Acknowledgement

Firstly, I would like to thank my supervisor, Dr Heather Hendrickson for the opportunity to be part of her team. It was my pleasure to work with such a supportive advisor, and I am grateful for the guidance, encouragement, and training over these several years I have received.

I am grateful to my co-supervisors, associated Professor Xue-Xian Zhang and Evelyn Sattlegger for the advice and discussions. Special thanks to Dr Mike Miller for performing RNA sequencing, the analysis, and assistance in turning population sequencing data into Muller plot. For assistance on the microcosmos essay and review of the second chapter, I thank Dr Gayle Ferguson.

Thanks to my lab mates in Hendrickson and Xue-Xian lab for their meaningful discussion - whom I have learnt from and assisted me to make this project possible. I am also thankful to my school for providing the scholarship and particularly Professor Dianne Brunton, head of the School of Natural and Computational Sciences.

Finally, I would like to express my gratitude to my lovely wife Mina, my parents, sister, and friends, for their endless support, motivation, and inspiration – without you I would not be where I am today.

Abstract

Predator-prey interactions are recognised to change the pace of evolution in microbial communities, but investigations into how selection for predation accelerates antagonistic behaviours, genomic evolution and the process of coadaptation are scarce. Here we performed a 20-day and an extended 90-day evolution experiment to investigate the adaptive traits that arise in in prey bacterium *Pseudomonas fluorescens* SBW25 on solid media in the presence and absence of a wild *Acanthamoeba* sp*.* Coevolution led to bacterial diversity, resistance to predation in coevolved bacterial lineages and evolution of predators. We show evidence of reciprocal adaptation, strong phenotypic and genotypic parallelism among prey lineages undergoing predation. We observed evolution of new colony morphotypes such as Wrinkly Spreader, Volcano and Mountain. Evolved morphotypes conferred grazing resistance and an increase in relative prey fitness that resulted in increased encystment and reduced replication of the protozoan populations. Mutation profiles of the coevolved phenotypes were associated with altered gene function in *amrZ*, *wspF*, *fadD1*, *fadD2* and putative hypothetical protein upstream of RND transporter. RNA sequencing results of the mutants also revealed a significant increase in the number of genes that up or downregulated while interacting with *Acanthamoeba sp*. We investigated the degree to which these mutations affect biofilm formation, capsulation, motility, mucoid and fatty acid degradation pathways. Some of these traits are associated with virulence in pathogenic organisms. We further found evidence of mutualisms where both prey and predator increased their survival relative to their respective ancestors. On the other side, we show promoted killing performance and higher generations upon feeding on WT bacteria in coevolved *Acanthamoeba* compared to their ancestors*.* Together, our findings demonstrate the emergence of

divergent colony morphologies and molecular parallelism that arise as an adaptation to predation and notably affects the fitness and evolution of predators suggesting Red Queen co-evolutionary dynamics between predators and prey. These findings suggest that protozoan predation can profoundly influence the course of genetic and phenotypic evolution in short and long-time scales.

Experimental Evolution Under Predation in *P. fluorescens* SBW25

A thesis presented in partial fulfilment of the

requirements for the degree of

Doctor of Philosophy

in

Microbiology & Genetics

at Massey University, Auckland, New Zealand.

Farhad Sadeghpour Golzar

2022

Table of Contents

List of Figures

List of Tables

Chapter 1

Overview

We are living in a microbial world. The bacteria that we encounter have been evolving for more than 3.5 billion years and have adapted to a wide range of lifestyles during that time [1–3]. One of the common strategies that bacteria have developed is virulence, or their capacity to harm eukaryotic hosts. Organisms that have adopted this lifestyle, can cause infectious diseases in humans or other animals [4–6]. These bacteria are referred to as bacterial pathogens.

Infectious diseases caused by bacterial pathogens are a major public health issue worldwide. Antimicrobial resistance, the emergence of new infectious diseases, outbreaks of water-borne and foodborne infectious diseases and bioterrorism have brought bacterial evolution to the forefront of concern [7,8]. A complete understanding of the factors that contribute to the evolution of bacterial pathogenicity can allow us to understand both how and why infectious diseases emerge. It is common to consider the evolution of virulence only in the context of multicellular hosts [9–11]. However, an alternative hypothesis by King et al. was developed as early as 1988 to suggest that the anti-predatory strategies that bacteria develop in response to protozoa, can also contribute to infection in multicellular hosts [12].

The hypothesis that protozoan predation is a natural and persistent phenomenon that can nourish and/or enhance bacterial resistance and virulence has received a little attention [13–15]. However, the mechanisms employed for resistance to protozoan predation are the same in many ways to the strategies employed in host infection; encapsulation, toxin secretion systems, invasion, siderophore expression, intracellular growth and extracellular adhesion are all traits found in both virulent bacteria and

bacteria either escaping or confronting protozoan predation [16–19]. If protozoan predation can stimulate evolution towards emergence of virulence traits, then evolution in response to protozoan predation would be expected to allow those same bacteria to invade and infect other higher host cell tissues. This is a hypothesis that we would like to test directly using experimental evolution.

From an ecological perspective, virulence can be framed as one extreme on the scale of intimate relationships between pairs of organisms; symbioses. The nature of symbiotic relationships can range between antagonistic (parasitism) to cooperative (mutualism) [20]. By directly testing the tendency of bacteria to evolve when challenged with protozoa and subsequently testing the downstream effects of this evolution on virulence in multicellular hosts, we will come to a clearer understanding of the potential of protozoa to effect symbiotic relationships in the environment.

The current project involves directly testing the evolution of a soil bacterium, *Pseudomonas fluorescens* SBW25 under heavy predation by model wild protozoa *Acanthamoeba sp*. This model system will provide an opportunity to measure the degree to which the prey-predator interaction may stimulate the evolution of adaptive traits in the prey bacterium. First, I will identify the nature of the molecular changes in the bacteria that have increased in their resistance to predation. I will then test the bacteria that have evolved under protozoan predation for the degree to which they have developed resistance against ancestral, coevolved and evolved predators and will evaluate the predator evolution as well.

In this introduction, I will give an overview of pathogenicity and describe the hypothesis I am testing. Next, I will focus on the host-bacterial interactions, the similarities and differences between multicellular hosts and protozoan predators from the perspective of bacterial cells. At the end of this literature review, I will focus on the establishment of symbiosis between two organisms and how these relationships depend on both organisms. This will be followed by a discussion specifically on different types of symbiotic relationships between bacteria-hosts such as mutualism, and parasitism. Then I will outline a set of common virulence factors in bacteria and how these affects either multicellular hosts or protozoan predators.

Introduction

Bacterial pathogenicity, significance of infectious diseases

In the rich microbial world, there are a small number of microorganisms that can be pathogenic [21]. Pathogenicity is a term that describes the ability of the microorganisms to cause disease by overwhelming a multicellular host's defence. Pathogens can be virulent, meaning that they can damage host cells and ultimately cause major infectious disease. Opportunistic pathogens are microorganisms that can become pathogenic but are generally non-harmful to healthy hosts [22]. For example, some strains of *E. coli* are mutualistic and generally do not cause harm in the normal habitat of the large intestine, but if these strains gain entry to other body locations, for example in the urinary tract, they can cause severe infectious disease [23]. Similarly, some human pathogens are classified as zoonotic, meaning a disease which emerges in animals and is subsequently transmitted to humans. An example of this is *Coxiella burnetii,* a major cause of a contagious disease called Q fever [24] or *Salmonella* sppl., [25] either of these can cause diseases in multiple hosts including humans [26].

It is estimated that infectious diseases are responsible for nearly 25% (15 million) of the annual deaths worldwide in 2002 [27] . Similarly, it has been estimated that 16 and 15 million deaths were caused by infectious diseases respectively in 1990 and 2010 [28,29]. New infectious diseases, the re-emergence of old infectious diseases and the growing number of antimicrobial resistant strains are a continuing threat to humans. Different pathogenic bacteria employ numerous common strategies to infect eukaryotes and cause disease. Many of these infectious strategies are related to the virulence associated traits [30,31]. Predation by Free-living amoebae (FLA) is a potent selective force driving bacterial evolution [32]. Failure to resist predation results in whole-cell ingestion and digestion of bacterial prey [33]. Amoebae are however inefficient and careless predators [34,35]. In other words, they are not capable of consuming 100% of the bacteria in their natural habitats or they are supplied with bacteria in abundance in the lab condition. Bacteria can escape protozoan predation by adopting anti-predatory behaviours such as cell elongation, secondary metabolite or toxin secretion, and mucoid phenotypes [32,36–42]. Moreover, FLA are known to interact with bacterial pathogens and in some instances can act as a source of bacterial infections. It has been shown that protozoan predators are regarded as reservoirs and vehicles of pathogenic bacteria leading to infection of multiple hosts [18,43]. An example of this relationship is evident in *Legionella* strains. These bacteria are engulfed by protozoa and have acquired several strategies to survive this ingestion. The ability of bacteria to survive within protozoa demonstrates that protozoan cells can act as safe harbours that provide stable conditions for bacteria to replicate and/or promote their pathogenicity before infecting further targets [44].

It has been previously proposed that bacteria-protozoa interactions have a role in increased bacterial pathogenicity and therefore, FLAs have been referred to as “training grounds” for bacterial pathogenicity [45]. This is due to the fact that the similar mechanisms used by amoebae and immune cells for engulfing and killing bacteria. The observation of the close association between pathogenic bacteria and protozoa led King et al. to propose a novel symbiotic hypothesis suggesting that the protozoa may drive changes in bacteria such as extracellular resistance and/or intracellular survival [12]. Further to this, these authors suggest that these intimate protozoan-bacterium interactions might lead to both ecological and evolutionary changes in the symbiotic associations, allowing bacteria to increase in their pathogenicity. This could subsequently affect their pathogenicity in infection of mammalian host cells.

A comparison of multicellular hosts and protozoa

Eukaryotes are identified as the group of organisms that possess a membrane bound nucleus. The multicellular and the unicellular organisms both belong to the eukaryotic phylogeny that diversified one billion years ago [46]. Eukaryotes generally possess a membrane-bound nucleus, a cytoskeleton and a complex endomembrane system [47].

The defence strategies that bacteria employ to avoid phagocytosis during strong predation pressure are similar to those used to escape pathogenesis by multiple host-specific pressures [48,49]. Some of these are important general defence features that have been observed in pathogenic bacteria while infecting other eukaryotic hosts [50]. It has been suggested that protozoa and phagocytic immune cells such as

macrophages are structurally similar [46,51–53]. Similar bactericidal strategies are used by amoebae and macrophage and mechanisms that bacteria employ to resist and exploit these hosts are similar in many bacteria [54–56]. In addition, the prey and predator interactions are not only omnipresent in nature, but bacteria and protozoa are both widespread and are members of gut microbiota in many organisms and it is plausible that they employ similar anti-phagocytosis traits to resist both predators and immune cells. Interactions between protozoa and bacteria may also change the structure of the gut microbiota and therefore affect hosts' health [57]. Following is a description of two different types of eukaryotic cells relevant to the hypothesis I am testing; unicellular and multicellular eukaryotes.

Multicellular and unicellular eukaryotic hosts (Immune cells)

Organisms that are made up from more than one cell are defined as multicellular species, almost all humans, animals, land plants and some of the well-developed fungi and algae are multicellular eukaryotes [58]. Many eukaryotes are multicellular and have complex body structures with multiple cell types and larger cell sizes (Fig. 1.1B). The body of the multicellular organisms consist of highly specialised compartments that perform various functions. In the case of an immune cell, the responses of these types of cells to pathogens are complex and activate a diverse number of cell types included in the immune system. The main organelles of immune cells include the cell membrane, endoplasmic reticulum, Golgi apparatus, lysosomes, mitochondria, nucleus and microfilaments [59]. Furthermore, multicellular cells have a long-life span and death of the one immune cell of a multicellular host does not affect the survival of the remaining cells.

In contrast to multicellular eukaryotes, protozoa belong to the main lineage of protists and are free-living. The term protist refers to the eukaryotic organisms with a unicellular level of organisation. In contrast to multicellular species, distinct division of tasks does not occur in unicellular organisms, a fundamental difference that distinguishes these two eukaryotes [60,61]. These organisms have organised nuclei, possess mitochondria, Golgi complex and ribosomes etc (Fig. 1.1A). Many unicellular hosts are free-living and have different types of vacuoles in their cells. They have a short life span and a single cell is responsible for its own survival, in the sense that simple cell damage can contribute to the rapid demise of the organism [62]

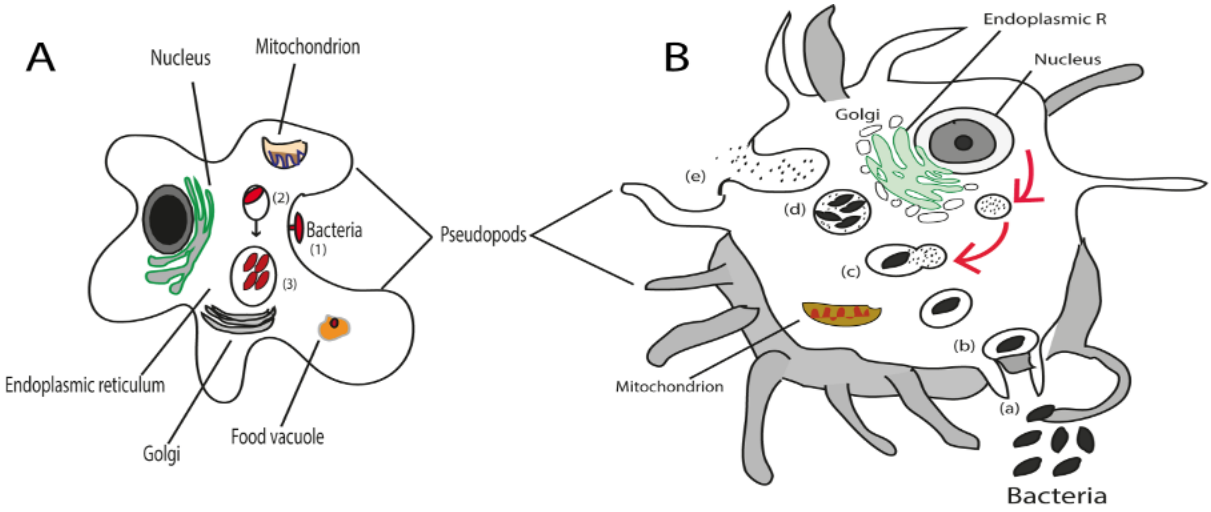

Figure 1. 1. Modelled schematics are a comparison of two different eukaryotic cells. A. Unicellular protozoan cell in the process of 1) phagocytosis of a bacterium (Red). (2) Upon engulfment, this bacterium employs a virulence factor (Type 4 Secretion System) to perform inhibition of endocytosis to be able to (3) colonise the protozoan host and possibly escape in order to infect other targets. B. Mammalian immune cell (leucocyte) in the process of engulfing a bacterium; (a) bacterium becomes attached to pseudopodia, (b) is ingested in a phagosome, (c) lysosomal enzymes produced by host cell (red arrows) fuse with phagosome to (d) digest and lyse the bacteria and (e) finally release the waste products from the immune cell.

Host-bacterial interaction

Bacterial microorganisms are widely distributed in diverse environments on earth [63]. This range of bacterial ubiquity puts prokaryotes in close contact with many eukaryotic organisms. Bacteria have long been the dominant organisms on this planet because of their inherent adaptive nature and ability to evolve rapidly. The inevitable consequences of large population sizes and short generation times allows bacteria to exploit the host and colonise every ecological space of the host. Indeed, selection drives microorganisms to compete for nutrients and enhance their adaptation to all suitable environments [64]. In comparison to their natural habitats in soil and water which have limited resources, the potential ecological niche within the host provides a new stable condition for bacterial life. This ideal environment is such that a multicellular host can therefore be seen as a reservoir with the potential to protect and enable bacteria to proliferate and increase their population [22,65,66].

Prey-predator interaction and adaptation to protozoa

Free-living protozoan predators are unicellular eukaryotes that are abundant in all environments (soil, river, ocean etc.) [67,68]. Some of these organisms are capable of causing severe infectious diseases in both humans and animals [13,69]. Several studies have shown the role of protozoans as vectors that can harbour pathogenic bacterial cells, resulting in the development of pathogenicity and emergence of new infectious disease. Ecologically FLA have roles in energy turnover, soil fertility and nutrient cycling in the environment. They compete with prokaryotes for nutrients, niche space, energy [70], and can feed on other prokaryotes, resulting in the bacterial community being limited as the daily turnover of bacterial communities is 60%[35].

However, some bacteria have developed numerous mechanisms to resist protozoan predation [36,65,71,72]. Importantly, resistance or pathogenic traits in bacteria are upregulated as a response to protozoan predation contribute to emergence of higher virulence functions [6,73,74]. Adaptation to protozoan predators increases the survival of bacteria in the environment [75]. For example, *Bacillus licheniformis* secretes lytic compounds to prevent phagocytosis by *Naegleria fowleri*. In some cases, after engulfment bacteria can establish a mutual relationship within the protozoan host called endosymbiosis from which both can benefit [34,76]. In general, there are two possible modes of prey-predator interaction when bacteria and protozoa encounter one another in their normal habitat; Intracellular lifestyles and extracellular life styles [36] (Fig. 1.2). In this thesis, we focus on extracellular lifestyles and traits associated with extracellular resistance. In either mode, bacteria can evolve adaptive characteristics to withstand the protozoan predator [77] (before ingestion or after ingestion) and therefore can increase their population [78]. Intracellular and extracellular bacterial strategies to protozoan predation are outlined further below.

Intracellular strategies after engulfment, fighting back

Once the bacteria are engulfed by free-living amoebae, some of them can avoid phagosomal lysis to maintain their intracellular viability (Fig. 1.2 a-c). *Legionella pneumophila* is a typical example of a bacterium able to survive inside the protozoan predators such as *Dictyostelium discoideum* [15]. Some bacteria have developed virulence strategies (adhesion and invasion) to penetrate into the host cell, resulting in host cell infection. If the defence system of the protozoan predator is ineffective to overcome the bacteria, the outcome can be co-adaptation and establishment of new symbiotic relationships which can either be cooperative or antagonistic. It has been

suggested that intracellular bacterial pathogens acquire similar mechanisms to infect both human macrophages and amoebae. Essentially, amoeba and human macrophages exhibit the same phagocytic strategies to kill the bacteria [19]. Therefore, close contact between protozoa and bacteria in the environment may support the evolution of bacterial pathogenicity and may be a cause of pathogen evolution [6].

Extracellular resistance to predation

A key focus of this thesis is extracellular lifestyles of bacteria and characteristics that contribute to extracellular resistance to amoeboid predation. Bacteria can evolve a complex set of anti-predatory strategies to maintain stable communities in the face of protozoan predation (Fig. 1.2 d-f). Biofilm formation is one of the predominant extracellular lifestyles of many prokaryotes and is considered to be an integral part of survival in many different environments. Growth in a biofilm allows prokaryotes to grow in a range of hostile environments and protects them from being phagocytosed by protozoans [79,80]. This indicates that free-living amoebae that reside in many habitats can be integral modulators of the bacterial community in biofilms. However, other phenomena including antibacterial agents, metal toxicity, acid exposure, and salinity also have a role in biofilm formation [81,82].

For instance, *P. aeruginosa* cells in the presence of the predator *Dictyostelium discoideum* form microcolonies which are the same size as the protozoa [83,84]. The establishment of microcolonies is the first stage of anti-predatory response, and increasing their survival against protozoan grazing [85,86]. At a later stage, bacterial microcolonies may produce various chemical components and secrete cytotoxins and

rhamnolipids [85]. The production of these components not only damages the amoebae, but it can also result in additional protection of the bacteria against a broad range of non-size-selective protozoans. Intriguingly, many of pathogenic traits developed by *P. aeruginosa* are common response strategies to all eukaryotes, multicellular and unicellular hosts. Therefore, it is plausible that the cause of parasitic bacteria may have origins in successful anti-predatory adaptations and in its inherent natural pressures [79,87].

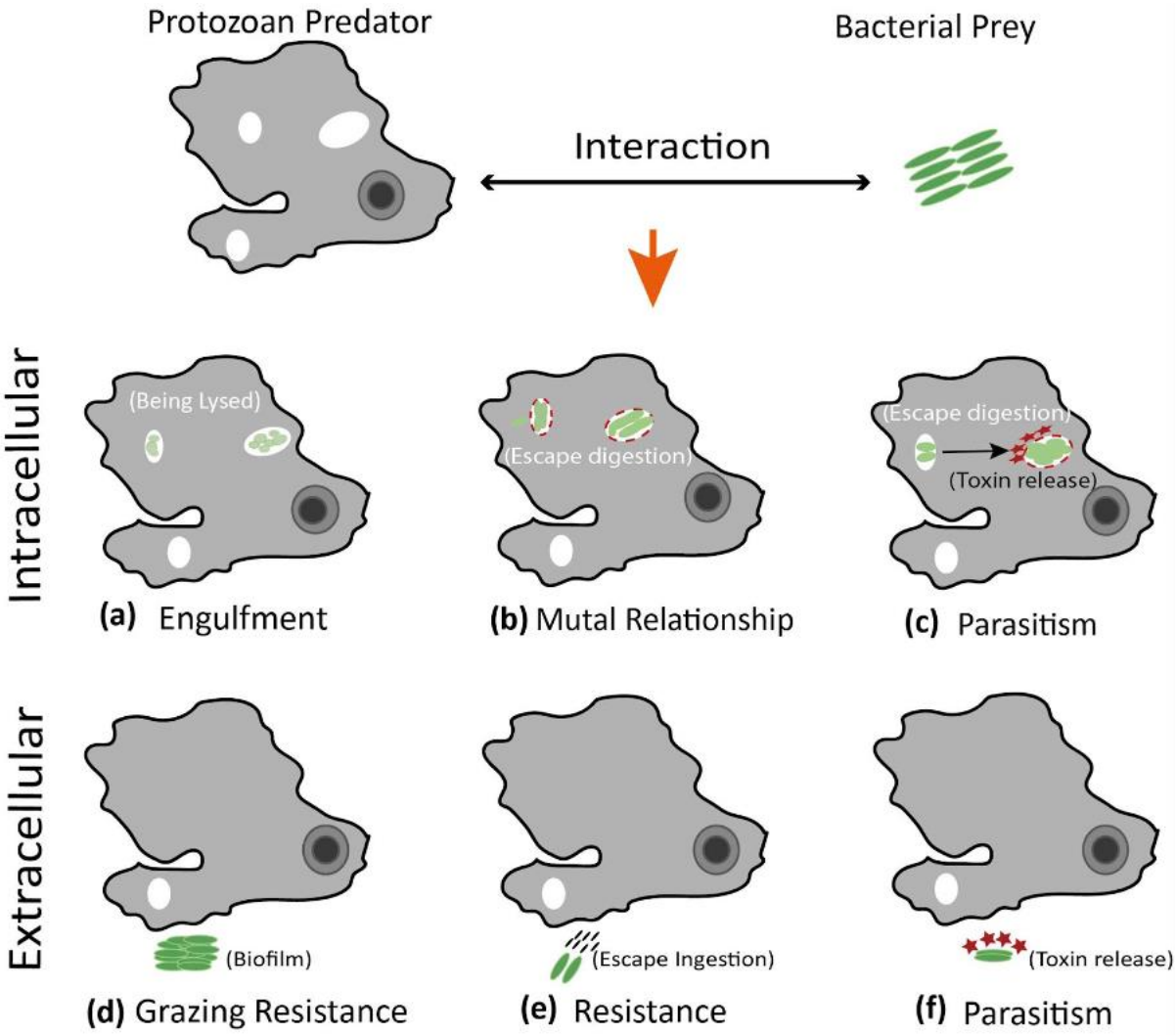

Figure 1. 2. Schematic model of predator-prey interactions and bacterial strategies towards symbiosis with protozoa. This overview is of the typical interactions that develop when bacteria and protozoa encounter one another. Shown are the several strategies that resistant bacteria exhibit in response to predation (adaptation strategies) leading to two distinct anti-predatory behaviours. (a-c) bacteria are engulfed and intracellular resistance factors by which bacteria may evolve to survive within protozoa.

Extracellular survival strategies such as (d) biofilm formation, (e) high speed and other virulence factors including (f) the release of distinct toxins that bacteria develop to escape from being phagocytosed by protozoa.

Symbiosis

A symbiosis is when two or more organisms live closely together, for example a bacterium and another species. Although symbiosis is most often used to describe the relationship between normal microbiota and host, the microbial world is also rife with interactions including protozoa-bacteria relationships [88]. Symbionts are defined as microorganisms that reside and colonise in a semi-permanent state and normally do not harm the host. However, a symbiosis can be any relationship that is intimate and need not describe a favourable relationship for either organism [14].

A typical example of a symbiosis occurs when a bacterium as an independent (free-living) organism colonises new ecological niches and develops a reliance on its host. Bacteria have developed several functions (detailed below) to gain access to and colonise new niches. The proliferation of prokaryotic cells within the host is a symbiotic interaction and can range from harmful to beneficial [89,90] (Fig. 1.2 a-c). Symbiotic interactions are important factor in the evolution of organisms. In natural ecosystems, numerous organisms have a tendency to interact and coevolve with each other, resulting in diverse beneficial or non-beneficial interactions [91]. Molecular phylogenetic studies from long-term symbioses of animal-associated bacteria have revealed many bacterial symbionts switched between mutualism and parasitism over time [92]. Once bacteria are established within the host, four different types of lifestyles can emerge: co-operation (mutualism - commensalism), parasitism, and amensalism. These are described in detail below.

Co-operation (mutualism)

In the symbiotic interaction termed mutualism, both species benefit. In rare cases intracellular growth and adaptation of both protozoa and bacteria can evolve successfully, resulting in the establishment of a mutually beneficial relationship between bacteria and amoebae. This relationship in which bacteria adapt and survive mutually within the free-living amoebae is termed endosymbiosis, from which both organisms benefit [93,94]. Free-living amoeba including *Acanthamoeba* spp., *Naegleria* and *Echinamoebae* have developed into a safe harbour for a variety of bacteria such as *Listeria* and *Legionella spp*. For example, in isolated free-living and pathogenic *Acanthamoebae* from humans and environmental samples, nearly 25% were carrying obligate endosymbionts [34]. Another example of a cooperative relationship in nature which has evolved for more than 65 million years, is established between *Rhizobium* species and plants known as *legumes* [95]. The symbiotic association between these two partners leads to nitrogen-fixation, a considerable ecological consequence that occurs in abundance on earth. Molecular nitrogen is an important element for the growth of plants. The *Rhizobia* naturally inhabit the soil and gain access to the root, infecting the cortex of the legume and intracellularly colonising in nodules that are able to fix nitrogen [96,97]. Nitrogen fixation makes the plant rich in an ingredient required for the production of proteins and can enhance crop yield [98]. On the other hand, rhizobia benefit from the host carbon sources and for a suitable environment for replication and survival [95]. This interaction is a successful mutualistic partnership that allows the plant to thrive in poor soils. In the case of *P. fluorescens* SBW25, several studies have shown it is able to colonise several distinct plant species [99]. Intriguingly, *P. fluorescens* SBW25 is able to establish a beneficial relationship both in soil and agar environments with plant hosts, resulting in the

promotion of the growth rates of a variety of plants such as tomato, wheat, pea and potato [100].

Parasitism

If the cooperative status is not established, protozoan-bacterial interactions can lead to a parasitic response leading to death of the protozoan cell [101]. This is another type of symbiosis in which one partner benefits while the other organism is adversely affected [102,103]. Many bacteria that contribute to the development of disease states in a host are parasites. For example, *Legionella pneumophila* and *Listeria monocytosis* are successful intracellular pathogens that have evolved various virulence functions to kill their protozoan hosts. These intracellular pathogens are able to exit the host cell in order to colonise other favourable niches [104,105]. Intriguingly, these bacteria can express a variety of strategies to infect either multicellular or unicellular eukaryotes [106,107]. Similarly, *L. pneumophila* in the early stages of the infection within mammalian cells can generate apoptosis in macrophages (programmed cell death). This involves the bacterial expression of an enzymatic regulator of apoptosis which modulates the activation of caspase-3 and induces cell necrosis in order to kill the host cell [108].

Intriguingly, both on ecological and evolutionary time scales, the evolution of virulence strategies and the range of harm caused by bacteria in damaging the host may be developed by a variety of factors (bacterial competition for nutrients) not only by host-pathogen interaction [109,110].

Commensalism

Commensalism is a kind of symbiotic interaction in which one organism benefits while the other is unaffected. These non-pathogenic microbes (as long as they do not invade the host) may generally gain access to the host's body from their natural environment in a short time after host birth and develop the mucous layer and skin epithelia. A vast majority of the microbes that shape the mammalian's normal flora (mucosal surface, eye, ear and external genitals surfaces) are commensals, although other kinds such as protozoa and fungi are found as well [111,112]. The commensal community under normal conditions does not cause any harm to the host. However, under certain conditions, if the immune responses are inappropriate against these bacteria, emergence of pathogenicity can result [113]. An example is the bacterium *Salmonella* that inhibits mammalian intestinal epithelial cells. Commensal bacteria modulate the innate and adaptive immune system of the host and are able to maintain a steady commensal state within the host [114]. This favourable environment within the host helps bacteria to replicate and reside as long as the host is alive. Intriguingly, hosts have evolved to incorporate bacterial colonisation of these commensal bacteria that contribute to maturation of the host immune system. Commensalism is also able to induce expression of some genes in mammals, resulting in the acquisition of strategies to enhance the immunity of the host tissue and therefore leads to protection against infectious pathogens [115].

Amensalism

A biological symbiotic association among distinct organisms in which one species is damaged and the other organism remains unharmed or benefits is classified as amensalism [116]. A common example of this interaction occurs between bacteria and

Penicillium as a bread mould where the outcome is the death of the many types of bacteria by penicillin secretion [117]. Amensalistic interaction basically involves two types of relationship; antibiosis (one species secrets molecular substance that kills the other species) and competition (a dominant species excludes another species from energy sources), black walnut tree is also a good example of this symbiotic relationship that prohibited from the growth of other plants habitat in its root zone [118].

Acanthamoeba sp. a model unicellular eukaryote

Protozoan predators are found in diverse habitats. Many are non-pathogens such as *Naegleria gruberi* [119] and some are potentially animal parasites, such as *Acanthamoeba*, *Balamuthia* [120,121] or *Naegleria fowleri*, a major cause of brain infection known as primary amoebic meningoencephalitis [122,123]. In general, these organisms in one stage of their life cycle possess flagella, cilia and pseudopodia that enable them to navigate. Free-living amoeba at least have developed two stages in their life cycle: the amoeboid form and cyst form (Fig. 1.3). Protozoans in the amoeboid form are able to engulf food by the process called phagocytosis and also are capable of establishing symbiotic relationships with other organisms. Fundamentally, protozoans are known for their potential pathogenicity and also as a major reservoir of pathogenic bacteria [124]. *Acanthamoebae* spp., the organism selected for this research project [125] is a wild protozoon that has a worldwide distribution. *Acanthamoeba* is a common soil based protozoan predator and grows in natural habitats and thrives in laboratory conditions. The life cycle of *Acanthamoeba* includes encysted form, for example in our experiment *Acanthamoeba* is in a cyst form when stored in a buffer and vegetative form, in which bacterial predation takes place (Fig.

1.3). In *Acanthamoeba*, the amoeba state is rounded, with a diameter of 15 μm and a reproduction rate of 1.6 hr when consuming bacteria [120].

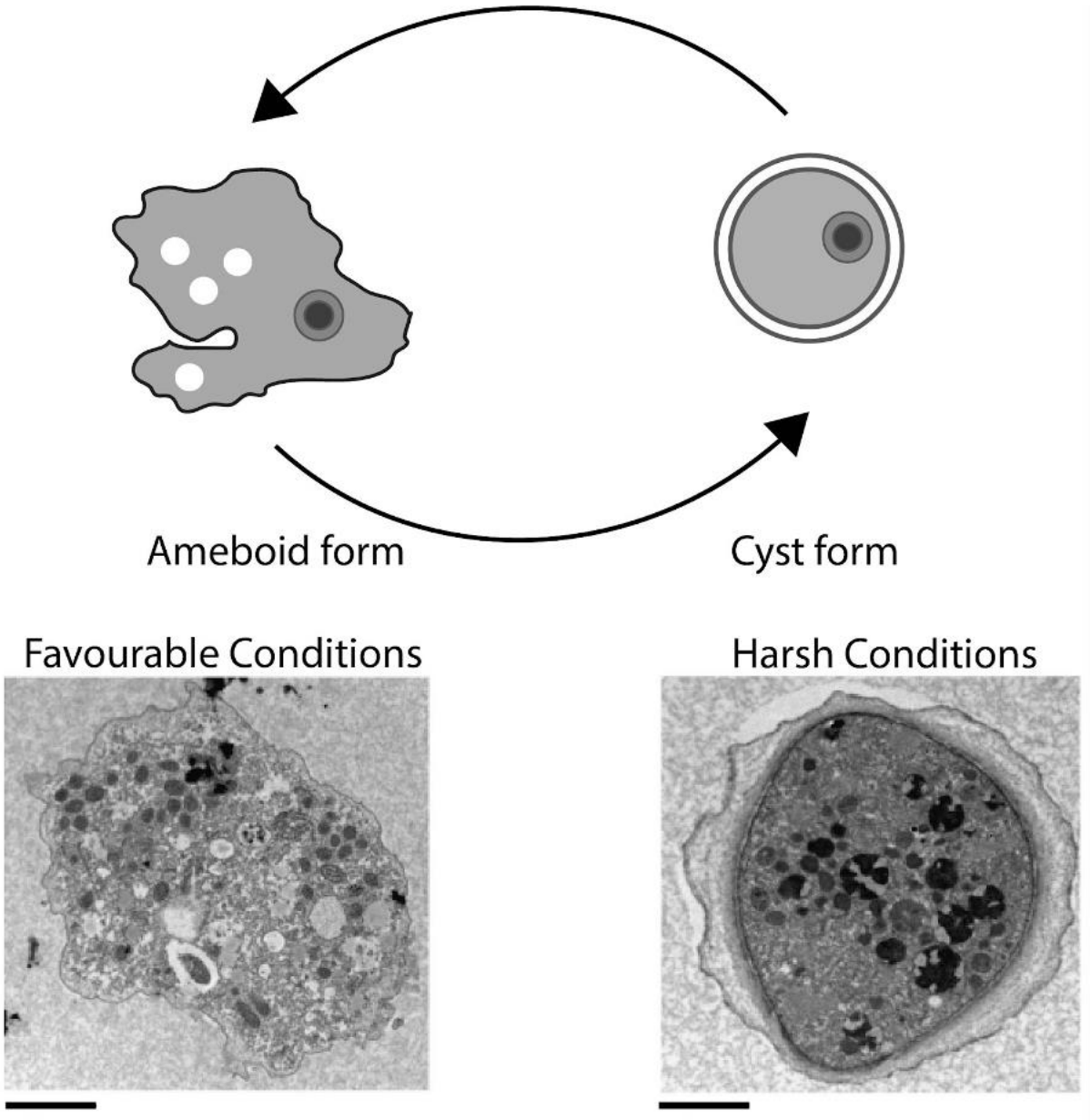

Figure 1. 2. The life cycle of *Acanthamoeba sp. Acanthamoeba* have two separate stages between which they transform; Cyst form and amoeba form for moving along a surface and consuming bacterium with large pseudopodia. Scale bars 2 μm.

Evolution of virulence factors

As mentioned previously, the hypothesis at the heart of this project suggests that resistance and virulence factors in bacteria can evolve as an adaptive response to protozoan predation and that these traits will negatively affect multicellular hosts [126]. It is therefore important to describe the functions of virulence factors and what is known of their evolution. Typically, virulence is defined as the amount of harm to the host resulting from an infection. This can range from illness to host mortality [8,65]. The evolution of virulence functions in parasitic bacteria is a major issue of evolutionary biology [59,127]. Virulence factors are produced by pathogenic microorganisms and help the bacteria to survive, replicate and harm the host and cause an infection via evading host defence [128]. Some well-known virulence factors in bacteria include capsules, toxins, adherence factors, invasion factors and siderophores. These are described in more detail below (Fig. 1.4).

Lipopolysaccharide capsule (LPS)

The bacterial outer membrane is the front line of defence against antimicrobial agents and other invading organisms [129]. The polysaccharide capsule (LPS) is present in the outer membrane of the gram-negative bacteria and considered as one of the main virulence factors produced by pathogenic bacteria to protect bacteria against phagocytosis by the host's immune system (Fig. 1.4) [130]. Polysaccharide capsules also known as O-antigen associated with the bacterial cell surface are highly hydrated molecules that are composed of individual monosaccharide capsules. A broad range of different capsular polysaccharide serotypes have been recognised that are related to specific infections. For instance, bacterial species that cause pneumonia and meningitis such as *Streptococcus pneumonia*e and *Haemophilus influenzae* produce

capsules that are fundamental to their virulence [8,131,132]. This is also found to be the effective defence mechanism of many bacteria such as *Salmonella* and *Klebsiella* against predation [114,133]. In our model bacterium *P. fluorescens* SBW25, LPS plays an important role in biofilm formation. It has been previously reported that a biofilm forming colony morphotype named Wrinkly Spreader (WS) arises in *P. fluorescens* SBW25 from smooth colony in response to environmental stressors such as lack of oxygen and predation pressure. The production of LPS in WS bacterial strain is crucial for adherence of these bacteria when they become attached to other cells or surfaces, resulting in successful resistance of the organism against a protozoan predator and an immune cell [71,134,135].

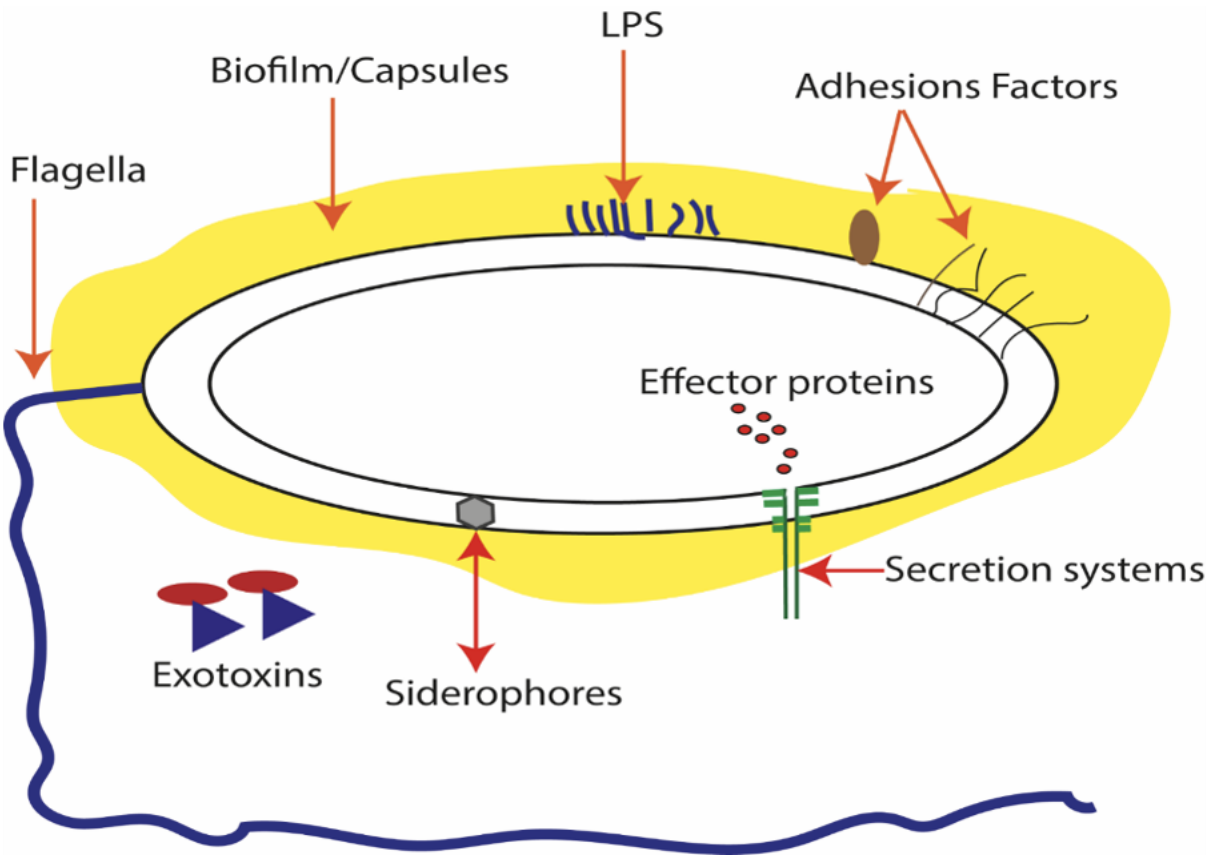

Figure 1. 3**.** Schematic encapsulated bacterial cell and the traits shown. Virulence trait is the ability that bacteria employ to harm other organisms to survive and grow.

Biofilm formation

Biofilms are firm aggregates of microorganisms that attach to a wide range of surfaces and produce extracellular polysaccharide, a serious problem and common amongst organisms that cause certain infectious diseases [136–138]. Biofilm formation is a co-operative behaviour that benefits bacteria by successfully repelling competition from other invading organisms [139]. Furthermore, by forming a dense biofilm, organisms can better resist predation and are more capable of withstanding the host immune system [126,140]. A commonly studied instance of biofilm formation is that of the air-liquid interface (A-L) by which bacteria have access to both oxygen (gaseous) and nutrient (liquid). In *P. fluorescens* SBW25 (our model bacterium) the colonisation of A-L interface arises through mutation when the ancestral smooth morphotype is grown in a spatially structured environment and gives rise to the WS. In this case, the expression and association of a LPS, cellulose matrix and a fimberial-like adherence factor that is initially produced, are essential components for the formation and development of the robust *P. fluorescens* SBW25 biofilm [135,141,142].

In *P. fluorescens* SBW25, the transcription of WSS cellulose synthase operon is thought to be encoded by three distinct regulatory pathways; Wsp chemosensory response system - awsXR and amrZ/fleQ. Thus, mutations on the *Wsp*, *amrZ* and *awsXR* system are well known to control cellular levels of secondary signalling molecule c-di-GMP and ultimately cause cells to constitutively over-express extracellular cellulose, resulting in formation of biofilm-producing mutants in WS strains [143–145] .

Secretion systems

Secretion systems of many bacterial pathogens play roles in adhesion, adaptation and increasing bacterial virulence during host-bacterial interaction [146]. These are complex molecular machines that translocate proteins through bacterial cytoplasm into multiple locations (target cell, extracellular space or outer membrane) resulting in recipient host tissue damage. Secretion systems of pathogenic bacteria are divided into diverse classes, based on their functions and structures [147]. Almost all common secretion systems, Type I secretion systems through Type VI are secreted by a wide range of Gram-negative pathogens [148]. In contrast, a small number of Gram-positive bacteria have these secretion systems. The Gram-positive bacteria possess only one lipid membrane which is surrounded by a thicker cell wall compared to Gram-negative bacteria [149].

The type 1 secretion system (T1SS) is a major virulence factor in an array of pathogenic bacteria, including *Vibrio Cholerae*, *Serratia marcescens* and *E. coli*. The TISS in these bacteria release toxins that can result in rupture of host tissue cells [150,151].

Type II secretion systems are made up of up to 15 diverse proteins that are known to be a general secretion system (Gsp) and have the ability to export an array of proteins outside of the bacterial cell into an extracellular environment [152]. Some of these are proteins including Xps in *P. aeruginosa* and Ecp in *V. cholera*. T2SS has an integral role in survival and replication of many pathogenic and non-pathogenic bacteria in environmental niches and/or within hosts. Secretion of hydrolysing enzymes including pseudolysin in *P. aeruginosa* and cholera toxin of *V. cholerae* are examples of

virulence factors that pathogenic bacteria use to cause severe infections in hosts [153].

Type III secretion systems are found in various Gram-negative pathogens and symbionts. They consist of 19-29 proteins that can secrete and inject a broad range of proteinaceous substrates into the cytoplasm or plasma membrane of recipient cells. These highly specialised delivery systems enhance the transport of bacterial effector molecules in order to alter or destroy specific target cell functions, resulting in successful invasion and proliferation of bacteria [154,155]. Pathogens *Salmonella spp*. and *Yersinia spp* use these tiny molecules such as InvJ and YscP to directly inject proteins into host cells cytoplasm. In the case of *salmonella* T3SS allows bacteria to invade eukaryotic cells by triggering pore complexes and decreasing phagosome lysosome fusion, leading to an infectious environment either within protozoan or animal cells [156,157]. Similarly, T3SS is identified in our model bacterium *P. fluorescens* SBW25. This secretion system (Rsp and Rsc) is essential for their growth and forming relationships with other host cells (microbe-host interactions) [158].

Another macromolecular system that can release substrates into a large number of target sites, including other bacteria, protozoan cells and mammalian's cells is known as Type IV secretion system (T4SS) [159]. These secretion complexes are capable of transferring either DNA or proteins and are therefore highly adaptable. Examples of bacteria that employ this as a virulence factor include *Helicobacter pylori*, *Brucella suis*, *L. pneumophila* and *Neisseria gonorrhoeae*. In *L. pneumophila* the T4SS plays a critical role in infecting both unicellular and multicellular eukaryotes. Bacteria with a T4SS can escape endocytosis by establishing a favourable environment in the

vacuole, inhibiting host defence and thereby allowing cells to successfully replicate within hosts [13,160].

Type V secretion systems (T5SS) or autotransporter systems are unique in that the substrate forms an individual polypeptide that can be transferred via secretion through the outer membrane. Besides their fundamental role as a major virulence secreting system, T5SS also serve in biofilm formation and adhesion process [161]. Some well-known substrates are protein YadA of *Y. enterocolitica* which enhances exportation of T3SS into host cell and participates in regulating resistance against host complement system and, immunoglobulin A protease in *N. gonorrhoeae* which adhere firmly to host antibodies [162].

Type VI secretion system (T6SS) has been found most recently and less is known about their mechanisms and structure. T6SS more commonly delivers the proteins into other bacterial cells and also eukaryotic cells. They are known for translocating effector proteins into other bacterial cells that may have a role in bacterial communication and interaction in many environments [163,164].

Type VII secretion systems (T7SS) are found in Gram-positive bacteria such as *Mycobacterium tuberculosis*, *Bacillus anthracis* and *L. monocytosis* that contain a thick cell wall layer. These bacteria therefore employ this specialised delivery mechanism to transfer proteins through their inner membrane to the extracellular environment. and have a variety of roles in pathogenicity of these bacteria. Many of the T7SS are divided into two ESX molecules (first identified in pathogenicity of *M. tuberculosis*) and PPE proteins [165,166].

Based on molecular structure and strategy of harm, toxins can be further divided into non-proteinaceous (endotoxins) and proteinaceous (exotoxins). These are described in more detail below.

Endotoxin

Bacterial cell walls are present in most Gram-negative and Gram-positive bacteria. The cell walls of bacteria can contain diverse structural toxic components that have a role in pathogenicity of bacteria [167]. These toxic components have different structures compared to conventional toxins (explained below). Bacterial LPS and teichoic acid produced by Gram-negative and Gram-positive organisms are known as endotoxins. These toxic molecules are potential virulence factors leading to mortality [168].

Exotoxin

Proteinaceous toxins are identified as general enzymes which can be secreted into the surrounding milieu in the eukaryotic host or be delivered directly into the cytoplasm of the host cell via secretion pathways such as T3SS. Bacterial exotoxins are divided into four types based on their role and amino acid composition [169]: 1) A-B toxins; subunit A have enzymatic activity and subunit B organise the toxin to be bound and delivered into the target cell (*E. coli* and *P. aeruginosa* are two distinct bacteria that contain this toxin). 2) Proteolytic toxins are responsible for destroying specific proteins in the host. These toxins block the release of the neurotransmitters in the nervous system of the host and cause the appearance of clinical symptoms of the disease such as paralysis (ie. *Clostridium botulinum* and *Clostridium tetani*). 3) pore-forming toxins;

can cause cell lysis and ultimately cell death via forming a pore in the host cell membrane. And 4) Other toxins not included in the other three categories [21,170].

Adhesion

Pathogenic bacteria employ numerous strategies to bind to the specific surface of the host tissue and start a biochemical process leading to host disease. Adhesion mechanisms are therefore a principal part of host-pathogen interactions. Microbial adherence factors can attach to host cell surfaces including the oral cavity, nasopharynx, lymphoid tissue, endothelial tissue, gastric and intestinal epithelia [171,172]. Adhesins can consist of polypeptides (protein), which are divided into two main groups; pili (fimbrial) and also non-pilus (afimbrial) or can be made by polysaccharides (carbohydrates or sugar). An example of this attachment is the bacterium *E. coli* adhesions that are necessary for infection in the urinary tract [173]. In response to the attack, host tissue cells produce a number of mechanical forces (saliva secretion, mucus flow, blood flow, coughing, sneezing and peristalsis) to avoid the bacteria binding to these surfaces [174].

One of these mechanical forces occurs against *Helicobacter pylori* in the mucosal surface of the stomach where the gastric epithelium releases a glycoprotein, known as mucin MUC1. *H. pylori* binding to the MUC1 prevents the adhesion of the bacteria to the cell surface and therefore limits the bacterial population. This results in limitation of the disease. Besides this role, MUC1 can act as a physical barrier against other bacteria to protect the epithelial surface [175].

Invasion

Once adhesion is complete the process of invasion can begin. At this stage, the bacterium may be able to penetrate the host cell, resulting in colonisation and the development of disease. Defensive systems of the host like the mucus layer act as a protective surface to limit and prevent the invasion of the pathogenic bacteria. Commensal organisms which form the normal microbiota residing on host mucosal surface, contribute to controlling pathogenic invasion by competing with pathogens for nutrients. An example of this mechanism is termed zipper and trigger entry which are specifically used by bacterial species such as *Yersinia pseudotuberculosis, Listeria monocytogenes, Shigella*, and *Salmonella* to gain entry to the host cell tissue [22,176].

Siderophores

Many bacteria and some plants produce molecules called siderophores. Siderophores are a virulence factor released by pathogenic bacteria to facilitate the uptake and storage of soluble iron ions. This acquisition of iron is considered to play a central role in the growth of pathogens within the host. To date, up to 500 siderophores have been recognised in bacteria, plant, and fungi [177], some of which are identified in plant growth-promoting *P. fluorescens* SBW25, plant pathogen *P. syringae*, and human pathogen *P. aeruginosa* [178,179]. In general, iron has an important role in metabolism and growth of all eukaryotic cells and many bacteria. This essential element is found abundantly on earth. However, iron is not a freely available supplement like in environments [180]. Bacteria develop several mechanisms for the acquisition of concentrated soluble iron from their hosts. In response, host's macrophages that have a main role in sequestering invasive bacteria employ a strategy called iron-withholding and utilise a protein (Nramp1) to vary their own internal iron status. However,

pathogenic bacteria require iron from iron-containing proteins (ferritin, haemoglobin, and transferrin) and therefore develop numerous mechanisms to combat this problem and to acquire the iron from the host [181,182]. For example, enterochelin is a siderophore that is secreted by *Escherichia* and *Salmonella* which is considered a crucial virulence strategy for the pathogenicity of these bacteria. Similarly, our model bacterium in this study, *P. fluorescens* SBW25 under certain conditions, produces the enzymatic yellow-greenish pyoverdine siderophore for the acquisition of iron from the environment [183]. *P. fluorescens* SBW25 in low-nutrient environments is able to compete without her organisms and can acquire iron, resulting in limitation of the growth of pathogens such as *Ralstonia solanacearum* [179].

The Red Queen dynamics

The Red Queen dynamics proposes both species can coexistence only if they continuously coevolve, improve and adapt to the selective pressure [184]. It has been suggested that the Red Queen includes two standard meanings; 1) According to Van Valen Red Queen hypothesis, populations of competing organisms can diversify, coexist and/or go extinct. 2) Describes interaction dynamics within two species based on negative frequency dependent selection, which explains the advantage of genetic recombination and sexual reproduction [184–186]. There are possible outcomes of coevolution of interacting populations in the predator-prey system: The prey populations develop defensive traits that are virulent that they cannot be overcome by predators, resulting in the surviving the prey population and extinction of the predators. Predators evolve offensive strategies that the current prey population is unable to resist, so the prey decrease in population to a degree that they go extinct and predators thrive. In order for both species to survive, both predator and prey

populations co-adapt and evolve in response to each other, so neither is extinct (the Red Queen effect) [187].

Our study (predator-prey coevolution)

P. fluorescens SBW25 is a plant-associated bacteria that was isolated in 1989 from the phyllosphere of a sugar beet grown in Oxfordshire [188]. *P. fluorescens* SBW25 has been used as a model organism for an array of studies with varying interests, including phenotypic changes [142] responses to bacteriophage, antibiotic exposure [189–192], biofilm formation and multicellularity [193], experimental evolution [143] and niche invasion [134]. An experimental evolution of harmless GFP labelled bacteria *P. fluorescens* SBW25 under predation by wild protozoa *Acanthamoeba* sp. provides us a novel approach to identify the molecular causes of evolutionary processes experimentally relative to no predation group. Furthermore, this provides the framework for an experimental evolution which can be used to understand the factors that prompt defensive traits in bacteria and how newly evolved bacteria can adapt to their predators.

Experimental evolution is a research approach that investigates the evolutionary process to identify evolutionary changes in experimental populations as a response to conditions established by the experimenter. Experimental evolution therefore uses adaptation of the bacterial population to the particular environment to observe the effects of evolution [194,195]. Here we are using this approach in the lab and using a basic protocol that imposes predation to follow the effects of predation on bacteria in this evolutionary experiment. Several empirical studies of bacterial evolution have been done to investigate evolutionary changes and subsequently to generate new

species [196]. In particular, the use of experimental evolution of bacterium *P. fluorescens* SBW25 can provide a rapid establishment of connection between molecular biology and evolutionary dynamics. *P. fluorescens* SBW25 is an experimentally well-studied organism that has previously been used to study a variety of topics [197–199]. An experimental evolution of *P. fluorescens* SBW25 and coevolving bacterial populations and phages provided an insight into bacterial morphological changes that contribute to their resistance against phages [190,192]. This study was done in microcosms containing King B media with propagating *P. fluorescens SBW25* with and without bacteriophages. After growing the bacteria for more than 400 generations, they found bacterial resistance relevant to the infection and disease. The finding of this study revealed that evolving *P. fluorescens* in the presence of phage phi2 can lead to the promotion of mutation rates, adaptation and phenotypically altered LPS and mucoid types in bacteria [200].

Similarly, populations of *P. fluorescens* SBW25 were evolved experimentally in broth microcosms (spatially heterogeneous environment) in order to create a range of niche specialist genotypes such as WS [135,201]. Colonisation of the WS phenotype in a static broth culture allows bacteria to survive and replicate in the anoxic conditions, implying that individual cells are more likely to attach and form a group. The evolution of WS genotype in *P. fluorescens* SBW25 indicates their cooperative behaviours that enable them to develop adhesive factors to survive in harsh conditions [142,201]. Bacterial prey and predator has recently received more attention because of the importance of the predators in the evolution of bacterial organisms. It has been reported that as a result of *P. fluorescens* SBW25 and lytic phage coevolution in microcosm environment the mucoid phenotype arose and persisted as an adaptive

response to predation by phage [190]. The coevolutionary experiment between bacterial prey *E. coli* and bacterial predator *M. xanthus* in liquid culture revealed that predator prompts phenotypic and genotypic evolution in bacterial prey and accelerates molecular parallelism in both species. In this study it was observed that bacterial prey increased extracellular mucoid production [202]. However, none of the above experiments were performed in a structured environment using single-cell amoeboid predators.

This experiment is novel and requires the development and testing of several aspects of the growth and viability of the *Acanthamoebae* in advance of starting the evolution experiment. These include the following: Measure the viability of *Acanthamoebae* at room temperature, at -80℃ and establish a protocol for storing protozoa in liquid N2. Develop methods for separating *Acanthamoebae* from bacteria and test proper solid media for culturing robust *Acanthamoebae.*

The main aim of my project is to characterise the evolutionary strategies that *P. fluorescens* SBW25 have developed under the predation regime in a structured environment. More generally, the ability to grow these two organisms in lab conditions provide an opportunity to understand how coevolution can influence both predator and prey evolution in their natural habitats. *Acanthamoeba* was selected as a protist predator because of its ability to phagocytose on surfaces and its direct impact on phenotypic and genotypic evolution of non-pathogenic prey bacteria on surfaces had remained largely unexplored. We chose solid media in order to allow the bacteria to adapt to phagocytosis which takes place in these conditions. Developing this novel system in this setting requires that we perform:

The first objective of my thesis is to characterise the evolution of prey in the presence and absence of predator *Acanthamoeba* in a short period of time (20-day co-evolution). To do this I will evolve prey bacteria in three lines in the presence and absence of predators on solid media. This will allow me to measure anti-predatory strategies that bacteria have developed in response to predation. I will also identify morphological and molecular changes by DNA and RNA sequencing in bacterial colonies that have altered phenotypes. Mutants will be allowed to grow with ancestral predators to measure their growth, survival and fitness, relative to WT prey. This is to determine how mutations affect the fitness of the strains in the presence and absence of predators. This also establishes a baseline for understanding the resistance traits in bacteria in a short period of time and for conducting the 90-day experiment. Understanding the results of the evolution experiment will help to better understand the future results.

2. My next objective is to conduct a 90-day experimental evolution of prey-predator and control (predation-free) in nine and three lines, respectively. This allows me to identify bacterial colony diversification and parallel phenotypic changes in co-evolved (CE) and prey-only (PO) groups. Next, I will measure colony morphotypes for anti-predatory traits (special relationship) that have developed in coevolved prey in the presence of all predator types (coevolved, evolved and ancestral *Acanthamoeba*) relative to WT bacteria. Furthermore, we will analyse predator specialisation and the effect of bacterial evolution on predator efficiency. This will allow us to further investigate reciprocal adaptation and Red Queen dynamics among the coevolved predator and prey populations.

3. Finally, I will characterise the genomic evolution among bacterial lines by identifying mutations in the colony morphotypes and evolved population lines (day 16, 40, 64 and 90). This is to investigate the mutations underlying these colony morphotypes and make progress in understanding the nature of bacterial survival to predation. In order to this we will reconstruct the mutations in wild type background and will test mutants for effect on *Acanthamoeba* by various microbiological techniques such as line test and performance test assays. In addition, we will perform RNA sequencing to study the differential gene expression in both coevolved bacteria and *Acanthamoeba*. By investigating the exact molecular mechanisms of bacterial survival during predation by predators, including the genomic basis of defensive traits, I will be able to determine the effect of predation on the coevolutionary processes leading to resistance traits in prey bacteria and reciprocal adaptation between predators and prey.

References

1. Xu F, Jerlström-Hultqvist J, Kolisko M, Simpson AGB, Roger AJ, Svärd SG, et al. On the reversibility of parasitism: adaptation to a free-living lifestyle via gene acquisitions in the diplomonad Trepomonas sp. PC1. BMC Biol. 2016;14: 1–15.
2. Holland HD. Evidence for Life on Earth More Than 3850 Million Years Ago. Science. 1997. pp. 38–39. doi:10.1126/science.275.5296.38
3. Gould SJ. The Evolution of Life on the Earth. Scientific American. 1994. pp. 84–91. doi:10.1038/scientificamerican1094-84
4. Donnenberg MS. Pathogenic strategies of enteric bacteria. Nature. 2000;406: 768–774.
5. Moradali MF, Ghods S, Rehm BHA. Pseudomonas aeruginosa Lifestyle: A Paradigm for Adaptation, Survival, and Persistence. Front Cell Infect Microbiol. 2017;0. doi:10.3389/fcimb.2017.00039

6. Adiba S, Nizak C, van Baalen M, Denamur E, Depaulis F. From grazing resistance to pathogenesis: the coincidental evolution of virulence factors. PLoS One. 2010;5: e11882.

7. Salyers AA, Whitt DD. Bacterial Pathogenesis: A Molecular Approach. Amer Society for Microbiology; 2002.

8. Wilson BA, Winkler M, Ho BT. Bacterial Pathogenesis: A Molecular Approach. John Wiley & Sons; 2020.

9. Entry of Bacteria into Nonphagocytic Cells. Bacterial Adhesion to Animal Cells and Tissues. 2014. pp. 113–126. doi:10.1128/9781555817800.ch7

10. Pizarro-Cerdá J, Cossart P. Bacterial Adhesion and Entry into Host Cells. Cell. 2006. pp. 715–727. doi:10.1016/j.cell.2006.02.012

11. Rahme LG, Stevens EJ, Wolfort SF, Shao J, Tompkins RG, Ausubel FM. Common virulence factors for bacterial pathogenicity in plants and animals. Science. 1995;268: 1899–1902.

12. King CH, Shotts EB Jr, Wooley RE, Porter KG. Survival of coliforms and bacterial pathogens within protozoa during chlorination. Appl Environ Microbiol. 1988;54: 3023–3033.

13. Hilbi H, Weber SS, Ragaz C, Nyfeler Y, Urwyler S. Environmental predators as models for bacterial pathogenesis. Environ Microbiol. 2007;9: 563–575.

14. Snelling WJ, Moore JE, McKenna JP, Lecky DM, Dooley JSG. Bacterial-protozoa interactions; an update on the role these phenomena play towards human illness. Microbes Infect. 2006;8: 578–587.

15. Steinert M, Heuner K. Dictyostelium as host model for pathogenesis. Cell Microbiol. 2005;7: 307–314.

16. Wells TJ, Henderson IR. Escherichia coli: Chapter 16. Type 1 and 5 secretion systems and associated toxins. Elsevier Inc. Chapters; 2013.

17. Bleves S, Voulhoux R, Ize B, Sana TG, Monack D. Protein Export and Secretion Among Bacterial Pathogens. Frontiers Media SA; 2020.

18. Van der Henst C, Vanhove AS, Drebes Dörr NC, Stutzmann S, Stoudmann C, Clerc S, et al. Molecular insights into Vibrio cholerae's intra-amoebal host-pathogen interactions. Nat Commun. 2018;9: 3460.

19. Matz C, Kjelleberg S. Off the hook--how bacteria survive protozoan grazing. Trends Microbiol. 2005;13: 302–307.

20. Huddleston E. Symbiotic Relationships. Core Library; 2020.

21. Wilson BA, Salyers AA, Whitt DD, Winkler ME. Bacterial Pathogenesis. 2011. doi:10.1128/9781555816162

22. Ezepchuk YV. Biological Concept of Bacterial Pathogenicity (Theoretical Review). Advances in Microbiology. 2017. pp. 535–544. doi:10.4236/aim.2017.77042

23. Ryan KJ, George Ray C, Sherris JC. Sherris Medical Microbiology: An Introduction to Infectious Diseases. 2004.

24. Esmaeili S, Golzar F, Ayubi E, Naghili B, Mostafavi E. Acute Q fever in febrile patients in northwestern of Iran. PLoS Negl Trop Dis. 2017;11: e0005535.

25. Kruse H, Kirkemo A-M, Handeland K. Wildlife as Source of Zoonotic Infections. Emerging Infectious Diseases. 2004. pp. 2067–2072. doi:10.3201/eid1012.040707

26. Wright SD. Wildlife and Emerging Zoonotic Diseases: The Biology, Circumstances and Consequences of Cross-Species Transmission. 315 Current Topics in Microbiology and Immunology. Journal of Wildlife Diseases. 2010. pp. 1345–1345. doi:10.7589/0090-3558-46.4.1345

27. Fauci AS. Emerging and reemerging infectious diseases: the perpetual challenge. Acad Med. 2005;80: 1079–1085.

28. Bouzid, Maha. Examining the Role of Environmental Change on Emerging Infectious Diseases and Pandemics. IGI Global; 2016.

29. Dye C. After 2015: infectious diseases in a new era of health and development. Philosophical Transactions of the Royal Society B: Biological Sciences. 2014. p. 20130426. doi:10.1098/rstb.2013.0426

30. Kado CI, Crosa JH. Molecular Mechanisms of Bacterial Virulence. Springer; 2012.

31. Kudva IT, Cornick NA, Plummer PJ, Zhang Q, Nicholson TL, Bannantine JP, et al. Virulence Mechanisms of Bacterial Pathogens. ASM Press; 2016.

32. Adiba S, Nizak C, van Baalen M, Denamur E, Depaulis F. From grazing resistance to pathogenesis: the coincidental evolution of virulence factors. PLoS One. 2010;5: e11882.

33. Vargas R, Hattori T. Protozoan predation of bacterial cells in soil aggregates. FEMS Microbiology Letters. 1986. pp. 233–242. doi:10.1111/j.1574-6968.1986.tb01733.x

34. Fritsche TR, Gautom RK, Seyedirashti S, Bergeron DL, Lindquist TD. Occurrence of bacterial endosymbionts in Acanthamoeba spp. isolated from corneal and environmental specimens and contact lenses. J Clin Microbiol. 1993;31: 1122–1126.

35. Clarholm M. Protozoan grazing of bacteria in soil—impact and importance. Microbial Ecology. 1981. pp. 343–350. doi:10.1007/bf02341429

36. Matz C, Kjelleberg S. Off the hook–how bacteria survive protozoan grazing. Trends Microbiol. 2005. Available: https://www.sciencedirect.com/science/article/pii/S0966842X05001344

37. Jürgens K, Matz C. Predation as a shaping force for the phenotypic and genotypic composition of planktonic bacteria. Antonie Van Leeuwenhoek. 2002;81: 413–434.

38. Pernthaler J. Predation on prokaryotes in the water column and its ecological implications. Nat Rev Microbiol. 2005;3: 537–546.

39. Van der Henst C, Vanhove AS, Drebes Dörr NC, Stutzmann S, Stoudmann C, Clerc S, et al. Molecular insights into Vibrio cholerae's intra-amoebal host-pathogen interactions. Nat Commun. 2018;9: 3460.

40. Jürgens K, Güde H. The potential importance of grazing-resistant bacteria in planktonic systems. Mar Ecol Prog Ser. 1994;112: 169–188.

41. Jousset A, Scheu S, Bonkowski M. Secondary metabolite production facilitates establishment of rhizobacteria by reducing both protozoan predation and the competitive effects of indigenous bacteria. Funct Ecol. 2008;22: 714–719.

42. Deines P, Matz C, JÜrgens K. Toxicity of violacein-producing bacteria fed to bacterivorous freshwater plankton. Limnology and Oceanography. 2009. pp. 1343–1352. doi:10.4319/lo.2009.54.4.1343

43. Guimaraes AJ, Gomes KX, Cortines JR, Peralta JM, Saramago Peralta RH. Acanthamoeba spp. as a universal host for pathogenic microorganisms: One bridge from environment to host virulence. Microbiological Research. 2016. pp. 30–38. doi:10.1016/j.micres.2016.08.001

44. Morozov AY, Adamson MW. Evolution of virulence driven by predator-prey interaction: Possible consequences for population dynamics. J Theor Biol. 2011;276: 181–191.

45. Miyake M, Watanabe T, Koike H, Molmeret M, Imai Y, Abu Kwaik Y. Characterization of Legionella pneumophila pmiA, a gene essential for infectivity of protozoa and macrophages. Infect Immun. 2005;73: 6272–6282.

46. Brinkmann H, Philippe H. The diversity of eukaryotes and the root of the eukaryotic tree. Adv Exp Med Biol. 2007;607: 20–37.

47. Vellai T, Vida G. The origin of eukaryotes: the difference between prokaryotic and eukaryotic cells. Proc Biol Sci. 1999;266: 1571–1577.

48. Hassett DJ, Sutton MD, Schurr MJ, Herr AB, Caldwell CC, Matu JO. Pseudomonas aeruginosa hypoxic or anaerobic biofilm infections within cystic fibrosis airways. Trends Microbiol. 2009;17: 130–138.

49. Worlitzsch D, Tarran R, Ulrich M, Schwab U, Cekici A, Meyer KC, et al. Effects of reduced mucus oxygen concentration in airway Pseudomonas infections of cystic fibrosis patients. Journal of Clinical Investigation. 2002. pp. 317–325. doi:10.1172/jci0213870

50. Espinoza-Vergara G, Hoque MM, McDougald D, Noorian P. The Impact of Protozoan Predation on the Pathogenicity of. Front Microbiol. 2020;11: 17.

51. Escoll P, Rolando M, Gomez-Valero L, Buchrieser C. From Amoeba to Macrophages: Exploring the Molecular Mechanisms of Legionella pneumophila

Infection in Both Hosts. Current Topics in Microbiology and Immunology. 2013. pp. 1–34. doi:10.1007/82_2013_351

52. Swart AL, Leoni Swart A, Harrison CF, Eichinger L, Steinert M, Hilbi H. Acanthamoeba and Dictyostelium as Cellular Models for Legionella Infection. Frontiers in Cellular and Infection Microbiology. 2018. doi:10.3389/fcimb.2018.00061

53. Thewes S, Soldati T, Eichinger L. Amoebae as Host Models to Study the Interaction with Pathogens. Frontiers Media SA; 2019.

54. Siddiqui R, Khan NA. Acanthamoeba is an evolutionary ancestor of macrophages: a myth or reality? Exp Parasitol. 2012;130: 95–97.

55. German N, Doyscher D, Rensing C. Bacterial killing in macrophages and amoeba: do they all use a brass dagger? Future Microbiol. 2013;8: 1257–1264.

56. Wheat WH, Casali AL, Thomas V, Spencer JS, Lahiri R, Williams DL, et al. Long-term survival and virulence of Mycobacterium leprae in amoebal cysts. PLoS Negl Trop Dis. 2014;8: e3405.

57. Chabé M, Lokmer A, Ségurel L. Gut Protozoa: Friends or Foes of the Human Gut Microbiota? Trends in Parasitology. 2017. pp. 925–934. doi:10.1016/j.pt.2017.08.005

58. Kirk DL. Volvox: A Search for the Molecular and Genetic Origins of Multicellularity and Cellular Differentiation. Cambridge University Press; 1998.

59. Kirk DL. A twelve-step program for evolving multicellularity and a division of labor. BioEssays. 2005. pp. 299–310. doi:10.1002/bies.20197

60. Jurkevitch E. Predatory Prokaryotes: Biology, Ecology and Evolution. Springer Science & Business Media; 2006.

61. Adl SM, Simpson AGB, Farmer MA, Andersen RA, Roger Anderson O, Barta JR, et al. The New Higher Level Classification of Eukaryotes with Emphasis on the Taxonomy of Protists. The Journal of Eukaryotic Microbiology. 2005. pp. 399–451. doi:10.1111/j.1550-7408.2005.00053.x

62. A Half-century of Research on Free-living Amoebae (1965-2017): Review of Biogeographic, Ecological and Physiological Studies. Acta Protozologica. 2018. doi:10.4467/16890027ap.18.001.8395

63. Bar-On YM, Phillips R, Milo R. The biomass distribution on Earth. Proc Natl Acad Sci U S A. 2018;115: 6506–6511.

64. Ghoul M, Mitri S. The Ecology and Evolution of Microbial Competition. Trends Microbiol. 2016;24: 833–845.

65. Brown SP, Cornforth DM, Mideo N. Evolution of virulence in opportunistic pathogens: generalism, plasticity, and control. Trends Microbiol. 2012;20: 336–342.

66. Leggett HC, Buckling A, Long GH, Boots M. Generalism and the evolution of parasite virulence. Trends in Ecology & Evolution. 2013. pp. 592–596. doi:10.1016/j.tree.2013.07.002

67. Fenchel T. Ecology of Protozoa: The Biology of Free-living Phagotropic Protists. Springer-Verlag; 2013.

68. Rodríguez-Zaragoza S. Ecology of free-living amoebae. Crit Rev Microbiol. 1994;20: 225–241.

69. Visvesvara GS. Pathogenic and Opportunistic Free-living Amoebae. Manson's Tropical Infectious Diseases. 2014. pp. 683–691.e5. doi:10.1016/b978-0-7020-5101-2.00051-0

70. Gallet R, Alizon S, Comte P-A, Gutierrez A, Depaulis F, van Baalen M, et al. Predation and disturbance interact to shape prey species diversity. Am Nat. 2007;170: 143–154.

71. Golzar FS, Ferguson GC, Hendrickson HL. Protozoan predation drives adaptive divergence in Pseudomonas fluorescens SBW25; ecology meets experimental evolution. doi:10.1101/2021.07.12.452127

72. Wieltschnig C, Fischer UR, Kirschner AKT, Velimirov B. Benthic Bacterial Production and Protozoan Predation in a Silty Freshwater Environment. Microbial Ecology. 2003. pp. 62–72. doi:10.1007/s00248-002-2040-x

73. Vasil ML, Darwin AJ. Regulation of Bacterial Virulence. American Society for Microbiology Press; 2012.

74. Hoque MM, Mozammel Hoque M, Noorian P, Espinoza-Vergara G, Cholan PM, Kim M, et al. Adaptation to an amoeba host drives selection of virulence-associated traits in Vibrio cholerae. The ISME Journal. 2021. doi:10.1038/s41396-021-01134-2

75. Song C, Mazzola M, Cheng X, Oetjen J, Alexandrov T, Dorrestein P, et al. Molecular and chemical dialogues in bacteria-protozoa interactions. Sci Rep. 2015;5: 12837.

76. Valdivia RH, Heitman J. Endosymbiosis: The Evil within. Current Biology. 2007. pp. R408–R410. doi:10.1016/j.cub.2007.04.001

77. McDougald D, Longford SR. Protozoa hosts lead to virulence. Nature Microbiology. 2020;5: 535–535.

78. Hilbi H. Molecular Mechanisms in Legionella Pathogenesis. Springer Science & Business Media; 2014.

79. Matz C, McDougald D, Moreno AM, Yung PY, Yildiz FH, Kjelleberg S. Biofilm formation and phenotypic variation enhance predation-driven persistence of Vibrio cholerae. Proceedings of the National Academy of Sciences. 2005. pp. 16819–16824. doi:10.1073/pnas.0505350102

80. Bramhachari PV. Implication of Quorum Sensing System in Biofilm Formation and Virulence. Springer; 2019.

81. Stewart PS, Costerton JW. Antibiotic resistance of bacteria in biofilms. Lancet. 2001;358: 135–138.

82. Donlan RM. Biofilms and device-associated infections. Emerg Infect Dis. 2001;7: 277–281.

83. Matz C, Bergfeld T, Rice SA, Kjelleberg S. Microcolonies, quorum sensing and cytotoxicity determine the survival of Pseudomonas aeruginosa biofilms exposed to protozoan grazing. Environ Microbiol. 2004;6: 218–226.

84. Wey JK, Jürgens K, Weitere M. Seasonal and successional influences on bacterial community composition exceed that of protozoan grazing in river biofilms. Appl Environ Microbiol. 2012;78: 2013–2024.

85. Scherwass A, Erken M, Arndt H. Grazing Effects of Ciliates on Microcolony Formation in Bacterial Biofilms. Microbial Biofilms - Importance and Applications. IntechOpen; 2016.

86. Chan SH, Ismail MH, Tan CH, Rice SA, McDougald D. Microbial predation accelerates granulation and modulates microbial community composition. BMC Microbiol. 2021;21: 91.

87. Cosson P, Zulianello L, Join-Lambert O, Faurisson F, Gebbie L, Benghezal M, et al. Pseudomonas aeruginosa virulence analyzed in a Dictyostelium discoideum host system. J Bacteriol. 2002;184: 3027–3033.

88. Catta-Preta CMC, Brum FL, da Silva CC, Zuma AA, Elias MC, de Souza W, et al. Endosymbiosis in trypanosomatid protozoa: the bacterium division is controlled during the host cell cycle. Front Microbiol. 2015;6: 520.

89. Dethlefsen L, McFall-Ngai M, Relman DA. An ecological and evolutionary perspective on human-microbe mutualism and disease. Nature. 2007;449: 811–818.

90. Nussbaumer AD, Fisher CR, Bright M. Horizontal endosymbiont transmission in hydrothermal vent tubeworms. Nature. 2006;441: 345–348.

91. Percival SL, Yates MV, Williams D, Chalmers R, Gray N. Microbiology of Waterborne Diseases: Microbiological Aspects and Risks. Academic Press; 2013.

92. Funk DJ, Helbling L, Wernegreen JJ, Moran NA. Intraspecific phylogenetic congruence among multiple symbiont genomes. Proc Biol Sci. 2000;267: 2517–2521.

93. Wingreen NS, Levin SA. Cooperation among Microorganisms. PLoS Biology. 2006. p. e299. doi:10.1371/journal.pbio.0040299

94. Uzuka A, Kobayashi Y, Onuma R, Hirooka S, Kanesaki Y, Yoshikawa H, et al. Responses of unicellular predators to cope with the phototoxicity of photosynthetic prey. Nat Commun. 2019;10: 5606.

95. Masson-Boivin C, Giraud E, Perret X, Batut J. Establishing nitrogen-fixing symbiosis with legumes: how many rhizobium recipes? Trends Microbiol. 2009;17: 458–466.

96. Ferguson BJ. Rhizobia and Legume Nodulation Genes ☆. Reference Module in Life Sciences. 2017. doi:10.1016/b978-0-12-809633-8.07071-0

97. Frugier F. The Nitrogen-Fixing Legume-Rhizobium Symbiosis. Academic Press; 2020.

98. Kumar V, Kumar M, Sharma S, Prasad R. Probiotics and Plant Health. Springer; 2017.

99. Naseby DC, Way JA, Bainton NJ, Lynch JM. Biocontrol of Pythium in the pea rhizosphere by antifungal metabolite producing and non-producing Pseudomonas strains. J Appl Microbiol. 2001;90: 421–429.

100. Jäderlund L. Fates and Impacts of the Genetically Modified Plant Growth-promoting Bacterium Pseudomonas Fluorescens SBW25: Under Controlled and Field Conditions. 2008.

101. Van der Henst C, Scrignari T, Maclachlan C, Blokesch M. An intracellular replication niche for Vibrio cholerae in the amoeba Acanthamoeba castellanii. ISME J. 2015;10: 897–910.

102. Eloe-Fadrosh EA, Rasko DA. The human microbiome: from symbiosis to pathogenesis. Annu Rev Med. 2013;64: 145–163.

103. Lee L-H, Mutalib N-SA, Wong SH, Chin S-F, Singh V. Human Microbiome: Symbiosis to Pathogenesis. Frontiers Media SA; 2021.

104. Gomez-Valero L, Buchrieser C. Intracellular parasitism, the driving force of evolution of Legionella pneumophila and the genus Legionella. Microbes Infect. 2019;21: 230–236.

105. Gao LY, Harb OS, Abu Kwaik Y. Utilization of similar mechanisms by Legionella pneumophila to parasitize two evolutionarily distant host cells, mammalian macrophages and protozoa. Infect Immun. 1997;65: 4738–4746.

106. Khweek AA, Amer A. Replication of Legionella Pneumophila in Human Cells: Why are We Susceptible? Front Microbiol. 2010;1: 133.

107. Hasni I, Jarry A, Quelard B, Carlino A, Eberst J-B, Abbe O, et al. Intracellular Behaviour of Three Legionella pneumophila Strains within Three Amoeba Strains, Including Willaertia magna C2c Maky. Pathogens. 2020. p. 105. doi:10.3390/pathogens9020105

108. Wall DM, McCormick BA. Bacterial secreted effectors and caspase-3 interactions. Cellular Microbiology. 2014. pp. 1746–1756. doi:10.1111/cmi.12368

109. Agosta SJ, Brooks DR. The Major Metaphors of Evolution: Darwinism Then and Now. Springer Nature; 2020.

110. Combes C. Parasitism: The Ecology and Evolution of Intimate Interactions. University of Chicago Press; 2001.

111. Hooper LV, Gordon JI. Commensal host-bacterial relationships in the gut. Science. 2001;292: 1115–1118.

112. Top FH, Wehrle PF. Communicable and Infectious Diseases. 1976.

113. Macpherson AJ, Harris NL. Interactions between commensal intestinal bacteria and the immune system. Nat Rev Immunol. 2004;4: 478–485.

114. Wildschutte H, Wolfe DM, Tamewitz A, Lawrence JG. Protozoan predation, diversifying selection, and the evolution of antigenic diversity in Salmonella. Proc Natl Acad Sci U S A. 2004;101: 10644–10649.

115. Casadevall A, Pirofski LA. Host-pathogen interactions: basic concepts of microbial commensalism, colonization, infection, and disease. Infect Immun. 2000;68: 6511–6518.

116. Townsend HM, Huyvaert KP, Hodum PJ, Anderson DJ. Nesting distributions of Galápagos boobies (Aves: Sulidae): an apparent case of amensalism. Oecologia. 2002;132: 419–427.

117. Veiga JP, Wamiti W, Polo V, Muchai M. Interphyletic relationships in the use of nesting cavities: mutualism, competition and amensalism among hymenopterans and vertebrates. Naturwissenschaften. 2013;100: 827–834.

118. Hochberg ME, Lawton JH. Competition between kingdoms. Trends Ecol Evol. 1990;5: 367–371.

119. Fritz-Laylin LK, Prochnik SE, Ginger ML, Dacks JB, Carpenter ML, Field MC, et al. The genome of Naegleria gruberi illuminates early eukaryotic versatility. Cell. 2010;140: 631–642.

120. Khan NA. Acanthamoeba: Biology and Pathogenesis. 2015.

121. Martinez AJ, Visvesvara GS. Free-living, amphizoic and opportunistic amebas. Brain Pathol. 1997;7: 583–598.

122. Siddiqui R, Khan NA. Primary Amoebic Meningoencephalitis Caused by Naegleria fowleri: An Old Enemy Presenting New Challenges. PLoS Neglected Tropical Diseases. 2014. p. e3017. doi:10.1371/journal.pntd.0003017

123. Gharpure R, Bliton J, Goodman A, Ali IKM, Yoder J, Cope JR. Epidemiology and Clinical Characteristics of Primary Amebic Meningoencephalitis Caused by Naegleria fowleri: A Global Review. Clin Infect Dis. 2021;73: e19–e27.

124. Greub G, Raoult D. Microorganisms resistant to free-living amoebae. Clin Microbiol Rev. 2004;17: 413–433.

125. Alan H. Carr, Amborski RL, Culley DD, Grace F. Amborski. Aerobic Bacteria in the Intestinal Tracts of Bullfrogs (Rana catesbeiana) Maintained at Low Temperatures. Herpetologica. 1976;32: 239–244.

126. Sun S, Noorian P, McDougald D. Dual Role of Mechanisms Involved in Resistance to Predation by Protozoa and Virulence to Humans. Front Microbiol. 2018;0. doi:10.3389/fmicb.2018.01017

127. Boots M, Sasaki A. “Small worlds” and the evolution of virulence: infection occurs locally and at a distance. Proceedings of the Royal Society of London. Series B: Biological Sciences. 1999. pp. 1933–1938. doi:10.1098/rspb.1999.0869

128. Peterson JW. Bacterial Pathogenesis. In: Baron S, editor. Medical Microbiology. Galveston (TX): University of Texas Medical Branch at Galveston; 2011.

129. Lerouge I. O-antigen structural variation: mechanisms and possible roles in animal/plant–microbe interactions. FEMS Microbiology Reviews. 2001. p. 0. doi:10.1016/s0168-6445(01)00070-5

130. Singh JK, Adams FG, Brown MH. Diversity and Function of Capsular Polysaccharide in Acinetobacter baumannii. Front Microbiol. 2019;0. doi:10.3389/fmicb.2018.03301

131. Iandolo JJ. The Genetics of Staphylococcal Toxins and Virulence Factors. Molecular Basis of Bacterial Pathogenesis. 1990. pp. 399–426. doi:10.1016/b978-0-12-307211-5.50023-4

132. Bartram J, Cotruvo JA, Cotruvo J, Exner M, Fricker C, Glasmacher A. Heterotrophic Plate Counts and Drinking-water Safety: The Significance of HPCs for Water Quality and Human Health. World Health Organization; 2003.

133. March C, Cano V, Moranta D, Llobet E, Pérez-Gutiérrez C, Tomás JM, et al. Role of bacterial surface structures on the interaction of Klebsiella pneumoniae with phagocytes. PLoS One. 2013;8: e56847.

134. Koza A, Kusmierska A, McLaughlin K, Moshynets O, Spiers AJ. Adaptive radiation of Pseudomonas fluorescens SBW25 in experimental microcosms provides an understanding of the evolutionary ecology and molecular biology of A-L interface biofilm formation. FEMS Microbiol Lett. 2017;364. doi:10.1093/femsle/fnx109

135. Spiers AJ, Rainey PB. The Pseudomonas fluorescens SBW25 wrinkly spreader biofilm requires attachment factor, cellulose fibre and LPS interactions to maintain strength and integrity. Microbiology. 2005;151: 2829–2839.

136. Bacterial biofilm and associated infections. J Chin Med Assoc. 2018;81: 7–11.

137. Gedefie A, Demsis W, Ashagrie M, Kassa Y, Tesfaye M, Tilahun M, et al. Biofilm Formation and Its Role in Disease Pathogenesis: A Review. Infect Drug Resist. 2021;14: 3711–3719.

138. Donlan RM. Biofilms: Microbial Life on Surfaces. Emerging Infectious Diseases. 2002. pp. 881–890. doi:10.3201/eid0809.020063

139. Hall-Stoodley L, Costerton JW, Stoodley P. Bacterial biofilms: from the natural environment to infectious diseases. Nat Rev Microbiol. 2004;2: 95–108.

140. Davey ME, O'toole GA. Microbial Biofilms: from Ecology to Molecular Genetics. Microbiology and Molecular Biology Reviews. 2000. pp. 847–867. doi:10.1128/mmbr.64.4.847-867.2000

141. Spiers AJ, Bohannon J, Gehrig SM. Biofilm formation at the air–liquid interface by the Pseudomonas fluorescens SBW25 wrinkly spreader requires an acetylated form of cellulose. Molecular. 2003. Available: https://onlinelibrary.wiley.com/doi/abs/10.1046/j.1365-2958.2003.03670.x

142. Gallie J, Bertels F, Remigi P, Ferguson GC, Nestmann S, Rainey PB. Repeated Phenotypic Evolution by Different Genetic Routes in Pseudomonas fluorescens SBW25. Mol Biol Evol. 2019;36: 1071–1085.

143. Lind PA, Farr AD, Rainey PB. Experimental evolution reveals hidden diversity in evolutionary pathways. eLife. 2015. doi:10.7554/elife.07074

144. Bantinaki E, Kassen R, Knight CG, Robinson Z, Spiers AJ, Rainey PB. Adaptive divergence in experimental populations of Pseudomonas fluorescens. III. Mutational origins of wrinkly spreader diversity. Genetics. 2007;176: 441–453.

145. Hickman JW, Tifrea DF, Harwood CS. A chemosensory system that regulates biofilm formation through modulation of cyclic diguanylate levels. Proc Natl Acad Sci U S A. 2005;102: 14422–14427.

146. Depluverez S, Devos S, Devreese B. The Role of Bacterial Secretion Systems in the Virulence of Gram-Negative Airway Pathogens Associated with Cystic Fibrosis. Front Microbiol. 2016;7: 1336.

147. Wang J, Li J, Zhao H, Sheng G, Wang M, Yin M, et al. Structural and Mechanistic Basis of PAM-Dependent Spacer Acquisition in CRISPR-Cas Systems. Cell. 2015;163: 840–853.

148. Gerlach RG, Hensel M. Protein secretion systems and adhesins: the molecular armory of Gram-negative pathogens. Int J Med Microbiol. 2007;297: 401–415.

149. Green ER, Mecsas J. Bacterial Secretion Systems: An Overview. Microbiol Spectr. 2016;4. doi:10.1128/microbiolspec.VMBF-0012-2015

150. Kanonenberg K, Spitz O, Erenburg IN, Beer T, Schmitt L. Type I secretion system—it takes three and a substrate. FEMS Microbiology Letters. 2018. doi:10.1093/femsle/fny094

151. Dolores JS, Agarwal S, Egerer M, Satchell KJF. Vibrio cholerae MARTX toxin heterologous translocation of beta-lactamase and roles of individual effector domains on cytoskeleton dynamics. Mol Microbiol. 2015;95: 590–604.

152. Korotkov KV, Sandkvist M. Architecture, Function, and Substrates of the Type II Secretion System. EcoSal Plus. 2019;8. doi:10.1128/ecosalplus.ESP-0034-2018

153. Zielke RA, Simmons RS, Park BR, Nonogaki M, Emerson S, Sikora AE. The type II secretion pathway in Vibrio cholerae is characterized by growth phase-dependent

expression of exoprotein genes and is positively regulated by σE. Infect Immun. 2014;82: 2788–2801.

154. Bacterial Type III Protein Secretion Systems. Current Topics in Microbiology and Immunology. 2020. doi:10.1007/978-3-030-52123-3

155. Cornelis GR. The type III secretion injectisome. Nature Reviews Microbiology. 2006. pp. 811–825. doi:10.1038/nrmicro1526

156. Büttner D. Protein export according to schedule: architecture, assembly, and regulation of type III secretion systems from plant- and animal-pathogenic bacteria. Microbiol Mol Biol Rev. 2012;76: 262–310.

157. Galán JE, Wolf-Watz H. Protein delivery into eukaryotic cells by type III secretion machines. Nature. 2006;444: 567–573.

158. Preston GM, Bertrand N, Rainey PB. Type III secretion in plant growth-promoting Pseudomonas fluorescens SBW25. Mol Microbiol. 2001;41: 999–1014.

159. Backert S, Grohmann E. Type IV Secretion in Gram-Negative and Gram-Positive Bacteria. Springer; 2018.

160. Christian G-R, Bhatty M, Christie PJ. Mechanism and Function of Type IV Secretion During Infection of the Human Host. Virulence Mechanisms of Bacterial Pathogens. 2016. pp. 265–303. doi:10.1128/9781555819286.ch10

161. Fan E, Chauhan N, Dbrkg U, Leo JC, Linke D. Type V Secretion Systems in Bacteria. Microbiology spectrum. 2016;4. doi:10.1128/microbiolspec.VMBF-0009-2015

162. Mikula KM, Kolodziejczyk R, Goldman A. Yersinia infection tools-characterization of structure and function of adhesins. Front Cell Infect Microbiol. 2012;2: 169.

163. Russell AB, Peterson SB, Mougous JD. Type VI secretion system effectors: poisons with a purpose. Nat Rev Microbiol. 2014;12: 137–148.

164. Logan SL, Thomas J, Yan J, Baker RP, Shields DS, Xavier JB, et al. The type VI secretion system can modulate host intestinal mechanics to displace gut bacterial symbionts. Proc Natl Acad Sci U S A. 2018;115: E3779–E3787.

165. Bowman L, Palmer T. The Type VII Secretion System of. Annu Rev Microbiol. 2021;75: 471–494.

166. Ates LS, Houben ENG, Bitter W. Type VII Secretion: A Highly Versatile Secretion System. Virulence Mechanisms of Bacterial Pathogens. 2016. pp. 357–384. doi:10.1128/9781555819286.ch13

167. Wilson BA, Winkler ME, Ho BT. Bacterial Pathogenesis: A Molecular Approach, Fourth Edition. 2019. doi:10.1128/9781555819415

168. Brown S, Santa Maria JP Jr, Walker S. Wall teichoic acids of gram-positive bacteria. Annu Rev Microbiol. 2013;67: 313–336.

169. Sastalla I, Monack DM, Kubatzky KF. Bacterial Exotoxins: How Bacteria Fight the Immune System. Frontiers Media SA; 2016.

170. Casadevall A, Pirofski L-A. Virulence factors and their mechanisms of action: the view from a damage-response framework. J Water Health. 2009;7 Suppl 1: S2–S18.

171. Liu Z, Liu H, Vera AM, Bernardi RC, Tinnefeld P, Nash MA. High force catch bond mechanism of bacterial adhesion in the human gut. Nature Communications. 2020. doi:10.1038/s41467-020-18063-x

172. Bouckaert J. Breaking down the wall: mutation of the tyrosine gate of the universal Escherichia coli fimbrial adhesin FimH. 2017. doi:10.2210/pdb5fx3/pdb

173. Finlay BB, Falkow S. Common themes in microbial pathogenicity revisited. Microbiol Mol Biol Rev. 1997;61: 136–169.

174. Sauer MM, Jakob RP, Eras J, Baday S, Eriş D, Navarra G, et al. Catch-bond mechanism of the bacterial adhesin FimH. Nat Commun. 2016;7: 10738.

175. Huang Y, Wang Q-L, Cheng D-D, Xu W-T, Lu N-H. Adhesion and Invasion of Gastric Mucosa Epithelial Cells by. Front Cell Infect Microbiol. 2016;6: 159.

176. Ribet D, Cossart P. How bacterial pathogens colonize their hosts and invade deeper tissues. Microbes Infect. 2015;17: 173–183.

177. Kramer J, Özkaya Ö, Kümmerli R. Bacterial siderophores in community and host interactions. Nat Rev Microbiol. 2020;18: 152–163.

178. Schalk IJ, Guillon L. Pyoverdine biosynthesis and secretion inPseudomonas aeruginosa: implications for metal homeostasis. Environmental Microbiology. 2013. pp. 1661–1673. doi:10.1111/1462-2920.12013

179. Moon CD, Zhang X-X, Matthijs S, Schäfer M, Budzikiewicz H, Rainey PB. Genomic, genetic and structural analysis of pyoverdine-mediated iron acquisition in the plant growth-promoting bacterium Pseudomonas fluorescens SBW25. BMC Microbiol. 2008;8: 7.

180. Haas H, Eisendle M, Turgeon BG. Siderophores in fungal physiology and virulence. Annu Rev Phytopathol. 2008;46: 149–187.

181. Lamont IL, Beare PA, Ochsner U, Vasil AI, Vasil ML. Siderophore-mediated signaling regulates virulence factor production in Pseudomonasaeruginosa. Proc Natl Acad Sci U S A. 2002;99: 7072–7077.

182. Neilands JB. Siderophores: Structure and Function of Microbial Iron Transport Compounds. Journal of Biological Chemistry. 1995. pp. 26723–26726. doi:10.1074/jbc.270.45.26723

183. Djibaoui, Djibaoui D, Bensoltane A. Effect of iron and growth inhibitors on siderophores production by Pseudomonas fluorescens. African Journal of Biotechnology. 2005. pp. 697–702. doi:10.5897/ajb2005.000-3129

184. van Valen L. Theory in Abstracts. BioScience. 1973. pp. 626–626. doi:10.2307/1296773

185. Decaestecker E, Gaba S, Raeymaekers JAM, Stoks R, Van Kerckhoven L, Ebert D, et al. Host-parasite “Red Queen” dynamics archived in pond sediment. Nature. 2007;450: 870–873.

186. Brockhurst MA. Sex, Death, and the Red Queen. Science. 2011. pp. 166–167. doi:10.1126/science.1209420

187. Dieckmann U, Marrow P, Law R. Evolutionary cycling in predator-prey interactions: population dynamics and the red queen. Journal of Theoretical Biology. 1995. pp. 91–102. doi:10.1006/jtbi.1995.0179

188. Rainey PB, Bailey MJ. Physical and genetic map of the Pseudomonas fluorescens SBW25 chromosome. Mol Microbiol. 1996;19: 521–533.

189. Escobar-Páramo P, Gougat-Barbera C, Hochberg ME. Evolutionary dynamics of separate and combined exposure of Pseudomonas fluorescens SBW25 to antibiotics and bacteriophage. Evol Appl. 2012;5: 583–592.

190. Scanlan PD, Buckling A. Co-evolution with lytic phage selects for the mucoid phenotype of Pseudomonas fluorescens SBW25. ISME J. 2012;6: 1148–1158.

191. Ramsayer J, Kaltz O, Hochberg ME. Evolutionary rescue in populations of Pseudomonas fluorescens across an antibiotic gradient. Evol Appl. 2013;6: 608–616.

192. Scanlan PD, Hall AR, Blackshields G, Friman V-P, Davis MR Jr, Goldberg JB, et al. Coevolution with bacteriophages drives genome-wide host evolution and constrains the acquisition of abiotic-beneficial mutations. Mol Biol Evol. 2015;32: 1425–1435.

193. Hammerschmidt K, Rose CJ, Kerr B, Rainey PB. Life cycles, fitness decoupling and the evolution of multicellularity. Nature. 2014;515: 75–79.

194. Lenski RE. Experimental evolution and the dynamics of adaptation and genome evolution in microbial populations. ISME J. 2017;11: 2181–2194.

195. Garland T, Rose MR. Experimental Evolution: Concepts, Methods, and Applications of Selection Experiments. Univ of California Press; 2009.

196. Dettman JR, Rodrigue N, Melnyk AH, Wong A, Bailey SF, Kassen R. Evolutionary insight from whole-genome sequencing of experimentally evolved microbes. Molecular Ecology. 2012. pp. 2058–2077. doi:10.1111/j.1365-294x.2012.05484.x

197. Rainey PB, Travisano M. Adaptive radiation in a heterogeneous environment. Nature. 1998;394: 69–72.

198. Beaumont HJE, Gallie J, Kost C, Ferguson GC, Rainey PB. Experimental evolution of bet hedging. Nature. 2009;462: 90–93.

199. Pentz JT, Lind PA. Forecasting of phenotypic and genetic outcomes of experimental evolution in Pseudomonas protegens. PLoS Genet. 2021;17: e1009722.

200. Scanlan PD, Buckling A, Hall AR. Experimental evolution and bacterial resistance: (co)evolutionary costs and trade-offs as opportunities in phage therapy research. Bacteriophage. 2015;5: e1050153.

201. Spiers AJ, Bohannon J, Gehrig SM, Rainey PB. Biofilm formation at the air--liquid interface by the Pseudomonas fluorescens SBW25 wrinkly spreader requires an acetylated form of cellulose. Mol Microbiol. 2003;50: 15–27.

202. Nair RR, Vasse M, Wielgoss S, Sun L, Yu Y-TN, Velicer GJ. Bacterial predator-prey coevolution accelerates genome evolution and selects on virulence-associated prey defences. Nat Commun. 2019;10: 4301.

Chapter 2

Protozoan predation drives adaptive divergence in *Pseudomonas fluorescens* SBW25: *ecology meets experimental evolution.*

Farhad S. Golzar[1], Michael E. Miller[1], Gayle C. Ferguson[1], and Heather Lyn Hendrickson[2]
[1]School of Natural and Computational Science, Massey University, Auckland, New Zealand.
[2]School of Biological Sciences, University of Canterbury, Christchurch, New Zealand.

Abstract

Protozoan predators affect the structure of bacterial communities, but investigations into how predation influences bacterial evolution and antagonistic behaviours are scarce. We performed a 20-day predator-prey evolution experiment on solid media to investigate the adaptive traits that arise in bacterial prey under continuous protozoan predation. We chose *Pseudomonas fluorescens* SBW25 and a wild *Acanthamoeba sp.* isolate as a predator prey pair that ecologically overlap in nature. Predation by *Acanthamoeba* led to the evolution of previously described bacterial colony morphotypes like Wrinkly Spreaders but also novel morphologies we describe as Fried Egg and Wrinkly Fried Egg. These evolved morphotypes conferred grazing resistance and an increase in relative prey fitness. When subjected to these evolved prey, *Acanthamoeba* sp. increased encystment and reduced replication. An investigation of the mutations responsible for predation resistance revealed that the Wrinkly Spreader and Fried Egg morphotypes were the result of mutations in *wspF* and that Wrinkly Fried Egg was caused by a mutation altering the transcriptional regulator *amrZ*. We investigated the degree to which these mutations affect biofilm formation, capsulation and motility. RNA sequencing results of WS and WFE also revealed a significant increase in the number of genes up or down regulated while interacting with

Acanthamoeba sp. The *amrZ* mutant withstands predation but this variant produces low levels of cellulose and limited swarming motility and increases amyloid fibril production. Our findings suggest that protozoan predation can profoundly influence the course of genetic and phenotypic evolution in a short period of time.

Introduction

The microbial world is replete with examples of competition and predation. These microbial melees impact the traits that bacteria evolve. Ultimately, the bacterial phenotypes that are successful in these contests affect agriculture, the environment and human health [1–3]. The predators of the microbial world include the free-living amoebae (FLA), single-celled eukaryotic protozoan predators that consume bacteria by phagocytosis and are ubiquitous in diverse environments [4]. Protozoan predation asserts a strong selective pressure on bacteria, reportedly eliminating 60% of bacteria in soils [5–8]. Despite their effects on decreasing bacterial abundance, FLAs are often neglected in considerations of microbial ecology [9,10]. They are, however, powerful agents involved in decomposition, recycling nutrients, and energy in ecosystems [1–3,11–13].

FLA predation is a potent selective force driving bacterial evolution [14]. Failure to resist predation results in whole-cell ingestion and digestion of bacterial prey [15]. Amoebae are however inefficient and careless predators, in the sense that they do not appear to consume all the bacteria they are provided [16,17]. Bacteria can escape protozoan predation by adopting anti-predatory behaviours such as cell elongation, secondary metabolite or toxin secretion, and mucoid phenotypes [14,18–24].

Investigating how predation drives bacterial diversity is fundamental to understanding how microorganisms evolve in the environment.

FLAs have been proposed to be a major driving force in the evolution of traits such as biofilm formation, intracellular growth and encapsulation in bacteria [25–28]. These complex sets of anti-predatory strategies benefit bacteria in the face of protozoan predation and help to maintain stable communities [18]. Biofilm formation is a common adaptation in prokaryotes contributing to survival in many different environments [29,30]. Growth in a multi-cell extracellular matrix affords protection from predatory phagocytosis whilst allowing bacteria to colonise a range of otherwise hostile environments [31,32], attaching to surfaces, and invading new niches [32–34]. In the presence of the amoeboid predator *Acanthamoeba castellanii*, *Pseudomonas aeruginosa* cells have been demonstrated to form protective biofilms, making the bacteria non-edible [28,35,36]. Biofilm formation can also be beneficial through the exclusion of competing organisms [37], and can increase resistance to harsh environmental conditions like antibacterial agents [38], metal toxicity, acid, and salinity [39,40].

In *P. fluorescens* SBW25 biofilm formation is a well-studied adaptation to oxygen limitation induced when growing at the air-liquid (AL) interface in standing liquid cultures [41,42]. In this system, mutations that induce the constitutive expression of extracellular polysaccharides are well documented (*wsp* mutations) [42,43]. Wrinkly Spreader (WS) phenotypes are biofilm forming mutants that arise from the ancestral Smooth (WT) colony morphotype, allowing access to the oxygen rich surface of the

liquid culture. Fuzzy Spreaders (*fuzY* mutations) are early colonisers of the surface that ultimately occupy the bottom of the microcosm [44–48].

Amoeboid predation has also been hypothesised to select for bacterial virulence as early as 1988 [49]. This hypothesis, sometimes called the "coincidental evolution hypothesis" suggests that adaptations to one environment, like protozoan predation, could result in virulence traits expressed in a similar environment, like a metazoan host. While tantalising correspondences have been observed between virulence and predation resistance, a direct test of this idea has not been attempted [14]. These ideas have recently experienced renewed interest and experimental attention [29,49,50]. Many pathogens have traits that deter predation. For example, *Klebsiella pneumoniae* cells are capable of producing lipopolysaccharide (LPS) and outer membrane proteases that limit amoeboid predation by *Dictyostelium discoideum* [51].

Whilst there is abundant literature describing a range of bacterial traits that may have evolved as anti-predatory devices, there is little or no experimental work that observes the traits that bacteria acquire in response to the pressure to survive FLA predation. In order to investigate the effect of continuous FLA predation on bacteria we used an experimental evolution approach in which populations of *P. fluorescens* SBW25 were continuously preyed upon amoeba, *Acanthamoeba* sp. on solid surfaces. We hypothesised that traits associated with virulence would arise in response to our protozoan predation regime.

Results

Experimental evolution of bacteria under amoeboid predation

To test the degree to which amoeboid predation contributes to the adaptive evolution of bacterial virulence, we established a coevolution experiment on solid media. Six lineages of GFP labelled strain of WT *P. fluorescens* SBW25, a non-pathogenic plant-associated bacterium, were established. Three lineages were maintained without predators as a media adaptation control with bacterial prey only (PO), and three of which were subjected to continuous predation by common soil-based amoeboid protozoan predator *Acanthamoeba* sp. (P) (Fig. 2.1 A and B). The *Acanthamoeba* sp. were added to a lawn of bacteria on a filter paper and the feeding front of active amoebae moving across the plate from the filter paper was visible as a loss of bacterial lawn as time passed (Fig. 2.1 C), *Acanthamoeba* and GFP labelled *P. fluorescens* SBW25 could be viewed by fluorescent, phase contrast microscopy (Fig. 2.1 C, inset).

As the coevolution progressed, viable cell counts of bacteria and amoebae were estimated by serial dilution and plating for CFU and PFU as appropriate, at each transfer (Fig. 2.1 C). The average number of the bacterial population in the PO lines has dramatically increased and reached its maximum density over 20 days of evolution (1×10^{11}, +/- 5×10^{2}) (Fig. 2.1 D). There was roughly a 100-fold reduction in the number of the bacteria observed on the predation plates, this remained relatively stable, and predation did not lead to extinction events. Similarly, the number of the amoebae cells in each prey-predator line was stable over 20-days of coevolution ranging between 2×10^{6} to 8×10^{6} over time (Fig. 2.1 D).

At each transfer, CFU plates were also inspected for changes in colony morphology that would indicate genetic changes in response to propagation on solid media or

predation pressure. The prey only (PO) plates retained a WT or smooth colony morphology throughout the 20-day experiment (Fig. 2.1 E). The bacterial colonies that came from the P or predation- positive plates, maintained WT morphologies for three transfers and it was only upon inspection of the CFU from the fourth transfer that novel morphologies were observed. These novel colony morphologies were associated with the appearance of microcolonies in the lawns of *P. fluorescens* SBW25 cells undergoing predation.

In order to study the nature of these colony variants, we selected four novel colonies that had shown distinct changes in their morphologies and two Like-WT (LWT) representatives from the three predation lines to represent the dominant types observed at the end of the evolution under predation (Day 20). These representative colonies were named: Wrinkly Spreader 1 and 2 (WS1, WS2), Fried Egg (FE), Wrinkly Fried Egg (WFE) and Like Wild Type (LWT) (Fig. 2.1 F). We named WS1 and WS2 'Wrinkly Spreaders' because of the similarity between these colony morphologies and those found in the AL adaptive radiation experiments previously described in *P. fluorescens* SBW25 [41]. WS1 is a classic Wrinkly Spreader colony morphology with undulate ridges throughout. WS2 is similar in appearance to WS1 but with an opaque central region that appears more smooth. FE colonies are primarily a Smooth or WT colony with a disrupted or rough opaque core at the colony centre. WFE is similar in appearance to FE but with a more rough appearance overall. We hypothesised that these colony morphology changes represented novel predator adaptations which might have increased virulence. These variants were single colony isolated, confirmed to be GFP labelled *P. fluorescens* SBW25 cells and preserved at -80°C for further analysis.

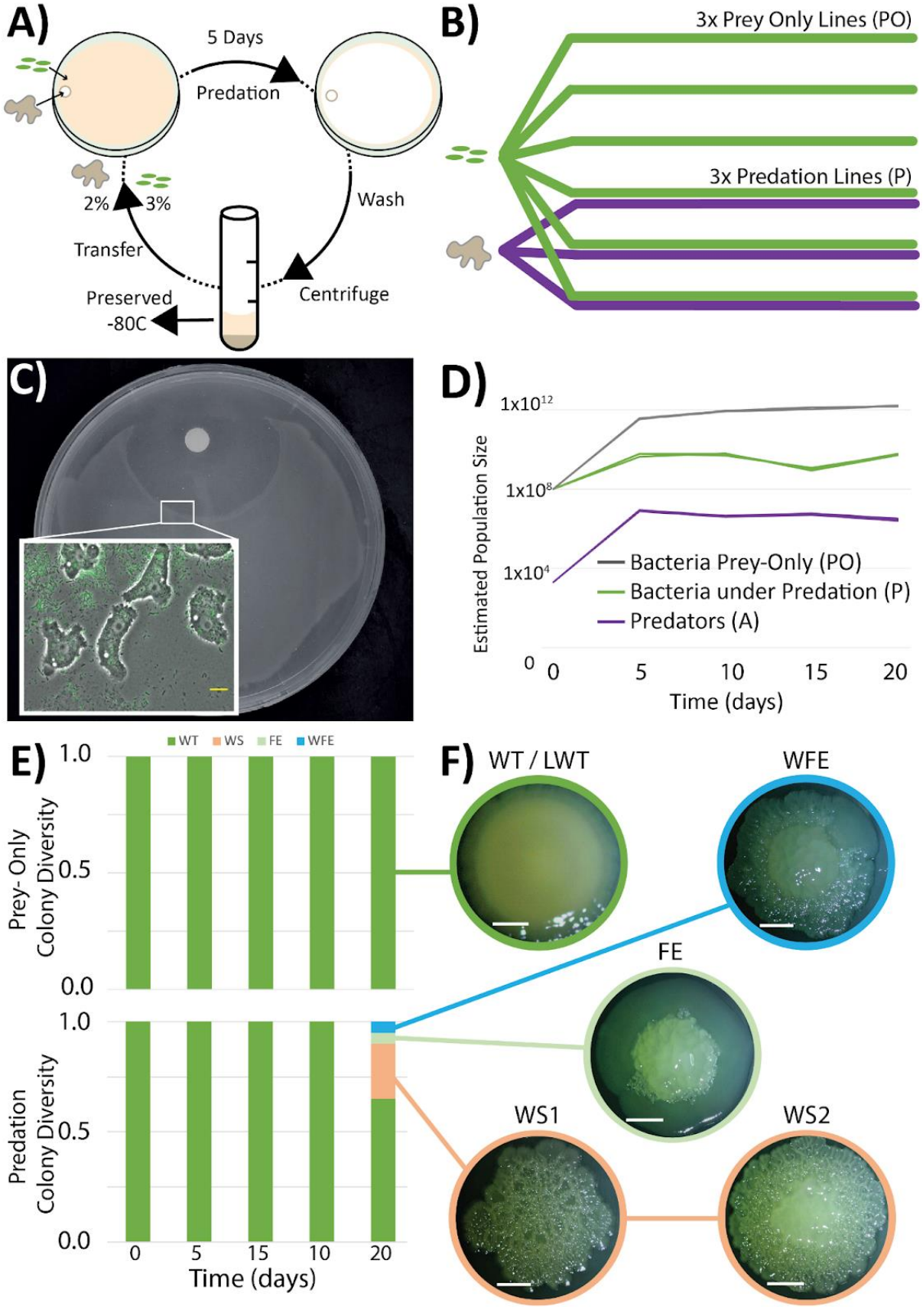
A)
5 Days
Predation
Wash
Centrifuge
Transfer
2%
3%
Preserved
-80C
B)
3x Prey Only Lines (PO)
3x Predation Lines (P)
C)
D)
Estimated Population Size
1x10^12
1x10^8
1x10^4
0
Bacteria Prey-Only (PO)
Bacteria under Predation (P)
Predators (A)
0
5
10
15
20
Time (days)
E)
WT
WS
FE
WFE
Prey- Only Colony Diversity
Predation Colony Diversity
1.0
0.5
0.0
0
5
15
10
20
Time (days)
F)
WT / LWT
WFE
FE
WS1
WS2

Figure 2. 1. Experimental co-evolution of *P. fluorescens* SBW25 and *Acanthamoeba sp.* drives bacterial diversification. A) Diagram of the experimental co-evolution protocol on solid media. B) A diagram showing the number of the prey-predator and control lines. C) A representative predation-evolution plate. The filter paper, containing ~10^3 *Acanthamoeba* cells can be seen at the top and the progress of the feeding front of amoeba consuming the bacterial lawn can be seen as a decrease in the thickness of the bacterial lawn (left). The feeding front contains active amoeba and the GFP labelled *P. fluorescens* SBW25, visible under fluorescent microscopy (scale bar, 100 µm). D) Estimates of the population size at each transfer for each organism in the predator-associated evolution and the prey-only control over 20-days of evolution. E) Divergence of the bacterial colony morphologies occurs in the presence of predators but not in their absence and the average frequency of the colonies in three evolved populations (scale bar, 10 mm). F) Colony morphologies pictured are representative of Wrinkly Spreader (WS), Fried Egg (FE), Wrinkly Fried Egg (WFE) and Like Wild Type (LWT). Note, a single representative Smooth, or “like WT" bacterial colony is shown.

Growth and survival of *Acanthamoeba* sp. on predation adapted bacteria

We observed the divergence of *P. fluorescens* SBW25 colony morphologies under amoeboid predation and hypothesised that these changes are adaptive or possibly increased bacterial virulence. In order to address these questions, we wanted to establish the degree to which *Acanthamoeba* were able to grow and subsist on the novel morphotypes isolated after 20 days of predation. We therefore measured ancestral *Acanthamoeba sp.* plaque formation on the six evolved bacterial isolates of interest and a WT control in a plaque test assay (Fig. 2.2 A).

We did not observe a significant difference in *Acanthamoeba* plaque formation on either of the two evolved LWT isolates compared to the *P. fluorescens* SBW25 WT (LWT1, LWT2). However, we did not observe obvious plaque formation when *Acanthamoeba* were plated on lawns of WS1, WS2, FE or WFE colony morphology mutants (Fig. 2.2 B). Despite the absence of prominent plaques on these isolates, we noted some deformation of the surface that suggested cryptic and possibly reduced predation and growth of the *Acanthamoeba sp.* This suggested either that the evolved

P. fluorescens SBW25 are directly inhibiting robust growth of the predator, or that the *Acanthamoeba* are unable to efficiently consume the mutant cells in quantities that produce robust observable plaques, or that some plaques were being formed underneath a layer of extracellular material produced by the bacteria.

In order to determine the degree to which predation-evolved isolates limit the strong growth of the *Acanthamoeba* cells we performed the plaque test assay once again, washing at T=0 and T=4 days in order to estimate the average number of amoebal generations on ancestral or evolved isolates. We found that in the presence of WT or LWT (evolved) bacteria, the *Acanthamoeba sp.* were able to divide approximately 19 times. However, when *Acanthamoeba* cells were grown in the same conditions on the evolved *P. fluorescens* SBW25 isolates, they achieved far fewer divisions. *Acanthamoeba* in the presence of lawns of WS1, WS2, FE, and WFE were only able to divide 11, 14, 10.3 and 9 times, respectively (Fig. 2.2 C). These results suggest that these mutants have a negative influence on replication and division of *Acanthamoeba* cells leading to the slow growth of protozoan predators.

Reduced division in the presence of evolved prey bacteria could be due to 1) increased cell death, 2) reduced access to bacterial prey as a food source or 3) reduced metabolic activity in an unfavourable environment (increased encystment). In order to evaluate the evidence for these possibilities, we subjected *Acanthamoeba sp.* to each of the evolved isolates of interest for four days, and measured life cycle stages and viability by flow cytometry (Supplementary Fig. 2.1), using propidium iodide staining to enumerate dead amoeboid cells.

We observed that up to 80% of the *Acanthamoeba* cells are in the active vegetative form when growing on WT and LWT isolates and less than 10% of their population was encysted (Two sample T test, P< 0.02 and P< 0.06). In contrast, more than 40% of the *Acanthamoeba* population was encysted when the prey was WS1, WS2, FE or WFE (Two sample T test, P< 0.002, P< 0.006, P< 0.00006, P< 0.00003) (Fig. 2.2 D). Further, amoebae cells have shown death rates of up to 11%, 9% and 10% in the presence of lawns of WT and LWT, respectively (Two sample T test, P< 0.01, P< 0.1); 3% death when exposed to the lawns of WS1, WS2 and FE (Two sample T test, P< 0.0001, P< 0.00001, P< 0.0001); and 1% death when growing with the WFE isolate (P< 0.000005) (Fig. 2.2 D).

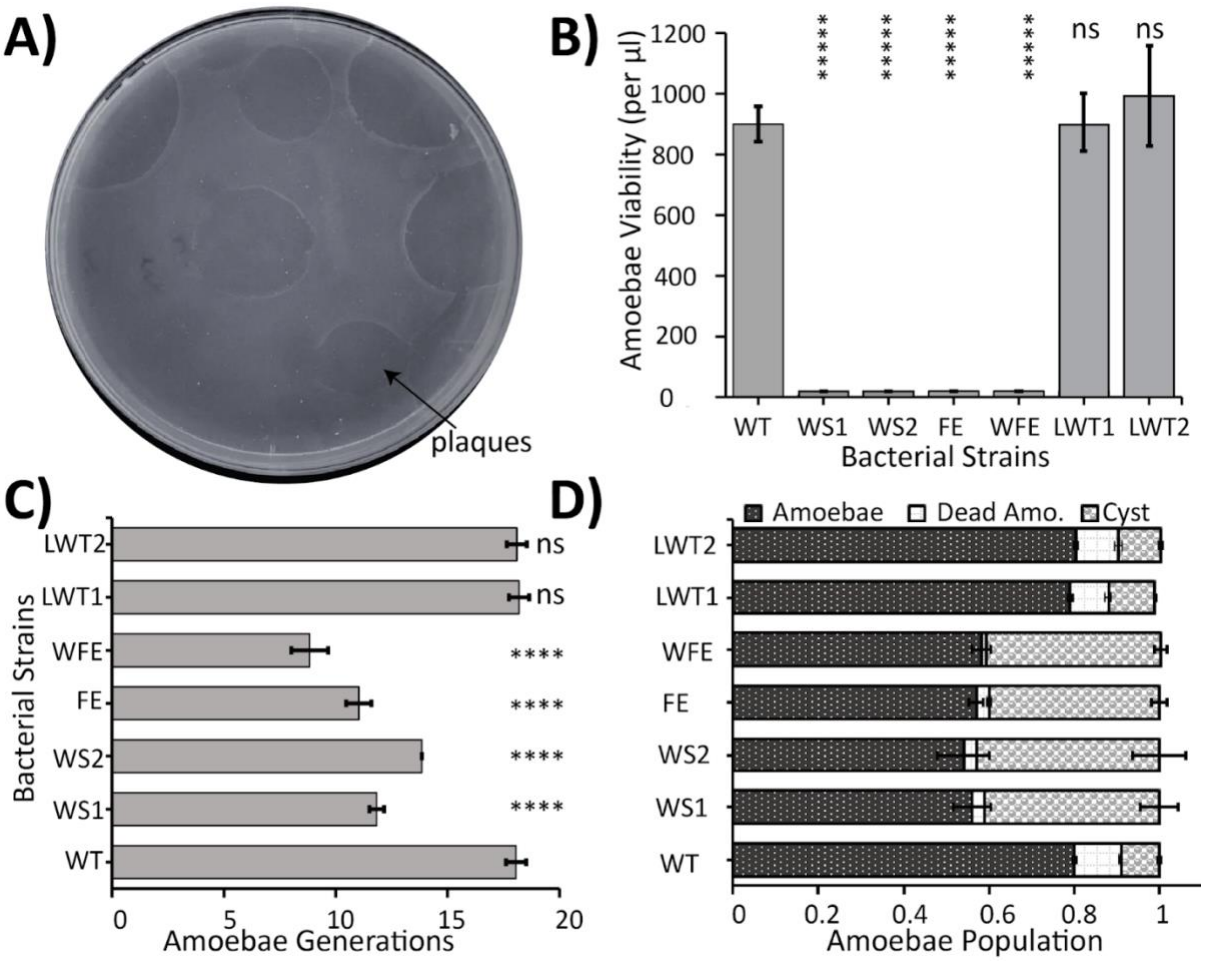

Figure 2. 2**.** Assays conducted to test the growth and survival of ancestral amoebae obtained on different predator-evolved bacterial isolates. A) *Acanthamoeba* cells form plaques on a bacterial lawn (each plaque indicative of one amoebae cell) when a single amoeba grows, divides and consumes a large number of bacterial cells over time. B) Estimates of the numbers of *amoeboid* cells when growing on each bacterial isolate based on plaque counts (n=6, *****P<0.00001, Two sample T tests). C) Average estimation of *Acanthamoeba* generation time over four days on various evolved bacteria (n=6, ****P≤ 0.00007, Two sample T tests). D) Measuring the approximate number of amoebae after they were confronted with each of the evolved mutants over four days (n=4). Error bars indicate standard deviation and stars denote statistical significance.

Predation resistance of novel pseudomonas isolates

The amoebae viability results suggest that an increase in bacterial virulence has not occurred; to the contrary, more non-viable amoebae are observed in the presence of the ancestral WT and LWT isolates than the morphologically distinct isolates of interest. When plated with a distinct morphotype as the sole food source, the amoebae appear to have increased the frequency with which they encyst, marking a transition to a dormant state [52,53]. This raises the possibility that the *P. fluorescens* SBW25 colony morphotypes under investigation have adopted a strategy that may make them more predation resistant. In order to establish the degree of evolved resistance to grazing by *Acanthamoeba* sp., we measured the speed of predation in line-test assays with the evolved isolates and a WT control strain as described previously [54] (Fig. 2.3 A). Line tests allow us to measure the predation rate by measuring the speed at which amoebae from a filter paper consume pre-grown lines of bacteria on a plate.

Predation rates on evolved morphotypes LWT were very similar to the true WT (Fig. 2.3 B grey and black, respectively). Predation by *Acanthamoeba* was resisted in this test by the WS1, FE and WFE morphotypes. We noted a difference between WS1 and WS2: the latter was consumed early in the line test assay and then the predator appeared to have stopped consuming these lines (Fig. 2.3 B). Line tests allow us to

calculate the predation rates (Fig. 2.3 C) and by accounting for the bacterial densities we can calculate relative prey fitness for the morphotypes tested. We note that the WT and LWT variants tested had low relative prey fitness whereas all the evolved morphologies had substantially improved prey fitness in the line test assay (Fig. 2.3 C). Together these results demonstrate that the WS1, WS2, FE and WFE morphotypes have evolved adaptations that improve their relative prey fitness by providing grazing resistance in the presence of an amoeboid predator.

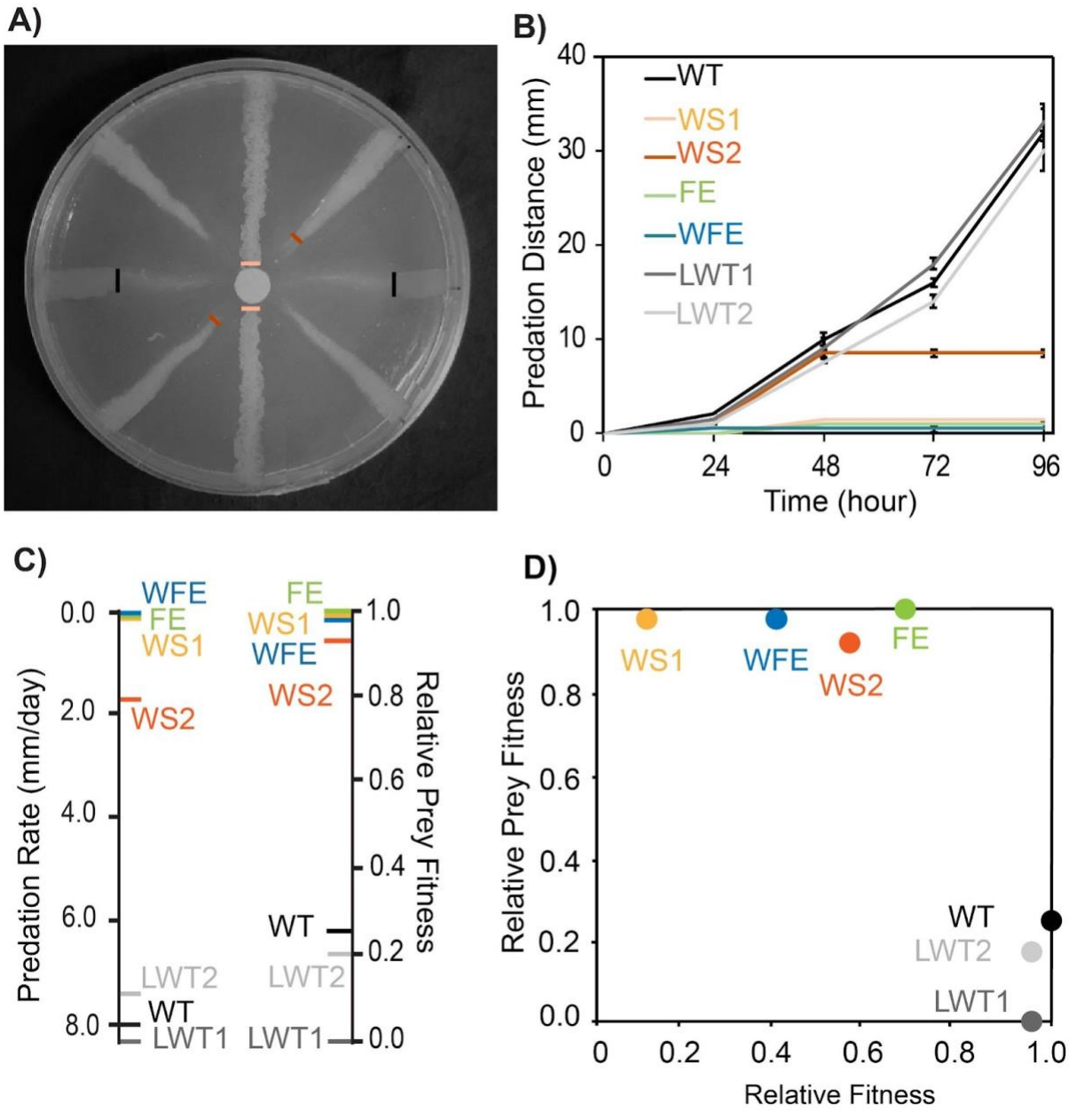

Figure 2. 3**.** Predation of ancestral *Acanthamoeba sp.* against evolved *P. fluorescens* SBW25 populations. A) A representative plate showing a line test assay after 72 hours. B) Line test disappearance produced by *Acanthamoeba* predation. Error bars indicate standard deviation (N=8). C) Rate of *Acanthamoeba* predation on the colony morphologies of interest as calculated in line tests and relative fitness of prey. D) Bacterial fitness on agar surface with and without ancestral predators. Bacteria were grown in the presence and absence of predator *Acanthamoeba* for four days on PM supplemented media.

Grazing resistance incurs a fitness cost

In order to understand the larger consequences of evolved grazing resistance we estimated bacterial fitness in the absence of the protozoan predators on agar plates. The ancestral WT strain was set to a fitness of 1 and LWT isolates 1 & 2 had a relative fitness of ~0.98. Colony morphotypes have adaptive predator resistance (WS1, WS2, FE and WFE) experience trade-offs in fitness in the absence of predators (Fig. 2.3 D). WS1 mutant replicated and grew with a low relative fitness of ~ 0.15. The three of the evolved mutants however gained a higher relative fitness (~ 0.4 - 0.67) than the WS1, their reproduction rate was lower than WT and LWT on plates over 4 days (Fig. 2.3 D). This suggests that evolved predation resistance imposes a fitness cost in this environment in the absence of predators.

Sequencing results

The colony morphologies that we observed after 20 days of evolution under protozoan predation are reminiscent of the WS mutations observed at the AL interface in *P. fluorescens* SBW25. In order to determine how similar, the underlying mutations might be, we subjected six evolved isolates from the prey-predator lines (four with colony morphology changes and two smooth colonies) and three smooth isolates from the PO (non-predation) plates to shotgun DNA sequencing.

Mutations in *wspF* are frequently observed in studies of *P. fluorescens* SBW25 during adaptive radiation at AL interfaces and are consistent with the “wrinkly” colony morphology observed (Fig. 2.4 A, Supplementary Table 1) [55] . The mutations in isolates WS1 and WS2 were in the CheY receiver domain of WspF [43]. The WS2 mutation was immediately adjacent to the phosphorylation domain within this receiver domain. The mutation in the WS2 isolate overlapped with previously identified *wspF* mutations that had arisen as constitutive cellulose producers in the AL interface experiments due to interruption of the receiver domain of WspF (Fig. 2.4, Table 2.1 & Supplementary Table 1) [56,57].

Table 2. 1. The locations and details of mutations observed in this study by whole-genome sequencing.

Isolate	**Gene name**	**PFLU**	**ORF Nuc. Change**	**ORF AA Change**	**Domain**	**Morph**
SBW25	_	_	_	_	_	Smooth
WS1	*wspF*	1224	∆231-236	∆VIV 76-78	CheY phosphorylation	Wrinkly Spreader
WS2 (x2)	*wspF*	1224	+166-180	+LMDLI 56-60	CheY phosphorylation	Wrinkly Spreader
FE	*wspF*	1224	T815C	L272P	CheB-type methylesterase	Fried Egg
WFE (x4)	*amrZ* (*algZ*)	4744	C97G	A33P	DNA binding	Wrinkly Fried Egg
LWT1	*LysR*	3329-30	∆TGGGCCACC	_	NA	Like Wild Type
LWT2 (x4)	_	_	_	_	_	Smooth
Prey-Only (x3)	_	_	_	_	_	Smooth

The FE isolate was also found to have acquired a mutation in the *wspF* gene, a single nucleotide change affecting the methyltransferase region of the CheB-type

methylesterase domain (Table 2.1, Fig. 2.4). This mutation is within 2 AA of a previously detected mutation at 274 discovered in the AL interface experiment (Supplementary Table 1) to lead to a robust WS morphology and constitutive expression of cellulose [43].

WFE had acquired mutations in AmrZ. The WFE mutant isolates included a single nucleotide change in the *amrZ* ORF (alginate and motility regulator). The AmrZ DNA binding protein has been implicated as a negative regulator of the Wsp operon [58,59], a positive regulator of algD (alginate synthesis) and a negative regulator of flagellum synthesis in *P. fluorescens* (Table 2.1, Fig. 2.4 D) [58]. To determine the degree to which the *amrZ* mutation might be disrupting function, we aligned the AA sequence of *amrZ* from *P. fluorescens* SBW25 and five other bacterial species [60] (Fig. 2.4 E). The AA identity at position 33 in *amrZ* is a highly conserved residue that lies outside of the dimerization zone. This alignment suggests that the mutation will cause some loss of function.

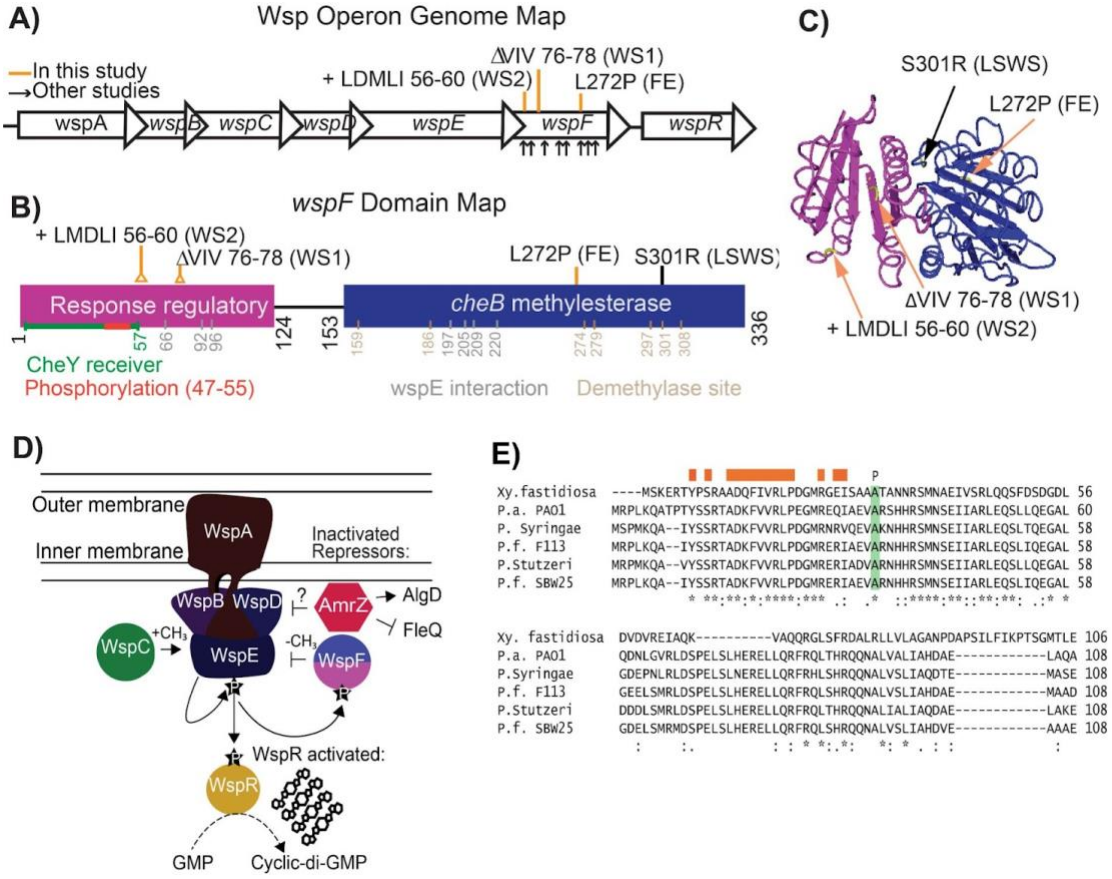

Figure 2. 4. Amoeboid predation resistance can be conferred by biofilm formation in *P. fluorescens* SBW25. A) The *wsp* operon in *P. fluorescens* SBW25, the *wspF* mutations found in this study (orange lines) resulting in Wrinkly Spreader phenotypes and those from AL interface studies (black arrows). B) The *wspF* domain map in *P. fluorescens* SBW25; predicted sites and the mutations identified in this study are shown above the domain map plus the LSWS positive control. C) WspF protein structure in SBW25 adopted from *Salmonella Typhimurium* (PDP ID; 1A2O). The protein consists of two domains: the CheB-type methylesterase domain (blue) and a response regulator-like *cheY* receiver domain in pink. Predicted mutational targets from this study and LSWS are highlighted in yellow and their names are shown (orange arrows). D) A model describing mutations that conferred resistance to amoeboid predation in *P. fluorescens* SBW25 during a short-term co-evolution experiment. FE mutation is in the methyltransferase domain and the WS mutations are both in the CheY domain. E) Amino acid alignment of AmrZ homologs in *P. fluorescens* SBW25 and other bacterial species. The orange box shows the dimerization domain of AmrZ and a mutation resulting in the WFE phenotype is shown in green.

Swarming and capsule formation assays

AmrZ is known to be a negative regulator for flagellum biosynthesis in some *Pseudomonads* [60]. To determine whether the AmrZ mutation affects motility we carried out a swarming test assay, comparing it to WT and ΔFleQ as a negative control

[61]. The WFE mutant AmrZ (A33P) showed a swarming defect compared to the WT *P. fluorescens* SBW25 that appeared to be mediated by obvious biofilm formation on the surface of the swarming plate (Fig. 2.5). The WFE mutant did not demonstrate a greater swarming distance than the ΔFleQ negative control in the first 21 hours. However, the swarming ability of the WFE mutant appeared to improve after the initial biofilm formation stage, when more cells appeared to breach the surface.

Capsule formation is a common virulence trait that has been implicated in parasite resistance in *P. fluorescens* SBW25 [62]. We therefore tested all isolates for capsule production by India ink staining and all were negative (Supplementary Fig. 2). The LWT isolate, despite having acquired a 12-bp deletion in a regulatory region between LysE family translocator *lysR* and transcriptional regulator *gcvA*, showed no change in either colony morphology or predation resistance; thus, the deletion is probably neutral in this context (Table 2.1).

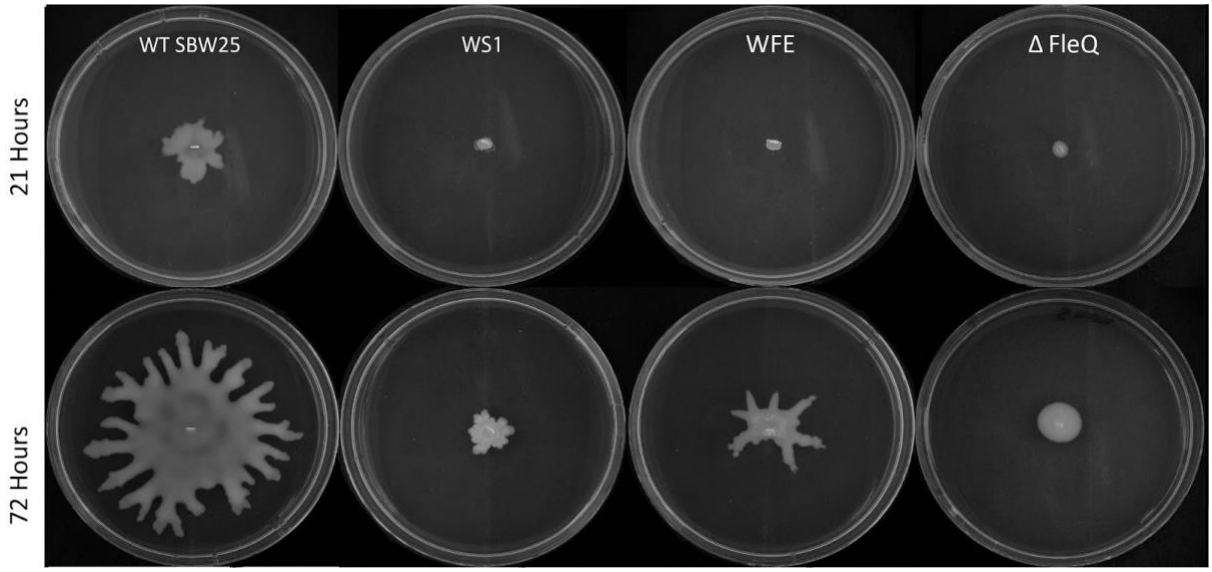

Figure 2. 5**.** Representative swarming images of the WT, WS1, WFE and FleQ mutants after 21 and 72 hours of growth on M9 plates.

Mat strength and cellulose expression

Three out of the four colony morphology mutants that we chose to focus on are mutations that are similar but not identical to those observed in the classic A-L interface experiments [44]. We therefore examined cellulose production on solid surfaces (Fig. 2.6 A, B and C) and adopted the glass bead strength test to measure the strength of biofilms formed (Fig. 2.5 D) [55]. We included the *P. fluorescens* SBW25 Large Spreading Wrinkly Spreader (LSWS) mutant as a positive control, as this mutant forms rapid and robust biofilms at the AL interface [43]. We initiated KB AL interfaces in standard microcosms from the colony morphology mutants of interest (shown) [44].

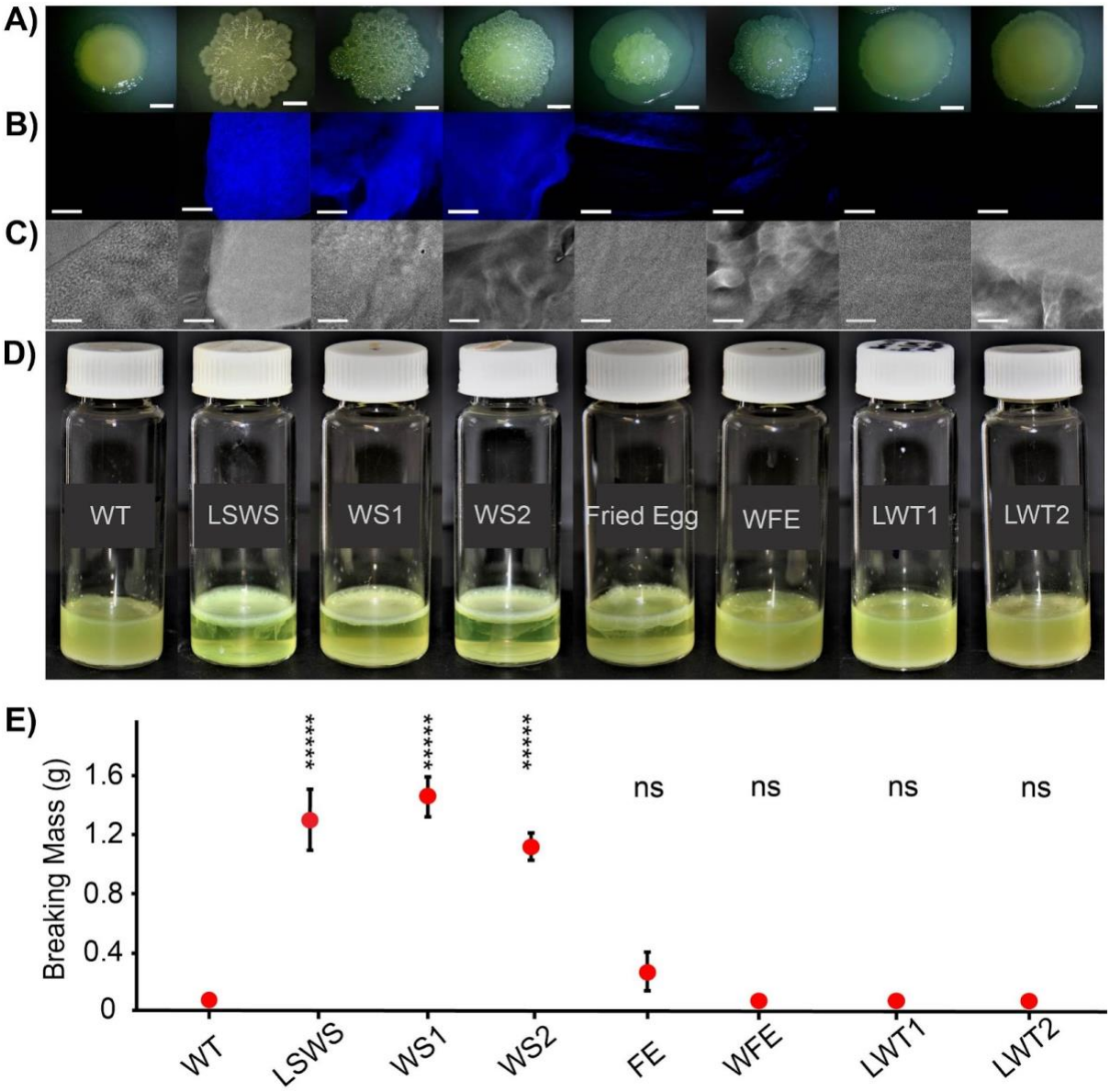

Figure 2. 6. Bacteria evolved under predation develop biofilm morphologies that are comparable to adaptive divergence phenotypes. A) Colony morphologies on LBA (Scale size: 10 mm). B) Visualisation of cellulose production grown on KB agar with a combination of calcofluor staining and microscopy. Scale bar: 30µm. C) Phase contrast image of colony segments shown in figure B. D) Microcosms after three days of growth in KB. E) Graph showing the summed mass of the beads that were added before the biofilm mat broke for each mutant type of interest (N=4, *****P<=0.0005, P values of over 0.05 were deemed insignificant (NS). All P values were pairwise T tests to WT. Error bars indicate standard deviation and stars denote statistical significance.

Within 24 hours, the positive control and four of our mutants of interest occupied the AL interface. As expected, LWT1, LWT2 and *P. fluorescens* SBW25 WT did not readily

form biofilms over this time period. The strength of mats formed by WS1 and WS2 (1.3 g +/- 0.18) were similar in strength to the LSWS (1.1 g +/- 0.4). These mutants produced significantly stronger mats than the WT (Fig. 2.6D & E). The FE mutant and WFE mutants were not as successful at colonising the AL interface and the mats produced were significantly less robust (0.15 g +/- 0.15), suggesting that these morphotypes are not robust biofilm producers. Calcofluor white staining confirmed the AL interface findings [63]. WS1 and WS2 each produced abundant extracellular cellulose whilst FE and WFE showed much less extracellular cellulose production (Fig. 2.6 B).

Differential gene expression in bacteria undergoing predation

Differentially expressed gene (DEG) profiles were made for two predator-evolved strains WS1 and WFE while predated by ancestral *Acanthamoeba*. In each case, WT *P. fluorescens* SBW25 was used as a baseline and significant differential expression was considered for genes with $\log_2$ FC ≥ 2, *P*-value ≤ 0.05 between conditions. For the WS condition, a total of 881 DEGs were identified, of which 424 were upregulated and 457 were downregulated. In the WFE condition, a total of 908 DEGs were identified, of which 475 were upregulated and 434 were downregulated. Among all DEGs, 335 upregulated and 313 downregulated genes were shared between the WS1 and WFE conditions. A heatmap of the top 100 most differentially expressed genes in the evolved strains illustrates the similarities and differences between the two evolved strains of interest (Fig. 2.7).

Differential gene expression in *Acanthamoeba* sp.

DEG profiles were made for ancestral *Acanthamoeba sp.* while predating upon WS1 AND WFE strains. In each case, ancestral *Acanthamoeba* with WT *Pseudomonas fluorescens* SBW25 was used as the baseline and significant differential expression was considered for genes with $\log_2$ FC ≥ 2, *P*-value ≤ 0.05 between conditions. Within the predator + WS1 condition, 408 DEGs were identified, of which 379 were upregulated and 29 were downregulated. Within the predator + WFE condition, 682 DEGs were identified, of which 513 were upregulated and 170 were downregulated (Fig. 2.8). A Venn diagram of DEGs shows 314 upregulated and 27downregulated DEGs are shared between the two conditions.

Gene Ontology (GO) Term Enrichment

Gene ontology terms associated with DEGs were trimmed for redundancy using REVIGO [64]. DEGs for each condition were then categorised by their GO category (Molecular Function; MF, Biological Process; BP, or Cellular Component; CC), subdivided by direction of regulation, and counted according to their InterProScan GO term (Supplementary Figs 3 to 5). To identify enriched GO terms within DEGs, DEG counts were compared to the counts of GO terms in the entire genome using a one-tailed Fisher's exact test. Results show that no GO terms were enriched for any cellular component DEGs. Within upregulated MF terms, WS1 and WFE had three and two enriched terms, respectively. WS1 enriched upregulated MF terms included 'levansucrase activity', 'oxidoreductase activity', and 'single-stranded RNA binding'. WFE enriched upregulated MF terms included 'levansucrase activity' and 'phosphoenolpyruvate carboxykinase (ATP) activity'. WS1 and WFE both had the same three enriched BP terms within upregulated DEGs, including 'protein folding',

‘trehalose catabolic process’, and ‘UTP biosynthetic process’. One enrichment was found within the downregulated DEGs for BP in WS1 – ‘L-arabinose transmembrane transport’. WS1 also had two enriched DEGs within downregulated MF terms – ‘chloromuconate cycloisomerase activity’ and ‘methylmalonate-semialdehyde dehydrogenase (acylating) activity’. One MF term was enriched for WFE in downregulated DEGs – ‘L-arabinose-importing ATPase activity’.

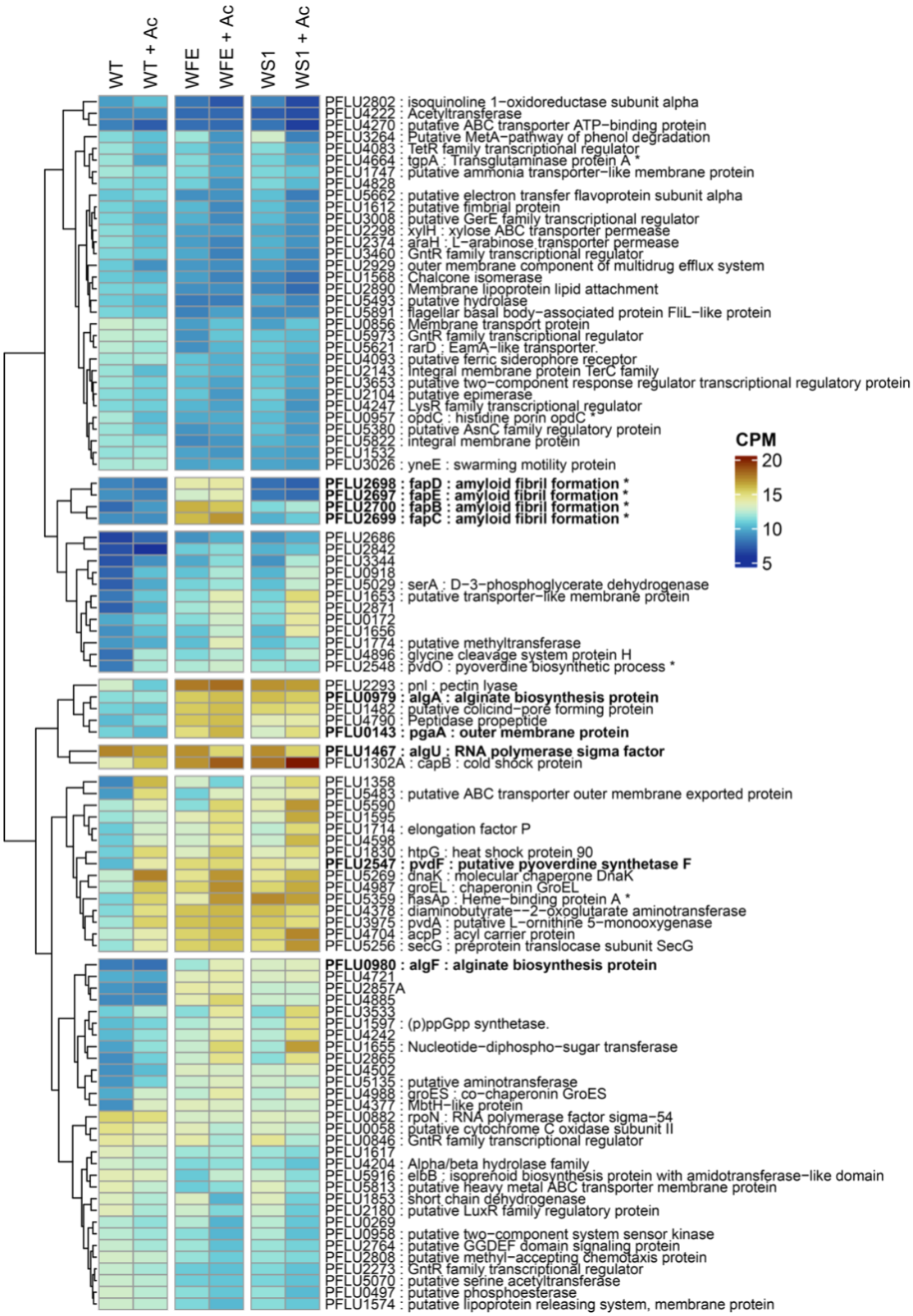

Figure 2. 7**.** Heatmap of the top differentially expressed genes among evolved strains WS1 and WFE when interacting with the ancestral predator (WS1 + predator, WFE + predator). All fold change calculations are made against SBW25 (WT) grown on solid media, without amoeba. CPM (counts per million) is a raw count of the number of reads mapped to a gene, normalised for library size (number of

total reads in a sample) and log transformed. Each row on the plot (genes) has at least one comparison ≥ 2 log_2FC (and P-value < 0.05) compared to the WT.

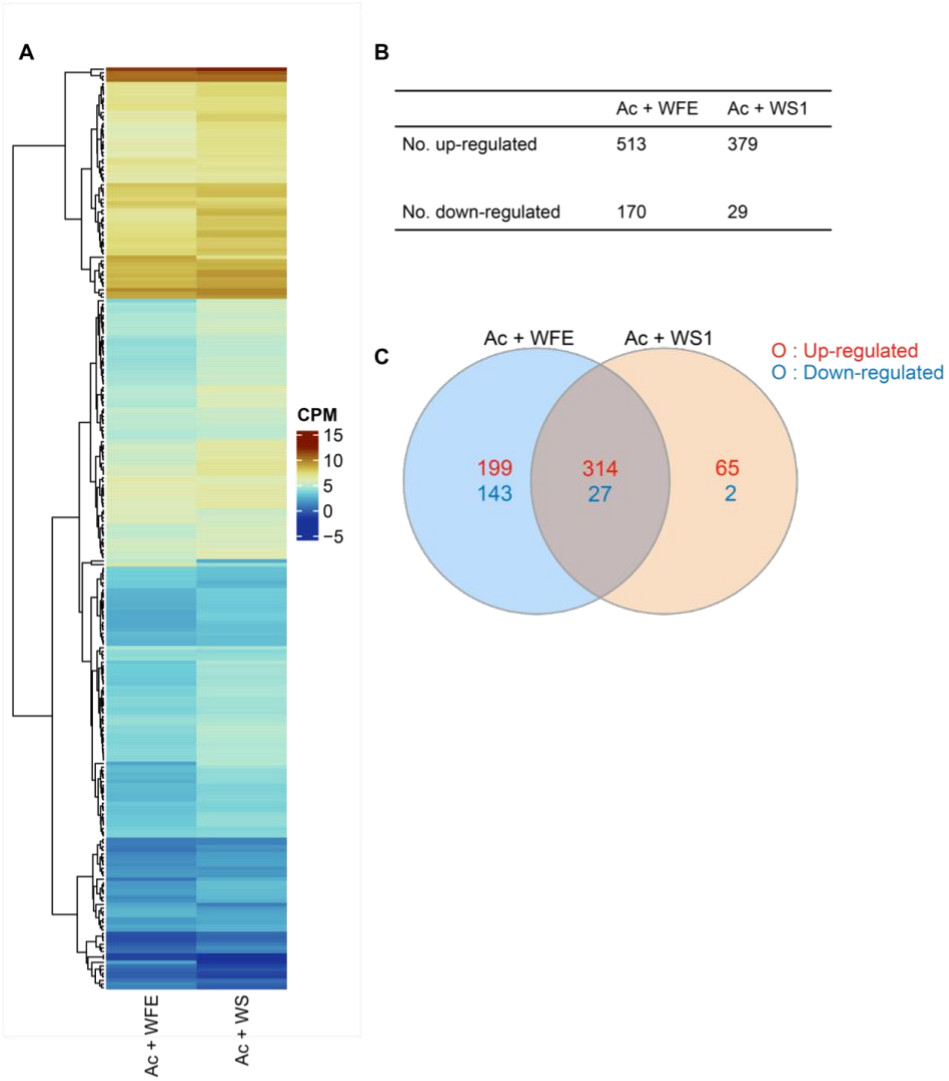

Figure 2. 8. Overview of significant changes in gene expression of *Acanthamoeba sp.* when predating upon evolved WFE and WS1 strains. A) Gene expression in log_2 counts per million (CPM) when interacting with each evolved strain as a heatmap clustered by count. B) The number of genes upregulated or downregulated (>2-fold change, p-value < 0.05). C) Venn diagram showing the number of overlapping genes differentially expressed between the two conditions. Ac; *Acanthamoeba sp.*, WFE; Wrinkly Fried Egg, WS1; Wrinkly Spreader-1.

Discussion

We conducted a 20-day predator-prey coevolution experiment in order to experimentally evaluate bacterial adaptations that increase resistance to amoeboid predation on solid surfaces. The predation-free lines did not develop recognisable colony variants or mutations, but after 20 days of predation a set of novel and not-so-novel bacterial colony morphologies were selected from the predation adapted bacterial lineages for further study. Two of the novel types closely resembled WS types observed in AL experiments performed previously in the same organism while the other two, WFE and FE, were not previously described.

All four colony variants evolved under predation regime demonstrated increased grazing resistance in plaque assays and line test assays and all four had substantially increased prey fitness relative to the WT. The strategies in place to resist predation appear however to be distinguishable.

As noted, two of the colony variants selected were classified as WS types. Complete genome sequencing revealed that the WS1 and WS2 isolates both had mutations in the phosphorylation domain of the well characterised *wspF* gene (Fig. 2.2). Similar mutations in this response regulatory domain are well known to increase cellular levels of cyclic-di-GMP and ultimately cause cells to constitutively over-produce extracellular cellulose, resulting in robust biofilms at the AL interface. In light of this genotype, we tested WS1 and WS2 in a classic AL interface experiment and found they produced high strength biofilms, comparable to a well-studied positive control (LSWS) [59]. This extracellular production strategy parallels the bacterial prey *Escherichia coli* and bacterial predator *Myxococcus xanthus* predation experiments that favour increased

extracellular mucoid production [65]. The evolution of constitutive biofilm production as an adaptive response to predation is consistent with expectations [18]. There is growing evidence that biofilm formation is a common response of *Pseudomonad*s to ecological challenges, aside from protozoan predation, including AL interfaces [44], the CF lung [53], and even space travel [66]. This may be an ecological consequence of the many negative repressors that contribute to the regulation of this trait, providing a large target for random mutations [59].

We observed trade-offs in the fitness of the majority of bacterial mutants that had acquired resistance to amoeboid predation (Fig. 2.4 B). This was particularly pronounced in the WS1 mutant, which lost an average of 23.8% generational growth compared to WT on these plates. The relative fitness of WS morphotypes measured in mixed colony fitness assays was 0.33 of WT over 100 generations [67]. In our hands, WT cells achieved an average of 9 generations over the 4-day experiment. A loss of 23.8% over a short time represents a substantial trade-off. However, trade-offs of this kind were not universal in these predation resistant mutants.

The FE mutation did not appear to impose a selective cost as measured by cell growth on solid media in the absence of predators (Fig. 2.4 B). This may suggest that the strategy of these cells to resist predation is optimal. It is also possible that we have failed to measure their growth in an environment in which deleterious fitness effects of this *wspF* mutation would be apparent.

The FE colony variant was also revealed to be a *wspF* mutation, however this one was in the demethylase domain of the WspF repressor. This mutation (L272P) is

comparable to the LSWS mutation, which is found in the same domain (Fig. 2.1 B & C). The result is a much less robust biofilm, which can only maintain the weight of 0.31 grams whereas the LSWS can support 1.1 grams. The cellulose production was also much less pronounced in the FE isolate as visualised by calcofluor staining (Fig. 2.6). This mutation is proximal (2 AA away) from the WSF (AA274) mutation observed previously in AL experiments (Supplementary Table 1) and shown to have a higher fitness than the LSWS in A-L competitions. Our results suggest that the FE mutation modulates the methylase activity of the WspF domain but the effect on the balance of Wsp and therefore c-di-GMP accumulation in the cell and cellulose production are not as dramatic as in the LSWS (S301R) mutation in the same domain [56].

The WFE colony variant also affects the function of a repressor that is implicated in c-di-GMP production via the Wsp regulatory system but this mutation was found in the AmrZ gene. AmrZ acts as a master regulator among *Pseudomonads* by binding to operator regions [60] and serves mostly as a transcriptional repressor of flagellar function, chemotaxis, and iron homeostasis in *Pseudomonas fluorescens* F113 [68]. AmrZ in *Pseudomonas fluorescens* is known to repress the Wsp system whilst simultaneously stimulating the production of alginate through AlgD and repressing production of the flagella through FleQ (Fig. 2.2 D & E) [58,59]. The *amrZ* mutation in evolved WFE appears to reduce the effectiveness of AmrZ as a regulator, possibly by changing its affinity for promoters or by reducing its abundance by inhibiting its production. We base this inference on the observation of multiple downstream changes in the biofilm pathway in WFE. AmrZ inhibits type VI secretion and pyoverdine synthesis in *Pseudomonas fluorescens* F113 [68]. Indeed, we observe evidence of

increased expression of a putative pyoverdine synthetase gene (pvdF, PFLU2547) in WFE as expected if AmrZ has decreased function.

Furthermore, AmrZ is involved in regulating 'functional amyloid of pseudomonas' (Fap) fibrils induce aggregation in *Pseudomonas aeruginosa* PA01 [69]. The greatest difference in expression observed between the WFE and WS1 was the upregulation of all four fap homologues in WFE (PFLU2697-2700). Furthermore, we found three *pga* genes (PFLU0143-0144) upregulated in WFE. The *pga* operon is necessary to produce exopolysaccharide (poly-beta-1,6-N-acetyl-D-glucosamine) involved in surface adhesion and mat formation [70]. In our hands, the mutation in AmrZ appeared to have a mild effect (similar to that of FE) in stimulating cellulose production, manifested as limited calcofluor staining and poor performance in the AL interface strength test (Fig. 2. 6). We interpret this as a partial loss of function of the AmrZ repressor. We have no evidence that this mutation increases flagella production concomitant with the observed increase in cellulose production [58], however our expression studies were performed on solid media, which would tend to repress flagellar synthesis. Our swarming motility assay result suggests that motility is impaired but this may be a consequence of cellulose production (Fig. 2.5). Impaired motility, which is predicted from the literature, in conjunction with slightly increased biofilm formation (cellulose and amyloid pilins), may explain the extremely weak biofilm formed in this instance at the AL interface.

Together, the differential expression results suggest expression of features that would be expected to increase biofilm formation in WFE according to previous studies [71]. However, increased expression of these traits may not lead to a stronger biofilm (as

suggested by our mat strength results), but may still provide predation resistance. For example, fibrils may increase the effective profile size of a bacterial cell. Increased Fap-mediated biofilm formation also induces increased alginate synthesis in *P. aeruginosa* PA01, an exopolysaccharide that protects mucoid *P. aeruginosa* against macrophage killing [69,72]. Interestingly, we found increased expression of alginate biosynthesis genes in both WFE and WS1 (*algA, algF*), suggesting alternate mechanisms leading to increased alginate production in these two strains.

We set out to determine if evolution under amoeboid predation would lead to an increase in bacterial virulence, focussing on altered colony morphologies in order to identify adaptive mutations. Given the focus on colony morphology, it is perhaps unsurprising that the isolates characterised were involved in biofilm formation to one degree or another. While biofilm formation has certainly been implicated as a virulence trait in some *Pseudomonads* [14,53], the WS1, WS2, FE and WFE variants were highly resistant to predation without increasing amoeboid mortality.

Contrary to our expectations, we found that predation of LWT or WT isolates resulted in higher mortality (10% cell death) in the *Acanthamoeba sp*. than predation of WS, FE or WFE isolates (Fig. 2.3 D). This increased mortality of predators likely results from the defensive traits expressed by WT *P. fluorescens* SBW25 in the presence of *Acanthamoeba*. For example, WT *P. fluorescens* SBW25 has been shown to produce viscosin, a cyclic lipopeptide biosurfactant implicated in increased motility and surface spreading and which has lethal effects on *N. americana* [61,73]. However, predators also demonstrated significantly better growth (19 generations) in the presence of the WT and Like-WT isolates than they did on the evolved isolates (9-14 generations). We

interpret the decreased growth observed in the presence of adapted bacterial isolates to suggest that the *Acanthamoeba* revert to their encysted state in response to food deprivation and that this, in turn, reduces their exposure to bacterial defences, reducing mortality [74]. Given the antagonistic starting point for our predator and prey, longer co-evolution experiments may yield isolates that increase in virulence, particularly given the tendency of experimental evolution protocols that require subculturing and transfer to select against biofilm-forming mutants over the long term [7].

Protozoan predation is an important mediator of bacterial populations in nature [6]. The power of these bacterial antagonists has been recognized previously but there has been a dearth of studies on the long-term molecular effects these keystone predators have on bacterial prey. Free-living amoebae can be integral modulators of the bacterial community in biofilms [75,76]. FLAs isolated from several environmental samples were recognised often to be in close contact with the bacterial biofilm community [4]. Similarly, biofilm formation has previously been demonstrated to be a successful defence strategy of *P. fluorescens* SBW25 against free-living ciliate predators in liquid environments [77–79].

Our findings support the suggestion that amoeboid predation can profoundly influence the course of genetic and phenotypic evolution in a short time span.

Materials and Methods

Strains and media. A strain of *P. fluorescens* SBW25 (NC_012660.1) that constitutively expresses GFP was used in order to easily confirm the genetic background of the strain and detect contamination [59]. The strain was regularly grown in 5 mL Lysogeny Broth (LB) [80] from -80°C frozen stock and incubated at 28°C in a shaker (180 rpm). Protozoan Strain *Acanthamoeba sp*. T2-5 (EF378666.1) was isolated from a tadpole 2 (Bullfrog, *Rana catesbeiana*) and propagated on solid PM media (4 g Difco Bacto Peptone, 2 g dextrose, 1.5 g K_2HPO_4, 1 g KH_2PO_4 and 20 g agar (2%) per litre H_2O) supplemented with 2% heat-inactivated Fetal Bovine Serum (FBS) (MEDIRAY, MG-FBS0820) and incubated in parafilm sealed plates at 28°C [81].

For the purpose of plaque assays (Plaque Forming Unit) (Fig. 2. 2A) in which only WT was present, PM media was supplemented with 33 mg of cholesterol (Sigma-Aldrich, C8867) per litre of PM agar in parafilm sealed plates and incubated at 28°C [82]. This was sufficient to allow for growth of *Acanthamoeba sp.* on the ancestral WT strain in order to measure PFU. However, in all other experiments, FBS was supplemented, as described above *Acanthamoeba sp.* stock was regularly stored in a 2 mM Tris HCL buffer (121.1 g Tris base in 800 mL H_2O, 60 mL HCl to get pH 7.6 (autoclaved or filter sterilised) at room temperature [74]. Amoebae were cultivated on WT bacterial prey before experimental evolution on medium-sized Petri plates (90 x 15mm).

Prey-predator experimental evolution. Experimental evolution was performed on solid PM agar plates, supplemented with 2% FBS to support long term *Acanthamoeba sp.* growth. Three replicates of prey-only (PO) treatment were used as a control by

spreading a lawn of $1x10^8$ *P. fluorescens* SBW25 cells in 100 µl on agar plates. Co-evolution of prey and predator (P) were started in the same way with the subsequent addition of $1x10^3$ protozoan cells in 2 µl of Tris HCl buffer on one side of the agar plate on a sterilised filter disk. Plates were wrapped in parafilm to prevent drying of the medium and incubated at 28°C to allow *Acanthamoeba sp.* to consume the bacterial lawn across the plate (Fig. 2.1 A, B and C).

Predation plates were developed for 5-day cycles, after which the lawn of the surviving prey bacteria and protozoan predators or prey-only controls were each washed with 3 mL of Tris buffer. The wash from the co-evolution plates was subjected to centrifugation at 400 g for 3 minutes in order to separate the amoebae (primarily in their encysted state) from bacterial cells. The supernatant was removed and 100 µl of Tris HCL was used to resuspend the amoebae pellet. Approximately 3% of the bacterial supernatant in 100 µl (3×10^7 - 1.6×10^8 for predator-evolved and 1×10^{10} - 3×10^{10} for prey-only) and 2% of the resuspended pellet containing protozoan cells in 2 µl (9×10^4 - 1.6×10^5) was transferred to fresh solid FBS supplemented PM plates for the next cycle. This cycle was performed every 5 days (4 cycles) for a total of 20 days. The remaining bacterial cells were frozen in equal parts for a final concentration of 4.25% NaCl and 35% glycerol at -80°C for further investigation. We were unable to reliably cryopreserve *Acanthamoeba sp.* during the course of the experiment.

Isolation of the Predation Adapted Bacteria. After 20 days of growth the evolved bacterial cells from the prey-predator and control group were plated for colony-forming units (CFU). Eight novel colony morphologies that appeared to have distinct phenotypes, along with five smooth isolates from three prey-predator lines were

selected for single colony isolation on LBA plates containing 100 µg/mL ampicillin and preserved at -80°C as above for further study. In addition, three smooth colonies from the prey-only plates were selected for single colony isolation and similarly preserved.

Predator growth on bacterial isolates. The ability of predator-evolved bacterial isolates to affect the viability of amoebae was established by growing ancestral *Acanthamoeba sp.* on evolved bacterial isolates and comparing PFU on these novel bacteria to PFU on WT *P. fluorescens* SBW25. Bacterial cultures were first grown overnight in 5 mL of LB in a shaker (180 rpm). The ancestral stock of *Acanthamoeba sp.* was diluted in order to yield 5-10 plaques on a total of six replicate plates [81]. Briefly, protozoan cells were transferred into the tubes that contained overnight test cultures of ~$1x10^8$ bacteria (100 µl), mixed thoroughly and spread onto PM agar plates. Plates were wrapped in parafilm and incubated at 28°C for four days. Plates were monitored daily for protozoal plaque formation and recorded (Fig. 2.2 A).

To evaluate the number of *Acanthamoeba sp.* generations (n) on each coevolved bacterial population, bacterial test isolates of interest were mixed with protozoan cells (10 +/- 2) and incubated as described above. The initial number of *Acanthamoeba sp.* cells placed on each plate were estimated by counting PFU at T=0 (ci). Protozoan cells were grown on predation-evolved bacterial isolates of interest for four days of growth at T=4 (cf). These plates were subsequently washed with 1.5 mL of Tris HCl (7.6 pH) buffer and plated for PFU as described above. The average number of generations that amoebae achieved on the various prey mutants was then calculated as:

cf= cell count final ci= cell count initial n= number of generations

$$logcf = logci + nlog2 \qquad n = \frac{logcf - logci}{log2} \qquad n = \frac{logcf - logci}{0.301} \qquad n = 3.3 \times log\left(\frac{cf-ci}{ci}\right)$$

Predator survival estimates. In order to determine the numbers of live or dead amoebae in either the encysted or amoeboid states after predation on the predator-evolved bacterial isolates, we performed flow cytometry. Briefly, $1x10^3$ ancestral protozoan cells were placed on one side of the PM plates and bacterial isolates were streaked with a 1 µl sterile loop from the side of the plates downwards. After 2-3 days of growth and once the amoebae had formed a visible clearing, 10 mm of the interaction zones containing approximately $8x10^4$ protozoan cells were gently harvested using a 1 µl loop and resuspended in 50 µl of Tris HCl buffer and instantly stained with 2% Propidium Iodide ($^V/_V$) (Thermo Scientific, P3566). PI stains cells that have lost membrane potential. Cells were incubated at room temperature for 10-20 minutes in the dark and examined by flow cytometry (BD FACSCanto™ II) using a PE-A channel. The ratio of stained to unstained cells in an appropriate gate was used to determine the proportion of the population that was not viable.

Line test assay. In order to measure the rate of predation by ancestral *Acanthamoeba* on the various bacterial isolates, line test assays were conducted as previously described [54]. Briefly, overnight cultures of six evolved isolates and the *P. fluorescens* SBW25 WT control were grown in LB from -80°C glycerol stocks. Approximately $1x10^3$ protozoan cells were added to a sterile filter paper placed in the middle of the PM plate supplemented with FBS. Bacterial isolates of interest were streaked as replicated paired lines on the plate with a 1 µl loop, from the centre of the plates outwards (Fig. 2.3 A). Plates were wrapped in parafilm and incubated at 28°C for five days. Plates were photographed every 24 hours and the distance of protozoan consumption of the

bacterial lines was recorded. Predation rates were calculated as the average of the rate of line disappearance over time for each evolved type over at least six replicate lines. These were adjusted for absolute bacterial density based on relative CFU of plugs of the plates. Relative prey fitness values were calculated by multiplying the overall rate of predation (mm/day) by the normalised cell density (cells/plate), normalising relative prey fitness (cells/day) to set the value of the least preferred mutants (WS1, FE, & WFE) to 1 and the most preferred mutant to 0 (LWT1) [54].

Bacterial Fitness Assay. Overnight cultures of bacterial isolates were grown in LB from -80°C glycerol stocks. The bacterial fitness assays were performed on solid PM agar plates. To estimate the growth rate of bacterial lines in the absence of protozoa, replicate cultures of $1x10^7$ bacteria (30 µl) were spread on small Petri plates (35 x10 mm). Plates were wrapped in parafilm and incubated at 28°C. After four days, plates were washed with 1.5 mL Tris HCl buffer, serially diluted, and plated for CFU. The fitness of the bacterial isolates was calculated based on the number of the bacterial populations after four days of growth in the absence of predators, relative to the density of WT strain.

Whole-genome sequencing of the bacterial isolates. Representative isolates from Predation and PO lines were revived from frozen -80°C stocks. DNA extraction was performed for whole-genomic DNA purification using the Promega™ Wizard™ Genomic DNA Kit (A1125, Promega). Genome quality and quantity were checked in 1% agarose gels stained with %0.0001 SYBR Safe and measured in a NanoDrop (ACTGene ASP-3700, Alphatech Systems), respectively. Genomes of all coevolved, prey-only controls, and ancestral *P. fluorescens* SBW25 WT were sent to MicrobesNG

(www.microbesng.com) for 250 bp paired-end, next-generation Illumina sequencing. Sequenced reads were trimmed, aligned, and mapped to the *P. fluorescens* SBW25 reference genome (NC_012660.1) [83] for a minimum and maximum sequencing depth of 60 and 190, respectively, across the genome using GENEIOUS version 9.0.5 [84]. Mutations in isolates were identified as being present in 90% of reads in the alignment by GENEIOUS using the “Find Variation/SNPs” tool.

Motility test assay (bacterial swarming). Bacterial swarming was examined on 0.5% agar M9 plates (100 mL M9 salt, 1 mL 1M $MgSo_4$, 10 mL 20% glycerol, 2.5 grams casamino acid and 50 µl 1M $CaCl_2$, adjusted to 500 mL with H_2O). Bacterial isolates were grown overnight in LB from frozen glycerol stocks. Assays were conducted by dipping the overnight bacterial culture and stabbing into the surface of agar plates using 1 µl inoculation Loops (n=10). Plates were incubated for 72 hrs at 28°C and photographed when required.

Microscopy and image analysis. Amoebae and bacteria visualisation: cells were harvested from actively growing PM plates using a 1 µl loop placed and distributed gently on a glass microscopic slide on an agarose pad (M9 media +1% agarose). Cells were allowed to dry and were then covered with a glass cover slip. Images were acquired using PH and GFP filter channels (excitation 80 and 250 nm, respectively) with a 100x phase objective lens (Olympus BX51) (Fig. 2.1 C).

Congo red staining: In order to visualise the cellulose production, congo red staining was performed. Cultures of interest were grown overnight from frozen stocks in 5 mL of LB broth. Cells were diluted to yield 10-15 colonies and plated onto LB agar plates

containing 0.004% congo red. Plates were allowed to incubate for 48 hrs at 28°C. Colony morphology images were carried out using a Zeiss dissecting microscope (Stemi 2000-C). Phase contrast images were acquired using SwiftCam x 0.5 and 1.2 objective (MA95011).

Cellulose staining: cell microscopy was performed using a fluorescence inverted microscope (Nikon Eclipse Ti2). Samples were grown overnight from glycerol stocks in 5 mL of KB broth [85]. From the overnight culture, 5 µl was dropped into fresh KB broth containing 200 µg mL^{-1} calcofluor white (Fluorescent Brightener 28, Sigma-Aldrich) and plates were incubated overnight at 28°C. Portions of the resulting bacterial colonies were sampled by scraping and placed directly on a glass microscope slide and covered with a glass coverslip. Images were captured using the Dapi filter channel (excitation 380 nm) using a 100x phase objective lens (Fig. 2.6 B).

Capsule staining: Capsule visualisation (Supplementary Fig. 2) was performed by growing the isolate of interest overnight in KB broth and mixing 10 µl of the culture with 10% India Ink ($^{V}/_{V}$) (PE316000). 2-5 µl of the mixed solution was then placed onto one side of the microscopic slide, thoroughly spread using the edge of the coverslip with an angle of 45° and allowed to dry for 5-10 minutes at room temperature. Slides were then viewed using phase contrast with a 100x phase objective lens (Olympus BX51).

Colony images: Colony morphology images were carried out using a Zeiss dissecting microscope (Stemi 2000-C). Phase contrast images were acquired using SwiftCam x 0.5 and 1.2 objective (MA95011). Cell and colony images were processed in ImageJ as described in figure legends (Fig. 2.1 F).

Microbial mat strength assay. To compare the strength of the biofilms across the various mutants that were isolated, a mat strength assay was performed as previously described [44]. Bacterial isolates of interest first were inoculated from frozen stocks kept at -80°C and grown overnight in 5 mL KB broth at 28°C. 5 µl of the overnight test isolates in four replicates were diluted into fresh 5 mL KB microcosms. Evolved bacterial isolates were incubated at 28°C in a static environment for 72 hours. Bacterial isolates were then tested for the strength of biofilm after 3-day growth in KB by gently placing the maximum number of 2 mm glass beads in the centre of the biofilm until the mat collapsed in the microcosm vial.

***Pseudomonas-Acanthamoeba* interaction assay.** Individual colonies of bacterial strains pre-cultured on LB agar were homogenised in LB broth and spread in single lines across PM agar plates using a 1ul transfer loop. Plates were allowed to dry before applying 2 µl of suspension containing ~10^3 *Acanthamoeba* cysts μl^{-1} at one end of the bacterial line. Plates were incubated at 28˚C for up to 1 week and the interaction zone was collected once the amoeba had formed a visible clearing. *Pseudomonas fluorescens* SBW25 strains were collected with *Acanthamoeba* from the bacteria-protozoa interaction zone and alone from the opposite end of the culture line with a transfer loop and immediately homogenised in RNA shield (n=4).

Transcriptional profiling. Total RNA was extracted from bacterial and amoebae cells using the Quick-RNA MiniPrep Kit (Zymo Research, USA). Preparations were dried in GenTegra RNA tubes according to manufacturer's instructions (Gentegra, USA) and sent to the Microbial Genome Sequencing (MiGS, USA) Center for Illumina Stranded RNA library preparation with RiboZero Plus rRNA depletion and sequencing on the

NextSeq 550 platform with 12M reads per bacterial sample or 50M reads per sample for bacteria-amoeba mixed samples. Bioinformatic analysis was carried out following a modified dual RNA-seq protocol from [86]. Briefly, reads were aligned to the *Acanthamoeba* reference genome using HiSat2 [87] unused reads were then aligned to the bacterial reference genome using Bowtie2 [88]. We used the closest reference sequence to our amoeba at the time of this work - *Acanthamoeba castellanii* strain NEFF (GCA_000313135.1). For bacterial sequences, reads were aligned to the *Pseudomonas fluorescens* SBW25 reference sequence (GCA_000009225.1). Sequence reads were assigned to genomic features using featureCounts [89]. Differential expression using GLM and count normalisation was calculated with edgeR [90]. Counts were normalised by library size (counts per million, CPM) with $\log_2$ transformation. Features with differential expression ≥ ±2 $\log_2$FC and *P*-value of ≤0.05 after correction for multiple testing using the FDR (Benjamini and Hochberg) method were considered significant.

References

1. Ghoul M, Mitri S. The Ecology and Evolution of Microbial Competition. Trends Microbiol. 2016 Oct;24(10):833–45.
2. Johansson JF, Paul LR, Finlay RD. Microbial interactions in the mycorrhizosphere and their significance for sustainable agriculture. FEMS Microbiol Ecol. 2004 Apr 1;48(1):1–13.
3. Foster RC, Dormaar JF. Bacteria-grazing amoebae in situ in the rhizosphere [Internet]. Vol. 11, Biology and Fertility of Soils. 1991. p. 83–7. Available from: http://dx.doi.org/10.1007/bf00336368.
4. Rodríguez-Zaragoza S. Ecology of free-living amoebae. Crit Rev Microbiol. 1994;20(3):225–41.
5. Hilbi H, Weber SS, Ragaz C, Nyfeler Y, Urwyler S. Environmental predators as models for bacterial pathogenesis. Environ Microbiol. 2007 Mar;9(3):563–75.

6. Fenchel T. Ecology of Protozoa: The Biology of Free-living Phagotropic Protists. Springer-Verlag; 2013. 197 p.

7. Gallet R, Alizon S, Comte P-A, Gutierrez A, Depaulis F, van Baalen M, et al. Predation and disturbance interact to shape prey species diversity. Am Nat. 2007 Jul;170(1):143–54.

8. Weekers PH, Bodelier PL, Wijen JP, Vogels GD. Effects of Grazing by the Free-Living Soil Amoebae *Acanthamoeba castellanii*, *Acanthamoeba polyphaga*, and *Hartmannella vermiformis* on Various Bacteria. Appl Environ Microbiol. 1993 Jul;59(7):2317–9.

9. Rønn R, McCaig AE, Griffiths BS, Prosser JI. Impact of protozoan grazing on bacterial community structure in soil microcosms. Appl Environ Microbiol. 2002 Dec;68(12):6094–105.

10. Luxmy BS, Nakajima F, Yamamoto K. Predator grazing effect on bacterial size distribution and floc size variation in membrane-separation activated sludge. Water Sci Technol. 2000;42(3-4):211–7.

11. Wright RT, Coffin RB. Measuring microzooplankton grazing on planktonic marine bacteria by its impact on bacterial production. Microb Ecol. 1984 Jun;10(2):137–49.

12. Leibold MA, Chase JM, Shurin JB, and, Downing AL. SPECIES TURNOVER AND THE REGULATION OF TROPHIC STRUCTURE [Internet]. Vol. 28, Annual Review of Ecology and Systematics. 1997. p. 467–94. Available from: http://dx.doi.org/10.1146/annurev.ecolsys.28.1.467.

13. Bar-On YM, Phillips R, Milo R. The biomass distribution on Earth. Proc Natl Acad Sci U S A. 2018 Jun 19;115(25):6506–11.

14. Adiba S, Nizak C, van Baalen M, Denamur E, Depaulis F. From grazing resistance to pathogenesis: the coincidental evolution of virulence factors. PLoS One. 2010 Aug 11;5(8):e11882.

15. Vargas R, Hattori T. Protozoan predation of bacterial cells in soil aggregates [Internet]. Vol. 38, FEMS Microbiology Letters. 1986. p. 233–42. Available from: http://dx.doi.org/10.1111/j.1574-6968.1986.tb01733.x.

16. Fritsche TR, Gautom RK, Seyedirashti S, Bergeron DL, Lindquist TD. Occurrence of bacterial endosymbionts in *Acanthamoeba spp*. isolated from corneal and environmental specimens and contact lenses. J Clin Microbiol. 1993 May;31(5):1122–6.

17. Clarholm M. Protozoan grazing of bacteria in soil—impact and importance [Internet]. Vol. 7, Microbial Ecology. 1981. p. 343–50. Available from: http://dx.doi.org/10.1007/bf02341429.

18. Matz C, Kjelleberg S. Off the hook–how bacteria survive protozoan grazing. Trends Microbiol [Internet]. 2005; Available from: https://www.sciencedirect.com/science/article/pii/S0966842X05001344.

19. Jürgens K, Matz C. Predation as a shaping force for the phenotypic and genotypic composition of planktonic bacteria. Antonie Van Leeuwenhoek. 2002 Aug;81(1-4):413–34.

20. Pernthaler J. Predation on prokaryotes in the water column and its ecological implications. Nat Rev Microbiol. 2005 Jul;3(7):537–46.

21. Van der Henst C, Vanhove AS, Drebes Dörr NC, Stutzmann S, Stoudmann C, Clerc S, et al. Molecular insights into Vibrio cholerae's intra-amoebal host-pathogen interactions. Nat Commun. 2018 Aug 27;9(1):3460.

22. Jürgens K, Güde H. The potential importance of grazing-resistant bacteria in planktonic systems. Mar Ecol Prog Ser. 1994;112(1/2):169–88.

23. Jousset A, Scheu S, Bonkowski M. Secondary metabolite production facilitates establishment of rhizobacteria by reducing both protozoan predation and the competitive effects of indigenous bacteria. Funct Ecol. 2008 Aug;22(4):714–9.

24. Deines P, Matz C, JÜrgens K. Toxicity of violacein-producing bacteria fed to bacterivorous freshwater plankton [Internet]. Vol. 54, Limnology and Oceanography. 2009. p. 1343–52. Available from: http://dx.doi.org/10.4319/lo.2009.54.4.1343.

25. Hass CC, Valenzuela D. Anti-predator benefits of group living in white-nosed coatis (Nasua narica). Behav Ecol Sociobiol. 2002 May 1;51(6):570–8.

26. Pérez J, Moraleda-Muñoz A, Marcos-Torres FJ, Muñoz-Dorado J. Bacterial predation: 75 years and counting! Environ Microbiol. 2016 Mar;18(3):766–79.

27. Van der Henst C, Scrignari T, Maclachlan C, Blokesch M. An intracellular replication niche for *Vibrio cholerae* in the amoeba *Acanthamoeba castellanii*. ISME J. 2016 Apr;10(4):897–910.

28. Matz C, Bergfeld T, Rice SA, Kjelleberg S. Microcolonies, quorum sensing and cytotoxicity determine the survival of *Pseudomonas aeruginosa* biofilms exposed to protozoan grazing [Internet]. Vol. 6, Environmental Microbiology. 2004. p. 218–26. Available from: http://dx.doi.org/10.1111/j.1462-2920.2004.00556.x.

29. Sun S, Noorian P, McDougald D. Dual Role of Mechanisms Involved in Resistance to Predation by Protozoa and Virulence to Humans. Front Microbiol. 2018 May 17;9:1017.

30. Lutz C, Erken M, Noorian P, Sun S, McDougald D. Environmental reservoirs and mechanisms of persistence of Vibrio cholerae. Front Microbiol. 2013 Dec 16;4:375.

31. Hall-Stoodley L, Costerton JW, Stoodley P. Bacterial biofilms: from the natural environment to infectious diseases. Nat Rev Microbiol. 2004 Feb;2(2):95–108.

32. O'Toole G, Kaplan HB, Kolter R. Biofilm Formation as Microbial Development [Internet]. Vol. 54, Annual Review of Microbiology. 2000. p. 49–79. Available from: http://dx.doi.org/10.1146/annurev.micro.54.1.49.

33. Makin SA, Beveridge TJ. The influence of A-band and B-band lipopolysaccharide on the surface characteristics and adhesion of *Pseudomonas aeruginosa* to surfaces

[Internet]. Vol. 142, Microbiology. 1996. p. 299–307. Available from: http://dx.doi.org/10.1099/13500872-142-2-299.

34. De Weger LA, van der Vlugt CI, Wijfjes AH, Bakker PA, Schippers B, Lugtenberg B. Flagella of a plant-growth-stimulating *Pseudomonas fluorescens* strain are required for colonization of potato roots. J Bacteriol. 1987 Jun;169(6):2769–73.

35. Matz C, Moreno AM, Alhede M, Manefield M, Hauser AR, Givskov M, et al. *Pseudomonas aeruginosa* uses type III secretion system to kill biofilm-associated amoebae. ISME J. 2008 Aug;2(8):843–52.

36. Matz C, McDougald D, Moreno AM, Yung PY, Yildiz FH, Kjelleberg S. Biofilm formation and phenotypic variation enhance predation-driven persistence of Vibrio cholerae [Internet]. Vol. 102, Proceedings of the National Academy of Sciences. 2005. p. 16819–24. Available from: http://dx.doi.org/10.1073/pnas.0505350102.

37. Davey ME, O'toole GA. Microbial Biofilms: from Ecology to Molecular Genetics [Internet]. Vol. 64, Microbiology and Molecular Biology Reviews. 2000. p. 847–67. Available from: http://dx.doi.org/10.1128/mmbr.64.4.847-867.2000.

38. Stewart PS, Costerton JW. Antibiotic resistance of bacteria in biofilms. Lancet. 2001 Jul 14;358(9276):135–8.

39. Donlan RM. Biofilms and device-associated infections. Emerg Infect Dis. 2001 Mar;7(2):277–81.

40. Donlan RM. Biofilms: Microbial Life on Surfaces [Internet]. Vol. 8, Emerging Infectious Diseases. 2002. p. 881–90. Available from: http://dx.doi.org/10.3201/eid0809.020063.

41. Spiers AJ, Rainey PB. The *Pseudomonas fluorescens* SBW25 wrinkly spreader biofilm requires attachment factor, cellulose fibre and LPS interactions to maintain strength and integrity. Microbiology. 2005 Sep;151(Pt 9):2829–39.

42. Spiers AJ, Bohannon J, Gehrig SM. Biofilm formation at the air–liquid interface by the *Pseudomonas fluorescens* SBW25 wrinkly spreader requires an acetylated form of cellulose. Molecular [Internet]. 2003; Available from: https://onlinelibrary.wiley.com/doi/abs/10.1046/j.1365-2958.2003.03670.x.

43. McDonald MJ, Gehrig SM, Meintjes PL, Zhang X-X, Rainey PB. Adaptive Divergence in Experimental Populations of *Pseudomonas fluorescens*. IV. Genetic Constraints Guide Evolutionary Trajectories in a Parallel Adaptive Radiation [Internet]. Vol. 183, Genetics. 2009. p. 1041–53. Available from: http://dx.doi.org/10.1534/genetics.109.107110.

44. Rainey PB, Travisano M. Adaptive radiation in a heterogeneous environment. Nature. 1998 Jul 2;394(6688):69–72.

45. Gallie J, Bertels F, Remigi P, Ferguson GC, Nestmann S, Rainey PB. Repeated Phenotypic Evolution by Different Genetic Routes in *Pseudomonas fluorescens* SBW25. Mol Biol Evol. 2019 May 1;36(5):1071–85.

46. Gallie J, Bertels F, Remigi P, Ferguson GC, Nestmann S, Rainey PB. Repeated phenotypic evolution by different genetic routes: the evolution of colony switching in *Pseudomonas fluorescens* SBW25 [Internet]. Available from: http://dx.doi.org/10.1101/414219.

47. Spiers AJ, Kahn SG, Bohannon J, Travisano M, Rainey PB. Adaptive divergence in experimental populations of *Pseudomonas fluorescens*. I. Genetic and phenotypic bases of wrinkly spreader fitness. Genetics. 2002 May;161(1):33–46.

48. Ferguson GC, Bertels F, Rainey PB. Adaptive divergence in experimental populations of *Pseudomonas fluorescens*. V. Insight into the niche specialist fuzzy spreader compels revision of the model Pseudomonas *radiation*. Genetics. 2013 Dec;195(4):1319–35.

49. King CH, Shotts EB Jr, Wooley RE, Porter KG. Survival of coliforms and bacterial pathogens within protozoa during chlorination. Appl Environ Microbiol. 1988 Dec;54(12):3023–33.

50. Levin BR, Svanborg Edén C. Selection and evolution of virulence in bacteria: an ecumenical excursion and modest suggestion. Parasitology. 1990;100 Suppl:S103–15.

51. March C, Cano V, Moranta D, Llobet E, Pérez-Gutiérrez C, Tomás JM, et al. Role of bacterial surface structures on the interaction of *Klebsiella pneumoniae* with phagocytes. PLoS One. 2013 Feb 15;8(2):e56847.

52. Leaver CJ, Lovett JS. An analysis of protein and RNA synthesis during encystment and outgrowth (germination) of *Blastocladiella* zoospores [Internet]. Vol. 3, Cell Differentiation. 1974. p. 165–92. Available from: http://dx.doi.org/10.1016/0045-6039(74)90028-1.

53. Malone JG. Role of small colony variants in persistence of *Pseudomonas aeruginosa* infections in cystic fibrosis lungs. Infect Drug Resist. 2015 Jul 29;8:237–47.

54. Wildschutte H, Wolfe DM, Tamewitz A, Lawrence JG. Protozoan predation, diversifying selection, and the evolution of antigenic diversity in *Salmonella*. Proc Natl Acad Sci U S A. 2004 Jul 20;101(29):10644–9.

55. Koza A, Kusmierska A, McLaughlin K, Moshynets O, Spiers AJ. Adaptive radiation of *Pseudomonas fluorescens* SBW25 in experimental microcosms provides an understanding of the evolutionary ecology and molecular biology of A-L interface biofilm formation. FEMS Microbiol Lett [Internet]. 2017 Jul 3;364(12). Available from: http://dx.doi.org/10.1093/femsle/fnx109.

56. Bantinaki E, Kassen R, Knight CG, Robinson Z, Spiers AJ, Rainey PB. Adaptive Divergence in Experimental Populations of *Pseudomonas fluorescens*. III. Mutational Origins of Wrinkly Spreader Diversity [Internet]. Vol. 176, Genetics. 2007. p. 441–53. Available from: http://dx.doi.org/10.1534/genetics.106.069906.

57. Hickman JW, Tifrea DF, Harwood CS. A chemosensory system that regulates biofilm formation through modulation of cyclic diguanylate levels. Proc Natl Acad Sci U S A. 2005 Oct 4;102(40):14422–7.

58. Giddens SR, Jackson RW, Moon CD, Jacobs MA, Zhang X-X, Gehrig SM, et al. Mutational activation of niche-specific genes provides insight into regulatory networks and bacterial function in a complex environment [Internet]. Vol. 104, Proceedings of the National Academy of Sciences. 2007. p. 18247–52. Available from: http://dx.doi.org/10.1073/pnas.0706739104.

59. Lind PA, Farr AD, Rainey PB. Experimental evolution reveals hidden diversity in evolutionary pathways. Elife [Internet]. 2015 Mar 25;4. Available from: http://dx.doi.org/10.7554/eLife.07074.

60. Baltrus DA, Dougherty K, Diaz B, Murillo R. Evolutionary Plasticity of AmrZ Regulation in. mSphere [Internet]. 2018 Apr 25;3(2). Available from: http://dx.doi.org/10.1128/mSphere.00132-18.

61. Alsohim AS, Taylor TB, Barrett GA, Gallie J, Zhang X-X, Altamirano-Junqueira AE, et al. The biosurfactant viscosin produced by *Pseudomonas fluorescens* SBW25 aids spreading motility and plant growth promotion. Environ Microbiol. 2014 Jul;16(7):2267–81.

62. Scanlan PD, Buckling A. Co-evolution with lytic phage selects for the mucoid phenotype of *Pseudomonas fluorescens* SBW25. ISME J. 2012 Jun;6(6):1148–58.

63. Spiers AJ, Bohannon J, Gehrig SM, Rainey PB. Biofilm formation at the air--liquid interface by the *Pseudomonas fluorescens* SBW25 wrinkly spreader requires an acetylated form of cellulose. Mol Microbiol. 2003;50(1):15–27.

64. Supek F, Bošnjak M, Škunca N, Šmuc T. REVIGO summarizes and visualizes long lists of gene ontology terms. PLoS One. 2011 Jul 18;6(7):e21800.

65. Nair RR, Vasse M, Wielgoss S, Sun L, Yu Y-TN, Velicer GJ. Bacterial predator-prey coevolution accelerates genome evolution and selects on virulence-associated prey defences. Nat Commun. 2019 Sep 20;10(1):4301.

66. Song B, Leff LG. Influence of magnesium ions on biofilm formation by *Pseudomonas fluorescens*. Microbiol Res. 2006 Mar 6;161(4):355–61.

67. Spiers AJ. Wrinkly-Spreader fitness in the two-dimensional agar plate microcosm: maladaptation, compensation and ecological success. PLoS One. 2007 Aug 15;2(8):e740.

68. Martínez-Granero F, Redondo-Nieto M, Vesga P, Martín M, Rivilla R. AmrZ is a global transcriptional regulator implicated in iron uptake and environmental adaption in P. fluorescens F113. BMC Genomics. 2014 Mar 26;15:237.

69. Leid JG, Willson CJ, Shirtliff ME, Hassett DJ, Parsek MR, Jeffers AK. The exopolysaccharide alginate protects *Pseudomonas aeruginosa* biofilm bacteria from IFN-gamma-mediated macrophage killing. J Immunol. 2005 Dec 1;175(11):7512–8.

70. Lind PA, Farr AD, Rainey PB. Evolutionary convergence in experimental Pseudomonas populations. ISME J. 2017 Mar;11(3):589–600.

71. Wang Y, Zhang S-P, Zhang M-Y, Kempher ML, Guo D-D, Han J-T, et al. The antitoxin MqsA homologue in *Pseudomonas fluorescens* 2P24 has a rewired regulatory circuit through evolution. Environ Microbiol. 2019 May;21(5):1740–56.

72. Herbst F-A, Søndergaard MT, Kjeldal H, Stensballe A, Nielsen PH, Dueholm MS. Major proteomic changes associated with amyloid-induced biofilm formation in *Pseudomonas aeruginosa* PAO1. J Proteome Res. 2015 Jan 2;14(1):72–81.

73. Mazzola M, de Bruijn I, Cohen MF, Raaijmakers JM. Protozoan-induced regulation of cyclic lipopeptide biosynthesis is an effective predation defense mechanism for *Pseudomonas fluorescens*. Appl Environ Microbiol. 2009 Nov;75(21):6804–11.

74. Marciano-Cabral F. Biology of Naegleria spp. Microbiol Rev [Internet]. 1988; Available from: https://www.ncbi.nlm.nih.gov/pmc/articles/pmc372708/.

75. Greub G, Raoult D. Microorganisms resistant to free-living amoebae. Clin Microbiol Rev. 2004 Apr;17(2):413–33.

76. Weitere M, Bergfeld T, Rice SA, Matz C, Kjelleberg S. Grazing resistance of *Pseudomonas aeruginosa* biofilms depends on type of protective mechanism, developmental stage and protozoan feeding mode. Environ Microbiol. 2005 Oct;7(10):1593–601.

77. Meyer JR, Kassen R. The effects of competition and predation on diversification in a model adaptive radiation. Nature. 2007 Mar 22;446(7134):432–5.

78. Hall AR, Meyer JR, Kassen R. Selection for predator resistance varies with resource supply in a model adaptive radiation. Evol Ecol Res. 2008;10(5):735–46.

79. Friman V-P, Jousset A, Buckling A. Rapid prey evolution can alter the structure of predator-prey communities. J Evol Biol. 2014 Feb;27(2):374–80.

80. Bertani G. Studies on lysogenesis. I. The mode of phage liberation by lysogenic Escherichia coli. J Bacteriol. 1951 Sep;62(3):293–300.

81. Heuser M, Razavi L. Chapter 13 Amebo-flagellates as Research Partners: The Laboratory Biology of *Naegleria* and *Tetramitus* [Internet]. Methods in Cell Biology. 1970. p. 341–476. Available from: http://dx.doi.org/10.1016/s0091-679x(08)61759-8.

82. Garg NK, Das SR. Lipid requirements for axenic cultivation of *Entamoeba histolytica* [Internet]. Vol. 2, Journal of Biosciences. 1980. p. 235–41. Available from: http://dx.doi.org/10.1007/bf02703249.

83. Silby MW, Cerdeño-Tárraga AM, Vernikos GS, Giddens SR, Jackson RW, Preston GM, et al. Genomic and genetic analyses of diversity and plant interactions of *Pseudomonas fluorescens*. Genome Biol. 2009 May 11;10(5):R51.

84. Kearse M, Moir R, Wilson A, Stones-Havas S, Cheung M, Sturrock S, et al. Geneious Basic: an integrated and extendable desktop software platform for the organization and analysis of sequence data. Bioinformatics. 2012 Jun 15;28(12):1647–9.

85. King EO, Ward MK, Raney DE. Two simple media for the demonstration of pyocyanin and fluorescin. J Lab Clin Med. 1954 Aug;44(2):301–7.

86. Marsh JW, Hayward RJ, Shetty AC, Mahurkar A, Humphrys MS, Myers GSA. Bioinformatic analysis of bacteria and host cell dual RNA-sequencing experiments. Brief Bioinform. 2018 Nov 27;19(6):1115–29.

87. Kim D, Langmead B, Salzberg SL. HISAT: a fast spliced aligner with low memory requirements. Nat Methods. 2015 Apr;12(4):357–60.

88. Langmead B, Salzberg SL. Fast gapped-read alignment with Bowtie 2. Nat Methods. 2012 Mar 4;9(4):357–9.

89. Liao Y, Smyth GK, Shi W. featureCounts: an efficient general purpose program for assigning sequence reads to genomic features. Bioinformatics. 2014 Apr 1;30(7):923–30.

90. Robinson MD, McCarthy DJ, Smyth GK. edgeR: a Bioconductor package for differential expression analysis of digital gene expression data. Bioinformatics. 2010 Jan 1;26(1):139–40.

91. Beaumont HJE, Gallie J, Kost C, Ferguson GC, Rainey PB. Experimental evolution of bet hedging [Internet]. Vol. 462, Nature. 2009. p. 90–3. Available from: http://dx.doi.org/10.1038/nature08504.

92. Lind PA. Evolutionary forecasting of phenotypic and genetic outcomes of experimental evolution in Pseudomonas [Internet]. Available from: http://dx.doi.org/10.1101/342261.

93. Lind PA, Libby E, Herzog J, Rainey PB. Predicting mutational routes to new adaptive phenotypes. Elife [Internet]. 2019 Jan 8;8. Available from: http://dx.doi.org/10.7554/eLife.38822.

Chapter 3

Reciprocal Adaptation in Predator-Prey lineages Mediates Coevolutionary Arms Race and Causes Specialised Traits in Prey Bacteria

Farhad S. Golzar[1] and Heather Lyn Hendrickson[2]
School of Natural and Computational Science, Massey University, Auckland, New Zealand
School of Biological Sciences, University of Canterbury, Christchurch, New Zealand

Abstract

Ecological interactions between predator and prey strongly influence the structure of microbial communities and evolutionary processes. Here we performed a 90-day predator-prey coevolution on solid media composed of *Pseudomonas fluorescens* SBW25 and a wild *Acanthamoeba sp.* to investigate the adaptive characteristics that arise in predator-prey lineages. We report how predator-prey interactions can lead to bacterial diversity, altered performance and evolution of predators. We show evidence of reciprocal adaptation, diversity and strong phenotypic parallelism among prey lineages undergoing predation. We found the evolution of novel colony morphologies such as Mountain and Volcano along with Wrinkly Spreaders specific to the predation groups. The bacterial isolates demonstrated a general resistance that resulted in reduced replication of the protozoan populations. We found evidence of mutualisms where both prey and predator increased their survival relative to their respective ancestors. Further, as a result of coevolution, evolved *Acanthamoeba* showed promoted killing performance and higher generations upon feeding on WT bacteria compared to the ancestral *Acanthamoeba sp.* Together, our findings show the emergence of divergent colony morphologies that arise as an adaptation to predation and notably affects the fitness and evolution of predators suggesting Red Queen co-evolutionary dynamics between predators and prey.

Introduction

Ecological interactions between prey and predator are among the oldest interactions in nature and have long been recognised to influence evolutionary processes [1,2]. Predator-prey interaction provides a strong driving force for rapid evolutionary changes in a range of ecosystems [3–5]. Predators are powerful agents capable of decreasing the abundance of prey populations and driving diversity [6,7]. They also play a pivotal role in maintaining the natural balance of microbial ecosystems by mediating rates of decomposition, nutrient recycling, and energy turnover [8,9]. Although bacterial adaptations to predation such as evolution of bacterial diversity have been observed in a wide range of environments, little is known about the direct effect of predator-prey interaction on phenotypic turnover in bacteria [7,10,11] and its effect on predator evolution in nature [12]. Ultimately, long term interactions between predator and prey can develop Red Queen dynamics, in which both species coexist only if they continuously coevolve, improve and adapt to the selective pressure [13,14].

The microbial world is replete with examples of competition and predation [11,15,16]. Due to high ecological abundance, prey bacteria may interact with a wide diversity of predators to survive in their natural habitats [17]. These predators include specialists (bacteriophages), semi-specialist (bacterial predators) and generalists (protists), all of which assert strong selective pressure on bacteria in the environment [6,7,12,18–21]. Predators with different behaviours appear to have different impacts on the evolution of prey bacteria [22]. Previous experiments have focused on rapid prey evolution and the development of antagonistic coevolution with specialist predators - phages [23,24], multiple predators (bacterial predator, phage and ciliates) from different trophic levels

[25–27] or semi-specialist bacterial predator such as *Myxococcus xanthus*. For example, *E. coli* bacteria that is exposed to *M. xanthus* have a greater chance of developing resistance due to an increased extracellular production. [12,28]. In test tubes, interactions among prey and predators can undergo rapid coevolution, however, surfaces are colonised by organisms more frequently and considered as an opening place for invasion [29]. Here we examine how a direct generalist protist and prey interactions on a solid surface promotes the evolution of parallel phenotypic diversity and turnover in prey bacteria, and determine the direct effects of bacterial evolution on fitness advantage of predatory protozoa in detail.

Free-living protozoan predator *Acanthamoeba sp*. has a worldwide distribution and is perhaps best known for causing severe keratitis and fatal encephalitis both in humans and animals [30–33]. *Acanthamoeba sp.* are unicellular eukaryotes that are found in several environments such as lakes, soil particles, animal tissues and thrive in laboratory conditions [6]. The life cycle of *Acanthamoeba* has two developmental stages: an encysted, dormant form, which is adopted when food is scarce and the vegetative motile form, in which bacterial predation takes place by phagocytosis on solid surfaces [34]. *Acanthamoeba* are also regarded as reservoirs and vehicles of pathogenic bacteria leading to infection of multiple hosts [35]. As a generalist predator, these amoebae feed upon a broad range of bacteria including bacterial pathogens [36,37]. For example, *Acanthamoeba* cells predate sufficiently upon pseudomonas species and decrease their population in the rhizosphere of *Arabidopsis thaliana,* contributing to improved growth of these plants [38–40]. Rhizosphere is a rich environment that presents up to 30-fold higher microbial populations including predator-prey communities than those in bulk soil [41]. *Pseudomonas fluorescens*

strains are proficient both in soil and phytosphere, and recognised to promote plant growth by competing and antagonising other pathogenic microbes [42,43]. Investigating how predator-prey interactions affect diversity and bacterial growth in soil is crucial to understand how they colonise future habitats [44]. *Acanthamoeba* was selected as a protist predator because it is a wild organism that has an ability to phagocytose on surfaces and its direct impact on phenotypic evolution of non-pathogenic prey bacteria on surfaces has received little attention.

We have previously reported on 20-day experimental co-evolution between *Acanthamoeba sp*. and *Pseudomonas fluorescens* SBW25 in which novel bacterial colony morphologies were investigated to reveal early mutations responsible for anti-predatory adaptations [5]. Biofilm formation through mutation in the *wspF* gene and the overexpression of amyloid fibrils were early adaptations to predation on solid surfaces. In that work, the effects of co-evolution on the predatory protozoa were not evaluated. Here, we report on an expanded 90-day experimental predator-prey co-evolution between these organisms with an increased number of parallel lines and the introduction of preserved protozoan predators. We explore the pattern and process of coadaptation and coevolution between protist and bacteria, particularly characteristics of bacterial survival, including the emergence of defensive traits and phenotypic evolution over coevolution. This approach allows us to study phenotypic turnover in the bacterial population and the effect of co-evolution on predator preferences in the co-evolutionary lineages. In addition, this approach enables us to observe reciprocal adaptation between predators and prey. We documented the co-evolutionary arms race between bacterial isolates and protozoan predator populations over an extended time scale. The experiment was established in two predator-prey and only-prey

groups. All replicate plates undergo 22 growth cycles (~4 days each) and 2% of each population was randomly transferred to a fresh plate for the next cycle giving ~5.6 and ~13.6 generations over four days of growth or 123.5 and 299.4 for the entire of the experiment in coevolved and prey-only populations, respectively (see method). However, we expected fluctuations in the number of cells and so in generation numbers each time that was transferred to a fresh plate and this is because of the heavy predation pressure that may limit the entirety of the prey bacteria.

Together, our experimental data show that divergent colony morphology arises as an adaptation to predation and notably affects the evolution and fitness of predators. Considering how coevolution between generalist protozoan predators and prey bacteria may structure bacterial diversity is fundamental to understanding how these organisms will evolve in the future.

Results

Ninety-day predator-prey coevolution drives bacterial diversification

In order to study the long-term effects of co-evolution between a ubiquitous generalist amoeboid predator and a non-pathogenic plant associated bacterium, we propagated nine lines of predator-prey co-evolution (CE) by washing and replating 2% of the surviving microbes and their predators on solid media for ninety days (Fig. 3.1 A). The prey bacteria, GFP labelled *P. fluorescens* SBW25, were subjected to continuous predation by a common soil-based amoeboid protozoan predator *Acanthamoeba* sp. (T2-5, EF378666.1) [45]. Alongside the nine CE lines, three lines of prey only (PO) bacterial control plates were propagated in parallel (Fig. 3.1 B).

The lines were monitored for colony morphology changes, indicative of genetic changes in individual cells, by inspecting colony forming unit (CFU) plates for non-Smooth (WT) colonies. A set of distinct colony morphologies were identified exclusively on the CE line plates. These were designated; Wrinkly Spreader (WS), Mountain (Mnt), and Volcano (Vol) (Fig. 3. 1C). Several Like Wild Type (LWT) colonies that retained the WT or Smooth colony morphology were also selected for further study. In the nine co-evolved lines, bacterial morphotypes remained Smooth for the first four transfers (16 days). After the fifth transfer novel colony morphologies were observed in the CFU plates. At this time point we also observed the appearance of microcolonies on the co-evolution plates (Fig. 3.1 D)

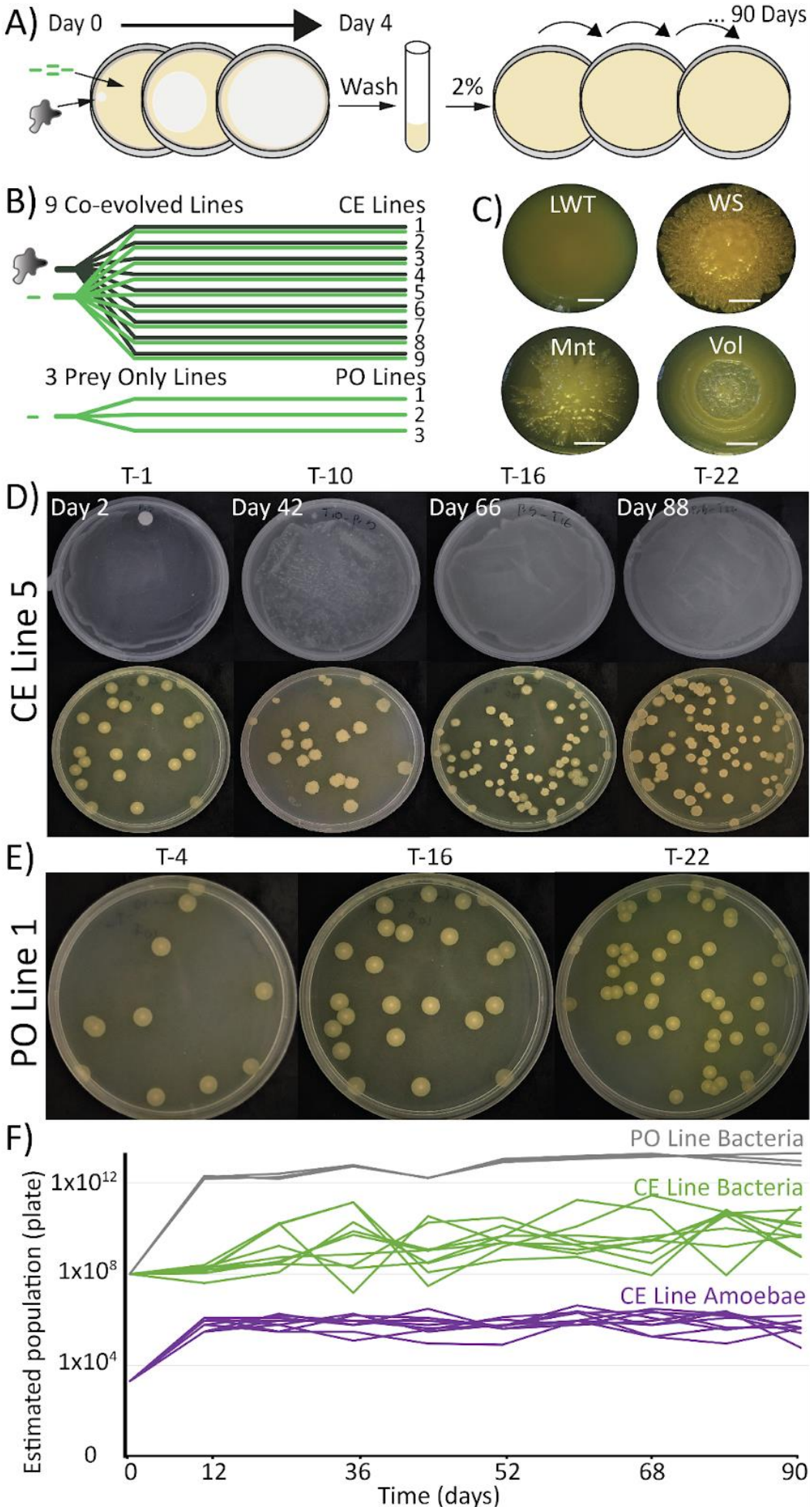
A)
Day 0
Day 4
Wash
2%
90 Days
B)
9 Co-evolved Lines
CE Lines
1
2
3
4
5
6
7
8
9
3 Prey Only Lines
PO Lines
1
2
3
C)
LWT
WS
Mnt
Vol
T-1
T-10
T-16
T-22
D)
CE Line 5
Day 2
Day 42
Day 66
Day 88
E)
T-4
T-16
T-22
PO Line 1
F)
PO Line Bacteria
CE Line Bacteria
CE Line Amoebae
Estimated population (plate)
1x10^12
1x10^8
1x10^4
0
0
12
36
52
68
90
Time (days)

Figure 3. 1**.** Experimental co-evolution of A GFP labelled *P. fluorescens* SBW25 and *Acanthamoeba* sp. A) Overview of plate transfer protocol for experimental co-evolution of *Acanthamoeba* sp. Preying on *P. fluorescens* SBW25 on solid PM plates for 90 days. Initially, $1x10^8$ bacterial cells were spread on the agar surface and $1x10^3$ amoebal cells were added on a filter paper set at the wall of the plate. Washing between transfers takes 2% of the amoebae and bacteria in the wash, the rest are cryogenically preserved for further study. B) Nine lines of CE (coevolved) predators and prey and three lines of PO (predator only) control plates were maintained for 90 days. C) Photographs of novel colony morphologies identified in the CE lines over 90-days. Four representative colony morphologies are depicted; Like Wild Type (LWT), Wrinkly Spreader (WS), Mountain (Mnt) and Volcano (Vol) phenotypes (scale bar, 15 mm). D) The appearance of the bacterial lawn during predation in the CE lines (CE Line 5 shown) at days 2, 42, 66, and 88 (top, black and white). The feeding front is visible in the first plate as amoebae emerge from the filter paper (top). Subsequent transfers include both amoebae and bacteria in washed solution so clearing and microcolonies are apparent but not a feeding front. CFU plates were used throughout evolution of the CE lines to estimate the population size at each transfer (bottom plates). Colony morphologies fluctuate as observed in CFU plates on LBA after washing the CE plate lines. E) CFU plates from the PO lines (PO Line 1 shown) do not alter in colony morphology days 16, 66 and 88 are shown. F) Population dynamics in PO and CE lines over time. Estimates obtained from CFU plate counts at the end of transfers.

As expected, colony morphologies on the three prey-only plates remained Smooth throughout the 90-day experiment. This confirmed our previous observations that growth on solid media alone does not select for mutations that manifest as colony variants [5] (Fig. 3.1 E).

Viable bacterial and amoeboid populations were monitored between passages by plating for CFU and plaque forming units (PFU) at every second transfer for 90 days and estimating the population size (Fig. 3.1 F). The three prey-only control lines reached their highest density at twelve days and remained relatively stable throughout, ranging in population from $2x10^{12}$, to $2x10^{13}$per plate. The populations of co-evolved amoebae remained relatively stable as well, ranging from $6x10^4$ to $5x10^6$ per plate in all experimental lineages (Fig. 3.1 F, Supplementary Fig. 1).

The CE prey exhibited reduced cell census counts compared to PO plates of ~10^3 fold on average per plate, presumably due to predation. There were no extinction events observed in any of the nine CE lines, but population estimates ranged over four orders of magnitude with a maximum $3x10^{11}$ per plate. In each instance in which co-evolved prey numbers were dramatically reduced, populations rapidly recovered.

Parallel phenotypic evolution in co-evolved prey

In contrast to the PO lines, bacteria from CE lines formed notably divergent colony morphologies that were apparent after 16 days of coevolution. We identified three distinct colony morphotypes; WS, Mnt, and Vol. WS colonies expected as they had been identified in the pilot predation experiment [5]. Mnt and Vol however were new colony morphologies; neither had been detected in our previous work.

We monitored the prevalence of each of these colony morphotypes on the CE lines by recording their frequencies on the CFU plates. The biofilm associated WS colony morphology performed well early on in lines 2, 4, and 5 (Fig. 3.2). However, the fate of this morphotype in each of these lineages was highly variable. In Line 2 the WS phenotype was rapidly replaced by LWT (Smooth) morphotypes at day 64, only to recover high frequency at day 90. In L4 the WS morphology dominates at the end and in L5 it is surpassed by the Mnt type. WS morphotypes were the most frequent at the end of 90 days in lines L2, L3 and L4 with final frequencies 1.0, 0.8 and 0.96, respectively (Fig. 3.2, Red).

The Mnt colony appeared after 40 days of coevolution and was found in all of the nine CE lines. In lines 2 and 9, Mnt morphotypes went completely extinct by 90 days.

However, the Mnt phenotype was the most frequent phenotype after 90 days of coevolution in L5, L6 and L8 with final frequencies of 0.7, 0.45 and 0.30, respectively (Fig. 3.2, Blue).

The Vol morphotype was never observed at high frequencies during the course of the experiment but at the end of 90 days it persisted in four lines; L1, L6, L7 and L8 at final frequencies of 0.45, 0.30, 0.60 and 0.30, respectively (Fig. 3.2, Green).

The Smooth morphotype (LWT) appeared to come to near fixation in CE line 9 after 90 days (0.99), replacing the Mnt morphotype in this line (Fig. 3.2, Black). This suggests that while we are focusing here on colony morphologies, there are fitness affecting mutations in this experiment that are not strongly influencing colony morphology. Representative isolates of LWT colony morphotypes isolated and preserved for further study (Supplementary Table 1).

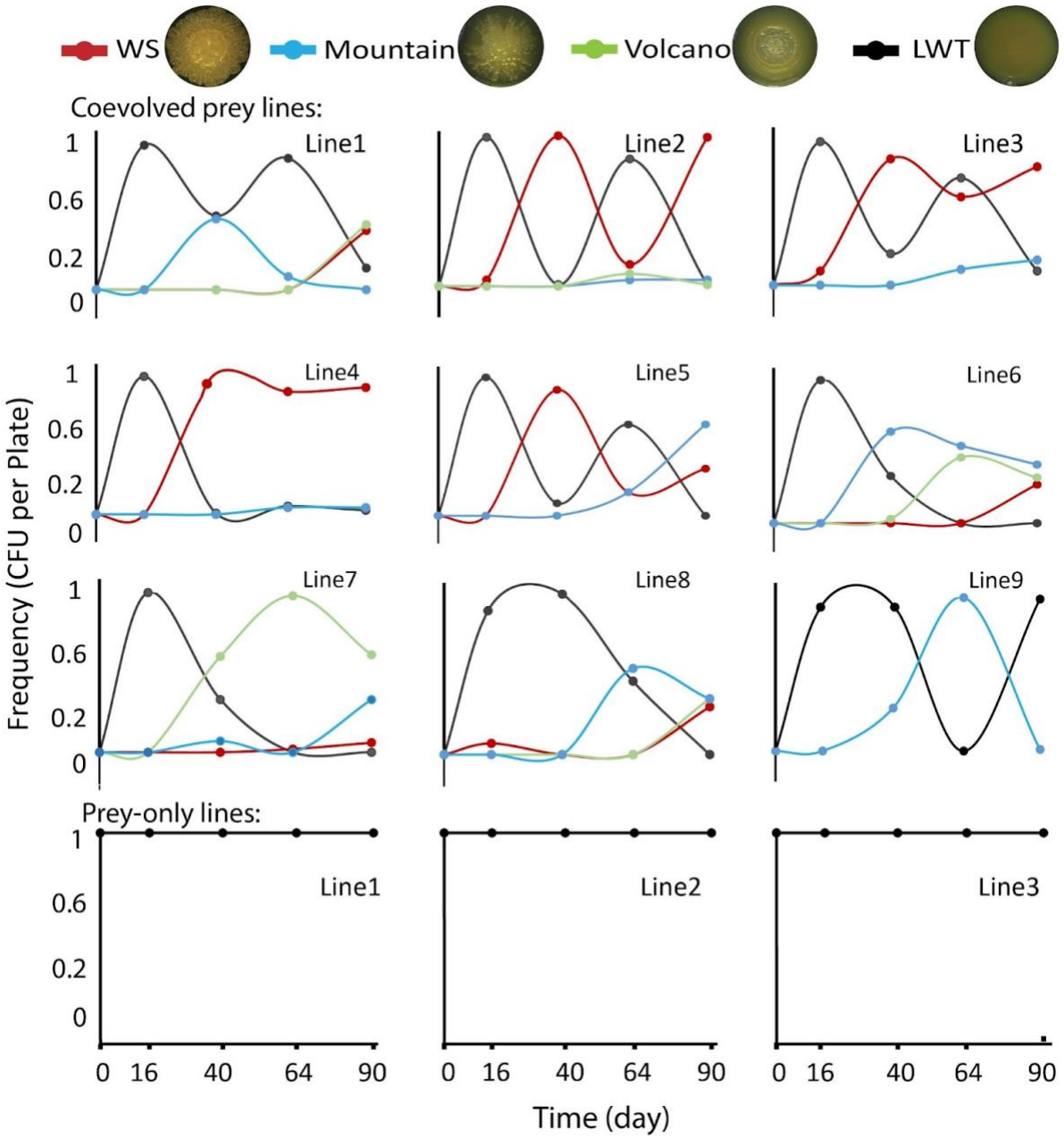

Figure 3. 2**.** Average frequency of the colonies in nine CE and three evolved PO populations based on CFU. Divergence of the bacterial colony morphologies occurs in the presence of predators but not in their absence.

Measuring colony morphotypes for anti-predator traits (investigation of special relationships)

The observation that phenotypically similar colony morphotypes (WS, Mnt and Vol) developed independently in the CE lines, and their absence in the PO lines, suggests that predation exerts a strong selection pressure on *P. fluorescens* SBW25 in these

conditions and that these bacterial colony morphotypes represent adaptations to protozoan predation. We also hypothesised that the CE *Acanthamoeba* were evolving in response to the prey and that we would see evidence of these amoebae adapting to familiar morphotypes.

We therefore performed line-test assays with a set of isolates from day 90 from different CE lines. Line-test assays allow us to measure the predation rate of the amoebae on various bacterial prey morphotypes by measuring the distance that amoebae travelled (Fig. 3.3 A). By selecting the prey and predators this assay allows us to measure the ability of CE or WT *P. fluorescens* SBW25 to resist specific predators when grown on plates. We selected five predators and 11 representative isolates; WS (L2, L6, L7), Mnt (L2, L6, L7, L9), Vol (L2, L6, L7), LWT (L9) morphotypes from different CE lines along with the WT. For each selected morphotype, we performed line tests with different *Acanthamoeba*, the ancestral predator (Anc.) or the Day 90 predator from CE lines L2, L6, L7 or L9. Ultimately, this allowed us to analyse predation by a naive ancestral predator, the co-evolved predator from the same CE line, and an evolved predator from a different CE line. In choosing the latter we attempted to identify predators with the least experience of that morphotype, though, particularly in the case of the common Mnt morphotype, this was not necessarily possible. An ancestral *P. fluorescens* SBW25 WT prey was also incorporated in the line tests as a reference.

The line test assay allows us to measure not only the predation rate of the amoebae on various bacterial prey morphotypes (Fig. 3.3 B & C) but by adjusting for prey density we can also use these data to estimate relative prey fitness, setting the least preferred

prey to 1 (Fig. 3.3 D) [46]. Based on the rate of line consumption we can confirm that the WS and Mnt colony morphologies are highly resistant to predation and that this resistance is generalizable to both Ancestral and unfamiliar CE predators (Fig. 3.3 C Red and Blue). As expected, the WS and Mnt morphotypes have higher relative prey fitness than either the WT or the LWT morphotypes indicating that the net effect of the mutations in these isolates confers generalizable resistance to predation.

We were surprised to find that the Vol morphotypes had the highest rate of line consumption and the corresponding lowest relative prey fitness of all morphotypes, including the WT (Fig. 3.3, green). This result contrasts with our observation that the Vol morphotypes appeared independently in five CE lineages and persisted until the end of the predation experiment in four of five CE lines (Fig. 3.2, Lines 1, 6, 7 & 8).

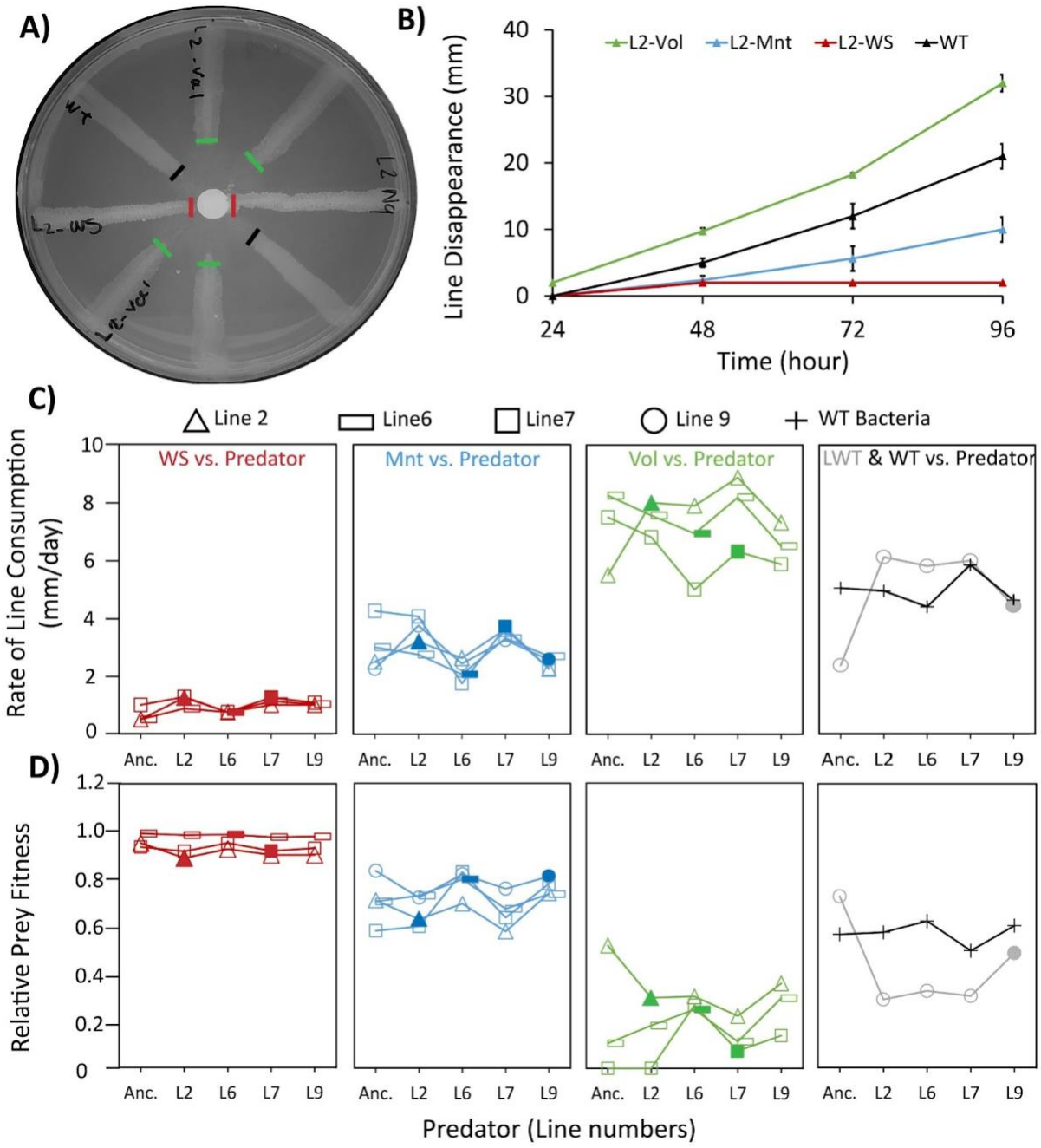

Figure 3. 3. Line test assay; Predation of ancestral and coevolved *Acanthamoeba sp.* against WT, new-evolved and coevolved *P. fluorescens* SBW25 populations. A) A representative plate showing a line test assay after 48 hours. B) Line test disappearance produced by *Acanthamoeba* predation on co-evolved isolates from line 2. Error bars indicate standard deviation (N=8). C) Predation rate of ancestral, new-evolved and co-evolved *Acanthamoeba* against evolved *P. fluorescens* SBW25 populations from the same line and the line they had not evolved within in the line test experiment. Predation rates (mm) shown per 24 hours (N=6). D) Relative prey fitness of each of the isolates in the presence of their coevolved predator and predators from the other three lines.

The line-test assay had previously been employed to measure predation resistance of both newly isolated and reconstructed prey bacteria against various amoeboid predators [45,46]. However, this method may underestimate phenotypic effects that are the result of proximity during growth. We therefore developed the Performance Assay (PA) which more closely replicates growth in the 90-day experiment by allowing bacteria and amoebae to grow near one another and estimating their respective fold population change relative to WT on full plates after four days (Fig. 3.4 A). We used the PA to test 15 CE isolate susceptibility in the presence of ancestral, CE or non-CE protozoan predation (Supplementary Table 1).

In keeping with our findings in the line test, the WS and Mnt CE isolates from distinct lines demonstrated a highly positive performance in the face of all three predator classes (ancestral, CE and Non-CE) relative to the WT prey (Fig. 3.4 B and Supplementary Fig. 3A - Red and Blue).

WS isolates exhibited increased fold survival against familiar and unfamiliar predators. Fold survival, relative to WT against the same predators, ranged from 1.9-fold to a maximum of 25-fold survival against the ancestral amoebae and from 3-fold to 35-fold increased survival in the presence of CE predators (Fig. 3.4 B & Supplementary Fig. 3A Red). The maximum observed was WS L1 which demonstrated a 782-fold increased survival over WT in the presence of non-CE L4 predators (Supplementary Fig. 3A Red).

Mnt isolates increased in their fold survival over WT from eightfold to 27-fold in the presence of ancestral predators and from 1.5-fold to as much as 27-fold in the presence of CE predators (Fig. 3.4 B, Blue).

In the presence of the ancestral *Acanthamoeba*, three out of the four Vol isolates we tested fared less well than the WT in the same conditions (Fig. 3.4 B, Green). The exception was Vol L7 which showed a 2.6-fold survival above the WT prey in the same conditions. However, what was striking was the contrast between the line test assays, and the PA test with respect to Vol survival against CE predators. In the presence of the predators that they had previously evolved with, the Vol isolates were much better off, demonstrating growth from 3.2-fold better up to a maximum of 170-fold better survival than the WT in the case of CE L1 predator (Fig. 3.4 B, Green). This result suggests that not only do the Line test assays not measure what is adaptive in the Vol isolates but that this quality requires that the bacteria be physically close during growth to their co-evolved predators. This surprising environmental factor, growth proximity to predators, did not appear to make a difference in the degree of predation resistance for either the WS or Mnt isolates.

In the presence of non-CE predators (those from other CE lines), the Vol isolates showed variable fold change differences (Supplementary Fig. 3A, Green). For example, the L4 predator was used in the PA for three of the four Vol isolates and though Vol isolates were never observed in L4, the fold values for this morphotype ranged from ~2-fold decrease in survival to a maximum of 80-fold increase in survival (relative to WT). These results suggest that the effects the Vol colonies are having on

interactions with predators can vary widely and may imply that this morphotype is a host to hidden mutational depths (Supplementary Fig. 3A, Green and Table 1).

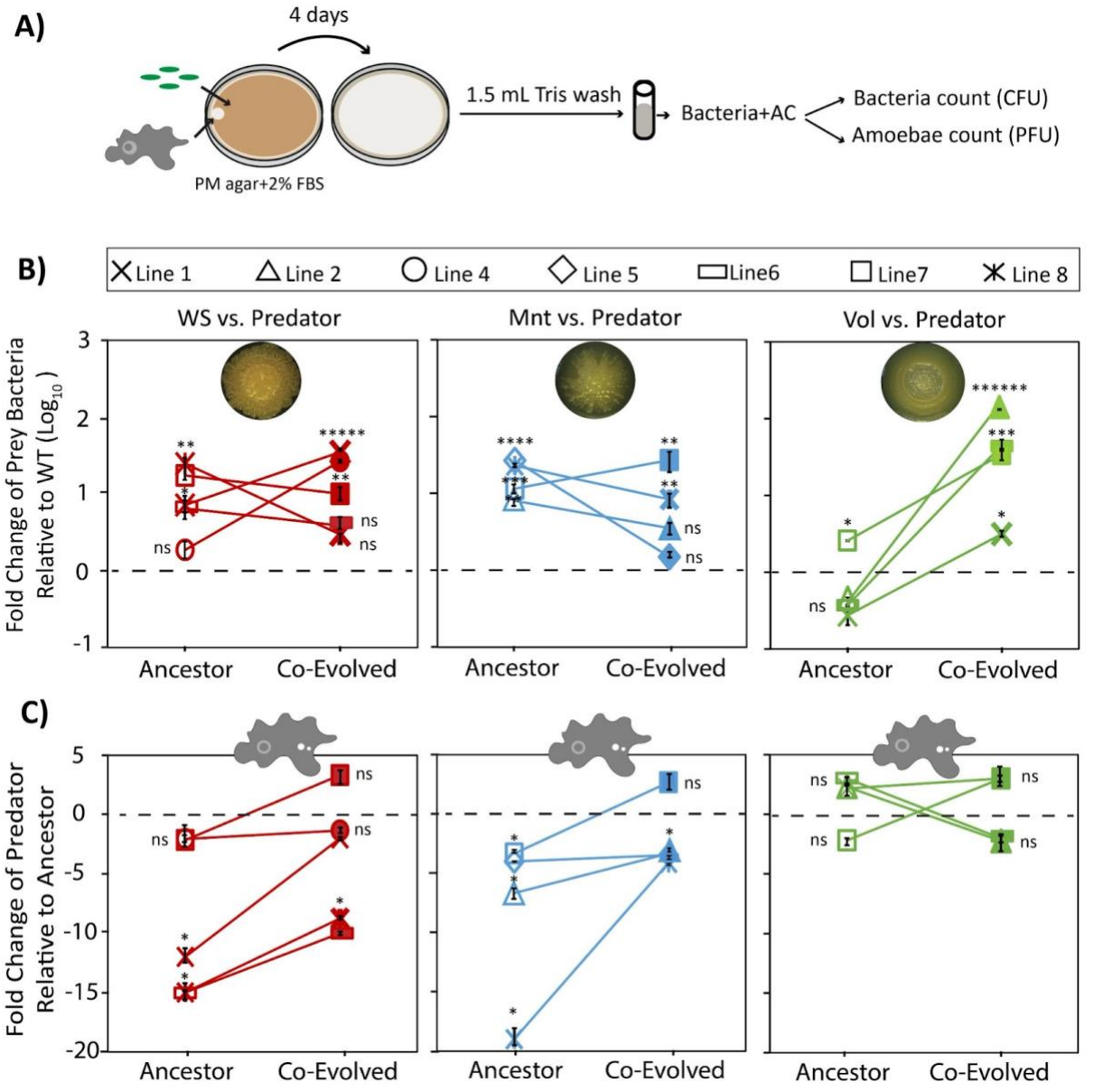

Figure 3. 4**.** Performance test assay results; A) A diagram describing the performance test assay the critical difference being that bacterial prey and amoeboid predators grow and divide in close proximity during predation in the PA. B) The fold change in the number of the bacterial population (CFU) after four days of predation by ancestral and coevolved *Acanthamoeba sp*. relative to WT prey while growing with ancestral predators (dashed lines) (n=6, *P≤ 0.08, **P≤ 0.007, ***P≤ 0.0003, ****P<0.00002, ******P< 0.0000009 Two sample T tests, relative to WT). C) Fold change in the number of ancestral and co-evolved *Acanthamoeba* (PFU) as a result of predating upon CE isolates relative to the population size of ancestral predators consuming the WT prey (dashed lines). Error bars represent standard deviation (n=6, *P≤ 0.08, Two sample T tests, relative to Ancestor).

Anti-predation strategies can take many forms. The success of the CE bacterial isolates could be explained by an evolved ability to limit the growth of *Acanthamoeba* by becoming toxic or otherwise inedible. Our pilot experiment showed that the WS phenotypes formed strong biofilms that made the bacterial prey inedible to the *Acanthamoeba* [5]. In order to gain insight into the wellbeing of the predators in the presence of these prey we took advantage of the PA PFU measurements to estimate the fold change in each of the three predator classes (Anc., CE, and non-CE) while growing on WS, Mnt or Vol isolates. We report these in terms of the fold change in population size after predation, relative to the growth of ancestral predator on the WT prey (Fig. 3.4 C).

When predating upon WS and Mnt isolates the *Acanthamoeba* cells did not replicate as well as the ancestral predator did on the WT prey (Fig. 3.4 C, Red and Blue). When the predators were provided with the WS or Mnt isolates with which they had co-evolved they generally performed better than the ancestral predators on the same strains but most did not grow better on these strains than they did on the WT. The exception was the CE L7 predator, which had marginally improved replication on CE WS and MNT prey over the ancestral *Acanthamoeba* growing on WT (Fig. 3.4 C). The L7 Mnt prey supported a 3-fold increase in L7 CE predator population and the L7 WS supported a 3.5-fold increase over ancestral predator on WT prey. These data suggest that the L7 predator has adapted to consuming these prey bacteria, this is also the single CE line in which Vol was thriving by the end of the 90 day experiment (Fig. 3.2).

The non-CE amoeba from selected lines demonstrated generally lower growth on either the WS isolates (~14 to 2-fold change) or the Mnt isolates (5 to 2-fold change)

(Supplementary Fig. 3B - blue and red lines). This supports the idea that the mutations that underlie these colony morphologies are general anti-predator strategies.

Interestingly, under the same conditions, the Vol isolates appear to support ancestral and CE growth better than the WS or Mnt isolates. Vol supported population growth closer to that of the WT ranging from fold differences of between -2.2 to 3. The growth of CE amoebae were similar (fold change difference from -2.25 to 3) (Fig. 3.4 C and - green lines). We found similar results when Volcano isolates were provided to non-CE predators with fold change differences ranging from -2.1 to 3.5 (Supplementart Fig. 3B - green lines). Remarkably, the Vol isolates consistently showed evidence of supporting roughly WT growth of the *Acanthamoeba,* whether they had coevolved with the predators or not. The Vol cells were being eaten less, particularly by the CE predators (Fig. 3. 4B, Green), but in our measurements, this was not having a negative effect on the population of the predators (Fig. 3.4 C, Green).

Predator specialisation

Acanthamoeba is a generalist predator that, under normal circumstances, maintains a flexible predation strategy in a diverse microbial prey environment. The observation that Ancestral, CE, and non-CE predators had varying success with diversifying prey raised the question as to whether predator adaptation to *P. fluorescens* SBW25 had also occurred during 90 days of coevolution. We first conducted line tests to calculate the efficiency of the evolved *Acanthamoeba* cells when predating upon WT prey populations. We observed that the ancestral predators were able to consume 20 mm of the WT prey over four days whereas, all CE predators with the exception of CE L3 appeared to have evolved increased consumption rates on ancestral prey of between

22 - 32 mm over four days (Supplementary Fig. 4). This suggested to us that during 90 days of CE our natural isolate of *Acanthamoeba* spp. have evolved to improve their predator efficiency on the WT *P. fluorescens* SBW25.

To further examine evolution in the CE predators we sought to determine if the increased speed in the line test assay resulted from a generally improved growth rate on agar plates. We performed the PA and calculated the number of the *Acanthamoeba* cells produced during predation upon WT prey. Similarly, we found all CE predators have a higher generation rate compared to the ancestral predator while consuming the WT bacteria (Fig. 3.5).

Line 9 exhibited a higher and Line 7 lower generation numbers (on average 11.5 and 9.5, respectively), but overall greater than ancestral *Acanthamoeba* (on average 9.2). This suggests that coevolution with prey conferred a rapid replication rate on coevolved predators in the presence of WT prey. Generally, CE predators demonstrated improved growth on P. fluorescens SBW25 WT as measured by the number of generations achieved on this prey. This indicates that the CE predators are doing better than the ancestral predator and suggests prey diversification had a positive effect on predator efficiency. Previous results point to the advantage of the coevolved over ancestral predator. To investigate the degree to which the speed and reproduction rate of the coevolved predators contributed to WT prey survival, we further allowed *Acanthamoeba* lines to predate upon WT prey for a 4-day-cycle under the same condition as in the 90-day experiment. The population sizes of the WT bacteria to a greater degree were reduced by all coevolved lines. WT prey bacteria demonstrated a greater survival when subjected to the ancestral predator ($2x10^8$),

while in the presence of the CE predators, WT bacteria exhibited notably a lower survival rate (ranging from 10^6 to $1.5x10^8$ cells) (Fig. 3.4 C).

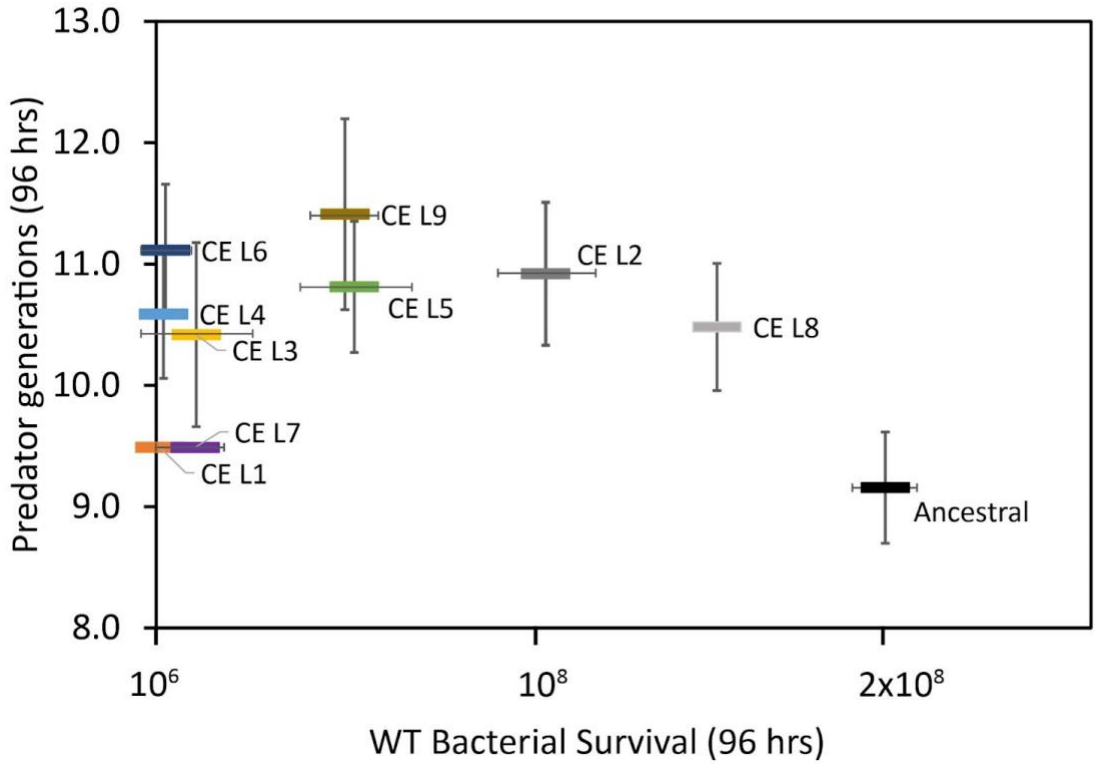

Figure 3. 5**.** Evidence of coevolved predator efficacy on WT prey. Performance test assay accomplished with CE and ancestral predators on WT prey. Generation rate estimated based on PFU of CE and ancestral *Acanthamoeba* after 4 days feeding upon WT prey; CE predators achieved more generations than their ancestors over four days while growing on WT prey and, lower survival of WT prey when encountered with CE predators in comparison with their ancestors. The differential survival rate in WT prey when subjected to CE predators is a product of the positive predator activity.

Discussion

Overall, experimental evolution has afforded a remarkable approach to understanding the ecological [47,48] and evolutionary process [49,50]. This experimental system allows us to identify evolutionary changes in bacteria as an adaptive response to protozoan predation and observe the effect of this on predator evolution. Here, we

conducted a 90-day predator-prey coevolution experiment on solid surfaces to evaluate the phenotypic turnover in *P. fluorescens* SBW25 prey population in response to predation and the effect of this coevolution on *Acanthamoeba spp*., a generalist amoeboid predator.

We observed stable populations of both prey and predator that do not appear to show waves of predominance predicted mathematically [51]. This may be because we do not have the time scale or numerical resolution to observe this effect [52]. Alternatively, this may be due to the conservative nature of *Acanthamoeba* as predators which switch to an encysted developmental state once local resources become limited [53]. We observed the maintenance of both populations in our pilot experiment as well [5]. The population sizes of predators remained relatively stable throughout ($6x10^4$ to $5x10^6$ cells/plate) and predation did not lead to extinction events in either the bacterial or amoebal populations. This is consistent with empirical studies between *E. coli* and *S. cerevisiae* that results in coexistence of both organisms [54]. This indicates coadaptation of both prey and predator over evolutionary time scale suggestive of Red Queen Coevolution. Importantly, in this extended solid surface propagation, prey-only lines did not develop new colony morphotypes over 90 days. However, at 16 days novel colony morphotypes were observed in the CE lineages. This strongly suggests that predation pressure drives higher prey diversity in this structured environment and that WS, Mnt and Vol morphotypes are anti-predator adaptations that evolved with a high degree of parallelism in the CE lines.

We have previously described the WS types that are the result of mutations in *wspF* and *amrZ* genes, responsible for anti-predatory adaptations [5]. However, as the

coevolution progressed other colony variants such as LWT, Vol and Mnt were observed as well. These morphotypes exhibited variable frequencies over the 90-day experiment, and were retained until the end of the predation experiment. Variation in a clonal level as an adaptation to a new niche is very common among bacterial populations [55] and this has been previously well observed in the populations of *P. fluorescens* SBW25 when competing for the resources in a liquid environment [56]. In this study we observed a high degree of parallel phenotypic evolution across CE lines undergoing predation on solid surfaces. Phenotypic convergence and evolution of similar traits in the replicates of multiple populations is very likely to arise among microorganisms [57] when exposed to homogenous environmental pressures [58,59]. High degrees of genotypic and phenotypic parallelism previously have been observed in the experimental coevolution of bacterial prey *Escherichia coli* and generalist bacterial predator *Myxococcus xanthus [12]*. However, such evolution of parallel colony diversification within prey populations undergoing predation in a structured environment have not been detected previously. Because of the strong identical predation pressure among coevolved prey and lower chance of bacterial competition for resources in a structured environment like the plate-constrained, it is not surprising to see the parallel adaptive phenotypic evolution in *P. fluorescens* SBW25.

In this study, parallel phenotypic evolution was found to be strongly accelerated under a predation regime. The WS and Mnt morphotypes were found in eight and nine of the CE lines, respectively and Vol was observed in four lines. Such observation predicts that predation pressure strongly tends to drive the evolution of defensive traits that can be beneficial in the face of stranger microorganisms. WS and Mnt isolates were highly resistant to all three *Acanthamoeba* classes (Ancestral, CE, and non-CE). Our results

strongly support that predation by generalist protists on a solid environment drives parallelism and colony morphology divergence that have emerged that have not been observed previously.

Strikingly in the line test assay we found the Vol morphotypes were defenceless against all three predator classes. This suggested that either the niche these bacteria were occupying in the experiment was not related to predator resistance, which seemed unlikely, or that our method of testing predation preference was not capturing this anti-predator strategy appropriately. This line of thought led us to develop a new method for measuring prey fitness which is closer to the conditions of the CE lines; the performance test assay. This method also has the advantage of measuring the populations of *Acanthamoeba* in the same experimental trial, which we will discuss in turn.

We subjected multiple WS, Mnt and Vol isolates to this modified performance test and observed that the WS and Mnt isolates consistently demonstrated increased survival (relative to WT) in the face of all three predator classes (ancestral, CE, and non-CE) (Fig. 3.4 B). These results suggest that the WS and Mnt morphotypes are generalisable anti-predator adaptations. In the case of the WS, the nature of this adaptation is most likely the production of extracellular cellulose. WS colony morphotypes of *P. fluorescens* SBW25, when investigated molecularly, have previously been demonstrated to be associated with mutations that increase cyclic di-GMP levels in the cell resulting in the production of extracellular cellulose [5,60,61]. As a response to predation, constitutive biofilm production is expected to evolve in bacteria as an adaptive mechanism [62]. Biofilm formation appears to be a common

response of *Pseudomonads* to ecological challenges, aside from protozoan predation, including AL interfaces [56], the CF lung [63], and even space travel [64]. It is likely that this is due to the numerous negative genetic repressors responsible for regualting this trait, which provide a large target for random mutations. [65]. Confirming the nature of the WS mutations in this experiment and investigating the nature of the Mnt mutations will be the subject of further research.

Intriguingly, in the performance test assay all the CE Vol strains performed very differently than they did in the line tests. Specifically, we observed that the Vol isolates were more resistant to predation than the WT when subjected to their CE predators (Fig. 3.4 A). Similarly, higher resistance of populations of *P. fluorescens* to their contemporary phages have been observed in soil environments when subjected to the lytic bacteriophage SBW25ϕ2 [66]. This result suggests not only co-adaptation between CE predators and prey, but also that some critical aspect of the relationship between them was not captured in the line tests. In the line test, the prey grows in advance of exposure to the predator and are therefore naive to their presence. The dramatic improvement in survival in the performance test (line test average fitness, 0.2 and 3.7 smaller than WT vs. performance test average fold change, 63 times greater than WT) suggests that exposure or proximity to the *Acanthamoeba* is stimulating the anti-predator trait in the bacteria in advance of phagocytosis. Several possibilities and parallels come to mind. It appears that the *P. fluorescens* Vol cells become predation resistant only in the presence of the *Acanthamoeba*. This suggests a molecular or gene regulation change that is taking place. This may be stimulated by cell to cell signalling on the part of the bacteria, similar to quorum sensing in the *P. aeruginosa,* [67] or this might be an indication that some molecular or chemical change in the

bacteria that is precipitated by the presence of the *Acanthamoeba* directly. Unravelling the molecular nature and mediator of this predator induced anti-predatory effect in the Vol morphotypes requires further study.

Changes in preference or behaviour were also noted in the predators during coevolution. Although in the performance assay the WS and Mnt morphotypes were able to extremely resist predation and the resulting *Acanthamoeba* populations were reduced compared to predation on WT prey, *Acanthamoeba* cells were able to persist in these environments. Moreover, amongst the Day 90 predators were the CE *Acanthamoeba* from Line 7, which had improved in their ability to eat either the WS or Mnt isolates to the degree that the ancestral predator did on the WT prey (3 and 3.5-fold increase respectively). We hypothesise that these WS or Mnt bacteria anti-predation traits are general, meaning that these strategies may confer resistance to other predators as well (cross-resistance) [68].

On the other hand, in the same experiment, when Ancestral or CE *Acanthamoebae* were grown on Vol isolates, the population sizes of the predators remained stable and were not significantly different from Ancestral predation on WT prey (Fig. 3.4 C). Taken together, it appears that the Vol morphotypes survive better when predated upon by their CE predators, whilst these predators do not suffer population declines in concert with this presumed prey “escape”. In the previous study we found that predation of WT prey resulted in higher mortality (10% cell death) in the *Acanthamoebae* but not in the presence of evolved isolates [5]. This may be the place where improvements are happening, less *Acanthamoeba* death and better bacterial replication. Once again, these results suggest a specific adaptation to predation and hint at a “special

relationship" evolving between the Vol isolates and their CE predators that merits further investigation (Fig. 3.4 C). Given that, in this study, we further confirmed an increase in the predation speed of the coevolved amoebae populations while predating upon WT prey (Supplementary Fig. 3). Coevolved predators appeared to achieve higher generations and their killing performance has accelerated compared to their ancestral amoebae (Fig. 3.5).

Protozoan predation is an important mediator of bacterial populations in nature [6]. The power of these bacterial antagonists has been recognized previously but there has been a dearth of studies on the long term genotypic and phenotypic effects these keystone predators have on bacterial prey on solid surfaces. Growth on the surface where most part of life happens [69] offer several advantages, some of which allow bacterial cells to first attach and aggregate and second increase their survival to a high-density form [70]. The establishment of dense populations on surfaces therefore provide microbes, nutrients and protection from various environmental stressors like predatory organisms, antibiotics and other invading bacteria [62,71,72]. Biofilm formation has previously been demonstrated to be a successful defence strategy of *P. fluorescens* SBW25 against free-living ciliate predators in liquid environments [73–75]. In addition, amoebae isolated from diverse environmental samples were recognised often to be in close contact with the bacterial biofilm community [76]. This suggests that predation by amoebae can contribute to the development of anti-predatory traits such as biofilm formation and this can be correlated with increased virulence of these bacterial organisms in the future [62,77,78].

The prey and predator interactions are not only omnipresent in nature. In this study the resistant strategies that bacteria have employed to avoid phagocytosis and increase their survival under strong predation pressure are similar to the scenarios where bacterial pathogens evolve under multiple host-specific pressures such as immune cells, lack of oxygen and antibiotic therapy [79,80]. Some of which are important general defensive-features that have been observed in pathogenic bacteria while infecting other eukaryotic hosts [81,82]. It has been suggested that *Acanthamoeba* and phagocytic immune cells such as macrophages are structurally similar [83–86]. Similar bactericidal strategies are used by amoebae and macrophage and mechanisms that bacteria employ to resist and exploit these hosts remained almost the same in many bacteria [87–89]. Thus, the coevolution power and the improved traits observed in prey and predator in this study are key factors to understand how organisms survive under strong selective pressure and how these traits benefit them while colonising other niches [90].

Finally, in our work, contrary to the ecological theory, the interaction between protozoa and bacteria resulted in the coexistence of both species [54] and stable populations [91]. In addition, from performance test assay the continual coadaptation and population trends of coevolved predator, suggests improved predator efficiency representative of a form of Red Queen coevolution [12,66,92]. This is consistent with previous empirical studies demonstrating that predator-prey coevolution increases molecular evolution, phenotypic divergence and specialised traits in both prey and predators. [54,93–95].

By showing the evolution of parallel colony variants in prey and that they are resistant to predation, we support both the ecological causes and the evolutionary significance of adaptive phenotypic diversification among *P. fluorescens* SBW25 populations. The consistent predation by a single predator can select for permanence in traits (like biofilm formation) that are generally regulated by gene expression changes. Predators that are phagocytic are a normal part of bacterial life on surfaces from soil particles, leaves or animal tissues. This experiment aims to help us understand the factors that prompt adaptation to predation over different time scales in this short time frame (of 90 days) therefore, we can better understand both the traits that they can deploy in a short time (hours). In addition, this can provide a framework to consider how long-term predation pressure may affect the suite of parallel defensive traits that a bacterium might deploy over evolutionary time scales to adjust its relationship with a consistent predator in the environment. The results of this work can apply to understand bacterial stability, function of ecological interactions, bacterial resistance, and the evolution of parasites.

Materials and Methods

Strains and media. A GFP tagged strain of *P. fluorescens* SBW25 (NC_012660.1) [96] grown in Lysogeny Broth (LB) [97] and protozoan strain *Acanthamoebae* sp. T2-5 (EF378666.1) propagated on modified solid PM media [98,99] were used as model organisms in this experiment as described in chapter 2.

Amoebae were cultivated on WT bacterial prey before experimental evolution on medium-sized Petri plates (90 x 15mm). *Acanthamoebae* stock was regularly stored in a 2 mM Tris HCL buffer (121.1 g Tris base in 800 mL H_2O, 60 mL HCl to get pH 7.6

(autoclaved or filter sterilised) at room temperature [101]. For long-term storage and where required, *Acanthamoebae* cells were frozen for a final concentration of 7.5% DMSO at -200°C in liquid Nitrogen (N2). Plaque Forming Unit was performed using supplemented PM media [100] as described previously.

Ninety-day experimental evolution. Nine replicate plates of predator-prey and three populations of only-prey were propagated on modified PM media supplemented with 2% FBS (4 g difco bacto peptone, 2 g dextrose, 1.5 g K2HPO4, 1 g KH2PO4 and 20 g agar (2%) per litre H2O) at 28°C [98,99]. In order to investigate the degree to which protozoan predation contributes to the evolution of bacterial characteristics, we established a 90-day evolution experiment. *P. fluorescens* SBW25, a non-pathogenic plant-associated bacterium, was subjected to continuous predation by common soil-based protozan predator *Acanthamoebae* sp. A single culture of GFP labelled WT *P. fluorescens* SBW25 bacteria was split into twelve populations and grown for 90 days on a solid PM supplemented media. Nine lineages were propagated with *Acanthamoebae* sp. protozoan predators and three lineages as control were propagated in the absence of protozoan predators**.**

We established nine predator-prey lines, where *Acanthamoebae* sp. were allowed to depend on prey and three predation-free lines, where *P. fluorescens* SWB25 solely were evolved. All organisms were cultivated in PM agar media that was supplemented with 2% Fetal Bovine Serum (FBS) to minimise the likelihood of extension events occurring in the populations of *Acanthamoeba sp.* coevolving with prey bacteria. Both predation and only-prey lineages undergo 22 growth cycles (~98 hours each and in a total of 90 days). At the end of each cycle, the lawn of the surviving prey bacteria and

protozoan predators or prey-only controls were each washed with 5 mL of Tris buffer. Randomly, 2% of the washed solution in 100 µl containing on average $2x10^5$ to $4x10^9$ bacterial and $2x10^3$ to $6x10^4$ protozoan cells was transferred to fresh solid FBS supplemented PM plates for the next cycle. Similarly, 2% of the prey-only control solution containing $3x10^{10}$ to $2x10^{11}$ bacterial cells were transferred to new plates as mentioned above. However, we expected that there might be fluctuations in the number of cells each time that was transferred to a fresh plate and this is because of the heavy predation pressure that may limit the availability of the prey bacteria.

At each transfer the wash from the coevolution plates were subjected to centrifugation at 400 g for 3 minutes in order to separate the amoebae (primarily in their encysted state) from bacterial cells. The supernatant containing bacterial cells along with the wash from the prey-only group was transferred to new tubes and subjected to centrifugation at 7000 g for 5 min to pellet the bacterial cells. Bacterial cells were frozen in equal parts for a final concentration of 4.25% NaCl and 35% glycerol at -80°C. To reliably cryopreserve *Acanthamoebae* sp*.,* during the course of the experiment, the pellet containing protozoan cells were frozen for a final concentration of 7.5% DMSO at -200°C in liquid Nitrogen (N2) for further investigation.

Colony morphology measurement. In order to examine the abundance of the colony morphotypes in each evolutionary line during the experiment, bacterial cultures from none-predation and predation groups on day 16, 40, 64 and 90 were grown overnight in LB from -80°C glycerol stocks. Cells were then serially diluted and plated for CFU on LBA pates in order to yield 20-30 colonies on a total of three replicate plated. Plates

were incubated at 28°C for 4-5 days, the number of colonies was recorded and photographed when required.

Line test assay and prey fitness. Line test assays were performed as previously described [46]. Predation rates were calculated as the average of the rate of line disappearance over time for each evolved type over at least eight replicate plates. These were adjusted for absolute bacterial density based on relative CFU of the lawn of the isolates. Prey fitness values were calculated by multiplying the overall rate of predation (mm/96 hours) by the normalised cell density (cells/mm), normalising relative prey fitness (cells/96 hours) to set the value of the least-preferred mutants (WS) to 1 and the most preferred mutant to 0 (Volcano).

Performance test assay. Overnight cultures of bacterial isolates were grown in LB from -80°C glycerol stocks. Co evolved and ancestral protozoan strains were revived from liquid N2 by incubating them at 35°C for 5 minutes. Protozoan cells were amplified in PM plates supplemented with 2% FBS by adding 10 µl of the cells on a lawn of WT bacteria. Plates were incubated up to five days at 28°C and harvested by washing off the plates using 1 µl sterile loop with 2 mM Tris HCL buffer. The washed solution was subjected to the centrifugation at 400 g for 3 minutes in order to separate the amoebae from bacteria. The pellets containing protozoan cells were collected, transferred into an Eppendorf tube containing 400 µl Tris buffer and stored at room temperature. Prior to the experiment, plaque test assay was performed in order to achieve the absolute number of the alive *Acanthamoeba* cells in each line. The bacterial performance assays were performed on solid PM agar plates supplemented with 2% FBS. To estimate the growth rate of bacterial lines in the absence of protozoa, replicate cultures of $1x10^7$ bacteria (30 µl) were spread on small Petri plates (35 x10

mm). For the predation group, $1x10^7$ bacteria (30 µl) were spread in the same way and quantities of ancestral, evolved, and coevolved *Acanthamoeba* cells in the volume of 2 µl ($1x10^3$) were subsequently added to one edge of each plate. All plates were wrapped in parafilm and incubated for days at 28°C. Plates were washed with 1.5 mL Tris HCl buffer, serially diluted, and plated for CFU and PFU on LBA and PM plates respectively in order to obtain 20-30 bacterial colonies and 5-10 protozoan plaques.

The fold numbers of the bacteria and protozoa were calculated based on the number of the bacterial and amoebae populations after four days of growth together on PM plates. The WT *P. fluorescens* SBW25 and ancestral *Acanthamoeba* populations while growing in the presence of each other were used as the baseline (equal 0). A simple estimate of absolute fold numbers was generated by using the formula: *(Y - X)/X* or equivalently *Y/X - 1.* Where Y is the number of WT + Ancestral cells in four days (original value), *X* is the estimated CFU/PFU of the bacterial/protozoan cells after 96 hours of growth, respectively (final value). Bacterial number was calculated while under predation by *Acanthamoeba* and amoebae population while predating upon bacterial isolates after four days as mentioned above.

Predator generation and prey survival. To evaluate the predator generation on WT prey bacteria, performance test assays were conducted. The bacterial and various protozoan strains of interest were prepared as mentioned above. Cells were allowed to interact for four days and then washed off using 1.5 mL Tris HCl. The wash solution containing *Acanthamoebae* was subsequently diluted and plated for PFU. A simple estimate of predator generation numbers were generated by assuming that the *Acanthamoebae* were undergoing binary fission and solving for *G* using the formula:

$F = S \times 2^G$. Where G is number of generations, *F* is the estimated PFU of the amoebae after 96 hours of predation, and S is the PFU of the amoebae plated when predation began. Bacterial survival was calculated after four days of predation by *Acanthamoeba* as mentioned above. Cells washed, diluted, and were plated for CFU on LBA to yield 10-15 colonies.

Microscopy and image analysis. Colony images: Colony morphology images were carried out using a Zeiss dissecting microscope (Stemi 2000-C). Phase contrast images were acquired using SwiftCam x 0.5 and 1.2 objective (MA95011). Cell and colony images were processed in ImageJ as described in figure legends.

Amoebae and bacteria visualisation: cells were harvested from actively growing PM plates using a 1 µl loop placed and distributed gently on a glass microscopic slide on an agarose pad (M9 media +1% agarose). Cells were allowed to dry and were then covered with a glass cover slip. Images were acquired using PH and GFP filter channels (excitation 80 and 250 nm, respectively) at 100x phase objective (Olympus BX51).

References

1. Pontarp M, Petchey OL. Ecological opportunity and predator–prey interactions: linking eco-evolutionary processes and diversification in adaptive radiations. Proceedings of the Royal Society B: Biological Sciences. 2018. p. 20172550. doi:10.1098/rspb.2017.2550.
2. Cavalier-Smith T. The phagotrophic origin of eukaryotes and phylogenetic classification of Protozoa. Int J Syst Evol Microbiol. 2002;52: 297–354.
3. Thompson JN. Rapid evolution as an ecological process. Trends in Ecology & Evolution. 1998. pp. 329–332. doi:10.1016/s0169-5347(98)01378-0

4. Hairston NG, Ellner SP, Geber MA, Yoshida T, Fox JA. Rapid evolution and the convergence of ecological and evolutionary time. Ecology Letters. 2005. pp. 1114–1127. doi:10.1111/j.1461-0248.2005.00812.x.

5. Golzar FS, Ferguson GC, Hendrickson HL. Protozoan predation drives adaptive divergence in *Pseudomonas fluorescens* SBW25; ecology meets experimental evolution. doi:10.1101/2021.07.12.452127.

6. Fenchel T. Ecology of Protozoa: The Biology of Free-living Phagotropic Protists. Springer-Verlag; 2013.

7. Gallet R, Alizon S, Comte P-A, Gutierrez A, Depaulis F, van Baalen M, et al. Predation and disturbance interact to shape prey species diversity. Am Nat. 2007;170: 143–154.

8. Bar-On YM, Phillips R, Milo R. The biomass distribution on Earth. Proc Natl Acad Sci U S A. 2018;115: 6506–6511.

9. Leibold MA, Chase JM, Shurin JB, and Downing AL. SPECIES TURNOVER AND THE REGULATION OF TROPHIC STRUCTURE. Annual Review of Ecology and Systematics. 1997. pp. 467–494. doi:10.1146/annurev.ecolsys.28.1.467.

10. Estes J, Crooks K, Holt RD. Predators, Ecological Role of. Encyclopedia of Biodiversity. 2013. pp. 229–249. doi:10.1016/b978-0-12-384719-5.00117-9.

11. Ghoul M, Mitri S. The Ecology and Evolution of Microbial Competition. Trends Microbiol. 2016;24: 833–845.

12. Nair RR, Vasse M, Wielgoss S, Sun L, Yu Y-TN, Velicer GJ. Bacterial predator-prey coevolution accelerates genome evolution and selects on virulence-associated prey defences. Nat Commun. 2019;10: 4301.

13. Van Valen L. Theory in Abstracts. BioScience. 1973. pp. 626–626. doi:10.2307/1296773.

14. The coevolution of predator—prey interactions: ESSS and Red Queen dynamics. Proceedings of the Royal Society of London. Series B: Biological Sciences. 1992. pp. 133–141. doi:10.1098/rspb.1992.0141.

15. Pernthaler J. Predation on prokaryotes in the water column and its ecological implications. Nat Rev Microbiol. 2005;3: 537–546.

16. Pérez J, Moraleda-Muñoz A, Marcos-Torres FJ, Muñoz-Dorado J. Bacterial predation: 75 years and counting! Environ Microbiol. 2016;18: 766–779.

17. Polis GA. Complex Trophic Interactions in Deserts: An Empirical Critique of Food-Web Theory. The American Naturalist. 1991. pp. 123–155. doi:10.1086/285208.

18. Hilbi H, Weber SS, Ragaz C, Nyfeler Y, Urwyler S. Environmental predators as models for bacterial pathogenesis. Environ Microbiol. 2007;9: 563–575.

19. Weekers PHH, Bodelier PLE, Wijen JPH, Vogels GD. Effects of Grazing by the Free-Living Soil Amoebae *Acanthamoeba castellanii*, *Acanthamoeba polyphaga*, and

Hartmannella vermiformis on Various Bacteria. Applied and Environmental Microbiology. 1993. pp. 2317–2319. doi:10.1128/aem.59.7.2317-2319.1993.

20. Pal C, Maciá MD, Oliver A, Schachar I, Buckling A. Coevolution with viruses drives the evolution of bacterial mutation rates. Nature. 2007;450: 1079–1081.

21. Chevallereau A, Pons BJ, van Houte S, Westra ER. Interactions between bacterial and phage communities in natural environments. Nat Rev Microbiol. 2021. doi:10.1038/s41579-021-00602-y.

22. Sommer U. The impact of herbivore type and grazing pressure on benthic microalgal diversity. Ecology Letters. 1999. pp. 65–69. doi:10.1046/j.1461-0248.1999.22052.x.

23. Brockhurst MA, Morgan AD, Fenton A, Buckling A. Experimental coevolution with bacteria and phage: The *Pseudomonas fluorescens*—Φ2 model system. Infect Genet Evol. 2007;7: 547–552.

24. Morgan AD, Buckling A. Parasites mediate the relationship between host diversity and disturbance frequency. Ecology Letters. 2004. pp. 1029–1034. doi:10.1111/j.1461-0248.2004.00670.x.

25. Filip J, Bauer B, Hillebrand H, Beniermann A, Gaedke U, Moorthi SD. Multitrophic diversity effects depend on consumer specialization and species-specific growth and grazing rates. Oikos. 2014. pp. 912–922. doi:10.1111/oik.01219.

26. Wohlgemuth D, Filip J, Hillebrand H, Moorthi SD. Prey diversity effects on ecosystem functioning depend on consumer identity and prey composition. Oecologia. 2017. pp. 653–661. doi:10.1007/s00442-017-3892-6.

27. Huang W, Traulsen A, Werner B, Hiltunen T, Becks L. Dynamical trade-offs arise from antagonistic coevolution and decrease intraspecific diversity. Nat Commun. 2017;8: 2059.

28. Hillesland KL, Velicer GJ, Lenski RE. Experimental evolution of a microbial predator's ability to find prey. Proc Biol Sci. 2009;276: 459–467.

29. Donlan RM. Biofilms: Microbial Life on Surfaces. Emerging Infectious Diseases. 2002. pp. 881–890. doi:10.3201/eid0809.020063.

30. Visvesvara GS, Moura H, Schuster FL. Pathogenic and opportunistic free-living amoebae: *Acanthamoebaspp*, *Balamuthia mandrillaris*, *Naegleria fowleri*, and *Sappinia diploidea*. FEMS Immunology & Medical Microbiology. 2007. pp. 1–26. doi:10.1111/j.1574-695x.2007.00232.x.

31. Marciano-Cabral F, Cabral G. *Acanthamoeba* spp. as agents of disease in humans. Clin Microbiol Rev. 2003;16: 273–307.

32. Martinez AJ, Visvesvara GS. Free-living, Amphizoic and Opportunistic Amebas. Brain Pathology. 1997. pp. 583–598. doi:10.1111/j.1750-3639.1997.tb01076.x.

33. Esteban GF, Fenchel TM. Ecology of Protozoa: The Biology of Free-living Phagotrophic Protists. Springer; 2021.

34. Weisman RA. Differentiation in *Acanthamoeba Castellanii*. Annual Review of Microbiology. 1976. pp. 189–219. doi:10.1146/annurev.mi.30.100176.001201.

35. Guimaraes AJ, Gomes KX, Cortines JR, Peralta JM, Peralta RHS. *Acanthamoeba* spp. as a universal host for pathogenic microorganisms: One bridge from environment to host virulence. Microbiol Res. 2016;193: 30–38.

36. Snelling WJ, Moore JE, McKenna JP, Lecky DM, Dooley JSG. Bacterial-protozoa interactions; an update on the role these phenomena play towards human illness. Microbes Infect. 2006;8: 578–587.

37. Winiecka-Krusnell J, Linder E. Bacterial infections of free-living amoebae. Research in Microbiology. 2001. pp. 613–619. doi:10.1016/s0923-2508(01)01240-2.

38. Sinclair JL, McClellan JF, Coleman DC. Nitrogen Mineralization by *Acanthamoeba polyphaga* in Grazed *Pseudomonas paucimobilis* Populations. Appl Environ Microbiol. 1981;42: 667–671.

39. Rønn R, McCaig AE, Griffiths BS, Prosser JI. Impact of protozoan grazing on bacterial community structure in soil microcosms. Appl Environ Microbiol. 2002;68: 6094–6105.

40. Rosenberg K, Bertaux J, Krome K, Hartmann A, Scheu S, Bonkowski M. Soil amoebae rapidly change bacterial community composition in the rhizosphere of Arabidopsis thaliana. The ISME Journal. 2009. pp. 675–684. doi:10.1038/ismej.2009.11.

41. Griffiths BS. A comparison of microbial-feeding nematodes and protozoa in the rhizosphere of different plants. Biology and Fertility of Soils. 1990. pp. 83–88. doi:10.1007/bf00335867.

42. Artursson V, Finlay RD, Jansson JK. Interactions between arbuscular mycorrhizal fungi and bacteria and their potential for stimulating plant growth. Environ Microbiol. 2006;8: 1–10.

43. Cook RJ, Thomashow LS, Weller DM, Fujimoto D, Mazzola M, Bangera G, et al. Molecular mechanisms of defense by rhizobacteria against root disease. Proc Natl Acad Sci U S A. 1995;92: 4197–4201.

44. Jousset A, Lara E, Wall LG, Valverde C. Secondary metabolites help biocontrol strain *Pseudomonas fluorescens* CHA0 to escape protozoan grazing. Appl Environ Microbiol. 2006;72: 7083–7090.

45. Wildschutte H, Lawrence JG. Differential Salmonella survival against communities of intestinal amoebae. Microbiology. 2007;153: 1781–1789.

46. Wildschutte H, Wolfe DM, Tamewitz A, Lawrence JG. Protozoan predation, diversifying selection, and the evolution of antigenic diversity in *Salmonella*. Proc Natl Acad Sci U S A. 2004;101: 10644–10649.

47. Friman V-P, Buckling A. Effects of predation on real-time host-parasite coevolutionary dynamics. Ecol Lett. 2013;16: 39–46.

48. Lawrence D, Fiegna F, Behrends V, Bundy JG, Phillimore AB, Bell T, et al. Species interactions alter evolutionary responses to a novel environment. PLoS Biol. 2012;10: e1001330.

49. Lenski RE. Experimental evolution and the dynamics of adaptation and genome evolution in microbial populations. ISME J. 2017;11: 2181–2194.

50. Kawecki TJ, Lenski RE, Ebert D, Hollis B, Olivieri I, Whitlock MC. Experimental evolution. Trends Ecol Evol. 2012;27: 547–560.

51. Cortez MH, Weitz JS. Coevolution can reverse predator-prey cycles. Proc Natl Acad Sci U S A. 2014;111: 7486–7491.

52. Van den Bergh B, Swings T, Fauvart M, Michiels J. Experimental Design, Population Dynamics, and Diversity in Microbial Experimental Evolution. Microbiol Mol Biol Rev. 2018;82. doi:10.1128/MMBR.00008-18

53. Anwar A, Khan NA, Siddiqui R. Combating *Acanthamoeba* spp. cysts: what are the options? Parasit Vectors. 2018;11: 26.

54. Barber JN, Sezmis AL, Woods LC, Anderson TD, Voss JM, McDonald MJ. The evolution of coexistence from competition in experimental co-cultures of *Escherichia coli* and *Saccharomyces cerevisiae*. ISME J. 2021;15: 746–761.

55. Sokatch J. The Biology of Pseudomonas. Elsevier; 2012.

56. Rainey PB, Travisano M. Adaptive radiation in a heterogeneous environment. Nature. 1998;394: 69–72.

57. Bolnick DI, Barrett RDH, Oke KB, Rennison DJ, Stuart YE. (Non) Parallel Evolution. Annual Review of Ecology, Evolution, and Systematics. 2018. pp. 303–330. doi:10.1146/annurev-ecolsys-110617-062240.

58. Bull JJ, Badgett MR, Wichman HA, Huelsenbeck JP, Hillis DM, Gulati A, et al. Exceptional Convergent Evolution in a Virus. Genetics. 1997. pp. 1497–1507. doi:10.1093/genetics/147.4.1497.

59. Rosenblum EB, Parent CE, Brandt EE. The Molecular Basis of Phenotypic Convergence. Annual Review of Ecology, Evolution, and Systematics. 2014. pp. 203–226. doi:10.1146/annurev-ecolsys-120213-091851.

60. McDonald MJ, Gehrig SM, Meintjes PL, Zhang X-X, Rainey PB. Adaptive Divergence in Experimental Populations of *Pseudomonas fluorescens*. IV. Genetic Constraints Guide Evolutionary Trajectories in a Parallel Adaptive Radiation. Genetics. 2009. pp. 1041–1053. doi:10.1534/genetics.109.107110.

61. Ferguson GC, Bertels F, Rainey PB. Adaptive Divergence in Experimental Populations of *Pseudomonas fluorescens*. V. Insight into the Niche Specialist Fuzzy Spreader Compels Revision of the Model Pseudom.onas Radiation. Genetics. 2013. pp. 1319–1335. doi:10.1534/genetics.113.154948

62. Matz C, Kjelleberg S. Off the hook–how bacteria survive protozoan grazing. Trends Microbiol. 2005. Available: https://www.sciencedirect.com/science/article/pii/S0966842X05001344.

63. Malone JG. Role of small colony variants in persistence of *Pseudomonas aeruginosa* infections in cystic fibrosis lungs. Infect Drug Resist. 2015;8: 237–247.

64. Song B, Leff LG. Influence of magnesium ions on biofilm formation by *Pseudomonas fluorescens*. Microbiol Res. 2006;161: 355–361.

65. Lind PA, Farr AD, Rainey PB. Experimental evolution reveals hidden diversity in evolutionary pathways. Elife. 2015;4. doi:10.7554/eLife.07074.

66. Hall AR, Scanlan PD, Morgan AD, Buckling A. Host-parasite coevolutionary arms races give way to fluctuating selection. Ecol Lett. 2011;14: 635–642.

67. Veselova MA. Quorum sensing regulation in Pseudomonas. Russian Journal of Genetics. 2010. pp. 129–137. doi:10.1134/s1022795410020018.

68. Wright RCT, Friman V-P, Smith MCM, Brockhurst MA. Cross-resistance is modular in bacteria–phage interactions. PLOS Biology. 2018. p. e2006057. doi:10.1371/journal.pbio.2006057

69. Grinberg M, Orevi T, Kashtan N. Bacterial surface colonization, preferential attachment and fitness under periodic stress. PLoS Comput Biol. 2019;15: e1006815.

70. Flemming H-C, Wingender J, Szewzyk U, Steinberg P, Rice SA, Kjelleberg S. Biofilms: an emergent form of bacterial life. Nat Rev Microbiol. 2016;14: 563–575.

71. Chavez-Dozal A, Gorman C, Erken M, Steinberg PD, McDougald D, Nishiguchi MK. Predation response of Vibrio fischeri biofilms to bacterivorus protists. Appl Environ Microbiol. 2013;79: 553–558.

72. O'Toole G, Kaplan HB, Kolter R. Biofilm formation as microbial development. Annu Rev Microbiol. 2000;54: 49–79.

73. Meyer JR, Kassen R. The effects of competition and predation on diversification in a model adaptive radiation. Nature. 2007;446: 432–435.

74. Hall AR, Meyer JR, Kassen R. Selection for predator resistance varies with resource supply in a model adaptive radiation. Evol Ecol Res. 2008;10: 735–746.

75. Friman V-P, Jousset A, Buckling A. Rapid prey evolution can alter the structure of predator-prey communities. J Evol Biol. 2014;27: 374–380.

76. Rodríguez-Zaragoza S. Ecology of free-living amoebae. Crit Rev Microbiol. 1994;20: 225–241.

77. Barker J, Brown MRW. Trojan Horses of the microbial world: protozoa and the survival of bacterial pathogens in the environment. Microbiology. 1994. pp. 1253–1259. doi:10.1099/00221287-140-6-1253.

78. Sun S, Noorian P, McDougald D. Dual Role of Mechanisms Involved in Resistance to Predation by Protozoa and Virulence to Humans. Front Microbiol. 2018;9: 1017.

79. Hassett DJ, Sutton MD, Schurr MJ, Herr AB, Caldwell CC, Matu JO. *Pseudomonas aeruginosa* hypoxic or anaerobic biofilm infections within cystic fibrosis airways. Trends Microbiol. 2009;17: 130–138.

80. Worlitzsch D, Tarran R, Ulrich M, Schwab U, Cekici A, Meyer KC, et al. Effects of reduced mucus oxygen concentration in airway Pseudomonas infections of cystic fibrosis patients. Journal of Clinical Investigation. 2002. pp. 317–325. doi:10.1172/jci0213870.

81. Thi MTT, Wibowo D, Rehm BHA. *Pseudomonas aeruginosa* Biofilms. International Journal of Molecular Sciences. 2020. p. 8671. doi:10.3390/ijms21228671.

82. Lutz C, Erken M, Noorian P, Sun S, McDougald D. Environmental reservoirs and mechanisms of persistence of Vibrio cholerae. Front Microbiol. 2013;4: 375.

83. Brinkmann H, Philippe H. The diversity of eukaryotes and the root of the eukaryotic tree. Adv Exp Med Biol. 2007;607: 20–37.

84. Escoll P, Rolando M, Gomez-Valero L, Buchrieser C. From Amoeba to Macrophages: Exploring the Molecular Mechanisms of *Legionella pneumophila* Infection in Both Hosts. Current Topics in Microbiology and Immunology. 2013. pp. 1–34. doi:10.1007/82_2013_351.

85. Swart AL, Leoni Swart A, Harrison CF, Eichinger L, Steinert M, Hilbi H. *Acanthamoeba* and *Dictyostelium* as Cellular Models for Legionella Infection. Frontiers in Cellular and Infection Microbiology. 2018. doi:10.3389/fcimb.2018.00061.

86. Thewes S, Soldati T, Eichinger L. Amoebae as Host Models to Study the Interaction with Pathogens. Frontiers Media SA; 2019.

87. Siddiqui R, Khan NA. Acanthamoeba is an evolutionary ancestor of macrophages: a myth or reality? Exp Parasitol. 2012;130: 95–97.

88. German N, Doyscher D, Rensing C. Bacterial killing in macrophages and amoeba: do they all use a brass dagger? Future Microbiol. 2013;8: 1257–1264.

89. Wheat WH, Casali AL, Thomas V, Spencer JS, Lahiri R, Williams DL, et al. Long-term survival and virulence of Mycobacterium leprae in amoebal cysts. PLoS Negl Trop Dis. 2014;8: e3405.

90. Espinoza-Vergara G, Mozammel Hoque M, McDougald D, Noorian P. The Impact of Protozoan Predation on the Pathogenicity of *Vibrio cholerae*. Frontiers in Microbiology. 2020. doi:10.3389/fmicb.2020.00017.

91. Chesson P. Mechanisms of Maintenance of Species Diversity. Annual Review of Ecology and Systematics. 2000. pp. 343–366. doi:10.1146/annurev.ecolsys.31.1.343

92. Stenseth NC, Smith JM. COEVOLUTION IN ECOSYSTEMS: RED QUEEN EVOLUTION OR STASIS? Evolution. 1984;38: 870–880.

93. Paterson S, Vogwill T, Buckling A, Benmayor R, Spiers AJ, Thomson NR, et al. Antagonistic coevolution accelerates molecular evolution. Nature. 2010;464: 275–278.

94. Scanlan PD, Buckling A. Co-evolution with lytic phage selects for the mucoid phenotype of *Pseudomonas fluorescens* SBW25. ISME J. 2012;6: 1148–1158.

95. Scanlan PD, Hall AR, Blackshields G, Friman V-P, Davis MR Jr, Goldberg JB, et al. Coevolution with bacteriophages drives genome-wide host evolution and constrains the acquisition of abiotic-beneficial mutations. Mol Biol Evol. 2015;32: 1425–1435.

96. Lind PA, Farr AD, Rainey PB. Experimental evolution reveals hidden diversity in evolutionary pathways. Elife. 2015;4. doi:10.7554/eLife.07074.

97. Bertani G. Studies on lysogenesis. I. The mode of phage liberation by lysogenic Escherichia coli. J Bacteriol. 1951;62: 293–300.

98. Heuser M, Razavi L. Chapter 13 Amebo-flagellates as Research Partners: The Laboratory Biology of *Naegleria* and *Tetramitus*. Methods in Cell Biology. 1970. pp. 341–476. doi:10.1016/s0091-679x (08) 61759-8.

99. Peretz A, Pastukh N, Geffen Y, Graffi S, Socea SD. Comparison of Fluorescence Microscopy and Different Growth Media Culture Methods for Acanthamoeba Keratitis Diagnosis. The American Journal of Tropical Medicine and Hygiene. 2015. pp. 316–318. doi:10.4269/ajtmh.15-0193.

100. Garg NK, Das SR. Lipid requirements for axenic cultivation of *Entamoeba histolytica*. Journal of Biosciences. 1980. pp. 235–241. doi:10.1007/bf02703249.

101. Marciano-Cabral F. Biology of Naegleria spp. Microbiol Rev. 1988. Available: https://www.ncbi.nlm.nih.gov/pmc/articles/pmc372708/.

Chapter 4

Virulence, cellular masking and grazing resistance in the struggle to survive under long term protozoan predation; the genetics of survival

Farhad S. Golzar[1], Michael E. Miller[1], and Heather Lyn Hendrickson[2]
[1]School of Natural and Computational Science, Massey University, Auckland, New Zealand
[2]School of Biological Sciences, University of Canterbury, Christchurch, New Zealand

Abstract

Generalist protozoan predators affect the pace of evolution in microbial communities, but investigations into the molecular consequences of predation for the genomic evolution of defence or coadaptation are scarce. We have previously performed a 90-day co-evolution experiment to address these effects using the bacterium *Pseudomonas fluorescens* SBW25 on solid media in the presence and absence of a wild *Acanthamoeba* sp. predator. Coevolution led to genomic divergence, altered phenotypes and resistance to predation in coevolved bacterial lineages. Strong parallel phenotypic evolution was observed among the coevolved replicates leading to Wrinkly Spreader, Volcano and Mountain colony phenotypes. Here, we describe the genomic mutations underlying this parallelism with a focus on these morphotypes. The Wrinkly Spreader colonies were predation resistant and caused by familiar mutations which alter the function of the protein methylesterase, WspF, inducing constitutive biofilm formation. Separately, the Volcano morphotype was caused by a fusion of the FadD2 and FadD1 proteins, a pair of long-chain-fatty-acid-CoA ligases responsible for directing long chain fatty acids to degradation in the tricarboxylic acid cycle. The presence of this mutation led to reduced predation but only when the cells had grown in close proximity to the predators. The Mountain morphotypes were the product of the deletion of a putative hypothetical protein upstream of a large transporter complex

which increases predation resistance, the basis of which is not clear. The mutations responsible for WS, Volcano and Mountain colony morphology appeared in eight, five and nine out of the nine coevolved population lines, respectively. Our results suggest that coevolution can prompt bacterial resistance and result in acquisition of novel beneficial mutations that are advantageous for bacterial survival in the natural ecosystem. In addition, we have observed remarkable levels of parallel molecular evolution that appear to be underpinned by 33 bp and 10 bp sequences tandem repeats in the case of both the Volcano and the Mountain mutations.

Introduction

Bacteria are the dominant organisms on this planet because of their inherent adaptive nature and ability to evolve rapidly [1]. Bacteria are widely distributed and interact with a wide diversity of competing organisms to survive in their natural habitats [2,3]. Competition drives phenotypic adaptation, the product of which varies according to environmental factors and leads to complex traits that exploit, eliminate or crowd out other organisms [4]. Apart from competition, interactions with either prokaryotic and eukaryotic organisms can include predation.

In soil, interactions between predator and prey have an important effect on shaping bacterial diversity [5,6] and maintaining the natural balance of microbial ecosystems, for example, by mediating rates of decomposition, nutrient recycling, and energy turnover [2,7]. Predation pressure can result in adaptive evolution of bacterial prey and therefore the adaptation to predation pressure may also protect bacteria in the absence of predators [8,9]

Predation by free-living amoebae (FLA) is a potent selective force driving bacterial evolution [10]. Predators are abundant in all natural habitats and recognised to affect the ecological and evolutionary processes for bacteria. Predation provides a strong driving force for rapid evolutionary changes in a range of ecosystems [11–13]. Bacterial adaptation to predation includes pre-phagocytic escape strategies such as cell elongation, biofilm formation, secondary metabolite or toxin secretion, and mucoid phenotypes [10,14–20]. These are anti-predatory behaviours that allow bacteria to survive, proliferate and exploit various niches.

Bacterial prey and predator interactions have recently received more attention because of the importance of the predators in the evolution of these organisms. Previous experimental evolutions have shown prey evolution can be influenced by predation from amoeboid predator *Acanthamoebae* spp. [13], protozoan ciliate *Tetrahymena thermophila* [21], and bacteriophages [22]. As a result of *P. fluorescens* SBW25 and lytic bacteriophage coevolution in a microcosm environment, the mucoid phenotype arose and persisted as an adaptive response to predation by phages [23]. It has been documented that predation by the specialised bacterial predator *Bdellovibrio bacteriovorus* leads to increased diversity in bacterial prey *Pseudomonas fluorescens* SBW25 [6]. An empirical coevolution study conducted in liquid media for ~87.5 days between bacterial predator *Myxococcus xanthus* and *E. coli* demonstrated genomic evolution of both prey and predators. The interaction led to evolution of resistant mucoid phenotype in bacterial prey and favoured them in the presence of predators [24]. However, studies of the molecular basis of resistant traits that arise in bacteria under amoeboid predation are scarce. Here we examine how a direct generalist protist and prey interactions on a solid surface promotes the parallel

genotypic evolution and determine the direct effects of these mutations on fitness advantage of prey bacteria in the face of predators.

Generalist protozoan predators such as *Acanthamoebae* species are ubiquitous in various environments [25] and feed upon a broad range of bacteria including bacterial pathogens [26,27]. *Acanthamoebae* are best known for causing severe keratitis and fatal encephalitis both in humans and animals [28–31]. *Acanthamoebae* are regarded as safe reservoirs and vehicles of fungi, viruses and pathogenic bacteria leading to infection of multiple hosts [32,33]. It has also been proposed that some bacteria including bacterial pathogens after exposure to predators can increase their pathogenicity, and this favours them while colonising future niches [34,35]. *Acanthamoebae* was selected as a protist predator because it is a wild organism that has an ability to phagocytose on surfaces and its direct impact on evolution of non-pathogenic prey bacteria on surfaces has received little attention. *Pseudomonas fluorescens* strains are proficient both in soil and phytosphere and recognised to promote plant growth by competing and antagonising other pathogenic microbes [36,37]. Investigating the interaction between wild *Acanthamoeba* and *P. fluorescens* SBW25 is important because in order to understand how bacteria are evolving in nature, we need to understand what adaptations arise under this common and ubiquitous evolutionary pressure [38].

Our previous work described the coevolution of *P. fluorescens* SBW25 and *Acanthamoebae* spp., focussing on the evolved anti-predator qualities of three morphotypes. These were Wrinkly Spreader (WS), Mountain (Mnt) and Volcano (Vol) morphologies. These three morphotypes were commonly observed in 4 CoEvolved

(CE) lines (2, 6, 7, 8), Mnt and WS in all but one line, and Vol in five out of nine. Evidence of pronounced parallel phenotypic evolution which we investigate further here. Coevolved WS and Mnt colonies demonstrated a high degree of predator resistance against ancestral, coevolved and separately evolved predators. The Vol morphotype was found to be highly resistant only against their coevolved predator and only when co-cultured near those predators.

Herein, we first report the evolution of prey *P. fluorescens* SBW25 in the presence and absence of amoeboid predator *Acanthamoeba spp.* over 90 days, then investigate the mutations underlying these phenotypes, and make progress in understanding the nature of bacterial adaptation. In this coevolution system, we show coevolved prey lineages acquire more colony morphology changes and associated mutations than the evolved prey-only lineages. Our experimental results show strong parallel genomic evolution within both population replicates and colony morphotypes unique to the coevolved prey. Coevolution led to an increased number of mutations among coevolved bacterial populations and affects the predator preferences in the coevolutionary lineages. Thus, we investigated the efficiency of the bacterial genomic evolution associated with anti-predatory traits that had arisen and caused the colony morphology changes among CE bacterial replicates. This allowed us to reconstruct the frequently repeated mutations in the wild type background and determine their contributions to protozoan predation adaptation. Further, this approach enabled us to describe the exact molecular mechanisms of bacterial survival during predation by predators, including the genomic basis of defensive traits and its effect on the coevolutionary processes leading to reciprocal adaptation between predators and prey. Considering how coevolution between generalist protozoan predators and prey

bacteria may structure the evolution of the bacterial genomes is fundamental to understanding how these organisms evolve in natural habitats.

Results

Predation leads to increased adaptation

The colony morphologies that we observed after 90 days of evolution under protozoan predation were reminiscent of the four main adaptive morphotypes; Wrinkly Spreader (WS), Mountain (Mnt), Volcano (Vol) and Like Wild Type (LWT). In order to determine the nature of the mutations that had arisen and caused the colony morphology changes among coevolved bacterial populations, we performed whole-genome population sequencing of Co-Evolved (CE) and Prey Only (PO) lineages to identify mutations above a detection threshold of %1. In addition, we sequenced 29 bacterial clones of various morphotypes from the end of the experiment (see materials and methods) in order to identify the genetic mutations that underlie these morphotypes and to determine their contributions to protozoan predation adaptation.

The CE and PO lineages underwent population sequencing at days 16, 40, 64 and 90. We first analysed the population sequencing for mutations that had achieved at least 1% frequency and observed that mutations had increased in frequency in the CE lines (with predation) but not in the PO (without predation) populations (Supplementary Table 1). In fact, we did not observe evidence of any mutations reaching fixation in the absence of predation (Fig. 4.1 A). Whilst the CE lines, those that had experienced predation, had acquired an average of eleven mutations by day 90 whilst the negative control populations had 2.3 (minimum detection threshold of 20%). PO lines had

accumulated ~3.3 mutations on average per line at day 16, but the number of mutations greater than 20% frequency decreased as the evolution progressed suggesting that mutations occurred but did not provide sufficient advantages on the solid PM media to sweep to fixation. On the contrary, CE population lines sustained ~4.7 mutations on average per line at day 16 but reached 11 mutations per line by the end of the experiment.

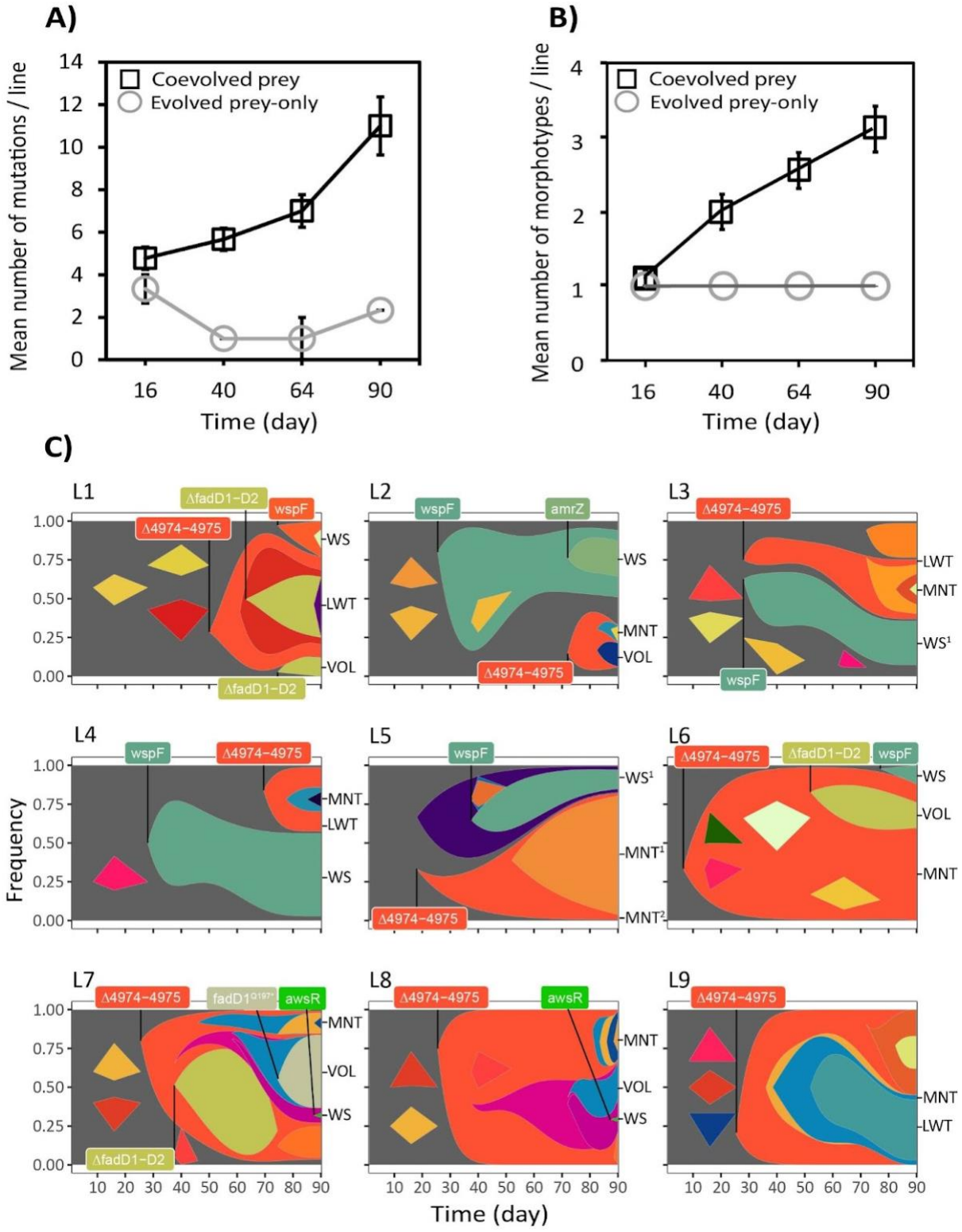

Figure 4. 1. Genotypic and phenotypic evolution in CE and PO *P. fluorescens* SBW25. A) Population sequencing revealed a higher number of mutations (threshold %20 and above) occurred in CE bacterial populations than in the evolved PO experimental lineages. B) More colony morphology classes were present among CE prey populations than the evolved PO lines in the 90-day experiment. C. Genotype abundance among CE bacterial populations visualised by Muller plots. Parallel genomic evolution in nine bacterial lines undergoing predation. Each colour indicates specific mutation and the labels are the

name and PFLU numbers of the mutated gene (Supplementary Fig. 1). Whole population sequencing with endpoint clone sequencing to determine mutation linkage. When multiple mutations were found within any time point at the same frequency, but their lineage could not be determined by endpoint clonal sequencing, these mutations were assumed to be within the same background and thus treated as a single genotype for the purpose of this visualisation.

The observation that predation drives diversification is consistent with our previous observations in a shorter study and this one regarding the numbers of the colony morphology variants observed in the CE vs PO populations (Chapter 2 & 3). During 90 days we observed an average of ~3.2 colony variant classes per line when predation was present whereas colony morphology in the PO lines remained unchanged (Fig. 4.1 B).

Remarkable levels of parallel genomic evolution under protozoan predation

We sequenced clones from day 90 of the experiment and used those data in combination with the population sequencing to predict the genetic history of the major combinations and classes of mutations that arose in the 90-day experiment (Supplementary Tables 1 & 2). This allowed us to produce Muller plots for each of the nine CE lines (Fig. 4. 1C). One of the hallmarks of adaptation to an environment is genetic parallelism in separate lineages. In analysing these population sequencing results we found three mutations that were frequently generated in separate CE lines. These were a deletion which included PFLU_4974 and PFLU_4975 (Δ4974-4975), a deletion that included PFLU_4830 and PFLU_ 4829 (ΔfadD2-D1) and a deletion in PFLU_1224, which eliminated five amino acids of the WspF protein product (wspFΔ51-55). These mutations frequently persisted until the end of the 90-day experiment (Fig. 4. 1C). Sequencing the colony variants at the end of the 90-day experiment also allowed us to associate each of these major mutations with a colony

morphology that was generally observed when they were present. These were as follows; The *wspF*Δ51-55 and a suite of other typical *wsp* associated genes were responsible for the WS colony morphologies. The behaviour in the population of this mutation in lines 2,3,4,5 and 9 was that of an early adaptive mutation that did not persist in our CE regime and was ultimately not able to sweep but could maintain a share of the phenotypic space whilst other variants were present (Fig. 4.1 C green).

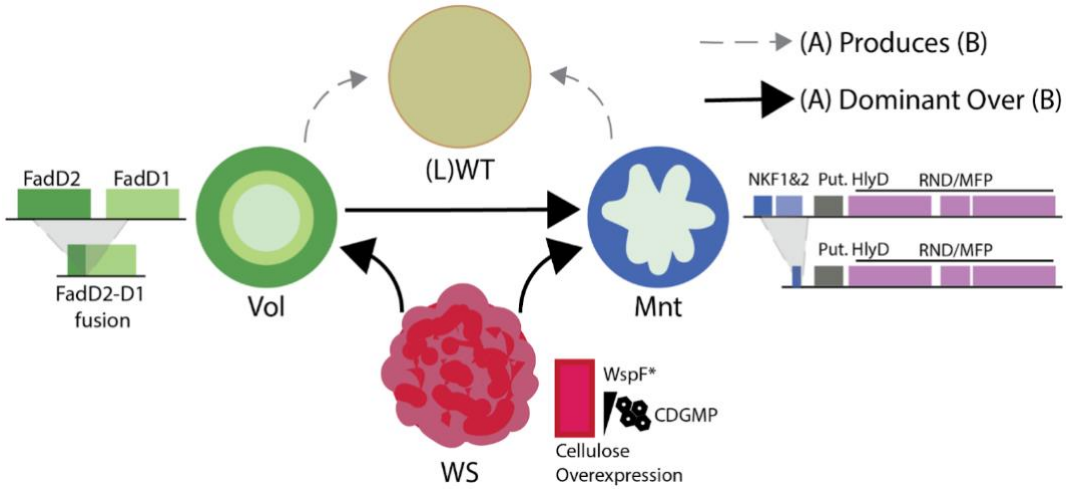

Figure 4. 2**.** Genotype to phenotype mapping. Three major classes of mutations were observed in the sequencing results, and these can be related to colony morphology phenotypes. The WS associated mutations were phenotypically dominant to the Mnt and Vol associated mutations, both of which were deletions. The Vol deletion (FadD2-D1 fusion) was phenotypically dominant over the Mnt deletion (PFLU_4974-4975), which was the most commonly observed. Both the Vol and Mnt colony morphotypes produced Smooth colonies (L)WT with some frequency.

The ΔfadD2-D1 mutation was always present in the colony morphs that we had named "Volcano" (Vol). Discovering the mutation responsible for Vol colonies was particularly interesting to us because the Vol colonies appeared to have disparate levels of predator resistance depending on how this trait was measured in our previous work (Chapter 3). The disruptions of FadD function arose through multiple mutational types (point mutations and deletions) twice in line 1, once in line 6, twice in Line 7. This

variability and the phenotypic consequences of this mutation suggested that this mutation requires further investigation.

The third major mutation of interest, ∆4974-4975, was responsible for the Mountain morphology (Mnt) but in instances where the ∆fadD2-D1 mutation was also present the colonies appeared Vol, indicating a phenotypic dominance of the Vol morphology (Supplementary table 1). As the co-evolution progressed, we observed the accumulation of various mutant sub-lineages more frequently within the primary mutant ∆4974-4975, none of which swept to fixation in CE bacterial populations (Fig. 4.1 C). The molecular underpinnings of the major morphotypes of interest (WS, Vol, and Mnt) will each be dissected further below.

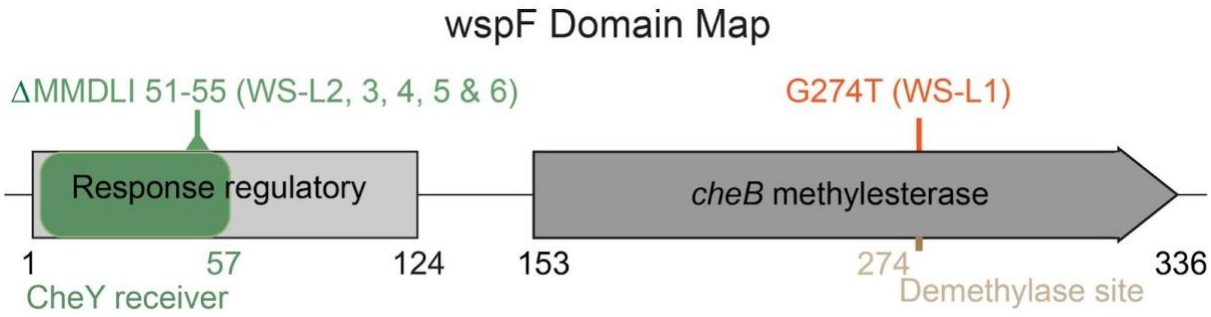

Figure 4. 3**.** Amoeboid predation resistance can be conferred by biofilm formation in *P. fluorescens* SBW25. The *wspF* domain map in *P. fluorescens* SBW25 illustrates similar mutations that are identified on CheY receiver in five out nine CE lines (wspF∆51-55) and on Demethylase site in line1 resulting in WS colony morphology.

The mutations responsible for WS colony morphology appeared in eight out of the nine CE population lines (Fig. 4.1 C Green). We found a 15-bp deletion mutation that eliminates 5 amino acids (∆LMDLI 51-55) from the wspF protein product (Fig. 4.3). This mutation arose in five out of nine lines (Lines 2, 3, 4, 5, and 6). In the CE lines at day 90 the frequency of this mutation was 0.11 to a maximum of 0.6 (Supplementary

table 1). In L1 and towards the end, we detected a single nucleotide change (G823T) that caused a substitution mutation on the wspF gene (final frequency; 0.25) which causes a similar phenotype (Fig. 4.2 & 3). Similarly, the mutation associated with WS colony morphologies in Lines 7 and 8 found to be substitution mutations on

gene (PFLU_5210). These mutations were detected through isolate-sequencing at day 90 to have arisen in the Δ4974-4975 genetic background at low frequency (0.03 and 0.04) (Fig. 4.1 C). WS isolates mostly had acquired mutations that were similar to *wspF, awsR* and *amrZ* mutations that had previously been investigated [13,39]. WS colonies are highly resistant to *Acanthamoebae* spp. and confer the highest level of prey fitness observed in our experiments [13]. As mentioned, wspFΔ51-55 mutants and mutations in other well characterised WSP complex associated genes (like *awsR*) generated WS colonies and few additional sub-mutations appear to have occurred in these cells. The exceptions were L2 in which a mutation occurred in AmrZ, a previously recognised WSP complex regulator. This suggests that the production of exopolysaccharides observed in WspF mutants of this kind, producing a biofilm on solid media, is a singularly successful strategy under amoeboid predation.

From the population sequencing results, the mutation responsible for Vol phenotype, ΔfadD2-D1, arose in five out of nine CE lines. As noted earlier, this Vol associated mutation also emerged later as a secondary mutant within the Δ4974-4975 populations in several CE lines and appears to be phenotypically dominant in those instances (Fig. 4.1 C). We also identified this mutation that occurred independently in L1 at a frequency of 0.1. In lines 2 and 8 the mutation responsible for this phenotype appeared to be a frameshift mutation in the *fadD1* (275 G>C) with the frequency of 0.07 and

0.23, respectively. However, in most instances the Vol associated *fadD* mutation (lines 1, 6 and 7) manifests as a deletion of 2,083 bp which eliminates (∆G350-T1689) of FadD2, fusing the upstream region of this protein with the downstream region of FadD1 (∆D1-G330) (Fig. 4.4 A). The deletion results in the creation of fadD2-fadD1 *(*fusion of fadD genes). The Vol associated ∆fadD2-fadD1 mutation in L6 and L7 reaches a final frequency of 0.2 and 0.26 respectively. Furthermore, in L7 we detected a frameshift mutation in the *fadD1* gene (Q197 Stop codon) within ∆4974-4975 and at the frequency of 0.5 at the end of this CE experiment (Fig. 4.3 and Supplementary Table 1).

Mutation associated with the Mountain colony morphology was present in all nine CE bacterial lines (Fig. 4.1 C). The mutation was caused by a 422-bp deletion of a *putative hypothetical protein* (PFLU_4974) accompanied by complete deletion of a *putative exported protein* (PFLU_4975) (∆A1-A1098) which included 212 bp of the regulatory region upstream of an RND (Resistance-Nodulation-Division) family efflux transporters. With a few exceptions, the wspF are the most abundant mutations, we found ∆4974-4975 mutants that arise and become the dominant one by the end of the 90-day in this CE experiment (lines 1, 3 and 5-9). The frequency of the Mnt mutations on day 90 was between 0.23 and 1.0 and they were observed in all CE lineages (Fig. 4.1 C – 4.2 and Supplementary Table1).

Evaluating the underlying causes of remarkable genetic parallelism

The two large deletion mutations, Vol associated ∆fadD2-fadD1 arose in five out of nine CE lines (5/9 or 55% of lines) and Mnt associated ∆4974-4975 was present in all lines (100% on lines). This observation either suggests that cross contamination of the

lines has been rampant or that these mutations are taking place in the population far more often than one would expect at random. Upon further inspection we noted that the join points of each deletion included tandem repeats.

The Vol associated ∆fadD2-fadD1 region has a pair of 33 bp tandem repeat (*CTGATCGTGGTCAACACCAACCCGCTGTACACC*) which is present within both the *fadD2* and the *fadD1* genes 2,083 bp apart. The distance between two tandem repeats was estimated from the end of the first 33 bp located on the fadD2 right before the deletion appears (5,308,307) to the second 33 bp on the fadD1 where deletion ends (5,310,390) (Fig. 4.4 A). This is not the only repeated sequence in this area as it appears that these genes are paralogs that have been subjected to a gene duplication event in the past. *fadD2* and *fadD1* are %66.37 identical at the nucleotide level (Fig 4.4).

The Mnt associated deletion ∆4974-4975 we identified identical 10 bp sequences (*CTGCGCGTCC*) at genome positions 5,460,377 and 5,462,137. Recombination between these sites, 1,734 bp apart, would be expected to take place with less frequency in the population than the longer repeats observed in the ∆fadD2-fadD1 fusion as the length of the homology is expected to determine the recombination frequency (Fig. 4.7 A) [40].

The population sequencing results of the PO group (No predation) revealed mutations that have emerged at lower frequency (ranging from 0.2 - 0.42) and these went completely extinct before 90 Days (Supplementary Table 1). There are parallel mutations observed in the Control (PO) lines. The substitution mutation on the

PFLU_4287 (transporter-like membrane protein) and PFLU_3789 were detected in three and two out of three PO lines, respectively. These mutations almost appeared earlier in this experiment, and we did not observe evidence of these mutations reaching to fixation indicating that they were not favourable mutations in this 90-day experiment. The frequency of the mutation on the PFLU_4287 was between 0.26 - 0.42 and on the PFLU_3879, 0.2 over 90 days among PO populations. Some of these mutations were detected in the CE lines earlier in the experiment as well, however, they have been observed at lower frequency and were not present by the end of the experiment (Fig. 4.1 C and Supplementary Table 1). The mutation on the transporter-like membrane protein (PFLU_4287) was observed in all nine CE lines with the average frequency of 0.06 - 0.37, but their frequency did not increase or fixed over 90 days. This may suggest that some cross contamination occurred, particularly early in the experiment, however we are unable to confirm or reject this hypothesis.

Investigating the molecular basis of predator adaptation (anti-predator traits)

Having identified the mutations responsible for the major colony morphotypes, we turned our attention to determining the degree to which the various mutations allowed bacteria to survive predation by ancestral, co-evolved or foreign evolved predators in the Performance Assay (PA) (Chapter 3). The PA allows us to simultaneously evaluate the survival of both a specific prey isolate and a predator population from a specific time point in an environment which closely replicates growth conditions during the 90-day experiment. Briefly, bacteria and amoebae grow in proximity to one another on solid media plates for four days after which we plate them as appropriate to estimate their respective fold population change relative to a naive WT prey with naive predators in identical conditions. We used the PA to test 15 representative CE isolates

in the presence of various protozoan populations from the CE and the ancestral predators. This approach has previously allowed us to choose predators that were either familiar (CE) or unfamiliar with the prey. In this instance, we used ancestral and evolved predators in order to determine how various genetic reconstructions of the Vol and Mnt morphotype mutations performed under predation. We chose WS, Mnt and Vol isolates along with subsets of the causal mutations outlined above (Supplementary Table 1 & 2).

WS and Mnt CE isolates from distinct lines demonstrated a highly positive performance in the face of CE predators relative to the performance of WT prey with the same predators.

It was found that WS isolates have an increased survival rate against familiar predators by 3-fold to 35-fold when CE predators are present. Mnt isolates increased in their fold survival over WT from 1.5-fold to as much as 27-fold in the presence of CE predators. Vol isolates demonstrate growth between 3.2-fold better up to a maximum of 170-fold better survival than the WT in the case of CE L1 predator (Chapter 3).

Investigating the nature of bacterial adaptation under predation

Whilst understanding the nature of the WS morphotypes confer high resistance is straightforward and has been discussed at length by ourselves and others [13,41], the explanation for predator resistance in both the Vol and Mnt morphotypes intrigued us. In order to investigate the nature of predation resistance in Vol we first analysed the *fadD* genes in *P. fluorescens* SBW25. The function of a FadD is to activate Long Chain Fatty Acids after they have been transported into the cell by FadL (Fig. 4.4 C).

Activation is accomplished through the acetyl-CoA transferase activity and requires ATP. The LCFA is subsequently beta oxidised and burned as fuel in the TCA cycle. We identified 4 *fadD* homologues in our reference genome (PFLUS; 4829, 4830, 3525, 1843). Their amino acid sequences were aligned to *P. aeruginosa* and *E. coli* via clustal.

The amino acid sequence analysis of ATP/AMP for *P. aeruginosa* PAO1 and *E. coli* were obtained from previous studies and compared with *P. fluorescens* SBW25 ATP/AMP and fatty acid binding motifs [42–44]. The results demonstrated a high degree of similarity of *fadD1* and *fadD2* genes to the *fadD* encoded motifs found in *P. aeruginosa* (95.24 and 90.70 identical, respectively) and *E. coli (*76.19 and 86.05 identical, respectively). The *fadD2-D1* fusion deletion found in Vol morphotype colonies in this study also demonstrated a high degree of similarities (66.37%) to motifs encoded by the *fadD1* gene in *P. fluorescens* and *P. aeruginosa* (Fig. 4.4 D).

Having determined that these genes had features which were suggestive of the annotated function we turned our attention towards determining if the FadD1 and FadD2 from *P. fluorescens* SBW25 are able to complement long chain fatty acid degradation in an Escherichia *coli* E2011*fadD*$^{-}$/*fadR*$^{-}$ strain. Further, we selected *fadD1*, *fadD2*, *fadD2* and *fadD1* and the *fadD2-D1* fusion for cloning into a plasmid for metabolic complementation.

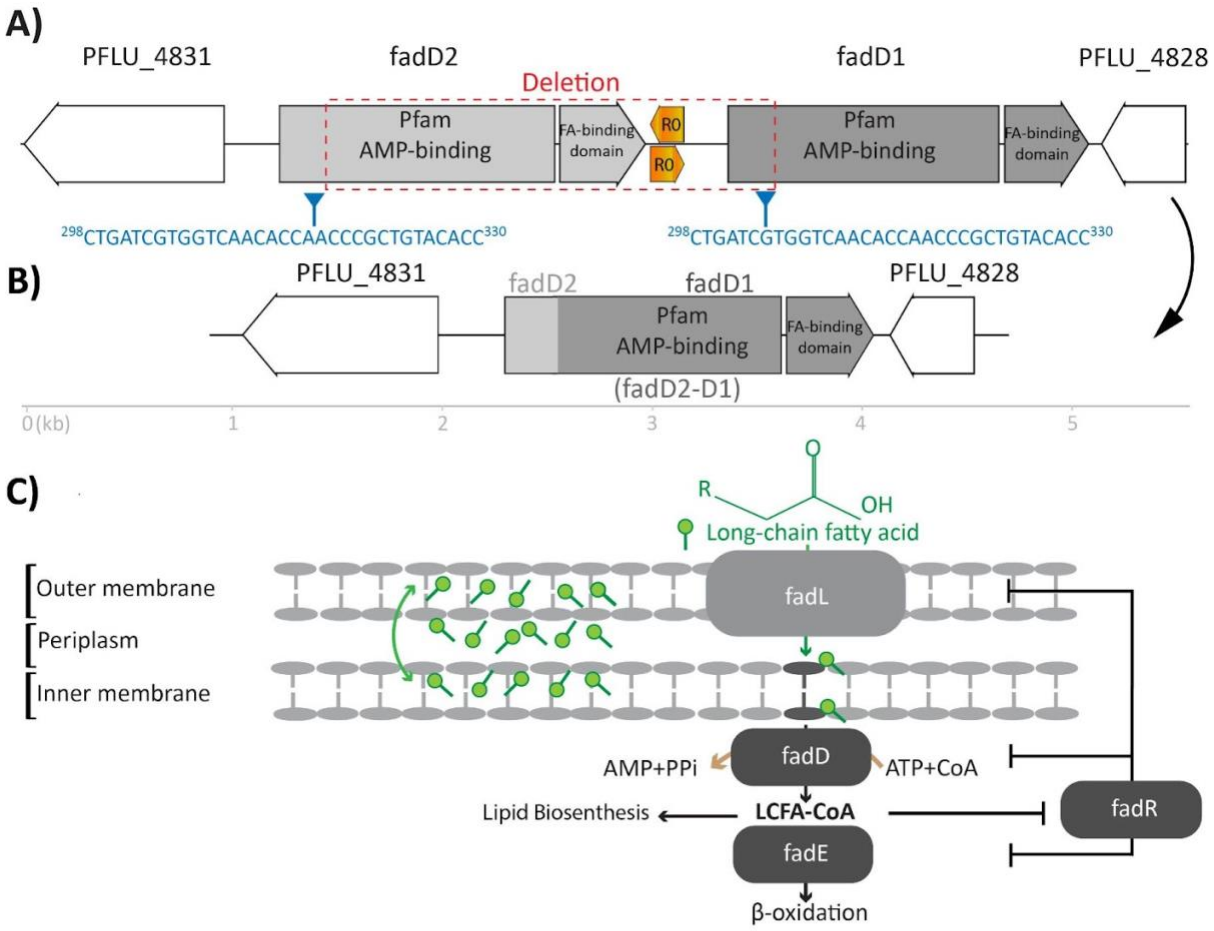

D)

	ATP/AMP Binding Motif	Fatty Acids Binding Motif
E. coli fadD	213YTGGTTGVAKGA224--356GYGLTE361--431NGWLHTGDIAVMDEEGFLRIVDRKK455	
P. aeruginosa fadD1	213YTGGTTGVAKGA225--357GYGMTE362--432DGWLKTGDIAIIQEDGYMRIVDRKK456	
P. f. SBW25 fadD1	214YTGGTTGVAKGA225--357GYGMTE362--432EGWLKTGDIAIIQPDGYMRIVDRKK456	
P. aeruginosa fadD2	213YTGGTTGVSKGA224--364GYGLTE369--441EGWLKTGDIAVIDEDGFVRIVDRKK465	
P. f. SBW25 fadD2	214YTGGTTGLAKGA225--364GYGLTE369--440EGWLKTGDIAVMDDDGFVRIVDRKK464	
P. aeruginosa fadD3	223HTGGTTGTPKLA234--366GYGLTE371--431DGWFNTGDLGRIDEDGYIWLTGRSK455	
P. f. SBW25 fadD3	222YTGGTTGDAKGV233--366GYGLTE371--447EGWLSTGDIGVMDARGYIRLVDRKK471	
P. aeruginosa fadD4	173YTSGTTGVPKGV184--334VYGMTE339--399DGFLRTGDKGEQDADGNLRLTGRMK423	
P. f. SBW25 fadD4	173YTSGTTGLPKGV184--334VYGMTE339--399DGFLRTGDKGEQDADGRLRLTGRLK423	
P. f. SBW25 fusion	214YTGGTTGVAKGA225--357GYGMTE362--432EGWLKTGDIAIIQPDGYMRIVDRKK456	

Figure 4. 4**.** *P. fluorescens* SBW25 *fadD* domain map and fatty acid degradation pathway. A) *fadD2* and *fadD1* genes with predicted domains and the deletion is shown in the red box and the precise locations of the two 33 bp repeats shown in blue colour. B) The predicted *fadD* fusion gene and domain after deletion that results in Volcano phenotypes. C) The fatty acid transport and biosynthesis model in *P. fluorescens* SBW25 based on the *E. coli* β-oxidation pathway. D) Alignment of amino acid sequences of *fadD* genes present in *P. fluorescens* SBW25 with *fadD* motifs in *E. coli* and *P. aeruginosa*. The FadD protein is composed of two highly conserved sequence elements corresponding to a proposed ATP/AMP signature motif [42,45] as well as a signature motif involved in FA substrate binding and specificity [44]. FadD appears to employ these two motifs to activate FAs in a two-step process [44,45].

We employed *E. coli* E2011, a *fadD*$^{-}$/*fadR*$^{-}$ Kmr mutant previously used to ascertain the function of *fadD* homologs from *P. aeruginosa* [43]. This strain is *fadD*$^{-}$ and is therefore unable to use exogenous LCFAs as a sole carbon source in minimal media without a functioning *fadD* provided in trans on the pTrc99a plasmid. In order to test these genes for function we compared growth on supplemented M9 minimal media with either Palmitic acid C16:0 (PA) or Oleic acid C18:1Δ9 (OA) (Sigma-Aldrich O1008-5G) to growth on rich media LBA plates (Fig. 4.5 A).

As expected, all of the strains exhibited strong growth on M9 agar media supplemented with glucose as the sole carbon source (Fig. 4.5 B). We used *E. coli* K12 AB1157 as a WT control, this had similar growth on M9 supplemented with PA or OA or M9 plus glucose. Whereas, *E. coli* E2011 without a plasmid and the empty pTrc99a vector control did not demonstrate growth on the media supplemented with PA or OA. The *E. coli* E2011 strain expressing *P. fluorescens* SBW25 FadD1, FadD2, FadD2+FadD1 and the FadD2-D1 fusion, all demonstrated growth on M9 supplemented with PA and/or OA. *E. coli* E2011, complemented with *fadD1* or ΔfadD2ΔfadD2 genes, appeared to have better growth than either the *fadD2* or the *fadD2-D1* fusion genes (Fig. 4.5 B). The amount of enhanced growth in the presence of *fadD1* and *fadD2* genes suggests that *fadD1, fadD2+fadD1* and the *fadD2-D1 fusion* each encode a functional acyl coenzyme A (CoA) synthetases. We see some evidence that the *fadD1* provides stronger growth on both PA and OA than the *fadD2* alone. We also infer from these data that the expression of FadD2 alone or the deletion leading to the *fadD2-D1* gene fusion effectively reduced the degree to which exogenous LCFAs are converted to coenzyme A (CoA) thioesters and are subsequently degraded by β-oxidation in *P. fluorescens* SBW25.

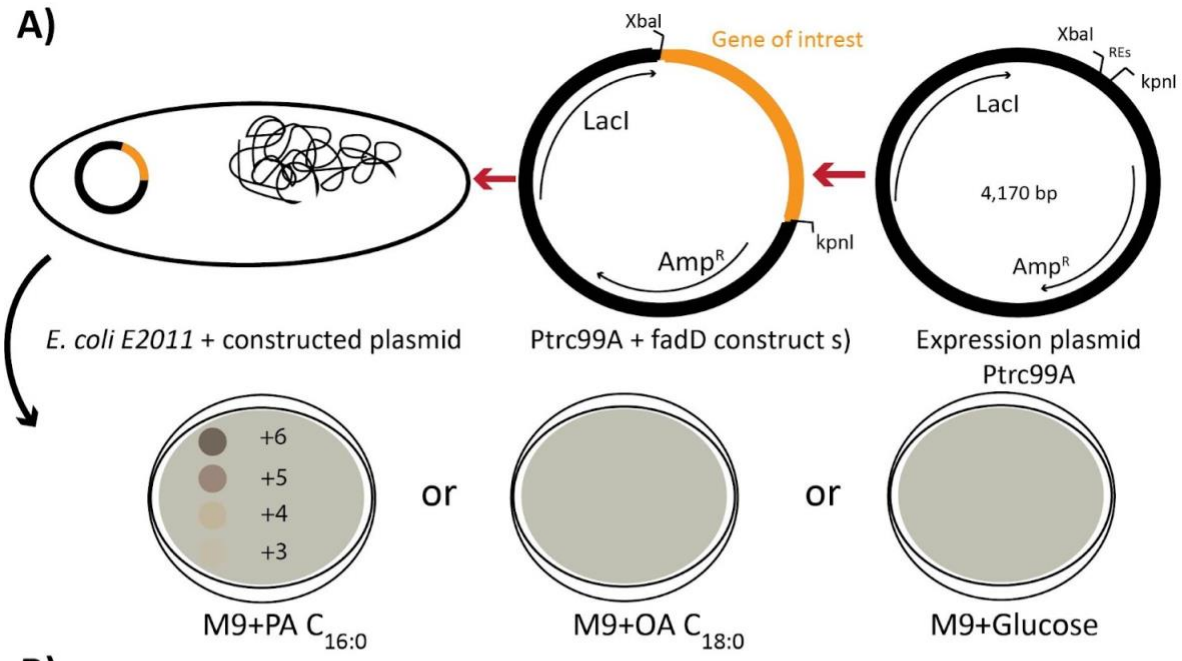

B)

Strains	PA $C_{16:0}$	OA $C_{18:0}^{\Delta 19}$	Glucose
E. coli K12	+6	+6	+6
E. coli E2011 (fadD⁻/fadR⁻)	0	0	+5
E. coli E2011 + pTrc99a	0	0	+5
E. coli E2011 + pTrc99a::fadD1	+5	+4	+6
E. coli E2011 + pTrc99a::fadD2	+4	+3	+6
E. coli E2011 + pTrc99a::fadD2fadD1	+5	+5	+5
E. coli E2011 + pTrc99a::fadD2-D1 (fusion)	+3	+3	+6

Figure 4. 5. *E. coli* E2011 complementation with *P. fluorescens* SBW25 *fadD* homologs. A) A diagram showing the different cloning steps; Genes of interest were cloned into the high copy expression plasmid Ptrc99A and the resulting plasmid introduced into E2011 double mutants (see materials and methods). B) A table showing the growth of E. coli K12 as a positive, E. coli E2011 as negative controls and E2011 harbouring an empty plasmid and fadD constructs on M9 media supplemented with different long chain fatty acids or Glucose as the sole carbon source. +1 denotes very poor growth, +3 denotes mild growth and +6 indicates heavy growth.

The previously reported effect of *Acanthamoebae* proximity on predation resistance (Chapter 3) led us to investigate the phenotypic changes induced in these reconstructed mutants by the presence or absence of predators. We therefore turned

our attention to the effect of the *Acanthamoebae* on the Vol colony morphology when these *fadD* mutations were reconstructed in the *P. fluorescens* SBW25 WT strain.

Our first observation is that in the absence of *fadD2*, colonies do not appear to express the Vol colony morphotype (*P. fluorescens* SBW25 Δ*fadD2,* Smooth colony frequency; 1.0). However, Vol morphology was more likely to manifest in *P. fluorescens* SBW25 Δ*fadD1* colonies (opaque central colony - Vol colony frequency; 1.0) (Table 1). This suggests that the lack of the *fadD1* gene causes the Vol colony morphotype. The *fadD2-D1* fusion produces an enzyme that retains the start of the *fadD2* and these results further support the assertion that this region of the protein or the expression that is driven by the promoter region upstream of this ORF is key.

In the absence of both *fadD1* and *fadD2* we observed a surprising activation of the Vol colony morphology (in the presence of the evolved predator) that may suggest that the other FadD homologs in *P. fluorescens* SBW25 are engaged when the *fadD2 and fadD1* under investigation here are absent or that FadD1 has a role in negatively regulating other FadD homologs in the cell [43]. Last but not least, we note that the presence of evolved *Acanthamoebae* appears to elicit a more substantial Vol colony morphology than the ancestral predator (Table 4.1). This suggests that behavioural memory of the interaction with *Acanthamoeba* survives more divisions after exposure to the evolved predators than those that are naive.

Table 4. 1. Colony morphology changes associated with Predators in reconstructed fadD mutations of interest in WT background. Colony morphology results of the Volcano mutants in the presence and absence of *Acanthamoebae* on PM agar media supplemented with 2% FBS. All plated colony morphotypes were consistent in each predation environment. “+” denotes the proportion of the colony that is caldera-like.

Strains	No Predator	Ancestral Predator	Ev. Predator
WT SBW25 + Δ*fadD1*	 + VOL	 + VOL	 ++ VOL
WT SBW25 + Δ*fadD2*	 SM	 SM	 SM
WT SBW25 + Δ*fadD2*Δ*fadD1*	 + VOL	 + VOL	 +++ VOL
WT SBW25 + Δ*fadD2-D1 (fusion)*	 + VOL	 ++ VOL	 +++ VOL
Evolved Vol-L1	 ++ VOL	 ++ VOL	 +++ VOL
Evolved Vol-L6	 + VOL	 ++ VOL	 +++ VOL

FadD mutants and their effect in resisting predation

We previously reported that Vol morphotypes persisted in five out of nine lines by the end of a 90-day co-evolution experiment and these Vol isolates had improved survival when grown with their coevolved but not ancestral predators (average fold change, 63 times greater than WT in the presence of coevolved than ancestral - chapter 3). We can now evaluate this adaptation in the context of its molecular cause; a deletion that produces a *fadD2-D1* fusion which effectively decreases the degradation of exogenous LCFAs by *P. fluorescens* SBW25. In order to investigate the effect of disrupted *fadD2* and *fadD1* on predation we carried out a 4-day-performance assay (PA), under the same conditions as in the 90-day experiment with these reconstructed mutants, the 90-day coevolved and ancestral WT bacteria (Table 4.2). The ancestral and 90 day evolved predators were used in addition to no predator controls.

The 90-day evolved Vol-L1 isolate performed poorly against the ancestral *Acanthamoeba* and was consumed 197-fold. This was reversed in the more experienced CE *Acanthamoeba* from Line 1 which only decreased the Vol-L1 by 17-

fold in the same amount of time. WT prey had an advantage over the Vol morphotype in the presence of the Ancestral predators and were only reduced by 24-fold. The evolved L1 CE *Acanthamoebae* were able to reduce the WT prey by 234-fold (Fig. 4.6 A). This suggests that the evolved predators had improved in their predation efficiency against WT cells and that the L1 Vol cells have an advantage against their co-evolved predators but not against the ancestral predators.

Table 4. 2. The name and genotype of each bacterial strain used in the performance test assay.

Bacterial Strains	Genotype
WT SBW25	-
Ev. Vol-L1	LuxR (PFLU_0925) & ΔfadD2-D1(fusion)
WT SBW25	ΔfadD1
WT SBW25	ΔfadD2
WT SBW25	ΔfadD2-D1 (fusion)
WT SBW25	ΔfadD2ΔfadD1
Ev. Mnt-L2	putative exported protein (PFLU_0924) & Δ4974-4975
Ev. Mnt-L5[2]	Δ4974-4975
WT SBW25	ΔPFLU_4974
WT SBW25	ΔPFLU_4975
WT SBW25	ΔPFLU_4974ΔPFLU_4975

In order to investigate the influence of the *fadD2* and *fadD1* genes on this phenomenon, we used the reconstructed mutations in the PA test. According to our *E. coli* E2011 experiments, the degree to which *P. fluorescens* SBW25 mutants were consumed (5-fold and 95-fold reduction in the presence of ancestral and evolved

predator, respectively) scaled with the degree of exogenous LCFA activation. In the presence of ancestral *Acanthamoebae,* the mutants with the lowest LCFA degradation activity (ΔfadD2 < ΔfadD1 = *fadD2-D1 fusion)* were the prey that have experienced more cell loss (11, 20 and 47-fold reduction, respectively). However, these did not differ significantly (*P≤ 0.02, Two sample T tests, relative to WT) from one another in the presence of the evolved Line 1 predator (17, 21 and 22-fold reduction) and any reduction of exogenous LCFA degradation appeared to result in the same fold change in prey reduction (Fig. 4.6 A). On the other hand, ΔfadD2ΔfadD1 mutation, is the least reduced by ancestral predator (5-fold reduction) but was overall reduced 95-fold by the evolved predator-L1 relative to the no predator group.

Vol-L1 isolate carries an additional mutation compared to the WT reconstruction carrying the *fadD2-D1* fusion. The addition of this LuxR/malT (PFLU_0925) mutation appears nonsubstantive against the Evolved L1 predator, but may be a disadvantage against the ancestral predator whereas the *fadD2-D1* fusion is reduced less than the Ev. Vol-L1 (Fig. 4.6). The double deletion ΔfadD2ΔfadD1 is more similar to WT in the presence of the ancestral and Line 1 *Acanthamoebae.* This is reminiscent of the colony morphology experiment (Table 4.1) and once again suggests that in the absence of these two copies of *fadD* other homologs in *P. fluorescens* SBW25 may be expressed but this has not been analysed further.

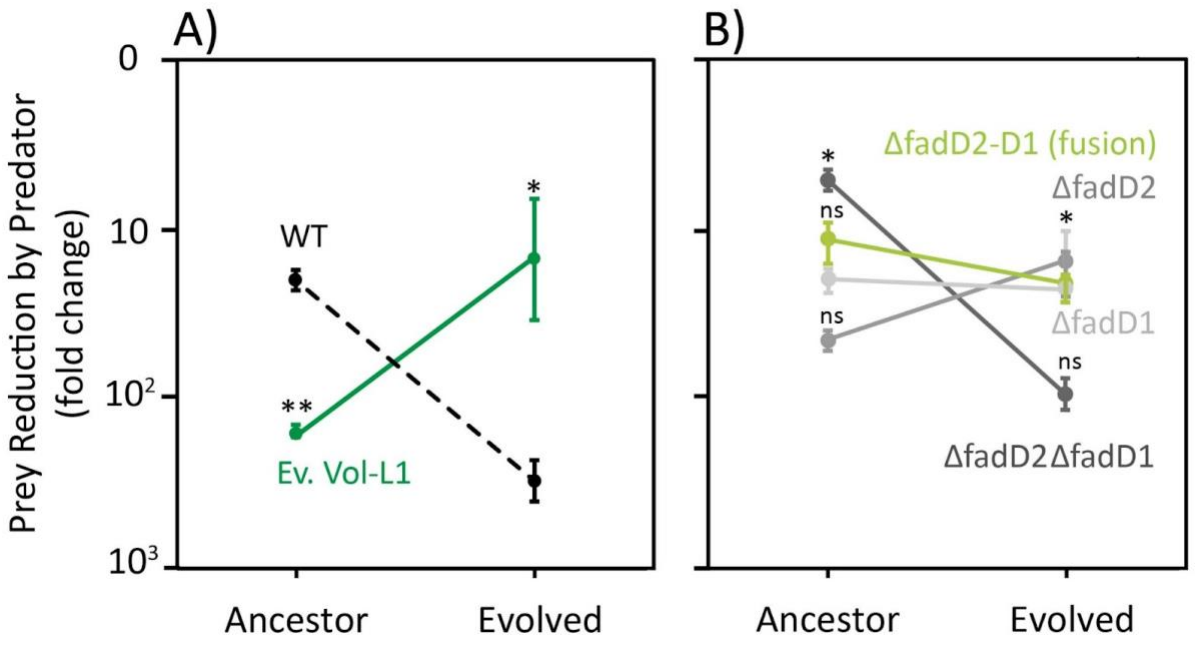

Figure 4. 6**.** The state of the *FadD* genes determines fold prey survival against Evolved L1 and Ancestral Predators**.** A) The *fadD* mutations substantially affect the performance of the bacterial mutants when encountered by predators. Contrary to WT prey survival, Ev. Vol L1 resist predation by Ev. L1 predator, but are more susceptible to ancestral predators. B) A single deletion of the *fadD* genes and Volcano deletion appear to have the same effect as the Ev. Vol-L1 in the presence of CE *Acanthamoebae*-L1, but not in the presence of the ancestral predator. The Δ*fadD2*Δ*fadD1* and Δ*fadD2-D1* mutants both exhibit the same trend as the WT prey, however the latter (deletion of *fadD2-D1*) appears to be more advantageous in the presence of the both Ev. L1 and ancestral predator types compared to other bacterial types. Error bars represent standard deviation (n=6, **P≤ 0.008, *P≤ 0.02, Two sample T tests, relative to WT prey in the presence of ancestral and evolved predators).

Differential Gene Expression in Vol-L1 Undergoing Predation

Further to these results, we made a profile of differentially expressed genes (DEG) for the coevolved Vol-L1 (Volcano L1; ΔfadD2-fadD1 & luxR T2675G) while predated by ancestral *Acanthamoebae*. WT *P. fluorescens* SBW25 was used as the baseline and significant differential expression was considered for genes with $\log_2$ FC ≥ 2, *P*-value ≤ 0.05 between conditions. We identified a total of 953 DEGs, of which 293 were upregulated and 660 were downregulated. Differential gene expression profiles were analysed with STRING and ReViGO, which revealed significant enrichments in several

gene clusters (where multiple enriched genes were involved in the same function) and gene ontology terms. Within Vol-L1 under predation by ancestral *Acanthamoebae* we found 21 upregulated genes, involved in O-antigen biosynthesis and presentation, a possible mechanism to resist predation [46–48]. Vol-L1 had enrichments in all three viscosin genes (a finding unique to the Vol-L1 strain) and lipopolysaccharide-A production. Furthermore, Vol-L1 had significant downregulation of seven efflux genes, most significantly PFLU_3263 (an efflux transporter), as well as a fatty acid transporter (PFLU_4903) (Fig. 4.9, Supplementary Fig. 3 & Table 4).

On the other hand, we performed a DEG profile for ancestral *Acanthamoebae* while predating upon Vol-L1 relative to the ancestral *Acanthamoebae* in the presence of WT SBW25. The latter was used as a baseline condition as described above. We identified 40 DEGs within ancestral *Acanthamoeba* while growing on Ev. Vol-L1, of which 25 were upregulated and 15 were downregulated. We found ACA1_141850, an NAD (P) H: quinone oxidoreductase the most upregulated gene in *Acanthamoebae* (as compared to predating on WT SBW25), and ACA1_061900, a translation elongation factor the most downregulated gene while interacting with Vol-L1 (Supplementary Fig. 2).

Mountain mutants and their effect in resisting predation

As described above, Mnt colony variants contain a 422bp deletion which deletes the nucleotides of two ORFS ΔA643-A1065 of PFLU_4974, and ΔA1-A1098 of PFLU_4975 including the intergenic space between these genes (Fig. 4.7 A and Supplementary Table 2). We hypothesised that this deletion effectively deletes a large section of the promoter region upstream of efflux RND transporter PFLU_4976,

bringing it under the regulatory control of the PFLU_4974 promoter. This specific mutation was identified in all nine CE bacterial populations and presented in 20/29 colonies at the end of the 90-day experiment. As reported above, we noted that the join points of Mnt associated Δ4974-4975 deletion has a pair of 10 bp tandem repeat (*CTGCGCGTCC*), which present within the PFLU_4974 and the intergenic space between genes PFLU_4975 & 4976 where deletion ends. Sequence identity of this mutation is predicted to have a strong effect on increasing the likelihood of a recombination event that would generate both duplications and deletions of the region in the population, suggesting that these mutations are taking place in the population far more often than one would expect at random.

In seven out of nine lines, Mnt isolates include at least one additional mutation (Supplementary Table 2). In our previous study we described that Mnt isolates are more resistant to *Acanthamoeba* spp. predation than *P. fluorescens* SBW25 WT cells. This suggested to us that the PFLU_4974-PFLU_4975 deletion (Δ4974-4975) is responsible for predation resistance in these cells. However, the two ORFS involved are both of unknown function and did not readily suggest functions. In order to investigate the consequences of this deletion we reconstructed the complete deletion of the two genes involved in the Mnt deletion in the WT background (Δ4974Δ4975) and deleted the ORFs PFLU_4974 and PFLU_4975 genes individually (Δ4974 and Δ4975). We also used two of the isolates from day 90 of the experiment, ΔMnt-L5^{2}; an evolved isolate that only carries the Δ4974-4975, and Ev. Mnt-L2 which carries an additional mutation (AA R264C) in an unknown protein (PFLU_0924) (Table 4.2).

We also noted that the downstream genes, whose expression might be affected by this deletion, encodes a putative HlyD and a large Resistance-Nodulation-Division

(RND) and Membrane Fusion Protein (MFP) Efflux pump complex [49]. The latter are associated with transporting antibiotics and toxins including fatty acids, outside of the cell (Fig. 4.7 A). We assessed the consequences of these deletions for predation resistance by conducting PA experiments under the same conditions as the 90-day experiment in the presence of ancestral and evolved predators relative to no predator population.

The Mnt deletion isolate with an additional mutation (Mnt-L2) had a slight disadvantage in the presence of the ancestral predator (Fig. 7B) however, in the presence of the co-evolved Line 2 predators, this strain proved to be 230-fold more resistant to predation than the WT *P. fluorescens* SBW25 which was readily predated. This was not observed however in the Ev. Mnt-L5^{2} (Δ4974-4975) which did not have any additional mutations. On the contrary, this strain performed on par with the WT prey but showed a distinct disadvantage in the presence of the CE L2 predator.

Ev. Mnt-L2 and WT demonstrated the same level of predation (~22 and 23-fold decreased) in the presence of ancestral predators, but as expected, Ev. Mnt-L2 was highly predator resistant when grown with their coevolved Line 2 predator, demonstrating 5-fold reduction over four days. While under the same conditions, the WT prey experienced 235-fold reduction relative to the no predation controls (Fig. 4.7 B).

The deletion of either ΔPFLU_4974 or ΔPFLU_4975 alone had a pattern that was more similar to that of the WT resulting in a slight reduction in these mutants in the presence of the predators (56-fold reduction). Further investigations of the effect of the Mnt

deletion (Fig. 4.7 C, Grey) in the predation resistance of these mutants however showed a pattern that was more similar to that of the WT, revealing a notable decrease in their population size in the presence of the evolved predator.

The EV. Mnt-L2 that also carries a substitution mutation (AA R264C) on the PFLU_0924 when predated by the evolved amoebae. However, the cell decrease caused by the ancestral predator was nearly the same as the WT (Supplementary table 2). Strikingly, the ∆4974∆4975 mutant was reduced to a great extent and higher than all other strains by both predator types (750 and 410-fold reduction, respectively) (Fig. 4.7 C).

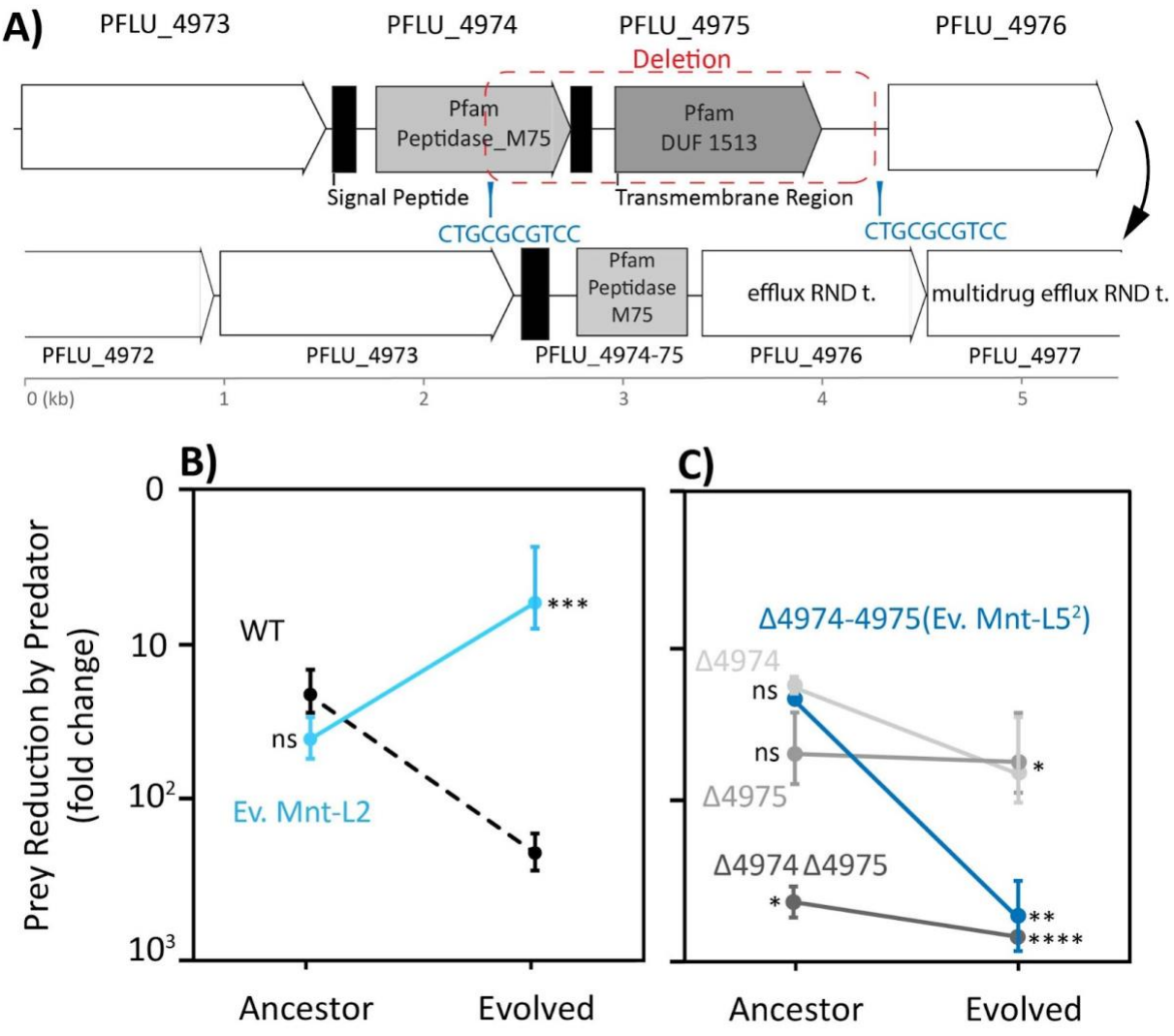

Figure 4. 7**.** Deletion of *Putative hypothetical* genes in *P. fluorescens* SBW25 was found in all of the coevolved lines at the end of the experiment. A) The genome and predicted domain map of genes involved in the mutation deletion and the 1,742bp deletion responsible for Mnt colony morphology is shown in the red dashed box - The mutation generated a 422-bp deletion (ΔA643-A1065) on PFLU_4974 and entire deletion of PFLU_4975 (ΔA1-A1098) including some part of the regulatory region. B) Prey Reduction based on PA test with Ev. Mnt-L2 (Δ4974-4975 + AA R264C on the PFLU_0924) substantially affects the performance of the bacterial mutants when predated by ancestral or CE L2 *Acanthamoebae*. Contrary to WT prey survival, Ev. Mnt-L2 resist predation by CE predators, but are more susceptible to ancestral predators. C) Prey Reduction with separate deletion of PFLU_4974, PFLU_4975, or both PFLU (Δ4974Δ4975) and Mnt deletion (Ev. Mnt-$L5^2$ = Δ4974-4975). The partial and complete deletions of PFLU_4974-PFLU_4975 decreases the survival under predation by Ev. L2 and ancestral predators. Error bars represent standard deviation (n=6, ****P≤ 0.00005, ***P≤ 0.0007, **P≤ 0.008, *P≤ 0.06, Two sample T tests, relative to WT prey in the presence of ancestral and evolved predators).

Capsule production

The Mnt colony morphologies were associated with a change in the appearance of the lawns of *P. fluorescens* SBW25 cells undergoing predation. Irrespective of the presence of predators when the Mnt colony morphologies appeared on the CFU plates, these were accompanied by lawns on the co-evolution plates that had a mucus-like appearance. We therefore investigated the capacity of the Mnt isolates for producing a colonic acid-like polymer [50]. Mnt isolates from different lines and the reconstructed mutants were stained with Indian ink (see materials and methods) and examined using light microscopy**.** We included a positive control named 6B4 [51] that makes large capsules in ~80% of the cells in LB broth. Though we did not find mutations in any of our predation-adapted genotypes in known encapsulation associated genes, most of Mnt isolates appeared to have increased capsule formation under standard laboratory conditions. Ev. Mnt-$L5^1$ strain that carries Δ4974-Δ4975 and additional mutation in ompR is the only evolved strain that was negative for capsule production. Similarly, none of the reconstructed Mnt mutants appeared to produce capsules (Fig. 4.8). The evolved Vol strains and Vol reconstructions were negative for

capsule production as well (data not shown). We therefore suggest the change in the expression of some genes in these mutants might be responsible for the increase in capsule production in these isolates.

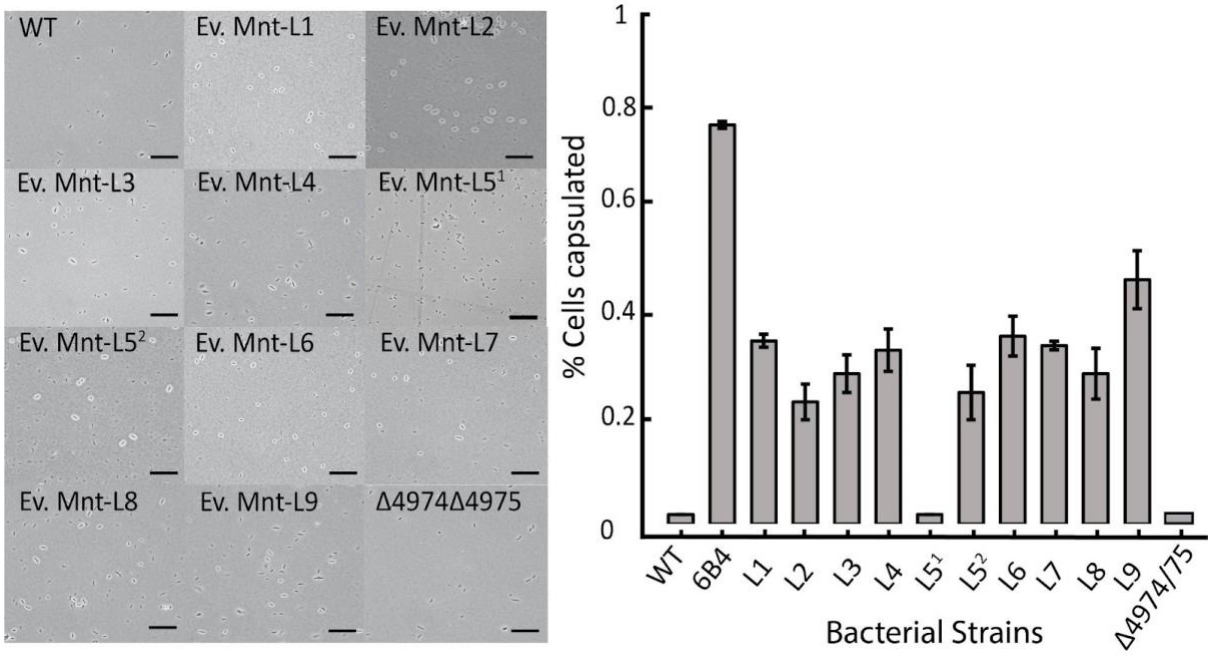

Figure 4. 8**.** Capsule production in *P. fluorescens* SBW25 Mnt mutants. The cells were picked up and stained while growing overnight in LB broth. Eight of the evolved Mnt strains were positive, while Mnt from evolved line5^1 and all reconstructions were negative for capsule formation. Error bars represent standard deviation (n=8). Scale bar: 30µm.

Differential gene expression in mountain undergoing predation

Differentially expressed gene (DEG) profiles were made for the coevolved strains Mnt-L2 (Mountain L2; ∆4974-4975 & PFLU_0924 C790T) while under predation by ancestral *Acanthamoebae*. In this case we also used WT *P. fluorescens* SBW25 without predation as a baseline as described previously. In this condition and compared to the WT SBW25, we identified a total of 209 DEGs, of which 118 were upregulated and 91 were downregulated. Differential gene expression profiles were analysed with STRING and ReViGO, which revealed significant enrichments in several

gene clusters (where multiple enriched genes were involved in the same function) and gene ontology terms. Within Mnt-L2 we found 12 upregulated genes, involved in O-antigen biosynthesis and presentation, a possible mechanism to resist predation [46–48]. Interestingly, the Mnt-L2 deletion resulted in upregulation of an RND pump downstream of the deletion (PFLU_4976) compared to WT (log2FC = 3.12 when interacting with *Acanthamoebae*, log2FC = 2 without *Acanthamoebae*) and a unique enrichment (5 genes) in the cyclophilin-like domain (immunophilin) (Fig. 4.9, Supplementary Fig. 3 & Table 4).

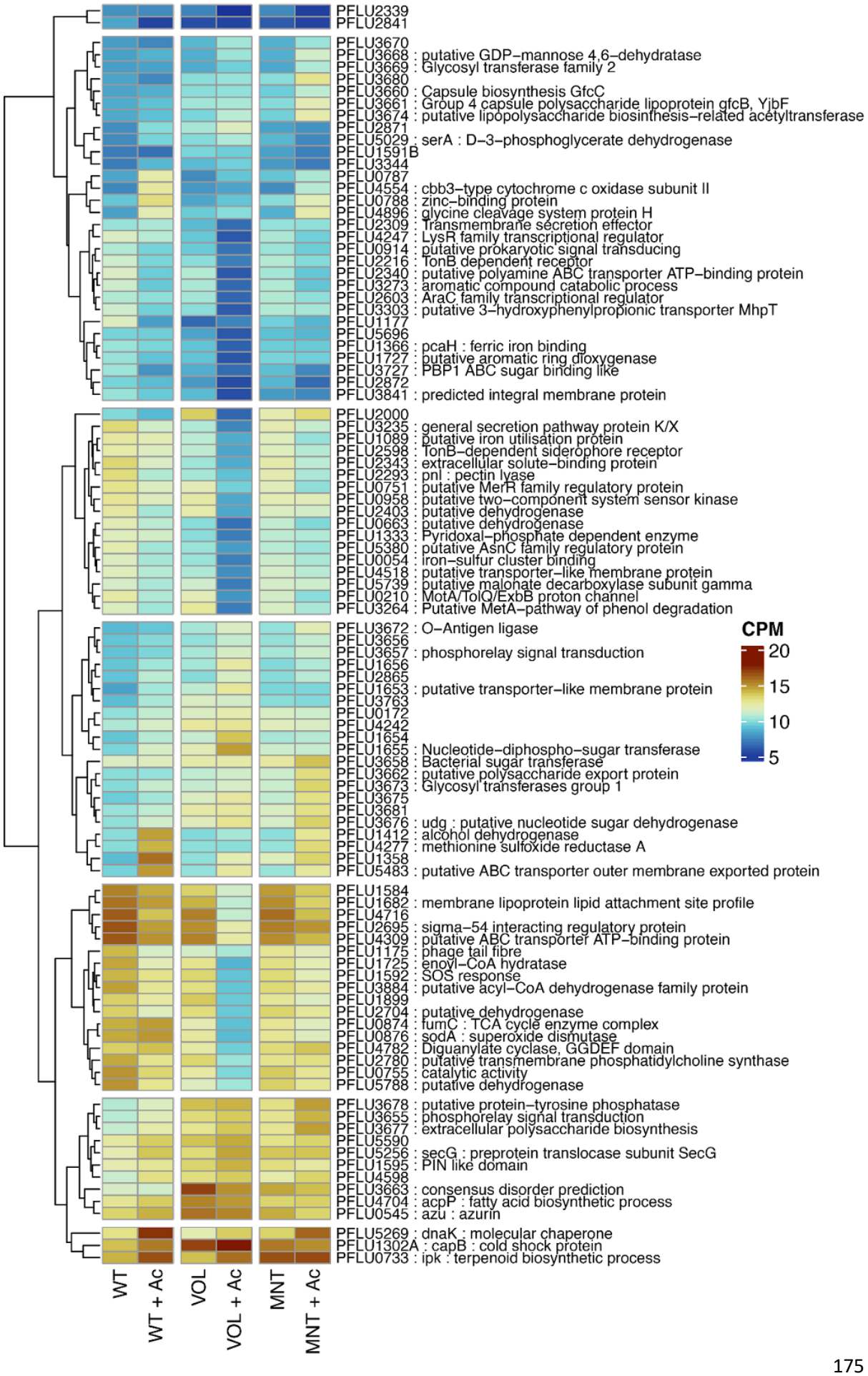
PFLU2339
PFLU2841
PFLU3670
PFLU3668 : putative GDP−mannose 4,6−dehydratase
PFLU3669 : Glycosyl transferase family 2
PFLU3680
PFLU3660 : Capsule biosynthesis GfcC
PFLU3661 : Group 4 capsule polysaccharide lipoprotein gfcB, YjbF
PFLU3674 : putative lipopolysaccharide biosinthesis−related acetyltransferase
PFLU2871
PFLU5029 : serA : D−3−phosphoglycerate dehydrogenase
PFLU1591B
PFLU3344
PFLU0787
PFLU4554 : cbb3−type cytochrome c oxidase subunit II
PFLU0788 : zinc−binding protein
PFLU4896 : glycine cleavage system protein H
PFLU2309 : Transmembrane secretion effector
PFLU4247 : LysR family transcriptional regulator
PFLU0914 : putative prokaryotic signal transducing
PFLU2216 : TonB dependent receptor
PFLU2340 : putative polyamine ABC transporter ATP−binding protein
PFLU3273 : aromatic compound catabolic process
PFLU2603 : AraC family transcriptional regulator
PFLU3303 : putative 3−hydroxyphenylpropionic transporter MhpT
PFLU1177
PFLU5696
PFLU1366 : pcaH : ferric iron binding
PFLU1727 : putative aromatic ring dioxygenase
PFLU3727 : PBP1 ABC sugar binding like
PFLU2872
PFLU3841 : predicted integral membrane protein
PFLU2000
PFLU3235 : general secretion pathway protein K/X
PFLU1089 : putative iron utilisation protein
PFLU2598 : TonB−dependent siderophore receptor
PFLU2343 : extracellular solute−binding protein
PFLU2293 : pnl : pectin lyase
PFLU0751 : putative MerR family regulatory protein
PFLU0958 : putative two−component system sensor kinase
PFLU2403 : putative dehydrogenase
PFLU0663 : putative dehydrogenase
PFLU1333 : Pyridoxal−phosphate dependent enzyme
PFLU5380 : putative AsnC family regulatory protein
PFLU0054 : iron−sulfur cluster binding
PFLU4518 : putative transporter−like membrane protein
PFLU5739 : putative malonate decarboxylase subunit gamma
PFLU0210 : MotA/TolQ/ExbB proton channel
PFLU3264 : Putative MetA−pathway of phenol degradation
PFLU3672 : O−Antigen ligase
PFLU3656
PFLU3657 : phosphorelay signal transduction
PFLU1656
PFLU2865
PFLU1653 : putative transporter−like membrane protein
PFLU3763
PFLU0172
PFLU4242
PFLU1654
PFLU1655 : Nucleotide−diphospho−sugar transferase
PFLU3658 : Bacterial sugar transferase
PFLU3662 : putative polysaccharide export protein
PFLU3673 : Glycosyl transferases group 1
PFLU3675
PFLU3681
PFLU3676 : udg : putative nucleotide sugar dehydrogenase
PFLU1412 : alcohol dehydrogenase
PFLU4277 : methionine sulfoxide reductase A
PFLU1358
PFLU5483 : putative ABC transporter outer membrane exported protein
CPM
20
15
10
5
PFLU1584
PFLU1682 : membrane lipoprotein lipid attachment site profile
PFLU4716
PFLU2695 : sigma−54 interacting regulatory protein
PFLU4309 : putative ABC transporter ATP−binding protein
PFLU1175 : phage tail fibre
PFLU1725 : enoyl−CoA hydratase
PFLU1592 : SOS response
PFLU3884 : putative acyl−CoA dehydrogenase family protein
PFLU1899
PFLU2704 : putative dehydrogenase
PFLU0874 : fumC : TCA cycle enzyme complex
PFLU0876 : sodA : superoxide dismutase
PFLU4782 : Diguanylate cyclase, GGDEF domain
PFLU2780 : putative transmembrane phosphatidylcholine synthase
PFLU0755 : catalytic activity
PFLU5788 : putative dehydrogenase
PFLU3678 : putative protein−tyrosine phosphatase
PFLU3655 : phosphorelay signal transduction
PFLU3677 : extracellular polysaccharide biosynthesis
PFLU5590
PFLU5256 : secG : preprotein translocase subunit SecG
PFLU1595 : PIN like domain
PFLU4598
PFLU3663 : consensus disorder prediction
PFLU4704 : acpP : fatty acid biosynthetic process
PFLU0545 : azu : azurin
PFLU5269 : dnaK : molecular chaperone
PFLU1302A : capB : cold shock protein
PFLU0733 : ipk : terpenoid biosynthetic process
WT
WT + Ac
VOL
VOL + Ac
MNT
MNT + Ac

Figure 4. 9**.** Heatmap of the top differentially expressed genes among evolved strains Vol-L1 and Mnt-L2 when interacting with the ancestral predator (Vol-L1 + predator, Mnt-L2 + predator). All fold change calculations are made against SBW25 (WT) grown on solid media, without amoeba. CPM (counts per million) is a raw count of the number of reads mapped to a gene, normalised for library size (number of total reads in a sample) and log transformed. Each row on the plot (genes) has at least one comparison ≥ 2 log_2FC (and P-value < 0.05) compared to the WT.

We further, analysed a DEG profile of ancestral *Acanthamoeba sp.* while predating upon Mnt-L2 strains. Ancestral *Acanthamoebae* while growing on WT SBW25 was used as a baseline and significant differential expression was considered for genes with log_2 FC ≥ 2, *P*-value ≤ 0.05 between two conditions. We identified a total of 163 DEGs within the predator in the presence of Ev. Mnt-L2, of which 159 were upregulated and 4 were downregulated. A Venn diagram of DEGs shows only 1 upregulated and no downregulated DEGs are shared between ancestral *Acanthamoebae* while predating upon the Mnt-L2 and Vol-L1 conditions. While predating upon Mnt-L2 (as compared to predating WT SBW25), the most upregulated gene in ancestral *Acanthamoeba* was ACA1_118780, an integral membrane protein of unknown function. Among significantly downregulated genes, while predating Mnt, *Acanthamoeba* downregulated ACA1_307560, a WD-40 domain containing protein (Supplementary Fig. 2).

Discussion

We have previously conducted a 90-day predator-prey coevolution experiment on solid surfaces to evaluate the genotypic evolution in *P. fluorescens* SBW25 prey population in response to predation and the effect of this coevolution on the fitness of *P. fluorescens* SBW25 genome. In that study, we described a set of colony

morphotypes that were common across the co-evolved lineages suggesting highly parallel phenotypic evolution under an amoeboid predation regime. We found on average ~3.2 colony morphology changes in the CE prey populations whereas the PO lines maintained the ancestral colony morphology (Fig. 4.1 B).

We observed the emergence of frequently repeated novel (Mountain and Volcano) and not so novel (Wrinkly Spreader) colony morphologies in the CE population lineages, but the molecular nature of the morphotypes had not been investigated. The Wrinkly Spreader and Mountain morphotypes were found in eight and nine of the CE replicates lines, respectively and, Vol was observed in four lines. Such observation predicted that predation pressure strongly tends to drive the evolution of defensive traits that can be beneficial in the face of other microorganisms (Chapter 2). These results and other empirical coevolution studies between bacterial predator and prey accomplished in liquid environments [21,24] strongly suggest that predator interactions are responsible for adaptation in CE prey that leads to positive selection for mutations.

In this study, we investigated the mutations that underpin the phenotypic diversity observed in the CE lines. Through a population sequencing, we observed nearly 3.7-fold more mutations overall among CE prey lines during the 90-day experiment and 4.7-fold more mutations per line at the end of the coevolution experiment compared to the PO lines. From the profile of mutations among PO lines, the substitution mutations on the PFLU_3879 and PFLU_4287 were found in two and three out of three PO lines, respectively. The latter was also observed in all nine CE replicate plates at lower

frequency. This suggests that there may have been instances of transfer between the CE and PO lines.

We found greater genetic divergence among CE populations (on average 28.4 mutations) than among PO lines (on average 7.6 mutations) during the experiment suggesting that predator interactions are responsible for adaptation in CE prey that leads to positive selection for mutations. In addition, we showed an average 3-fold more genes that were separately mutated among CE compared to the evolved control lines. Similar results have been observed in the empirical coevolution studies between *P. fluorescence* and phage that resulted in higher genetic divergence with nearly 13-fold more mutations within coevolved genotype compared to the evolved control [9]. It has been proposed that a high degree of phenotypic convergence and molecular parallelism in the replicates of multiple populations when exposed to an environment with identical selective pressures is very likely to arise among microorganisms [52–55]. We found mutations responsible for WS and Mnt colony morphology in eight and nine lines, respectively and Vol colony phenotype in four out of the nine lines. High degree of parallelism more often occurs between biological populations in experimental evolution indicating a similar evolutionary response to environmental stressors [56,57]. However, such frequent identical mutations in independent lineages have not to our knowledge been reported among microorganisms. Whilst phenotypic convergence under a strong evolutionary pressure would not be seen as amiss, the observation of identical deletions arising in 100% of a set of coevolution lineages is not expected. This observation required some further explanation in order to put aside the reasonable suspicion that this represents massive cross contamination [58].

After 90 days of evolution, 29 colonies were isolated, 20 of these had evidence of the Mnt associated deletion of PFLU_4974 and PFLU_4975 (∆4974-4975), 5 of which had the WspF ∆MMDLI mutation and 5 out of 29 carried the Δ*fadD2-D1* deletion (Supplementary Table 2). Further investigation suggested that the Δ*fadD2-D1* deletion join point harboured a 33 bp tandem repeat 2,038 bp apart whilst the ∆4974-4975 join point contained a 10 bp tandem repeat 1,734 bp apart. Sequence identity of this kind is both predicted and experimentally measured to have a strong effect on increasing the likelihood of a recombination event that would generate both duplications and deletions of the region in the population. Homology lengths of between 50 and 100 increase the recombination frequency to between 10^{-2} or 10^{-1} and identical tandem repeats of only 10 bp can be expected to recombine ~10^{-5} [40]. In populations of 10^{8-10} bacterial cells under predation pressure, we can expect many of these mutations to occur randomly in this and any other evolution experiment which uses *P. fluorescens* SBW25 as a result of these tandem repeats.

We therefore suggest that the 10 and 33 bp direct tandem repeats reported herein regularly create a sub-population of prey cells with either one of these deletions (in addition to the corresponding duplications) in the PFLU_4974-PFLU_4975 and *fadD2/fadD1* regions of the genome. However, only in the CE populations did these random deletions proved to be beneficial predation adaptations that subsequently increased in frequency through natural selection. As a result of this frequent subpopulation, parallel phenotypic and genotypic evolution was found between the coevolved lineages.

The profile of mutations in coevolved prey populations demonstrate a complete or partial loss of gene function on *fadD1*, *fadD2*, *wspF* and putative hypothetical proteins (PFLU_4974 and PFLU_4975). In addition, altered gene function was separately identified in these mutants (Supplementary table 2). Mutations in the response regulatory and demethylase domain of *wspF* gene are well known to increase cellular levels of cyclic-di-GMP and ultimately cause cells to constitutively over-produce extracellular cellulose, resulting in robust biofilms in the structured [13] and unstructured environment [59]. Three distinct regulatory pathways are believed to encode *wss* transcription; Wsp chemosensory response system - awsXR and amrZ/fleQ. In this study among CE lines, we identified various mutations on the Wsp and awsXR system resulting in the formation of WS morphotype that showed extensive resistance against the predators (Chapter 3). These three pathways control the activation of the secondary signalling molecule c-di-GMP leading to formation of biofilm-producing mutants in WS strains [60–62].

We used genetic reconstruction and a complementation assay to begin to investigate the nature of the Vol mutants *fadD2-D1* fusion mutation. *P. fluorescens* SBW25 has four fadD homologs which are annotated as having a role in fatty acid degradation. In the complementation assay we tested the two homologs in the fusion, in addition to the fusion to determine the level of growth observed in *E. coli* E2011 (*fadD*$^{-}$/*fadR*$^{-}$ Km^{r}). We determined that both the *fadD1* and *fadD2* genes encoded proteins were functional in long chain fatty acid degradation. However, we observed that the FadD1 protein, provided in trans, supported a greater degree of growth of the *E. coli E*2011 mutant on minimal media supplemented with either PA or OA. This suggests that FadD1 is

likely primary in converting exogenous LCFA into acyl-CoA for in *P. fluorescens* SBW25.

We further investigated the role of the *fadD* genes in contribution to the development of Volcano morphology. We created multiple fadD deletions in the WT *P. fluorescens* SBW25 background using two-steps allelic exchange and tested the resulting strains in the presence and absence of predators in the same condition as in the 90-day experiment. Our CFU mediated observation of reconstructed mutants confirmed that either the complete deletion of *fadD1* or the partial deletion of *fadD1* (as in the fusion) leads to the formation of Volcano morphotype in the presence of ancestral or evolved amoebae (Table 4.2). The deletion of *fadD2* did not produce the same effect. We also noted that the Vol colony morphology was more pronounced in the presence of the ancestral and evolved predators and was less pronounced in the absence of these predators. These findings indicate that the Vol phenotype is the product of the loss of *fadD1* function. This is significant in that *fadD1* is implicated in being the primary FadD in exogenous LCFA conversion to acyl CoA. This implies that the *P. fluorescens* SBW25 cells with this fusion mutation may be accumulating exogenous LCFA in their membranes.

We previously showed that the *P. fluorescens* Vol cells became predation resistant only in the presence of the evolved *Acanthamoebae* and that if they were grown in the absence of the *Acanthamoebae* they were not subsequently resistant to predation. This suggested a molecular or gene regulation change that is taking place in the presence of the predators. This would appear to indicate a molecular or chemical change in the bacteria that is precipitated by the presence of the *Acanthamoeba*

directly. The PA test measures predator and prey success simultaneously and in the case of the *fadD2-D1* deletion mutant this test revealed that loss of these genes increases their survival during predation by coevolved *Acanthamoebae.* Consistent with expectations, Ev. Vol-L1 (*fadD2-D1* deletion & LuxR mutation) exhibits a high degree of resistance to their coevolved L1 predator. However, the latter demonstrated poor survival during predation by ancestral WT *Acanthamoebae* (197-fold reduction). The clean *fadD2-D1* deletion in WT *P. fluorescens* SBW25 background results in similar levels of resistance to that of the Ev. Vol-L1 in the presence of the coevolved predator.

Fatty acids are the main part of the membrane structure and have a pivotal role in membrane function [63]. FadD is an acetyl-CoA synthesis protein and plays a major role in degrading exogenous LCFA [64].

Increasing the concentration of host associated LCFA in the membrane may mask prey cells in some way. This could involve making the *Acanthamoebae* less likely to consume them because the bacteria are recognised as self, rather than as prey. *Acanthamoebae* have LCFA incorporated into their own membranes. The primary LCFA in *Acanthamoebae* are oleic acids (40-50%), and longer polyunsaturated fatty acids (20-30%) and this might be the reason that *Acanthamoebae* cells are less rapidly consuming Vol cells [65]. On the other hand, phagocytosis is inescapably a membrane mediated activity. It is therefore possible that the bacteria are affecting the flow of LFCA in the Vol mutants in order to decrease the membrane fluidity in their *Acanthamoebae* predators, by increasing the abundance of saturated LCFAs. This would decrease the speed and therefore the rate of prey consumption on the part of

the predators. If the bacteria are preferentially enriching their membranes in immobile branched chain LCFA or unsaturated LCFA then these may be incorporated into the *Acanthamoebae,* either through passive diffusion or through export into the extracellular milieu by the bacteria. We did observe that *Acanthamoebae* actively take up fluorescently labelled LCFA from media and these are enriched first in phagosomes (Supplementary Fig. 9), suggesting that these are organelles whose function may be susceptible to alterations that involve changing available LCFA.

Finally, the degradation of LCFA by beta-oxidation produces reactive oxygen species [66]. It is formally possible that the decrease in FadD function that is accomplished by fusing the FadD proteins in Vol mutants is beneficial because it decreases cell death due to mutagenesis in the presence of exogenous LCFA provided by the *Acanthamoebae*. We do not favour this hypothesis, but it is a possibility. Future work in determining the LCFA present in the *Acanthamoeba* and the Vol mutants will shed light on how changes in LCFA degradation may be leading to an increase in prey fitness in the presence of the Evolved *Acanthamoebae*. This work may thereby also shed light on the consumption of exogenous LCFA by other pathogens such as *P. aeruginosa* and *Mycobacterium tuberculosis* [67–69].

In our previous work the Mnt colony morphotype proved to be highly resistant to amoeboid predation (17 and 10-fold increased survival over WT prey in the presence of ancestral and coevolved predator, respectively). This resistance was not influenced by the nature of the predation assay used, as was the case for the Vol colonies. Here we described the nature and dominance of the Mnt colony mutations. The genes affected by the Mnt deletion included PFLU_4974 and PFLU_4975 and a tandem

repeat of 10 bp was determined to be responsible, in part, for the frequency of this mutation in our CE lines. PFLU_4974 is a *putative hypothetical protein* (1,065 bp) and PFLU_4975 is a *putative exported protein* (1,098 bp). In order to better understand how the deletion of all of PFLU_4975 and most of PFLU_4974 would bring about predation resistance we deleted each gene alone and both of the genes entirely and reconstructed these in the WT *P. fluorescens* SBW25 background. In addition, we tested the Ev. Mnt-L2 (∆4974-4975 & PFLU_0924 C790T4) and the Ev. Mnt-L5^2 (∆4974-4975) alongside the reconstructed mutants (Table 4.2).

In our PA test we found that the mutants (for example Ev. Mnt-L2) carrying ∆4974-4975 and an additional substitution mutation on the putative exported protein (pflu_0924) exhibited a greater degree of resistance to predation with their coevolved predator (628-fold less reduction compared to Ev. Mnt-L5^2 that only carries ∆4974-4975 mutation). In contrast, the mutants with complete loss of either PFLU_4974 and PFLU_4975 (∆4974∆4975) were not beneficial in the presence of the coevolved predators and resulted in a 633-fold reduction by the predator. This deletion was also not beneficial during predation by ancestral *Acanthamoebae* (Fig. 4.7 A and Supplementary Table 2). This suggested that the additional substitution mutation (AA R264C) on the PFLU_0924, or correlation of the two mutations together (for example; ∆4974-4975 & PFLU_0924 C790T4) benefits these cells in the presence of the coevolved predator.

Seven out of nine Mnt isolates carry at least one additional mutation (Supplementary table 2) given the poor performance of the Mnt deletion alone (in Mnt-L5^2) under predation. The predation resistance of Ev. Mnt-L2, shows the evolution of anti-

predatory behaviours in these mutants suggesting that the Δ4974Δ4975 and Δ4974-4975 mutation deletions alone make bacteria more susceptible to predators and is not sufficient to produce predation resistance. The frequent co-occurrence of additional mutations in distinct genes appears to be required for increased survival and predation resistance.

On the predator side, we previously reported increased fitness on the WT prey as measured in generation numbers and increased predation rates in the coevolved *Acanthamoeba* compared to their ancestors (Chapter 3). In this experiment, the interaction between non-evolved prey-predator (WT prey + ancestral *Acanthamobae*) and coevolved prey-predator (Vol-L2 + *Acanthamoebae*-L2) after 90 days resulted in the same amount of reduction (24 and 23-fold, respectively) in the prey bacteria (Fig. 4.6). In addition, consistent with previous study, the higher cell reduction in WT prey by the evolved predator line1 and 2 (20 and 173-fold more reduction compared to when predated by ancestral predator, respectively) suggested strong predator evolution. This strongly indicates evidence of potent coadaptation among coevolved prey and predator populations. The heavy loss in the population sizes of the WT bacteria by the evolved predators is the consequence of predator evolution (Chapter 3). Our finding therefore confirms that coevolution accelerates prey-predator evolution and contributes to both sides compared to the non-evolved prey-predator. These results are therefore the product of a phenomenon that shows evolution takes place on both the prey and predator sides representing early stages of Van Valen's "Red Queen" Coevolution [70–72]. This is also consistent with previous empirical studies demonstrating that predator-prey coevolution increases molecular evolution and specialised traits in both prey and predator in unstructured environments [8,9,23,24].

Theoretical and empirical studies of microbial communities have revealed that predation asserts strong selective pressure on bacterial prey resulting in diversification and evolution of defensive traits [73,74]. This has been observed in experimental evolution of bacteria during predation by bacterial predators *Bdellovibrio bacteriovorus* and *Myxococcus xanthus* [6,24], protists *Tetrahymena thermophila* and *Acanthamoeba* [13,21], and phages [22]. An experimental coevolution between populations of *P. fluorescens* SBW25 and bacteriophages showed morphological changes in the prey bacteria that contributed to bacteriophage resistance [9,23]. This study was done in microcosms containing King B media for more than 400 generations with propagating *P. fluorescens* SBW25 with and without bacteriophages. Findings of this study revealed that evolving *P. fluorescens* in the presence of bacteriophage phi2 can lead to the increased mutation rates, the promotion of adaptations such as altered LPS and mucoid types in *P. fluorescens* SBW25 [75].

In this experiment the WS phenotype had a pronounced advantage over other evolved morphotypes. WS is a well-studied biofilm forming mutant and the property of forming a biofilm is a common virulence factor of many human pathogens such as *V. cholera* and *P. aeruginosa* [76,77] and biofilm forming mutants have been known to evolve in response to antibiotics as well [78]. WS colony morphotype is a common response of *Pseudomonad*s to ecological challenges including AL interfaces [59] and even space travel [79]. Intriguingly, the formation of exopolysaccharide through the activation of cyclic-di-GMP has previously been demonstrated to be a successful defence strategy of *P. fluorescens* SBW25 against free-living ciliate predators and bacteriophages in liquid environments [22,80–82].

The observation that this phenotype is advantageous during predation by *Acanthamoebae* may support the previous hypotheses that this is a direct adaptation in some bacteria to protect against amoeboid predation [14]. This also opens the door for this adaptation to being relevant in the more medically important parallel bacterial defence against phagocytic immune cells. The notion that traits that are common in bacterial pathogens might be entrained or evolved in response to predation pressure by amoeboid predators was first proposed by [83] and quickly embraced [10,84]. The evidence of traits that are found in pathogens being selected through predation pressure has however been lacking.

Volcano and Mountain were also major phenotypes evolved from WT strains after exposure to generalist protozoan predators. Vol was caused by a reduction in the effective FadDs, CoA ligase synthases that operate on LCFA and are present in many organisms such as *E. coli* and pathogenic bacteria *P. aeruginosa* [85,86]. In *P. aeruginosa, fadD* genes are considered virulence factors that are crucial for bacterial survival during lung infection in CF patients via degradation of lipids, specifically FAs that allow bacteria to proliferate and colonise within CF lungs [87]. Further work on why amoeboid predation brings about a decrease in the number of functional FadDs and the relationship between amoeboid LCFAs and resistance to predation in this study may lead to new insights into why pathogens take up exogenous host LCFAs in these closely related systems.

Formation or production of polysaccharide capsule (PLS), a common virulence factor of some bacterial pathogens has been observed in our experiment in Mnt phenotypes as a response to predation as well. Capsule formation is a common virulence trait that

has been implicated in parasite resistance in *P. fluorescens* SBW25 [23] and other bacterial pathogens [88,89]. We found production of capsules in all the Mnt isolates except in Ev. Mnt-L5[1] strain that carries ∆4974-4975 and a frameshift deletion mutation on the *ompR* gene (G112). It is believed that mutations in a SNP in rpoD and carB genes (PFLU_5592 and 5265, respectively) may be sufficient for the cause of capsule switching behaviour in *P. fluorescens* SBW25 [51,90]. Capsule formation has been reported among *P. fluorescens* SBW25 populations as a response to lytic phages as well [23] and observed in the experimental evolutions of *P. fluorescens* SBW25 in microcosm environments, where bacteria compete for both nutrient and oxygen acquisition in order for survival and replication [51], however, here we did not observe a correlation between predation resistance and capsule formation in our data.

Furthermore, O-antigen structures (a surface polysaccharide of gram-negative bacteria known as LPS) [91] associated with the bacterial cell surface is a known defence mechanism of many bacterial pathogens such as *salmonella spp* and *Klebsiella* against predation [46–48]. In this study, from the DEG profile of Mnt-L2 and Vol-L1 while predated by the ancestral *Acanthamoebae* we found 12 and 21 upregulated genes in O-antigen biosynthesis, respectively. The polysaccharide capsule (LPS) is considered as one of the main virulence factors produced by pathogenic bacteria to protect bacteria against phagocytosis by the host's immune system as well [92]. We found enrichments in lipopolysaccharide-A production and three viscosin genes in Vol-L1 (a finding unique to the Vol-L1 strain). Vol-L1 had significant downregulation of seven efflux genes, most significantly PFLU_3263 (an efflux transporter), as well as a fatty acid transporter (PFLU_4903). These results, taken with the finding of altered survivability only when evolved strains are grown with

Acanthamoebae and the abundance of mutations found in FadD genes, led to our hypothesis that the evolved bacteria might be altering transporters to counter increased exposure to LC fatty acids from the *Acanthamoeba* by increased oxidative stress from LC fatty acid degradation, masking, etc. Furthermore, we found upregulation of an efflux RND transporter downstream of the deletion (PFLU_4976) and a unique enrichment (5 genes) in the cyclophilin-like domain (immunophilin) in Mnt-L2. Among all DEGs, 72 upregulated and 66 downregulated genes were shared between the Vol-L1 and Mnt-L2 conditions. A heatmap of the top 100 most differentially expressed genes in the evolved strains illustrates the similarities and differences between the two resistant strains of interest (Fig. 4.9).

Consistent with our findings, prey responses such as surface masking and biofilm formation were found in pathogenic *V. cholerae* as defence mechanisms against protozoan grazing. These are also considered as important virulence factors for exploiting and infecting higher eukaryotic hosts [93].

These observations predict that predation pressure strongly tends to drive the evolution of general defensive traits that can be beneficial in the face of predators. Evolutionary responses such as biofilm formation, o-antigen variation (LPS), altered transporters, masking and other alteration of gene functions can provide protection from an array of invading microorganisms in ecological communities. We suggest these traits associated with virulence make bacteria less available to predators and limit the strength of the predators in rapid prey hunting [48,91]. For example, the decreased growth observed in the presence of adapted bacterial isolates such as WS suggested that the *Acanthamoeba* revert to their encysted state in response to food

deprivation and that this, in turn, reduces their exposure to bacterial defences [13], reducing mortality [94].

Co-evolution of prey and predators on a solid environment drives genomic parallelism and colony morphology divergence. The mutations that underlie the prevailing colony types are a mix of some of the best studied adaptations to AL interfaces and a pair of completely new mutations that have not previously been studied. Herein we have observed striking parallelism, driven by previously undescribed tandem repeats that led to identical mutations in independent lineages underlying the Vol and Mnt morphotypes. Once again, the study of adaptive evolution in *P. fluorescens* SBW25 populations is shown to bear fruit. Consistent predation by a single predator can select for constitutive expression of previously regulated traits (like WS and Mnt). It also selects for traits that are altered by the presence of the predator as in the case of the Vol resistance phenotype.

Amoebae and their phagocytic predation are a normal part of bacterial life on surfaces from soil or submerged particles and leaves to animal tissues. In this experiment we aimed to understand the genetic underpinnings of bacterial adaptation to predation over 90 days. In doing so, we can begin to investigate the traits that bacteria deploy when faced with this pressure. In addition, this can provide a framework to consider how long-term predation pressure may affect the suite of parallel defensive traits that a bacterial lineage might evolve over much longer time scales when faced with a consistent predator in the environment. The result of this work forms a foundation for a new line of enquiry into the evolution of bacterial stability, the function of ecological interactions, predation resistance, and the evolution of pathogens.

Materials and Methods

Strains and media. A GFP labelled strain of *P. fluorescens* SBW25 (NC_012660.1) and wild protozoan train *Acanthamoebae* sp. T2-5 (EF378666.1) were used in this work, grown and stored as described previously (chapter 2 & 3 – Materials and Methods). Plaque Forming Unit assay was done in the same as explained previously (Chapter 2 – Materials and Methods).

Whole-genome sequencing. We sequenced whole populations of 9 coevolving predation and 3 prey-only replicates. We sequenced the populations at days 16, 40, 64, and 90, in total of 36 coevolved and 12 evolved prey-only populations. In addition, we selected 33 clones at the end of the experiment (day-90) 3-4 clones per predation line and one clone per non-predation line to send for shotgun DNA sequencing. We revived each population or clone from frozen -80°C stocks in LB culture as described above. DNA extraction was performed for whole-genomic DNA purification using Promega™ Wizard™ Genomic DNA Kit (A1125, Promega). Genome quality and quantity were checked in %1 agarose gels stained with %0.0001 SYBR Safe and measurement in a NanoDrop (ACTGene ASP-3700, Alphatech Systems) respectively. Genomes of all coevolved, prey-only control, and ancestral *P. fluorescens* SBW25 WT were sent to Custom Science (www.customscience.co.nz) for 250 bp paired-end, next-generation Illumina sequencing. Sequenced reads were trimmed, aligned, and mapped to the *P. fluorescens* SBW25 reference genome (NC_012660.1) [95] for a minimum and maximum sequencing depth of 140 and 240 respectively across the genome using GENEIOUS version 9.0.5 [96]. Mutations were identified as being present in 99%, 90% or 20% of reads in the alignment by GENEIOUS version 9.0.5 using the “Find Variation/SNPs” tool in isolates and populations, respectively [96].

Muller plots. Muller plots were generated with EvoFreq [97]. A list of known mutations from endpoint clones was used as search criteria for variants in whole genome population samples and the frequency of each mutation was determined using Free Bayes (*arXiv:1207.3907*). Large deletions (4974-4975 and fadD1-D2) that could not be identified with Free Bayes were estimated by dividing the average read depth in deletion loci by the average read depth of the surrounding locus. Sequencing of endpoint clones, together with relative abundance of mutations at each timepoint from population sequencing, was used to determine mutation linkage and lineage. Mutations identified at the same time point and frequency were grouped when their lineage could not be determined. Unique mutations were assigned unique colours so that parallelism can be observed across experimental lines.

Bacterial strains and growth media for complementation assay. To determine whether genes (long chain fatty acid CoA ligase) that have been partially deleted after 90-day predation experiment in Volcano strains perform the function that has been deleted in the *E. coli fadD*$^{-}$ *fadR*$^{-}$ Km^{r} mutant (E2011), we introduced fadD1, fadD2 and fadD1/2 as well as in frame fusion deletion from evolved Line7-Volcano into E2011, respectively. We tested their growth individually on M9 medium as described previously [43]. For the complementation study, E2011 double mutant strains harbouring *P. fluorescens* SBW25 fadD genes were first grown overnight in LB from frozen stock at 37°C with a shaking speed of 180 rpm. 100 µl of the overnight culture was subjected to centrifugation (6000g for 5 min) LB media discharged and the bacterial pellet was treated with M9 media (200 mL M9 salt, 2 mL 1M $MgSo_4$, and 100 µl 1M $CaCl_2$, adjusted to 1 L with H_2O) in order to obtain pure bacterial cells. Bacterial

growth (spot test assay) was performed in 1x M9 medium +1% (w/v) Brij-58 supplemented with 0.2% (w/v) fatty acids (palmitic acid, C16:0 and/or oleic acid, C18:1$^{\Delta 9}$) or 20 mM glucose (Glu) + 0.25 mM IPTG and 1.5% agar. Briefly, 5 µl of the pure bacterial washed cells in six replicate plates were spotted onto the M9 plates and allowed them to dry. Plates then were incubated for four days at 37°C and bacterial growth was monitored. Note, +1 indicates very poor and +6 denotes heavy growth compared to the K12 growth on Glucose at day four.

Volcano morphology assessment. In order to examine the appearance of the Vol colony morphotypes and whether this special phenotype is correlated with altered function of fadD genes, *P. fluorescens* SBW25 harbouring fadD1, fadD2, fadD2fadD1 and fadD2-fadD1 deletions were grown in the absence and presence of ancestral, evolved and coevolved *Acanthamoeba*. Overnight cultures of bacterial mutants were grown in LB from -80°C glycerol stocks. Coevolved and ancestral protozoan strains were revived from liquid N2 as described previously (Chapter 3). The prey-predator growth was performed on solid PM agar plates supplemented with and without 2% FBS. 1x10^{7} bacteria (30 µl) was spread in the absence and presence of quantities of ancestral, evolved, and coevolved *Acanthamoeba* cells in the volume of 2 µl (1x10^{3}) by subsequently adding to one edge of each plate. All plates were wrapped in parafilm and incubated for 4-5 days at 28°C. Plates were washed with 1.5 mL Tris HCl buffer, serially diluted, and plated for CFU on LBA plates in order to yield 5-10 bacterial colonies. Plates were incubated at 28°C and monitored for 4-5 days for change in the shape.

Molecular techniques. Complementation of the *E. coli fadD*$^{-}$*/fadR*$^{-}$ Km^{r} mutant (E2011) with *P. fluorescens* SBW25 fadD1 and fadD2 genes; *E. coli* strain E2011 used in this study was kindly provided by Professor Tung T. Hoang, University of Hawaii [67]. In order to introduce *P. fluorescens* SBW25 fadD genes into E2011, fadD1, fadD2, fadD1/2 and fusion genes were individually amplified by PCR. PCR products were first cloned into pCR8/GW/TOPO (Life Technologies) easy vector. The resulting colon harbouring the gene of interest was validated by whole plasmid sequencing (www.migscenter.com). The obtained vector was digested as XbaI and KpnI restriction fragments, ligated with expression plasmid Ptrc99A, downstream of the lacI promoter, yielding Ptrc99A+fadD1, Ptrc99A+fadD2, Ptrc99A+fad1/2 and Ptrc99A+fusion gene. The resulting colons, and an empty vector as a control were proceeded to the final transformation with *E. coli* strain E2011 for the expression of each of the *FadD* genes. To test whether the final transformation worked, PCR was performed to amplify the insertion from the grown cultures.

Constructions of mutants; splicing by overhang extension polymerase chain reaction (SOE PCR) [98] was used to generate the fadD1, fadD2, fadD1/2 and fusion deletion in ancestral *P. fluorescens* SBW25. To generate deletion mutants, two sets of primers designed, and two PCR reactions were performed to amplify ~550 bp upstream (fragment A) and ~550 bp downstream (fragment B) of the fadD1, fadD2 and fadD1/2 from *P. fluorescens* SBW25. The yield primary fragments were mixed in equal concentration (v/v) and a third PCR was performed to obtain the final product (flanking region). This was to SOE-en the primary PCR products to generate the full-length product containing fadD1, fadD2, fadD1/2 flanking region. Final construct was first cloned into the pCR8/GW/TOPO easy vector, and their fidelity was validated by whole

plasmid sequencing (www.migscenter.com). Full-length fragments of the gene of interest individually ligated into the pUIC3 plasmid [99] as BgIII and were then introduced to *E. coli* strain DH5α λpir. Plasmids carrying each deletion cassette were introduced into *P. fluorescens* SBW25 by using triparental conjugations protocol with the helper plasmid pRK2013 [100], harbouring the mob and tra genes required for conjugation. The FadD deletion mutants were acquired following the two-step allelic exchange method described previously [101].

Similarly, deletion constructs of PFLU_4974, 4975 and 4974-4975 were obtained as described above. Deletion reconstructs of the exact Volcano and Mountain mutants were generated by using the Volcano and Mountain strains as templates. In order for this, ~550-bp upstream and 550-bp downstream of the deletion region were amplified to yield the flanking region. The resulting product was first cloned into the pCR8/GW/TOPO and further proceeded as described above.

Performance test assay with mutants. This experiment was conducted as described above (Chapter 3 - Materials and Methods). The fold numbers of the bacterial isolates were calculated based on the number of the bacterial populations after four days of growth in the absence of predators on PM plates. A simple estimate of absolute fold numbers was generated by using the formula: *(Y - X)/X* or equivalently *Y/X - 1.* Where Y is the number of cells in four days without predation (original value), *X* is the estimated CFU of the cells after 96 hours of predation (final value). Bacterial number was calculated after four days of predation by *Acanthamoeba* as mentioned above. Cells washed, diluted and were plated for CFU on LBA to yield 10-15 colonies for both predation and non- predation groups.

***Pseudomonas-Acanthamoeba* interaction assay.** Individual colonies of bacterial strains pre-cultured on LB agar were homogenised in LB broth and spread in single lines across PM agar plates using a 1ul transfer loop. Plates were allowed to dry before applying 2 ul of suspension containing ~10^3 *Acanthamoeba* cysts μl^{-1} at one end of the bacterial line. Plates were incubated at 28˚C for up to 1 week and the interaction zone was collected once the amoeba had formed a visible clearing. *Pseudomonas fluorescens* SBW25 strains were collected with *Acanthamoeba* from the bacteria-protozoa interaction zone and alone from the opposite end of the culture line with a transfer loop and immediately homogenised in RNA shield (n=4).

Transcriptional profiling. Total RNA was extracted from bacterial and amoebae cells using the Quick-RNA MiniPrep Kit (Zymo Research, USA). Preparations were dried in GenTegra RNA tubes according to manufacturer's instructions (Gentegra, USA) and sent to the Microbial Genome Sequencing (MiGS, USA) Center for Illumina Stranded RNA library preparation with RiboZero Plus rRNA depletion and sequencing on the NextSeq 550 platform with 12M reads per bacterial sample or 50M reads per sample for bacteria-amoeba mixed samples. Bioinformatic analysis was carried out following a modified dual RNA-seq protocol from [102]. Briefly, reads were aligned to the *Acanthamoeba* reference genome using HiSat2 [103] unused reads were then aligned to the bacterial reference genome using Bowtie2 [104]. We used the closest reference sequence to our amoeba at the time of this work - *Acanthamoeba castellanii* strain NEFF (GCA_000313135.1). For bacterial sequences, reads were aligned to the *Pseudomonas fluorescens* SBW25 reference sequence (GCA_000009225.1). Sequence reads were assigned to genomic features using feature Counts [105]. Differential expression using GLM and count normalisation was calculated with edgeR

[106]. Counts were normalised by library size (counts per million, CPM) with $\log_2$ transformation. Features with differential expression ≥ ±2 $\log_2$FC and *P*-value of ≤0.05 after correction for multiple testing using the FDR (Benjamini and Hochberg) method were considered significant.

Acknowledgements: The *E. coli* E2011 strain and pTrc99a plasmid were a kind gift from Professor Tung T. Hoang, University of Hawaii, USA and Associated Professor Xue-Xian Zhang, Massey University, Auckland, New Zealand, respectively.

References

1. Woese CR. Bacterial evolution. Microbiological Reviews. 1987. pp. 221–271. doi:10.1128/mmbr.51.2.221-271.1987.
2. Bar-On YM, Phillips R, Milo R. The biomass distribution on Earth. Proc Natl Acad Sci U S A. 2018;115: 6506–6511.
3. Polis GA. Complex Trophic Interactions in Deserts: An Empirical Critique of Food-Web Theory. The American Naturalist. 1991. pp. 123–155. doi:10.1086/285208
4. Ghoul M, Mitri S. The Ecology and Evolution of Microbial Competition. Trends Microbiol. 2016;24: 833–845.
5. Fenchel T. Ecology of Protozoa: The Biology of Free-living Phagotropic Protists. Springer-Verlag; 2013.
6. Gallet R, Alizon S, Comte P-A, Gutierrez A, Depaulis F, van Baalen M, et al. Predation and disturbance interact to shape prey species diversity. Am Nat. 2007;170: 143–154.
7. Leibold MA, Chase JM, Shurin JB, and Downing AL. SPECIES TURNOVER AND THE REGULATION OF TROPHIC STRUCTURE. Annual Review of Ecology and Systematics. 1997. pp. 467–494. doi:10.1146/annurev.ecolsys.28.1.467.
8. Paterson S, Vogwill T, Buckling A, Benmayor R, Spiers AJ, Thomson NR, et al. Antagonistic coevolution accelerates molecular evolution. Nature. 2010;464: 275–278.
9. Scanlan PD, Hall AR, Blackshields G, Friman V-P, Davis MR Jr, Goldberg JB, et al. Coevolution with bacteriophages drives genome-wide host evolution and constrains the acquisition of abiotic-beneficial mutations. Mol Biol Evol. 2015;32: 1425–1435.

10. Adiba S, Nizak C, van Baalen M, Denamur E, Depaulis F. From grazing resistance to pathogenesis: the coincidental evolution of virulence factors. PLoS One. 2010;5: e11882.

11. Thompson JN. Rapid evolution as an ecological process. Trends in Ecology & Evolution. 1998. pp. 329–332. doi:10.1016/s0169-5347(98)01378-0.

12. Hairston NG, Ellner SP, Geber MA, Yoshida T, Fox JA. Rapid evolution and the convergence of ecological and evolutionary time. Ecology Letters. 2005. pp. 1114–1127. doi:10.1111/j.1461-0248.2005.00812.x.

13. Golzar FS, Ferguson GC, Hendrickson HL. Protozoan predation drives adaptive divergence in *Pseudomonas fluorescens* SBW25; ecology meets experimental evolution. doi:10.1101/2021.07.12.452127.

14. Matz C, Kjelleberg S. Off the hook–how bacteria survive protozoan grazing. Trends Microbiol. 2005. Available: https://www.sciencedirect.com/science/article/pii/S0966842X05001344.

15. Jürgens K, Matz C. Predation as a shaping force for the phenotypic and genotypic composition of planktonic bacteria. Antonie Van Leeuwenhoek. 2002;81: 413–434.

16. Pernthaler J. Predation on prokaryotes in the water column and its ecological implications. Nat Rev Microbiol. 2005;3: 537–546.

17. Van der Henst C, Vanhove AS, Drebes Dörr NC, Stutzmann S, Stoudmann C, Clerc S, et al. Molecular insights into *Vibrio cholerae*'s intra-amoebal host-pathogen interactions. Nat Commun. 2018;9: 3460.

18. Jürgens K, Güde H. The potential importance of grazing-resistant bacteria in planktonic systems. Mar Ecol Prog Ser. 1994;112: 169–188.

19. Jousset A, Scheu S, Bonkowski M. Secondary metabolite production facilitates establishment of rhizobacteria by reducing both protozoan predation and the competitive effects of indigenous bacteria. Funct Ecol. 2008;22: 714–719.

20. Deines P, Matz C, JÜrgens K. Toxicity of violacein-producing bacteria fed to bacterivorous freshwater plankton. Limnology and Oceanography. 2009. pp. 1343–1352. doi:10.4319/lo.2009.54.4.1343.

21. Huang W, Traulsen A, Werner B, Hiltunen T, Becks L. Dynamical trade-offs arise from antagonistic coevolution and decrease intraspecific diversity. Nat Commun. 2017;8: 2059.

22. Brockhurst MA, Morgan AD, Fenton A, Buckling A. Experimental coevolution with bacteria and phage: The *Pseudomonas fluorescens*—Φ2 model system. Infect Genet Evol. 2007;7: 547–552.

23. Scanlan PD, Buckling A. Co-evolution with lytic phage selects for the mucoid phenotype of *Pseudomonas fluorescens* SBW25. ISME J. 2012;6: 1148–1158.

24. Nair RR, Vasse M, Wielgoss S, Sun L, Yu Y-TN, Velicer GJ. Bacterial predator-prey coevolution accelerates genome evolution and selects on virulence-associated prey defences. Nat Commun. 2019;10: 4301.

25. Rodríguez-Zaragoza S. Ecology of free-living amoebae. Crit Rev Microbiol. 1994;20: 225–241.

26. Snelling WJ, Moore JE, McKenna JP, Lecky DM, Dooley JSG. Bacterial-protozoa interactions; an update on the role these phenomena play towards human illness. Microbes Infect. 2006;8: 578–587.

27. Winiecka-Krusnell J, Linder E. Bacterial infections of free-living amoebae. Research in Microbiology. 2001. pp. 613–619. doi:10.1016/s0923-2508(01)01240-2

28. Visvesvara GS, Moura H, Schuster FL. Pathogenic and opportunistic free-living amoebae: *Acanthamoebaspp*.*Balamuthia mandrillaris*, *Naegleria fowleri*, and *Sappinia diploidea*. FEMS Immunology & Medical Microbiology. 2007. pp. 1–26. doi:10.1111/j.1574-695x.2007.00232.x.

29. Marciano-Cabral F, Cabral G. Acanthamoeba spp. as agents of disease in humans. Clin Microbiol Rev. 2003;16: 273–307.

30. Martinez AJ, Visvesvara GS. Free-living, Amphizoic and Opportunistic Amebas. Brain Pathology. 1997. pp. 583–598. doi:10.1111/j.1750-3639.1997.tb01076.x.

31. Esteban GF, Fenchel TM. Ecology of Protozoa: The Biology of Free-living Phagotrophic Protists. Springer; 2021.

32. Guimaraes AJ, Gomes KX, Cortines JR, Peralta JM, Peralta RHS. *Acanthamoeba* spp. as a universal host for pathogenic microorganisms: One bridge from environment to host virulence. Microbiol Res. 2016;193: 30–38.

33. Chekabab SM, Daigle F, Charette SJ, Dozois CM, Harel J. Survival of enterohemorrhagic *Escherichia coli* in the presence of *Acanthamoeba castellanii* and its dependence on Pho regulon. Microbiologyopen. 2012;1: 427–437.

34. Mattana A, Serra C, Mariotti E, Delogu G, Fiori PL, Cappuccinelli P. *Acanthamoeba castellanii* promotion of in vitro survival and transmission of coxsackie b3 viruses. Eukaryot Cell. 2006;5: 665–671.

35. Casadevall A. Amoeba provide insight into the origin of virulence in pathogenic fungi. Adv Exp Med Biol. 2012;710: 1–10.

36. Artursson V, Finlay RD, Jansson JK. Interactions between arbuscular mycorrhizal fungi and bacteria and their potential for stimulating plant growth. Environ Microbiol. 2006;8: 1–10.

37. Cook RJ, Thomashow LS, Weller DM, Fujimoto D, Mazzola M, Bangera G, et al. Molecular mechanisms of defense by rhizobacteria against root disease. Proc Natl Acad Sci U S A. 1995;92: 4197–4201.

38. Jousset A, Lara E, Wall LG, Valverde C. Secondary metabolites help biocontrol strain *Pseudomonas fluorescens* CHA0 to escape protozoan grazing. Appl Environ Microbiol. 2006;72: 7083–7090.

39. Giddens SR, Jackson RW, Moon CD, Jacobs MA, Zhang X-X, Gehrig SM, et al. Mutational activation of niche-specific genes provides insight into regulatory networks and bacterial function in a complex environment. Proceedings of the National Academy of Sciences. 2007. pp. 18247–18252. doi:10.1073/pnas.0706739104.

40. Fujitani Y, Yamamoto K, Kobayashi I. Dependence of frequency of homologous recombination on the homology length. Genetics. 1995;140: 797–809.

41. Spiers AJ, Rainey PB. The *Pseudomonas fluorescens* SBW25 wrinkly spreader biofilm requires attachment factor, cellulose fibre and LPS interactions to maintain strength and integrity. Microbiology. 2005;151: 2829–2839.

42. Black PN, DiRusso CC, Metzger AK, Heimert TL. Cloning, sequencing, and expression of the fadD gene of *Escherichia coli* encoding acyl coenzyme A synthetase. J Biol Chem. 1992;267: 25513–25520.

43. Zarzycki-Siek J, Norris MH, Kang Y, Sun Z, Bluhm AP, McMillan IA, et al. Elucidating the *Pseudomonas aeruginosa* fatty acid degradation pathway: identification of additional fatty acyl-CoA synthetase homologues. PLoS One. 2013;8: e64554.

44. Black PN, Zhang Q, Weimar JD, DiRusso CC. Mutational Analysis of a Fatty Acyl-Coenzyme A Synthetase Signature Motif Identifies Seven Amino Acid Residues That Modulate Fatty Acid Substrate Specificity. Journal of Biological Chemistry. 1997. pp. 4896–4903. doi:10.1074/jbc.272.8.4896.

45. Weimar JD, DiRusso CC, Delio R, Black PN. Functional Role of Fatty Acyl-Coenzyme A Synthetase in the Transmembrane Movement and Activation of Exogenous Long-chain Fatty Acids. Journal of Biological Chemistry. 2002. pp. 29369–29376. doi:10.1074/jbc.m107022200.

46. Leong W, Poh WH, Williams J, Lutz C, Mozammel Hoque M, Poh YH, et al. Adaptation to an amoeba host leads to *Pseudomonas aeruginosa* isolates with attenuated virulence. Appl Environ Microbiol. 2022 [cited 2 Feb 2022]. doi:10.1128/aem.02322-21.

47. March C, Cano V, Moranta D, Llobet E, Pérez-Gutiérrez C, Tomás JM, et al. Role of Bacterial Surface Structures on the Interaction of *Klebsiella pneumoniae* with Phagocytes. PLoS One. 2013;8: e56847.

48. Wildschutte H, Wolfe DM, Tamewitz A, Lawrence JG. Protozoan predation, diversifying selection, and the evolution of antigenic diversity in *Salmonella*. Proc Natl Acad Sci U S A. 2004;101: 10644–10649.

49. Nikaido H, Takatsuka Y. Mechanisms of RND multidrug efflux pumps. Biochimica et Biophysica Acta (BBA) - Proteins and Proteomics. 2009. pp. 769–781. doi:10.1016/j.bbapap.2008.10.004.

50. Beaumont HJE, Gallie J, Kost C, Ferguson GC, Rainey PB. Experimental evolution of bet hedging. Nature. 2009;462: 90–93.

51. Gallie J, Bertels F, Remigi P, Ferguson GC, Nestmann S, Rainey PB. Repeated Phenotypic Evolution by Different Genetic Routes in *Pseudomonas fluorescens* SBW25. Mol Biol Evol. 2019;36: 1071–1085.

52. Bolnick DI, Barrett RDH, Oke KB, Rennison DJ, Stuart YE. (Non) Parallel Evolution. Annual Review of Ecology, Evolution, and Systematics. 2018. pp. 303–330. doi:10.1146/annurev-ecolsys-110617-062240.

53. Bull JJ, Badgett MR, Wichman HA, Huelsenbeck JP, Hillis DM, Gulati A, et al. Exceptional Convergent Evolution in a Virus. Genetics. 1997. pp. 1497–1507. doi:10.1093/genetics/147.4.1497.

54. Wichman HA, Badgett MR, Scott LA, Boulianne CM, Bull JJ. Different trajectories of parallel evolution during viral adaptation. Science. 1999;285: 422–424.

55. Rosenblum EB, Parent CE, Brandt EE. The Molecular Basis of Phenotypic Convergence. Annual Review of Ecology, Evolution, and Systematics. 2014. pp. 203–226. doi:10.1146/annurev-ecolsys-120213-091851.

56. Alto BW, Wasik BR, Morales NM, Turner PE. Stochastic temperatures impede RNA virus adaptation. Evolution. 2013;67: 969–979.

57. Vasi F, Travisano M, Lenski RE. Long-Term Experimental Evolution in *Escherichia coli*. II. Changes in Life-History Traits During Adaptation to a Seasonal Environment. The American Naturalist. 1994. pp. 432–456. doi:10.1086/285685.

58. van Raay K, Stolyar S, Sevigny J, Tirado AM, Draghi JA, Lenski RE, et al. Evolution with private resources reverses some changes from long-term evolution with public resources. doi:10.1101/2021.07.11.451942.

59. Rainey PB, Travisano M. Adaptive radiation in a heterogeneous environment. Nature. 1998;394: 69–72.

60. Bantinaki E, Kassen R, Knight CG, Robinson Z, Spiers AJ, Rainey PB. Adaptive Divergence in Experimental Populations of *Pseudomonas fluorescens*. III. Mutational Origins of Wrinkly Spreader Diversity. Genetics. 2007. pp. 441–453. doi:10.1534/genetics.106.069906.

61. Malone JG, Williams R, Christen M, Jenal U, Spiers AJ, Rainey PB. The structure-function relationship of WspR, a *Pseudomonas fluorescens* response regulator with a GGDEF output domain. Microbiology. 2007;153: 980–994.

62. Hickman JW, Tifrea DF, Harwood CS. A chemosensory system that regulates biofilm formation through modulation of cyclic diguanylate levels. Proceedings of the National Academy of Sciences. 2005. pp. 14422–14427. doi:10.1073/pnas.0507170102.

63. Zhang Y-M, Rock CO. Membrane lipid homeostasis in bacteria. Nature Reviews Microbiology. 2008. pp. 222–233. doi:10.1038/nrmicro1839

64. Pech-Canul Á, Nogales J, Miranda-Molina A, Álvarez L, Geiger O, Soto MJ, et al. FadD is required for utilization of endogenous fatty acids released from membrane lipids. J Bacteriol. 2011;193: 6295–6304.

65. Ulsamer AG, Wright PL, Wetzel MG, Korn ED. Plasma and phagosome membranes of Acanthamoeba castellanii. J Cell Biol. 1971;51: 193–215.

66. Fujita Y, Matsuoka H, Hirooka K. Regulation of fatty acid metabolism in bacteria. Mol Microbiol. 2007;66: 829–839.

67. Kang Y, Zarzycki-Siek J, Walton CB, Norris MH, Hoang TT. Multiple FadD Acyl-CoA Synthetases Contribute to Differential Fatty Acid Degradation and Virulence in *Pseudomonas aeruginosa*. PLoS ONE. 2010. p. e13557. doi:10.1371/journal.pone.0013557.

68. Rindi L, Fattorini L, Bonanni D, Iona E, Freer G, Tan D, et al. Involvement of the fadD33 gene in the growth of Mycobacterium tuberculosis in the liver of BALB/c mice. Microbiology. 2002. pp. 3873–3880. doi:10.1099/00221287-148-12-3873.

69. Cox JS, Chen B, McNeil M, Jacobs WR Jr. Complex lipid determines tissue-specific replication of Mycobacterium tuberculosis in mice. Nature. 1999;402: 79–83.

70. Stenseth NC, Smith JM. COEVOLUTION IN ECOSYSTEMS: RED QUEEN EVOLUTION OR STASIS? Evolution. 1984;38: 870–880.

71. Van Valen L. Molecular evolution as predicted by natural selection. Journal of Molecular Evolution. 1974. pp. 89–101. doi:10.1007/bf01796554.

72. Van Valen L. Theory in Abstracts. BioScience. 1973. pp. 626–626. doi:10.2307/1296773.

73. Bell T, Bonsall MB, Buckling A, Whiteley AS, Goodall T, Griffiths RI. Protists have divergent effects on bacterial diversity along a productivity gradient. Biol Lett. 2010;6: 639–642.

74. Jousset A. Ecological and evolutive implications of bacterial defences against predators. Environ Microbiol. 2012;14: 1830–1843.

75. Scanlan PD, Buckling A, Hall AR. Experimental evolution and bacterial resistance: (co)evolutionary costs and trade-offs as opportunities in phage therapy research. Bacteriophage. 2015;5: e1050153.

76. Malone JG. Role of small colony variants in persistence of *Pseudomonas aeruginosa* infections in cystic fibrosis lungs. Infect Drug Resist. 2015;8: 237–247.

77. Sengupta C, Mukherjee O, Chowdhury R. Adherence to Intestinal Cells Promotes Biofilm Formation in Vibrio cholerae. J Infect Dis. 2016;214: 1571–1578.

78. Davarzani F, Saidi N, Besharati S, Saderi H, Rasooli I, Owlia P. Evaluation of Antibiotic Resistance Pattern, Alginate and Biofilm Production in Clinical Isolates of *Pseudomonas aeruginosa*. Iranian Journal of Public Health. 2021. doi:10.18502/ijph.v50i2.5349.

79. Song B, Leff LG. Influence of magnesium ions on biofilm formation by *Pseudomonas fluorescens*. Microbiol Res. 2006;161: 355–361.

80. Meyer JR, Kassen R. The effects of competition and predation on diversification in a model adaptive radiation. Nature. 2007;446: 432–435.

81. Hall AR, Meyer JR, Kassen R. Selection for predator resistance varies with resource supply in a model adaptive radiation. Evol Ecol Res. 2008;10: 735–746.

82. Friman V-P, Jousset A, Buckling A. Rapid prey evolution can alter the structure of predator-prey communities. J Evol Biol. 2014;27: 374–380.

83. King CH, Shotts EB Jr, Wooley RE, Porter KG. Survival of coliforms and bacterial pathogens within protozoa during chlorination. Appl Environ Microbiol. 1988;54: 3023–3033.

84. Levin BR, Svanborg Edén C. Selection and evolution of virulence in bacteria: an ecumenical excursion and modest suggestion. Parasitology. 1990;100 Suppl: S103–15.

85. Black PN, DiRusso CC. Molecular and biochemical analyses of fatty acid transport, metabolism, and gene regulation in *Escherichia coli*. Biochim Biophys Acta. 1994;1210: 123–145.

86. Kang Y, Nguyen DT, Son MS, Hoang TT. The *Pseudomonas aeruginosa* PsrA responds to long-chain fatty acid signals to regulate the fadBA5 β-oxidation operon. Microbiology. 2008. pp. 1584–1598. doi:10.1099/mic.0.2008/018135-0.

87. Son MS, Matthews WJ Jr, Kang Y, Nguyen DT, Hoang TT. In vivo evidence of *Pseudomonas aeruginosa* nutrient acquisition and pathogenesis in the lungs of cystic fibrosis patients. Infect Immun. 2007;75: 5313–5324.

88. Rubens CE. Type III Capsular Polysaccharide of Group B Streptococci: Role in Virulence and the Molecular Basis of Capsule Expression. Molecular Genetics of Bacterial Pathogenesis. 2014. pp. 327–339. doi:10.1128/9781555818340.ch21.

89. Iandolo JJ. The Genetics of Staphylococcal Toxins and Virulence Factors. Molecular Basis of Bacterial Pathogenesis. 1990. pp. 399–426. doi:10.1016/b978-0-12-307211-5.50023-4.

90. Gallie J, Libby E, Bertels F, Remigi P, Jendresen CB, Ferguson GC, et al. Bistability in a Metabolic Network Underpins the De Novo Evolution of Colony Switching in *Pseudomonas fluorescens*. PLOS Biology. 2015. p. e1002109. doi:10.1371/journal.pbio.1002109.

91. Lerouge I, Vanderleyden J. O-antigen structural variation: mechanisms and possible roles in animal/plant-microbe interactions. FEMS Microbiol Rev. 2002;26: 17–47.

92. Singh JK, Adams FG, Brown MH. Diversity and Function of Capsular Polysaccharide in *Acinetobacter* baumannii. Front Microbiol. 2019;0. doi:10.3389/fmicb.2018.03301

93. Lutz C, Erken M, Noorian P, Sun S, McDougald D. Environmental reservoirs and mechanisms of persistence of *Vibrio cholerae*. Front Microbiol. 2013;4: 375.

94. Marciano-Cabral F. Biology of Naegleria spp. Microbiol Rev. 1988. Available: https://www.ncbi.nlm.nih.gov/pmc/articles/pmc372708/.

95. Silby MW, Cerdeño-Tárraga AM, Vernikos GS, Giddens SR, Jackson RW, Preston GM, et al. Genomic and genetic analyses of diversity and plant interactions of *Pseudomonas fluorescens*. Genome Biol. 2009;10: R51.

96. Kearse M, Moir R, Wilson A, Stones-Havas S, Cheung M, Sturrock S, et al. Geneious Basic: an integrated and extendable desktop software platform for the organization and analysis of sequence data. Bioinformatics. 2012;28: 1647–1649.

97. Gatenbee CD, Schenck RO, Bravo RR, Anderson ARA. EvoFreq: visualization of the Evolutionary Frequencies of sequence and model data. BMC Bioinformatics. 2019;20: 710.

98. Horton RM, Hunt HD, Ho SN, Pullen JK, Pease LR. Engineering hybrid genes without the use of restriction enzymes: gene splicing by overlap extension. Gene. 1989;77: 61–68.

99. Rainey PB. Adaptation of *Pseudomonas fluorescens* to the plant rhizosphere. Environ Microbiol. 1999;1: 243–257.

100. Ditta G, Stanfield S, Corbin D, Helinski DR. Broad host range DNA cloning system for gram-negative bacteria: construction of a gene bank of Rhizobium meliloti. Proc Natl Acad Sci U S A. 1980;77: 7347–7351.

101. Zhang X-X, Rainey PB. Construction and validation of a neutrally-marked strain of *Pseudomonas fluorescens* SBW25. Journal of Microbiological Methods. 2007. pp. 78–81. doi:10.1016/j.mimet.2007.07.001.

102. Marsh JW, Hayward RJ, Shetty AC, Mahurkar A, Humphrys MS, Myers GSA. Bioinformatic analysis of bacteria and host cell dual RNA-sequencing experiments. Brief Bioinform. 2018;19: 1115–1129.

103. Kim D, Langmead B, Salzberg SL. HISAT: a fast spliced aligner with low memory requirements. Nat Methods. 2015;12: 357–360.

104. Langmead B, Salzberg SL. Fast gapped-read alignment with Bowtie 2. Nat Methods. 2012;9: 357–359.

105. Liao Y, Smyth GK, Shi W. featureCounts: an efficient general purpose program for assigning sequence reads to genomic features. Bioinformatics. 2014;30: 923–930.

106. Robinson MD, McCarthy DJ, Smyth GK. edgeR: a Bioconductor package for differential expression analysis of digital gene expression data. Bioinformatics 2010;26: 139–140.

Chapter 5

Concluding Remarks

Overall, experimental evolution has provided an extraordinary approach to understanding the ecological [1,2] and evolutionary process [3,4]. We use an experimental system to address the evolutionary changes in bacteria as an adaptive response to protozoan predation and the effect of this on predator evolution. Herein, we conducted a pilot 20-day and extended 90-day predator-prey coevolution experiment on solid surfaces to first evaluate bacterial adaptations that increase resistance to amoeboid predation and second to evaluate the phenotypic and genotypic evolution in *P. fluorescens* SBW25 prey population in response to predation and finally the effect of this coevolution on *Acanthamoeba* spp., a generalist amoeboid predator.

We overall observed stable populations of both prey and predator during the evolutionary experiment that do not appear to show waves of predominance predicted mathematically [5]. One possible reason for this is, we were not sampling often enough (every transfer) but these dynamics could be at play. However, we observed the maintenance of both populations in our 20 [6] and 90-day experiments (Fig. 3.1). The population sizes of predators remained relatively stable throughout and predation did not lead to extinction events in either the bacterial or amoebal populations. This is consistent with previous experimental studies that result in the coexistence of both *E. coli* and *S. cerevisiae* [7] suggesting coadaptation of both prey and predator over evolutionary time scale representative of early stages of Red Queen Coevolution.

Importantly, in our short and long-term solid surface propagation, prey-only lines did not develop recognisable colony variants. However, in bacterial lines undergoing predation, a set of bacterial colony morphologies were observed. From the 20-day experiment, two of the novel types were similar to WS types observed in air-liquid (A-L) experiments reported previously in the same organism, while the other two, WFE and FE, were not previously reported (Fig. 2.1). In the extended 90-day experiment we observed other colony variants such as Volcano (Vol) and Mountain (Mnt) as well (Fig. 3.1). This strongly suggests that predation pressure drives higher prey diversity in the solid surface and that WSs, WFE, FE, Mnt and Vol morphotypes are anti-predator adaptations that evolved with a high degree of parallelism in the bacterial lines undergoing predation.

In the 20-day experiment, from the profile of the mutation, WS isolates had mutations in the phosphorylation and FE colony in the demethylase domain of the well characterised WspF repressor. The WFE colony variant was found in the *AmrZ* gene, known as the negative regulator of Wsp (Table 2.1).

All four evolved colony variants from the 20-day experiment demonstrated increased grazing resistance and had substantially increased prey fitness relative to the WT. We observed trade-offs in the fitness of the majority of bacterial mutants that had acquired resistance to amoeboid predation. This was particularly striking in the WS mutants (23.8% less generational growth compared to WT). The relative fitness of WS morphotypes measured in mixed colony fitness assays was 0.33 of WT over 100 generations [8]. In our hands, WT cells achieved an average of 9 generations over the

96-hr experiment. A loss of 23.8% over a short time represents a notable trade-off (Fig. 2.3).

In the AL interface strength assay, we observed the formation of robust biofilms in WS isolates (holding a weight of ~1.33 grams), whilst this was much less pronounced in the WFE and FE isolates, as visualised by calcofluor staining. The WS phenotypes also had a strong cellulose production compared to other evolved morphotypes, but, to some extent, all adopted isolates were able to resist predation.

Furthermore, predators also demonstrated significantly reduced growth (9-14 generations) in the presence of all evolved isolates than they did on the WT isolates (19 generations) (Fig. 2.2). We interpret that the adapted bacterial isolates decreased predator growth, suggesting that *Acanthamoeba* may revert to their encysted state in response to food deprivation and that this, in turn, decreases their exposure to bacterial defences.

In the extended 90-day coevolution study, we found strong parallel phenotypic and genotypic evolution across coevolved lines under a predation regime on solid surfaces (Fig. 3.2 and Fig. 4.1). It is plausible to see the evolution of similar traits in the replicates of multiple populations among microorganisms [9] when exposed to identical environmental selections [10,11]. Although this has been previously reported in empirical studies of bacterial predator and prey in unstructured environments [12], such evolution of high parallel phenotypic and genotypic evolution within prey populations while under predation from amoeboid predators in a structured environment have not been detected.

From the mutation profile of the population sequencing, we showed nearly 3.7-fold more mutations overall among coevolved prey replicates during the 90-day experiment and 4.7-fold more mutations per line at the end of the coevolution experiment compared to the no predator control lines. In addition, during this experiment we found higher genetic divergence among bacterial lineages (on average 28.4 mutations) undergoing predation than among the no predator lines (on average 7.6 mutations). Such observations suggest that predator interactions are responsible for adaptation in coevolved prey that leads to positive selection for mutations (Fig. 4.1 A & B).

In this experiment and among nine coevolved lines, the majority of the morphotypes were found to be the WS (8 out of 9) and Mnt (9 out of 9). The volcano was also observed in four lines (Fig. 3.2). Similarly, through a combination of population and colony sequencing at the end of the experiment we identified the *WspF* ΔMMDLI mutation associated with WS phenotype, deletion of PFLU_4974 and PFLU_4975 (Δ4974-4975) responsible for Mnt isolates, and the Δ*fadD2-D1* deletion responsible for Volcano isolates (Fig. 4.1). Further investigation suggested that the Δ4974-4975 join point in Mnt isolates contained a 10 bp tandem repeat 1,734 bp apart whilst the Δ*fadD2-D1* deletion join point in Vol variants harboured a 33 bp tandem repeat 2,038 bp apart (Figs. 4.4 & 4.7). Sequence identity of this kind is both predicted and experimentally measured to have a strong effect on increasing the likelihood of a recombination event that would generate both duplications and deletions of the region in the population [13]. In populations of 10^{8-10} bacterial cells under predation pressure, we can expect many of these mutations to occur randomly in this and any other evolution experiment which uses *P. fluorescens* SBW25 as a result of these tandem repeats.

In this work, the WS morphotype demonstrated a pronounced advantage over other adopted isolates. We found the WS isolates to be highly resistant and demonstrated increased survival (relative to WT) to all three *Acanthamoeba* classes (Ancestral, CE, and non-CE). In our short and long-term predation studies, we identified various mutations on the Wsp, awsXR system and amrZ/fleQ that showed extensive resistance against the predators. These three separate regulatory pathways are believed to encode *wss* transcription and thus control the activation of the secondary signalling molecule c-di-GMP resulting in the formation of WS morphotype in several environments [6,14] (Fig. 2.3 - Figs. 3.3 and 3.4). WS is a well-studied biofilm-forming mutant, and the property of forming a biofilm is a common virulence factor of many human pathogens such as *V. cholera* and *P. aeruginosa* [15,16]. The notion that traits that are common in bacterial pathogens might be entrained or evolved in response to predation pressure by amoeboid predators was first proposed by [17] and quickly embraced [18,19]. The evidence of traits that are found in pathogens being selected through predation pressure has however been lacking.

Biofilm formation has previously been demonstrated to be a successful defence strategy of *P. fluorescens* SBW25 against free-living ciliate predators and phages in liquid environments [20–22]. This suggests that predation by amoebae can contribute to the development of anti-predatory traits such as biofilm formation, and this can be correlated with increased virulence of these bacterial organisms in the future [23–25].

Volcano and Mountain were also major phenotypes evolved from WT strains after exposure to generalist protozoan predators. In the line test and performance assay (PA), Mnt isolates were found to be highly resistant. Intriguingly, these phenotypes

showed higher survival (relative to WT) to all three predator types (Ancestral, CE, and non-CE) while Vol morphotypes were susceptible to all Acanthamoeba classes (Figs. 3.3 & 3.4). However, in the PA which is closer to the conditions of the coevolution experiment, surprisingly all the coevolved Vol strains performed very differently than they did in the line tests. We observed that the Vol isolates were more resistant to predation than the WT when subjected to their coevolved predators.

Together, it appears that the Vol morphotypes survive better from predation by their coevolved predators, whilst these predators do not suffer such population declines observed in coevolved *Acanthamoeba* while predating upon WS and Mnt. This suggests a specific adaptation to predation and hints at a "special relationship" (possibly cooperative) evolving between the Vol isolates and their coevolved predators that merits further investigation (Fig. 3.4 C). However, further work is required to understand the underlying mechanism here and how this mutation is responsible for Vol phenotype driving this particular effect.

The *P. fluorescens* Vol cells became predation resistant only in the presence of the evolved *Acanthamoebae*. We used genetic reconstruction to begin to investigate the nature of the Vol mutants *fadD2-D1* fusion mutation that was detected four times among CE replicates. *P. fluorescens* SBW25 has four fadD homologs which are annotated as having a role in fatty acid degradation. FadD is an acetyl-CoA synthesis protein and has a major role in degrading exogenous LCFA [26]. We found that both the *fadD1* and *fadD2* genes encoded proteins were functional in long chain fatty acid degradation. Furthermore, our CFU mediated observation of reconstructed mutants confirmed that either the complete deletion of *fadD1* or the partial deletion of *fadD1*

(as in the fusion) leads to the formation of Volcano morphotype in the presence or absence of predators (Figs. 4.4, 4.5 and Table 4.1).

We measured the success of the *fadD2-D1* deletion mutant in the PA test and found that loss of these genes increases their survival during predation by coevolved *Acanthamoebae.* Consistent with this, Ev. Vol-L1 that carries *fadD2-D1* deletion and an additional mutation on *LuxR* gene showed a high degree of resistance to their coevolved L1 predator (Fig. 4.6).

We hypothesise that increasing the concentration of host-associated LCFA in the membrane may mask prey cells in the way that this could involve making the *Acanthamoebae* less likely to uptake them because the bacteria are recognised as self, rather than as prey. Furthermore, it is a possibility that the degradation of LCFA by beta-oxidation produces reactive oxygen species [27]. It is formally possible that the reduced activity of FadD function that is accomplished by fusing the FadD proteins in Vol variants is beneficial because it decreases cell death due to mutagenesis in the presence of exogenous LCFA provided by the *Acanthamoebae*. From the RNA sequencing results, the Vol-L1 had significant downregulation of seven efflux genes, most significantly PFLU_3263 (an efflux transporter), as well as a fatty acid transporter (PFLU_4903). These results, taken with the finding of increased survivability of Vol strains only when grown with their evolved *Acanthamoebae* and the abundance of mutations identified in fadD genes, led to our hypothesis that the evolved bacteria might be altering transporters to counter increased exposure to LCFA from the *Acanthamoeba* by increased oxidative stress from LCFA degradation. However, further work is required in determining the LCFA present in the *Acanthamoebae* and

the Vol mutants to shed light on how changes in LCFA degradation may be leading to an increase in coevolved prey and predator fitness in the presence of each other. This work may thereby also explain the consumption of exogenous LCFA by pathogens such as *P. aeruginosa* and *M. tuberculosis* [28–30].

Mountain colony was one of the frequently observed mutants in the 90-day experiment. These morphotypes that have shown mucus-like appearance when growing on the surface, demonstrated resistance and increased survival to all predator types (Fig. 3.1 C). The genes affected by the Mnt deletion included PFLU_4974 and PFLU_4975, and a tandem repeat of 10 bp was determined to be responsible, in part, for the frequency of this mutation in eight out of nine coevolved lines (Fig. 4.7). In addition, from the mutation profile of the colony sequencing, seven out of nine Mnt isolates carry at least one additional mutation. Although, all the Mnt isolates except in Ev. Mnt-L51 (Δ4974-4975 & G112 on *ompR* gene) were positive for the production of capsules, none of which was found to have a mutation in known encapsulation associated genes (Chapter 4, Supplementary Table 2). We showed that the Mnt deletion alone (in Mnt-L52; Δ4974-4975) showed poor performance under predation, whereas the Ev. Mnt-L2 that carries Δ4974-4975 and an additional substitution mutation on the putative exported protein (PFLU_0924) exhibited a greater degree of resistance to predation with their coevolved predator. The predation resistance of Ev. Mnt-L2 demonstrates the evolution of anti-predatory behaviours in these mutants suggesting that the Δ4974Δ4975 and Δ4974-4975 mutation deletions alone make bacteria more susceptible to predators and is not sufficient to produce predation resistance (Fig. 4.7).

In this study, we did not find a correlation between the Mnt deletion mutation (Δ4974-4975) alone and resistance of this phenotype against predation, considering that Mnt isolates except in two lines had at least one additional mutation that may have conferred resistance in these colonies. Furthermore, from the RNA sequencing profile of Mnt-L2 while under predation, 12 genes were found to be upregulated in O-antigen biosynthesis, a surface polysaccharide of gram-negative bacteria known as LPS [31]. The polysaccharide capsule (LPS) is a known defence trait of many pathogenic bacteria against phagocytosis from protozoan predators and the host's immune system [32]. In addition, in Mnt-L2 we found upregulation of an efflux RND transporter downstream of the deletion (PFLU_4976) and a unique enrichment (5 genes) in the cyclophilin-like domain (immunophilin). We did not investigate the nature of additional mutations due to their abundance, however, with confirmation in hand that the Mnt isolates had a mucus-like appearance while growing on a plate and demonstrated increased upregulation of genes in the outer membrane and efflux RND transported, we hypothesis that these traits might be responsible for the resistance of these colony variants against predators (Figs. 4.8 & 4.9).

On the predator side, changes in preference or behaviour were also noted in the predators during 90-days of coevolution with prey. These predator populations persisted while growing on their prey over 90-days. Although in the performance assay the WS and Mnt morphotypes were extremely resistant to predation and the resulting *Acanthomobae* populations were reduced compared to predation on WT prey, *Acanthamoeba* cells were able to persist in these environments (Fig. 3.4 C). We measured increased fitness on the WT prey as measured in generation numbers and increased predation rates in the coevolved *Acanthamoeba* compared to their

ancestors (Fig. 3.5). Consistent with this, the significant loss in the population sizes of the WT bacteria by the evolved predator line 1 and 2 indicates improved predator efficiency and is the consequence of predator evolution. This strongly indicates evidence of potent coadaptation among coevolved prey and predator populations and thus, confirms that coevolution accelerates prey-predator evolution compared to the non-evolved prey and predator (WT prey + Ancestral predator).

This is also consistent with previous empirical studies demonstrating that predation in liquid environments increases genotypic and phenotypic evolution in prey and affects predator behaviours [12,33–35]. Contrary to the ecological theory, in our short and long predation studies, the interaction between protozoa and bacteria did not lead to extinction of the species [7] and both organisms overall demonstrated stable populations [36].

This thesis presents new insights on how co-evolution of prey and amoeboid predators on a solid surface drives genomic parallelism and divergence in prey populations. The mutations that underlie the prevailing colony types are some of the best-studied adaptations to AL interfaces, a mix of completely new mutations (Mnt, Vol, FE, and WFE) and a high number of other individual mutations that have not previously been studied. By showing the evolution of parallel molecular changes in prey and that they are resistant to predation, we support both the ecological causes and the evolutionary significance of adaptive evolution among *P. fluorescens* SBW25 populations.

Using experimental evolution, I was able to demonstrate that a number of resistant mutants can be evolved from WT *P. fluorescens* SBW25 within a relatively short period of time. I have identified strategies that evolved bacteria employ to adapt to their

amoeboid predator. The consistent predation by a single predator can select for permanence in traits such as biofilm formation. Phagocytic single-cell predators are a normal part of bacterial life on several surfaces (soil, leaves, and tissues). This coevolution experiment aims to help us determine the adaptation factors to predation over different time scales in this short time frame. Thus, we can better understand the defence strategies that they can employ in a short time (hours). The results of this work can apply to understanding bacterial divergence, bacterial stability, the function of ecological interactions, bacterial resistance, and the evolution of pathogens.

References

1. Friman V-P, Buckling A. Effects of predation on real-time host-parasite coevolutionary dynamics. Ecol Lett. 2013;16: 39–46.
2. Lawrence D, Fiegna F, Behrends V, Bundy JG, Phillimore AB, Bell T, et al. Species interactions alter evolutionary responses to a novel environment. PLoS Biol. 2012;10: e1001330.
3. Lenski RE. Experimental evolution and the dynamics of adaptation and genome evolution in microbial populations. ISME J. 2017;11: 2181–2194.
4. Kawecki TJ, Lenski RE, Ebert D, Hollis B, Olivieri I, Whitlock MC. Experimental evolution. Trends Ecol Evol. 2012;27: 547–560.
5. Cortez MH, Weitz JS. Coevolution can reverse predator-prey cycles. Proc Natl Acad Sci U S A. 2014;111: 7486–7491.
6. Golzar FS, Ferguson GC, Hendrickson HL. Protozoan predation drives adaptive divergence in *Pseudomonas fluorescens* SBW25; ecology meets experimental evolution. doi:10.1101/2021.07.12.452127.
7. Barber JN, Sezmis AL, Woods LC, Anderson TD, Voss JM, McDonald MJ. The evolution of coexistence from competition in experimental co-cultures of *Escherichia coli* and Saccharomyces cerevisiae. ISME J. 2021;15: 746–761.
8. Spiers AJ. Wrinkly-Spreader fitness in the two-dimensional agar plate microcosm: maladaptation, compensation and ecological success. PLoS One. 2007;2: e740.
9. Bolnick DI, Barrett RDH, Oke KB, Rennison DJ, Stuart YE. (Non)Parallel Evolution. Annual Review of Ecology, Evolution, and Systematics. 2018. pp. 303–330. doi:10.1146/annurev-ecolsys-110617-062240.

10. Bull JJ, Badgett MR, Wichman HA, Huelsenbeck JP, Hillis DM, Gulati A, et al. Exceptional Convergent Evolution in a Virus. Genetics. 1997. pp. 1497–1507. doi:10.1093/genetics/147.4.1497.

11. Rosenblum EB, Parent CE, Brandt EE. The Molecular Basis of Phenotypic Convergence. Annual Review of Ecology, Evolution, and Systematics. 2014. pp. 203–226. doi:10.1146/annurev-ecolsys-120213-091851.

12. Nair RR, Vasse M, Wielgoss S, Sun L, Yu Y-TN, Velicer GJ. Bacterial predator-prey coevolution accelerates genome evolution and selects on virulence-associated prey defences. Nat Commun. 2019;10: 4301.

13. Fujitani Y, Yamamoto K, Kobayashi I. Dependence of frequency of homologous recombination on the homology length. Genetics. 1995;140: 797–809.

14. Rainey PB, Travisano M. Adaptive radiation in a heterogeneous environment. Nature. 1998;394: 69–72.

15. Malone JG. Role of small colony variants in persistence of *Pseudomonas aeruginosa* infections in cystic fibrosis lungs. Infect Drug Resist. 2015;8: 237–247.

16. Sengupta C, Mukherjee O, Chowdhury R. Adherence to Intestinal Cells Promotes Biofilm Formation in *Vibrio cholerae*. J Infect Dis. 2016;214: 1571–1578.

17. King CH, Shotts EB Jr, Wooley RE, Porter KG. Survival of coliforms and bacterial pathogens within protozoa during chlorination. Appl Environ Microbiol. 1988;54: 3023–3033.

18. Adiba S, Nizak C, van Baalen M, Denamur E, Depaulis F. From grazing resistance to pathogenesis: the coincidental evolution of virulence factors. PLoS One. 2010;5: e11882.

19. Levin BR, Svanborg Edén C. Selection and evolution of virulence in bacteria: an ecumenical excursion and modest suggestion. Parasitology. 1990;100 Suppl: S103–15.

20. Meyer JR, Kassen R. The effects of competition and predation on diversification in a model adaptive radiation. Nature. 2007;446: 432–435.

21. Hall AR, Meyer JR, Kassen R. Selection for predator resistance varies with resource supply in a model adaptive radiation. Evol Ecol Res. 2008;10: 735–746.

22. Friman V-P, Jousset A, Buckling A. Rapid prey evolution can alter the structure of predator-prey communities. J Evol Biol. 2014;27: 374–380.

23. Barker J, Brown MRW. Trojan Horses of the microbial world: protozoa and the survival of bacterial pathogens in the environment. Microbiology. 1994. pp. 1253–1259. doi:10.1099/00221287-140-6-1253.

24. Sun S, Noorian P, McDougald D. Dual Role of Mechanisms Involved in Resistance to Predation by Protozoa and Virulence to Humans. Front Microbiol. 2018;9: 1017.

25. Matz C, Kjelleberg S. Off the hook–how bacteria survive protozoan grazing. Trends Microbiol. 2005. Available: https://www.sciencedirect.com/science/article/pii/S0966842X05001344.

26. Pech-Canul Á, Nogales J, Miranda-Molina A, Álvarez L, Geiger O, Soto MJ, et al. FadD is required for utilization of endogenous fatty acids released from membrane lipids. J Bacteriol. 2011;193: 6295–6304.

27. Fujita Y, Matsuoka H, Hirooka K. Regulation of fatty acid metabolism in bacteria. Mol Microbiol. 2007;66: 829–839.

28. Kang Y, Zarzycki-Siek J, Walton CB, Norris MH, Hoang TT. Multiple FadD Acyl-CoA Synthetases Contribute to Differential Fatty Acid Degradation and Virulence in *Pseudomonas aeruginosa*. PLoS ONE. 2010. p. e13557. doi:10.1371/journal.pone.0013557.

29. Rindi L, Fattorini L, Bonanni D, Iona E, Freer G, Tan D, et al. Involvement of the fadD33 gene in the growth of *Mycobacterium tuberculosis* in the liver of BALB/c mice. Microbiology. 2002. pp. 3873–3880. doi:10.1099/00221287-148-12-3873.

30. Cox JS, Chen B, McNeil M, Jacobs WR Jr. Complex lipid determines tissue-specific replication of *Mycobacterium tuberculosis* in mice. Nature. 1999;402: 79–83.

31. Lerouge I, Vanderleyden J. O-antigen structural variation: mechanisms and possible roles in animal/plant-microbe interactions. FEMS Microbiol Rev. 2002;26: 17–47.

32. Singh JK, Adams FG, Brown MH. Diversity and Function of Capsular Polysaccharide in *Acinetobacter baumannii*. Front Microbiol. 2019;0. doi:10.3389/fmicb.2018.03301

33. Paterson S, Vogwill T, Buckling A, Benmayor R, Spiers AJ, Thomson NR, et al. Antagonistic coevolution accelerates molecular evolution. Nature. 2010;464: 275–278.

34. Scanlan PD, Buckling A. Co-evolution with lytic phage selects for the mucoid phenotype of *Pseudomonas fluorescens*

SBW25. ISME J. 2012;6: 1148–1158.

35. Scanlan PD, Hall AR, Blackshields G, Friman V-P, Davis MR Jr, Goldberg JB, et al. Coevolution with bacteriophages drives genome-wide host evolution and constrains the acquisition of abiotic-beneficial mutations. Mol Biol Evol. 2015;32: 1425–1435.

36. Chesson P. Mechanisms of Maintenance of Species Diversity. Annual Review of Ecology and Systematics. 2000. pp. 343–366. doi:10.1146/annurev.ecolsys.31.1.343.

Future Directions

The present thesis provides new insight into how protozoan predation leads to the evolution of parallel defensive traits in non-pathogenic bacteria. In this project, we established a 20- and 90-day experiment to investigate the evolution of a soil bacterium, *P. fluorescens* SBW25 in the presence and absence of a wild protozoa *Acanthamoeba sp*. This model system presents an opportunity to measure the degree to which the prey-predator interaction may stimulate the evolution of adaptive traits in both predator and prey populations. As a result of heavy predation pressure, we found a number of parallel mutations in *amrZ*, *wspF*, *fadD1, fadD2* and *putative hypothetical protein* specific to the predation group. We reported the evolution of novel colony morphologies such as WFE, FE, Mnt and Volcano along with WS in bacterial lines undergoing predation. The evolved bacterial isolates demonstrated anti-predatory defensive traits that resulted in reduced replication of the protozoan populations. We investigated that these traits associated with virulence arise in response to our protozoan predation. However, the direct testing of the isolates for increased virulence has not been addressed in this work. Additional research is needed to determine whether the evolved isolates are capable of causing death in multicellular model organisms. In order to test the accuracy of the virulence hypothesis, isolates could be tested for increased virulence against a common lab model, *Caenorhabditis elegans.* Testing virulence factors using multicellular models has long been an area of interest in pathogens such as *P. aeruginosa* and *V. cholera.* Demonstration of increased virulence requires an additional plate assay where 5-10 synchronous young adult hermaphrodite N2 worms can be transferred on a plate to initiate their exposure to bacterial strains of interest. A WT *P. fluorescens* SBW25

strain and a virulent strain of *P. aeruginosa PAO1* would be used as negative and positive controls.

There is also further research into the novel phenotypes we found in the populations of *P. fluorescens* SBW25 undergoing predation. Whilst understanding the nature of WS morphotypes conferring resistance is straightforward and has been discussed extensively both by ourselves and others, the explanation for predator resistance in both the Vol and Mnt morphotypes intrigued us. In this work, we proposed line test and performance test assays to investigate the resistance of bacterial isolates including Vol phenotype against all predator types. It appeared that in the line test assay, the Vol morphotypes were highly susceptible to all predator types. Contrary to this, in the performance test assay the Vol isolates survived better when predated upon by their coevolved predators, whilst these predators do not suffer population declines in concert with this presumed prey "escape". The increased bacterial survival suggested that exposure or proximity to the *Acanthamoeba* is stimulating the anti-predator trait in the bacteria in advance of phagocytosis. We found that the *P. fluorescens* Vol cells become predation-resistant only in the presence of coevolved amoebae. Therefore, we predict a molecular or gene regulation change that is taking place. This may be stimulated by cell-to-cell signalling on the part of the bacteria, like quorum sensing in the *P. aeruginosa,* or this might be an indication that some molecular or chemical change in the bacteria that is precipitated by the presence of the *Acanthamoeba* directly. Molecular investigations suggested that the Vol cells harboured a deletion mutation on the *fadD1-fadD2* genes. FadD is an acetyl-CoA synthesis protein and plays a major role in degrading exogenous LCFA. We predict host associated LCFA may mask prey cells if they accumulate in the membrane. In this case, the bacteria would be recognised as self rather than prey, which would

reduce their consumption by the *Acanthamoebae*. To explore this further, we are interested in investigating the composition of fatty acids in Vol isolates and their coevolved predators while growing together and by itself. This is to find out if Vol demonstrates a similar FA structure as their coevolved protozoa. The FA acid profile of the bacteria and amoebae could be obtained by using the Bligh and Dyer method following the methylation method. After the lipids are extracted the amount of fatty acids in the oil can be quantified by capillary gas chromatography (GC). It is hoped that this investigation will deepen our understanding of why Vol cells have been stablish a special relationship by their coevolved predators.

Chapter 2 Supplementary

DRC 16

MASSEY UNIVERSITY
GRADUATE RESEARCH SCHOOL

STATEMENT OF CONTRIBUTION
DOCTORATE WITH PUBLICATIONS/MANUSCRIPTS

We, the candidate and the candidate's Primary Supervisor, certify that all co-authors have consented to their work being included in the thesis and they have accepted the candidate's contribution as indicated below in the *Statement of Originality*.

Name of candidate:	Farhad Golzar
Name/title of Primary Supervisor:	Dr Heather Hendrickson
Name of Research Output and full reference:	
In which Chapter is the Manuscript /Published work:	Chapters 2 & 4
Please indicate:	
• The percentage of the manuscript/Published Work that was contributed by the candidate:	90%
and	
• Describe the contribution that the candidate has made to the Manuscript/Published Work:	
Chapter 2: All work with the exception of the biofilm strength assay. Capther 4: All work with the exception of RNA sequencing.	
For manuscripts intended for publication please indicate target journal:	
Munuscript 1: Plos bio - Manuscript 2: ISME - Manuscript 3: MBE	
Candidate's Signature:	Golzar, Farhad Digitally signed by Golzar, Farhad Date: 2022.03.03 16:29:28 +13'00'
Date:	03/03/2022
Primary Supervisor's Signature:	Heather Hendrickson Digitally signed by Heather Hendrickson Date: 2022.03.04 08:44:48 +13'00'
Date:	04/03/2022

(This form should appear at the end of each thesis chapter/section/appendix submitted as a manuscript/ publication or collected as an appendix at the end of the thesis)

GRS Version 4– January 2019

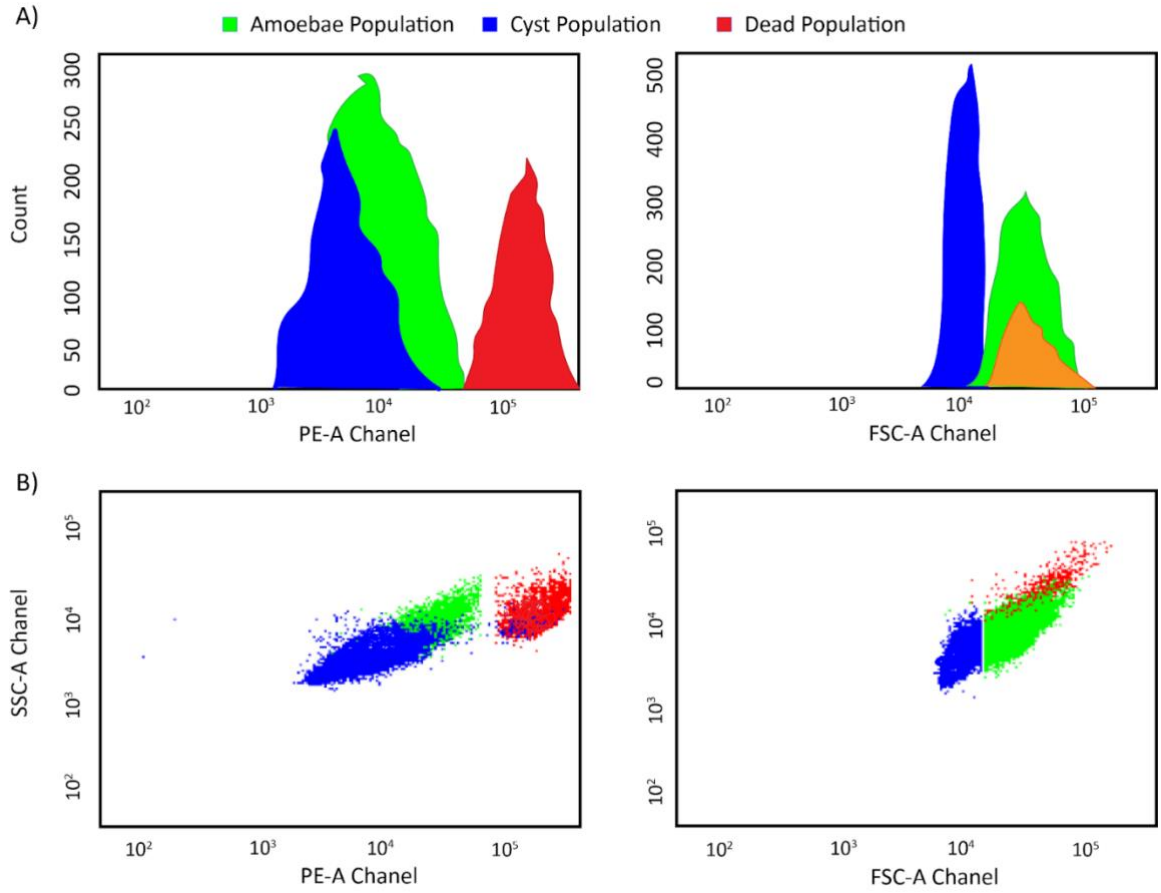

Supplementary Figure 1. Results of flow cytometry showing *Acanthamoeba* populations distinguished by morphology and viability using PE-A and FSC-A channels. Active amoeba, cyst and dead populations are shown in green, blue and red, respectively.

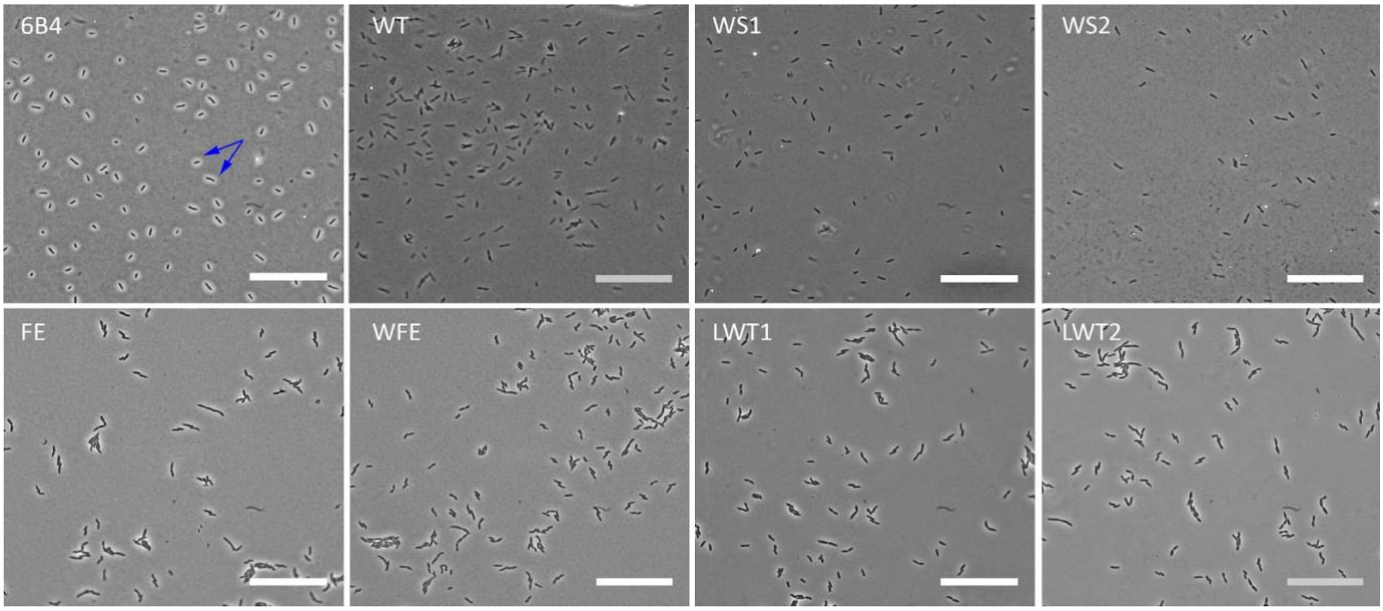

Supplementary Figure 2. Capsule Staining. We examined the predator-evolved phenotypes for production of a colanic acid-like polymer [92] by visualising them with India Ink (see Materials and Methods) and observed them using phase contrast microscopy**.** We included a positive control named 6B4 [45] that makes large capsules. None of the mutants were able to produce a capsule. There were no mutations found in any of our predation-adapted genotypes in known encapsulation associated genes and the evolved isolates do not appear to have increased capsule formation under standard laboratory conditions. Scale bar: 30μm.

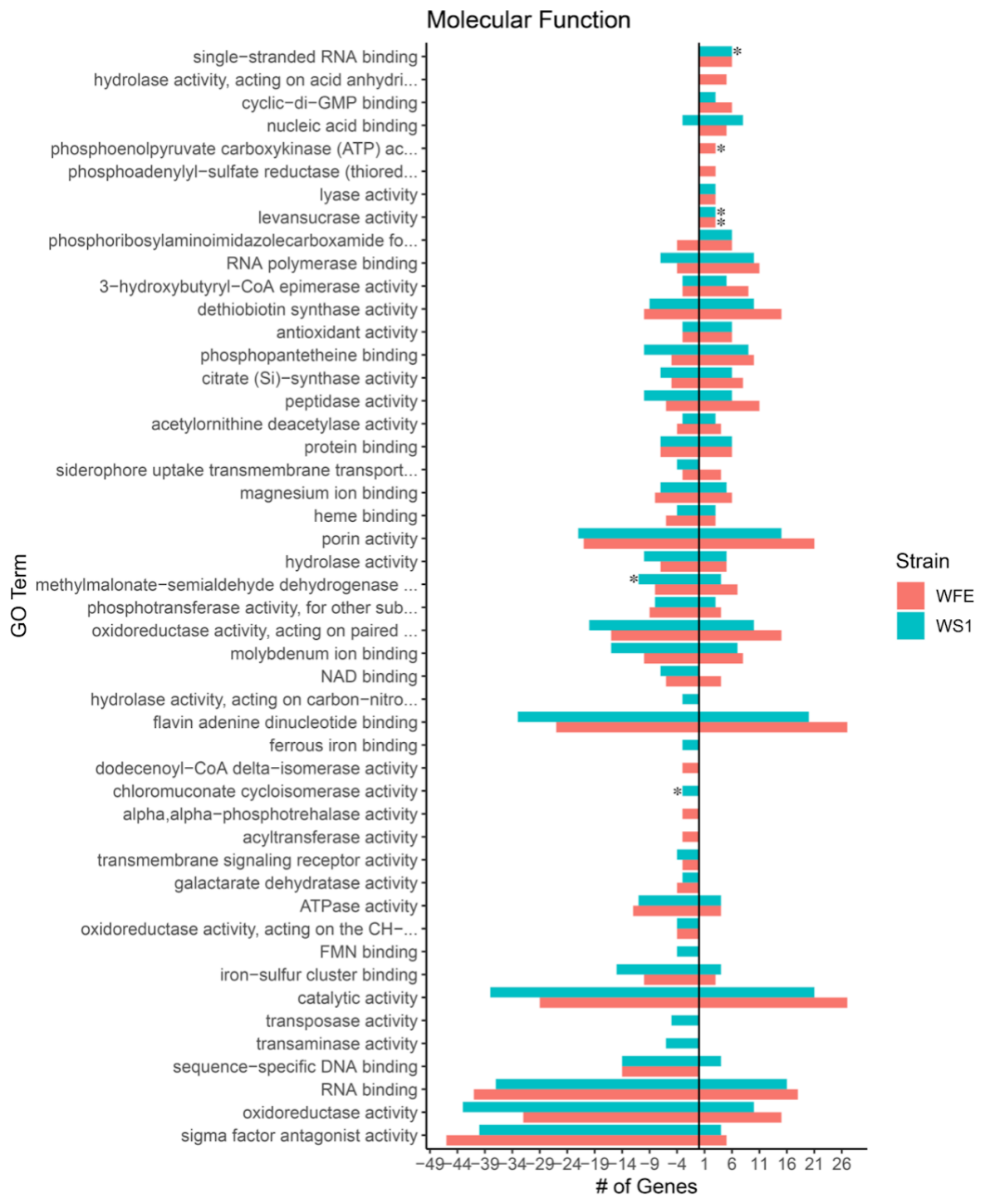

Supplementary Figure 3. Distribution of gene ontology (GO), molecular function classifications. GO analysis of upregulated (right) and downregulated (left) genes in WS1 and WFE when exposed to ancestral *Acanthamoeba sp.* as indicated. Stars denote enriched GO terms (One-tailed Fisher's exact test, P value <0.05).

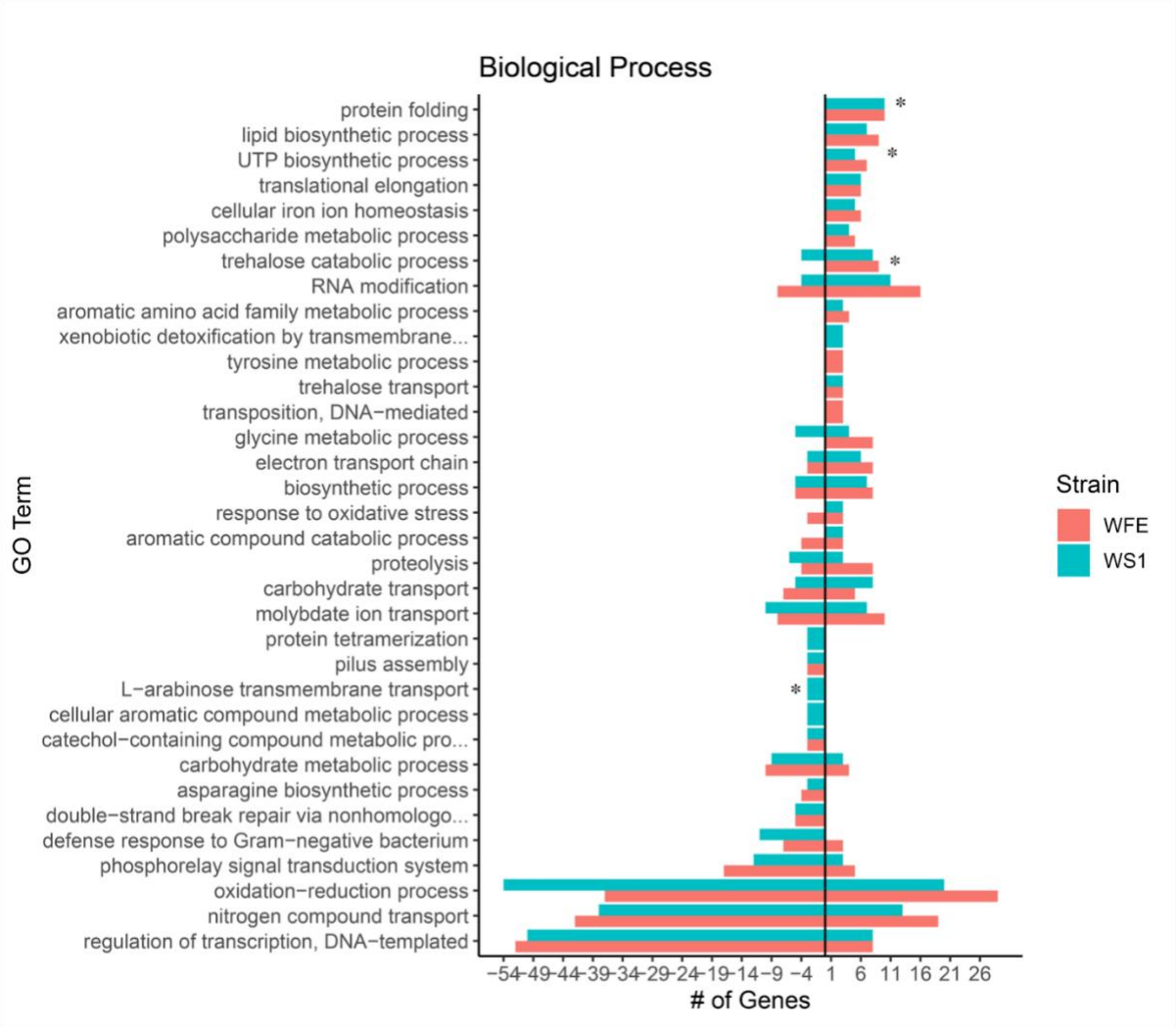

Supplementary Figure 4. Distribution of gene ontology (GO), biological process classifications. GO analysis of upregulated (right) and downregulated (left) genes in WS1 and WFE interacting with *Acanthamoeba sp.* as indicated. Stars denote enriched GO terms (One-tailed Fisher's exact test, P value <0.05).

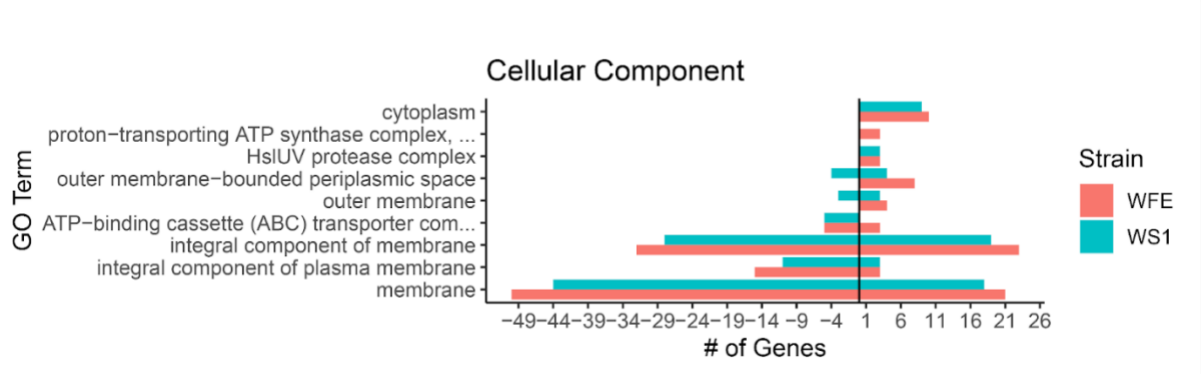

Supplementary Figure 5. Distribution of gene ontology (GO), cellular component classifications. GO analysis of upregulated (right) and downregulated (left) genes in WS1 and WFE interacting with *Acanthamoeba sp.* as indicated.

Supplementary Table 1. *WspF* mutations associated with Wrinkly Spreader Phenotype in this study and the previous literature.

WS genotype	Gene	Nucleotide change	AA change	Reference
WS1	*wspF*	Δ231-236	ΔVIV 76-78V	This study
WS2	*wspF*	+166-180	+LMDLI 56-60	This study
FE	*wspF*	T815C	L272P	This study
LSWS	*wspF*	A901C	S301R	[69]
WSA	*wspF*	T14G	I5S	[69]
WSB	*wspF*	Δ620-674	P206Δ	[69]
WSC	*wspF*	G823T	G275C	[69]
WSE	*wspF*	G658T	V220L	[69]
WSF	*wspF*	C821T	T274I	[69]
WSG	*wspF*	C556T	H186Y	[69]
WSJ	*wspF*	Δ865-868	R288Δ	[69]
WSL	*wspF*	G482A	G161Δ	[69]
WSN	*wspF*	A901C	S301R	[69]
WSO	*wspF*	Δ235-249	V79Δ	[69]
WSU	*wspF*	Δ823-824	T274Δ	[69]
WSW	*wspF*	Δ149	L49Δ	[69]
WSY	*wspF*	Δ166-180	ΔL51-I55	[69]
WS	*wspF*	-	0297K	[93]
WS	*wspF*	-	V271G	[93]
WS	*wspF*	-	G270R	[93]
WS	*wspF*	-	P47L	[94]
WS	*wspF*	-	ΔR66-L 107	[94]
WS	*wspF*	-	S159L	[94]
WS	*wspF*	-	H186Y	[94]
WS	*wspF*	-	Q297R	[94]
WS	*wspF*	-	ΔT226-G275	[94]

Supplementary Table 2. Genes with differential expression (>2 log_2 FC) in WS1 or WFE when interacting with *Acanthamoeba*, compared to interaction with WT SBW25.

Gene ID	Log$_2$ Fold Change		Gene Name	Product Description
	WS1 + Ac	WFE + Ac		
PFLU0020	-2.289	-2.463	hypothetical protein	hypothetical protein
PFLU0030	-3.038	-2.753	putative 2-dehydro-3-deoxygalactonokinase	putative 2-dehydro-3-deoxygalactonokinase
PFLU0058	-2.023	-2.220	putative cytochrome C oxidase subunit II	putative cytochrome C oxidase subunit II
PFLU0071	-2.408	-2.474	hydroperoxidase II	hydroperoxidase II
PFLU0089	-2.798	-4.584	hypothetical protein	NA
PFLU0091	-4.855	-5.285	hypothetical protein	hypothetical protein
PFLU0108	3.023	2.279	hypothetical protein	NA
PFLU0109	4.231	3.950	hypothetical protein	NA
PFLU0143	3.973	5.235	outer membrane protein PgaA	outer membrane protein PgaA
PFLU0144	3.084	4.237	outer membrane N-deacetylase	outer membrane N-deacetylase
PFLU0145	2.685	3.620	N-glycosyltransferase	N-glycosyltransferase
PFLU0148A	2.198	2.424	putative transposase	putative transposase
PFLU0150	2.379	2.867	hypothetical protein	NA
PFLU0161	2.033	2.033	putative lipoprotein	NA
PFLU0163	2.177	2.550	putative lipoprotein	NA
PFLU0172	4.662	3.374	hypothetical protein	NA
PFLU0173	2.281	3.216	hypothetical protein	NA
PFLU0187	2.181	2.064	sulfate ABC transporter sulfate-binding protein	sulfate ABC transporter sulfate-binding protein

PFLU0191	**-2.840**	**-2.218**	**hypothetical protein**	**NA**
PFLU0192	**-2.130**	**-2.134**	**putative regulatory protein**	**putative regulatory protein**
PFLU0196	**-2.495**	**-2.590**	**AraC family transcriptional regulator**	**AraC family transcriptional regulator**
PFLU0210	**-2.283**	**-2.261**	**putative transporter-like membrane protein**	**NA**
PFLU0215	**2.077**	**2.062**	**hypothetical protein**	**NA**
PFLU0218	**-3.899**	**-3.341**	**hypothetical protein**	**NA**
PFLU0244	**2.132**	**2.232**	**amino acid ABC transporter ATP-binding protein**	**amino acid ABC transporter ATP-binding protein**
PFLU0292	**-2.727**	**-2.067**	**hypothetical protein**	**hypothetical protein**
PFLU0300	**2.119**	**2.787**	**putative cell morphology-like protein**	**NA**
PFLU0305	**3.367**	**4.114**	**cell morphology-like protein**	**NA**
PFLU0307	**3.340**	**3.074**	**cell morphology-like protein**	**cell morphology-like protein**
PFLU0308	**2.352**	**2.131**	**cell morphology-like protein**	**NA**
PFLU0313	**2.909**	**3.177**	**putative amino acid ABC transporter membrane protein**	**NA**
PFLU0322	**2.363**	**2.088**	**hypothetical protein**	**hypothetical protein**
PFLU0340	**3.062**	**3.020**	**preprotein translocase subunit SecB**	**preprotein translocase subunit SecB**
PFLU0345	**2.338**	**3.013**	**putative lipoprotein**	**NA**
PFLU0347	**2.652**	**2.332**	**hypothetical protein**	**NA**
PFLU0348	**2.613**	**3.228**	**glutamine synthetase**	**glutamine synthetase**
PFLU0351	**3.154**	**3.468**	**hypothetical protein**	**NA**
PFLU0364	**-2.713**	**-3.464**	**putative histidine ABC transporter membrane protein**	**putative histidine ABC transporter membrane protein**
PFLU0376	**2.471**	**2.676**	**putative ABC transporter exported protein**	**putative ABC transporter exported protein**

PFLU0398	3.661	3.956	ATP-dependent protease ATP-binding subunit HslU	ATP-dependent protease ATP-binding subunit HslU
PFLU0399	3.036	3.398	ATP-dependent protease peptidase subunit	ATP-dependent protease peptidase subunit
PFLU0403	4.994	3.419	50S ribosomal protein L31	50S ribosomal protein L31
PFLU0440	2.767	3.300	hypothetical protein	NA
PFLU0497	-2.536	-2.038	putative phosphoesterase	putative phosphoesterase
PFLU0533	2.485	3.281	30S ribosomal protein S6	30S ribosomal protein S6
PFLU0534	3.052	3.810	30S ribosomal protein S18	30S ribosomal protein S18
PFLU0536	2.480	3.324	50S ribosomal protein L9	50S ribosomal protein L9
PFLU0549	-2.426	-2.584	putative dehydrogenase	putative dehydrogenase
PFLU0575	2.883	2.810	curved DNA-binding protein	curved DNA-binding protein
PFLU0612	2.159	2.140	bifunctional phosphoribosylaminoimidazolecarboxamide formyltransferase/IMP cyclohydrolase	bifunctional phosphoribosylaminoimidazolecarboxamide formyltransferase/IMP cyclohydrolase
PFLU0613	3.054	2.537	DNA-binding protein Fis	DNA-binding protein Fis
PFLU0625	2.298	2.398	translation initiation factor Sui1	translation initiation factor Sui1
PFLU0640	-2.331	-3.573	putative two-component system response regulator	putative two-component system response regulator
PFLU0641	-3.423	-3.205	hypothetical protein	NA
PFLU0652	-2.302	-2.500	putative lipoprotein	NA
PFLU0662	2.455	3.070	hypothetical protein	NA
PFLU0672	2.474	2.457	TetR family transcriptional regulator	TetR family transcriptional regulator
PFLU0673	-3.746	-3.619	putative purine transporter-like permease	putative purine transporter-like permease
PFLU0729	2.114	2.296	GTP-dependent nucleic acid-binding protein EngD	GTP-dependent nucleic acid-binding protein EngD
PFLU0731	3.877	4.562	50S ribosomal protein L25/general stress protein Ctc	50S ribosomal protein L25/general stress protein Ctc

PFLU0733	4.017	2.600	4-diphosphocytidyl-2-C-methyl-D-erythritol kinase	4-diphosphocytidyl-2-C-methyl-D-erythritol kinase
PFLU0752	-2.484	-2.340	hypothetical protein	NA
PFLU0755	-3.432	-3.565	hypothetical protein	hypothetical protein
PFLU0765	5.924	4.467	30S ribosomal protein S20	30S ribosomal protein S20
PFLU0795	2.180	2.176	hypothetical protein	NA
PFLU0824	2.631	2.681	putative outer membrane porin	putative outer membrane porin
PFLU0826	2.011	2.014	dipeptide ABC transporter substrate-binding protein	dipeptide ABC transporter substrate-binding protein
PFLU0828	2.486	3.392	hypothetical protein	NA
PFLU0840	3.565	2.589	30S ribosomal protein S9	30S ribosomal protein S9
PFLU0848	2.109	3.353	phosphatidylcholine-hydrolyzing phospholipase C	NA
PFLU0852	-2.712	-2.397	D-galactarate dehydratase	D-galactarate dehydratase
PFLU0855	3.011	2.113	hypothetical protein	hypothetical protein
PFLU0856	-2.045	-2.071	hypothetical protein	hypothetical protein
PFLU0859	2.005	2.110	putative lipoprotein A-like protein	putative lipoprotein A-like protein
PFLU0869	-2.948	-3.438	putative hydrolase	putative hydrolase
PFLU0882	-2.049	-2.014	RNA polymerase factor sigma-54	RNA polymerase factor sigma-54
PFLU0893	2.227	2.129	hypothetical protein	NA
PFLU0907	-2.458	-2.284	hypothetical protein	NA
PFLU0918	5.486	4.960	hypothetical protein	NA
PFLU0932	2.495	2.682	putative phospholipid-binding lipoprotein	NA
PFLU0934	4.632	4.302	hypothetical protein	NA

PFLU0957	-2.435	-2.036	hypothetical protein	hypothetical protein
PFLU0979	4.239	4.629	alginate biosynthesis protein	alginate biosynthesis protein
PFLU0980	5.272	5.470	alginate biosynthesis protein	alginate biosynthesis protein
PFLU0981	3.598	3.892	alginate biosynthesis protein	alginate biosynthesis protein
PFLU0982	4.029	4.184	poly(beta-D-mannuronate) O-acetylase	poly(beta-D-mannuronate) O-acetylase
PFLU0983	3.199	3.532	poly(beta-D-mannuronate) lyase	poly(beta-D-mannuronate) lyase
PFLU0985	2.653	3.100	poly(beta-D-mannuronate) C5 epimerase	NA
PFLU0988	2.930	2.995	putative alginate biosynthesis-like protein	putative alginate biosynthesis-like protein
PFLU0990	3.765	3.841	GDP-mannose 6-dehydrogenase	GDP-mannose 6-dehydrogenase
PFLU1004	-3.034	-2.702	hypothetical protein	hypothetical protein
PFLU1010	-2.159	-2.339	putative outer membrane usher protein	putative outer membrane usher protein
PFLU1017	-3.176	-3.465	putative response regulator receiver domain-containing protein	putative response regulator receiver domain-containing protein
PFLU1018	-2.272	-2.272	putative response regulator receiver domain-containing protein	putative response regulator receiver domain-containing protein
PFLU1026	2.447	3.189	putative fumarylacetoacetase	putative fumarylacetoacetase
PFLU1031	2.829	2.579	hypothetical protein	NA
PFLU1035	2.480	2.066	L-serine dehydratase 1	L-serine dehydratase 1
PFLU1039	-2.227	-2.490	LysR family transcriptional regulator	LysR family transcriptional regulator
PFLU1070	2.010	2.436	ATP-dependent protease	ATP-dependent protease
PFLU1074	-2.900	-2.979	putative sugar transporter-like, membrane protein	putative sugar transporter-like, membrane protein
PFLU1075	-3.617	-4.065	putative dehydrogenase	putative dehydrogenase
PFLU1103	2.287	2.253	putative amino acid transporter-like membrane protein	putative amino acid transporter-like membrane protein

PFLU1139	2.129	2.323	glutamate/aspartate ABC transporter periplasmic binding protein	NA
PFLU1148	-2.734	-3.201	putative formate dehydrogenase	putative formate dehydrogenase
PFLU1155	-3.107	-3.569	putative exported flagellar protein	NA
PFLU1163	2.077	2.242	ferredoxin I	ferredoxin I
PFLU1170	2.926	3.318	hypothetical protein	NA
PFLU1171	2.726	3.181	putative phage assembly-like protein	NA
PFLU1172	2.606	2.977	hypothetical protein	NA
PFLU1177	2.773	3.504	hypothetical protein	NA
PFLU1178	3.204	3.666	putative phage tail-like protein	NA
PFLU1180	2.537	2.881	phage protein	NA
PFLU1182	2.462	2.830	hypothetical protein	NA
PFLU1228	2.053	2.181	lysyl-tRNA synthetase	lysyl-tRNA synthetase
PFLU1265	2.595	2.405	hypothetical protein	NA
PFLU1271	2.110	2.938	elongation factor Ts	elongation factor Ts
PFLU1279	3.117	2.758	hypothetical protein	hypothetical protein
PFLU1302A	6.648	5.109	cold shock protein	cold shock protein
PFLU1335	-4.336	-4.079	putative lipoprotein	NA
PFLU1341	3.308	3.930	hypothetical protein	NA
PFLU1357	3.331	2.236	hypothetical protein	NA
PFLU1358	7.120	2.719	hypothetical protein	NA
PFLU1369	-2.672	-2.568	3-carboxy-cis,cis-muconate cycloisomerase	3-carboxy-cis,cis-muconate cycloisomerase
PFLU1382	2.943	2.356	putative carbon compunds degradation-like protein	putative carbon compunds degradation-like protein
PFLU1412	3.283	3.264	alcohol dehydrogenase	alcohol dehydrogenase
PFLU1418	-2.597	-2.767	putative transporter-like membrane protein	putative transporter-like membrane protein

PFLU1433	**-2.849**	**-3.745**	**hypothetical protein**	**NA**
PFLU1436	**-3.190**	**-3.521**	**ribosomal small subunit pseudouridine synthase A**	**ribosomal small subunit pseudouridine synthase A**
PFLU1439	**-2.656**	**-2.507**	**putative lipoprotein**	**NA**
PFLU1482	**4.065**	**5.092**	**putative colicind-pore forming protein**	**putative colicind-pore forming protein**
PFLU1483	**-2.185**	**-2.104**	**hypothetical protein**	**hypothetical protein**
PFLU1504	**-3.008**	**-3.163**	**LysR family transcriptional regulator**	**LysR family transcriptional regulator**
PFLU1505	**-3.133**	**-3.074**	**hypothetical protein**	**NA**
PFLU1519	**2.000**	**2.321**	**putative nitroreductase**	**putative nitroreductase**
PFLU1522	**-2.250**	**-2.827**	**hypothetical protein**	**NA**
PFLU1525	**-2.845**	**-2.937**	**putative lipoprotein**	**NA**
PFLU1532	**-2.001**	**-2.263**	**hypothetical protein**	**NA**
PFLU1533	**-2.570**	**-2.322**	**LysR family transcriptional regulator**	**LysR family transcriptional regulator**
PFLU1534	**-2.422**	**-2.229**	**LamB/YcsF family protein**	**LamB/YcsF family protein**
PFLU1542	**-2.369**	**-2.134**	**aconitate hydratase**	**NA**
PFLU1568	**-2.381**	**-2.044**	**hypothetical protein**	**hypothetical protein**
PFLU1574	**-2.002**	**-2.410**	**putative lipoprotein releasing system, membrane protein**	**putative lipoprotein releasing system, membrane protein**
PFLU1591A	**4.042**	**3.222**	**hypothetical protein**	**NA**
PFLU1592	**-3.317**	**-3.085**	**hypothetical protein**	**NA**

PFLU1595	**4.863**	**3.393**	**hypothetical protein**	**NA**
PFLU1596	**2.830**	**2.017**	**hypothetical protein**	**NA**
PFLU1597	**4.567**	**3.206**	**hypothetical protein**	**hypothetical protein**
PFLU1605	**-2.813**	**-2.337**	**putative two-component system sensor kinase**	**putative two-component system sensor kinase**
PFLU1610	**-2.885**	**-2.894**	**putative fimbrial usher outer membrane protein**	**putative fimbrial usher outer membrane protein**
PFLU1631	**2.241**	**2.310**	**putative proline iminopeptidase**	**putative proline iminopeptidase**
PFLU1636	**3.017**	**3.002**	**putative peptide ABC transporter substrate-binding protein**	**putative peptide ABC transporter substrate-binding protein**
PFLU1652	**3.081**	**2.529**	**hypothetical protein**	**hypothetical protein**
PFLU1653	**7.121**	**5.807**	**putative transporter-like membrane protein**	**putative transporter-like membrane protein**
PFLU1655	**7.462**	**5.934**	**hypothetical protein**	**NA**
PFLU1656	**5.250**	**3.891**	**hypothetical protein**	**NA**
PFLU1658	**2.675**	**2.069**	**NAD dependent epimerase/dehydratase**	**NAD dependent epimerase/dehydratase**
PFLU1659	**3.001**	**2.340**	**UDP-N-acetylglucosamine2-epimerase**	**UDP-N-acetylglucosamine2-epimerase**
PFLU1662	**4.052**	**3.083**	**hypothetical protein**	**hypothetical protein**
PFLU1666	**2.224**	**2.084**	**putative 3-oxoacyl-(Acyl-carrier-protein) synthase III**	**putative 3-oxoacyl-(Acyl-carrier-protein) synthase III**
PFLU1669	**3.780**	**3.999**	**hypothetical protein**	**NA**
PFLU1673	**-2.723**	**-2.649**	**hypothetical protein**	**NA**
PFLU1682	**-2.291**	**-2.642**	**putative lipoprotein**	**NA**
PFLU1683	**-2.539**	**-2.120**	**hypothetical protein**	**NA**
PFLU1691	**2.743**	**3.139**	**hypothetical protein**	**NA**
PFLU1696	**2.369**	**2.145**	**transcription elongation factor**	**transcription elongation factor**
PFLU1714	**4.481**	**4.217**	**elongation factor P**	**elongation factor P**
PFLU1725	**-4.247**	**-4.048**	**enoyl-CoA hydratase**	**enoyl-CoA hydratase**

PFLU1726	3.385	3.637	cold-shock dead-box protein A	cold-shock dead-box protein A
PFLU1728	-2.722	-2.407	thiopurine S-methyltransferase	thiopurine S-methyltransferase
PFLU1743	-2.184	-2.151	EAL domain-containing protein	NA
PFLU1749	-5.064	-5.035	hypothetical protein	NA
PFLU1758	2.609	2.219	cytochrome c biogenesis protein CcmA	cytochrome c biogenesis protein CcmA
PFLU1767	2.048	2.392	putative lipoprotein	NA
PFLU1773	2.652	4.209	hypothetical protein	hypothetical protein
PFLU1774	2.686	4.725	putative methyltransferase	putative methyltransferase
PFLU1793	-3.774	-4.220	putative metalloprotease	putative metalloprotease
PFLU1810	-2.412	-2.442	hypothetical protein	NA
PFLU1815	3.099	3.310	type II citrate synthase	type II citrate synthase
PFLU1819	2.362	2.527	succinate dehydrogenase iron-sulfur subunit	succinate dehydrogenase iron-sulfur subunit
PFLU1820	2.062	2.547	2-oxoglutarate dehydrogenase E1 component	2-oxoglutarate dehydrogenase E1 component
PFLU1823	2.139	2.939	succinyl-CoA synthetase subunit beta	succinyl-CoA synthetase subunit beta
PFLU1830	4.105	4.840	heat shock protein 90	heat shock protein 90
PFLU1853	-2.024	-3.015	short chain dehydrogenase	short chain dehydrogenase
PFLU1876	-2.143	-2.740	putative transporter-like membrane protein	putative transporter-like membrane protein
PFLU1886	3.606	2.197	hypothetical protein	NA
PFLU1893	-2.089	-2.280	hypothetical protein	hypothetical protein
PFLU1895	-2.328	-2.076	putative cytochrome C dehydrogenase-like protein	putative cytochrome C dehydrogenase-like protein
PFLU1896	-2.307	-2.523	hypothetical protein	hypothetical protein

PFLU1898	-4.960	-6.071	putative transporter-like membrane protein	putative transporter-like membrane protein
PFLU1907	2.062	2.391	hypothetical protein	NA
PFLU1924	3.139	2.173	putative HTH-type regulatory protein	putative HTH-type regulatory protein
PFLU1983	3.948	3.689	hypothetical protein	hypothetical protein
PFLU1990	-2.111	-2.126	putative transporter-like membrane protein	putative transporter-like membrane protein
PFLU1992	-2.724	-3.214	hypothetical protein	NA
PFLU1995	-3.226	-4.524	hypothetical protein	hypothetical protein
PFLU1997	-2.075	-3.317	acetyl-CoA carboxylase biotin carboxylase subunit	acetyl-CoA carboxylase biotin carboxylase subunit
PFLU2009	-3.538	-4.115	threonine synthase	NA
PFLU2010	-2.162	-3.100	putative AsnC family regulatory protein	putative AsnC family regulatory protein
PFLU2012	2.012	2.067	putative dehydrogenase	putative dehydrogenase
PFLU2013	2.894	2.883	D-serine/D-alanine/glycine transporter	D-serine/D-alanine/glycine transporter
PFLU2027	2.282	3.137	FKBP-type peptidyl-prolyl cis-trans isomerase	FKBP-type peptidyl-prolyl cis-trans isomerase
PFLU2041	2.193	2.385	putative ABC transporter substrate-binding protein	putative ABC transporter substrate-binding protein
PFLU2054	-5.277	-7.013	hypothetical protein	NA
PFLU2102	-2.276	-2.375	putative transporter-like membrane protein	putative transporter-like membrane protein
PFLU2116	2.313	2.425	6-pyruvoyl tetrahydrobiopterin synthase	NA
PFLU2127	-3.820	-2.447	hypothetical protein	NA
PFLU2128	-3.863	-3.154	hypothetical protein	hypothetical protein

PFLU2129	-2.483	-2.801	hypothetical protein	NA
PFLU2133	-4.281	-3.726	hypothetical protein	NA
PFLU2156	-2.241	-2.113	hypothetical protein	NA
PFLU2176	-4.446	-2.232	putative isomerase	putative isomerase
PFLU2180	-2.518	-2.017	putative LuxR family regulatory protein	putative LuxR family regulatory protein
PFLU2193	2.007	2.352	putative riboflavin biosynthesis deaminase	putative riboflavin biosynthesis deaminase
PFLU2219	-4.025	-2.472	hypothetical protein	hypothetical protein
PFLU2244	2.569	2.638	putative two-component system response regulator	putative two-component system response regulator
PFLU2246	3.266	3.069	hypothetical protein	NA
PFLU2248	-2.367	-3.026	putative two-component system response regulator	putative two-component system response regulator
PFLU2271	-2.322	-2.080	putative exported isoquinoline 1-oxidoreductase subunit beta	putative exported isoquinoline 1-oxidoreductase subunit beta
PFLU2293	4.013	5.379	pectin lyase	NA
PFLU2294	2.427	3.610	levansucrase	levansucrase
PFLU2298	-2.059	-2.018	xylose ABC transporter permease	xylose ABC transporter permease
PFLU2301	-2.340	-3.079	xylose isomerase	xylose isomerase
PFLU2308	-5.129	-5.048	hypothetical protein	NA
PFLU2310	-3.208	-2.229	putative monooxygenase	putative monooxygenase
PFLU2329	-2.674	-2.140	putative amino acid transporter-like protein	putative amino acid transporter-like protein

PFLU2335	**-2.238**	**-3.022**	**putative oxidoreductase**	**putative oxidoreductase**
PFLU2340	**-3.173**	**-2.568**	**putative polyamine ABC transporter ATP-binding protein**	**putative polyamine ABC transporter ATP-binding protein**
PFLU2341	**-2.094**	**-2.349**	**putative polyamine ABC transporter membrane protein**	**putative polyamine ABC transporter membrane protein**
PFLU2342	**-2.982**	**-3.015**	**putative polyamine ABC transporter membrane protein**	**putative polyamine ABC transporter membrane protein**
PFLU2352	**-2.945**	**-2.078**	**putative oxidoreductase**	**putative oxidoreductase**
PFLU2353	**-3.314**	**-3.445**	**hypothetical protein**	**NA**
PFLU2368	**-3.172**	**-3.084**	**putative transporter-like membrane protein**	**putative transporter-like membrane protein**
PFLU2370	**-3.008**	**-2.957**	**putative aldehyde dehydrogenase**	**putative aldehyde dehydrogenase**
PFLU2371	**-3.992**	**-4.152**	**putative calcium-binding protein**	**NA**
PFLU2373	**-2.322**	**-2.378**	**L-arabinose transporter ATP-binding protein**	**L-arabinose transporter ATP-binding protein**
PFLU2374	**-2.034**	**-2.766**	**L-arabinose transporter permease**	**L-arabinose transporter permease**
PFLU2376	**-3.496**	**-4.057**	**putative short-chain dehydrogenase/reductase**	**putative short-chain dehydrogenase/reductase**
PFLU2381	**-3.181**	**-4.746**	**hypothetical protein**	**hypothetical protein**
PFLU2384	**-2.385**	**-2.591**	**hypothetical protein**	**NA**
PFLU2411	**-3.118**	**-3.252**	**hypothetical protein**	**NA**
PFLU2412	**-2.620**	**-2.868**	**putative TonB-ferrisiderophore receptor protein**	**putative TonB-ferrisiderophore receptor protein**

PFLU2419	-2.882	-2.152	putative type II secretion pathway protein G	putative type II secretion pathway protein G
PFLU2436	-7.397	-3.026	hypothetical protein	NA
PFLU2442	-2.768	-2.582	LysR family transcriptional regulator	LysR family transcriptional regulator
PFLU2454	3.501	2.463	putative hydratase	putative hydratase
PFLU2461	-2.303	-2.051	hypothetical protein	NA
PFLU2462	-6.235	-4.504	hypothetical protein	NA
PFLU2498	2.728	2.293	putative methyl-accepting chemotaxis protein	putative methyl-accepting chemotaxis protein
PFLU2509	2.786	2.677	putative TonB-receptor protein	NA
PFLU2509A	2.948	2.648	hypothetical protein	NA
PFLU2529	-4.060	-3.574	putative IcrL family regulatory protein	putative IcrL family regulatory protein
PFLU2530	-5.704	-5.264	putative LuxR family regulatory protein	putative LuxR family regulatory protein
PFLU2532	-3.499	-3.439	GntR family transcriptional regulator	GntR family transcriptional regulator
PFLU2537	-3.528	-2.811	putative ATP-binding protein	putative ATP-binding protein
PFLU2543	2.226	3.488	peptide synthase	peptide synthase
PFLU2544	2.124	3.477	peptide synthase	peptide synthase
PFLU2545	2.655	4.148	ferripyoverdine receptor	ferripyoverdine receptor
PFLU2546	2.218	3.340	putative ABC transporter ATP-binding protein	putative ABC transporter ATP-binding protein
PFLU2547	3.586	5.048	putative pyoverdine synthetase F	putative pyoverdine synthetase F
PFLU2548	3.482	4.771	hypothetical protein	NA
PFLU2551	2.378	3.301	hypothetical protein	NA
PFLU2559	-3.074	-3.702	AsnC family regulatory protein	AsnC family regulatory protein

PFLU2573	-2.951	-3.783	putative transmembrane protein	NA
PFLU2582	2.285	2.157	hypothetical protein	NA
PFLU2584	-2.198	-2.267	putative ABC transporter ATP-binding protein	putative ABC transporter ATP-binding protein
PFLU2586	2.819	3.126	putative DnaK suppressor protein	putative DnaK suppressor protein
PFLU2591	2.902	3.226	hypothetical protein	NA
PFLU2598	-2.336	-2.078	TonB-dependent siderophore receptor	TonB-dependent siderophore receptor
PFLU2605	2.267	2.089	hypothetical protein	NA
PFLU2612	3.592	3.371	hypothetical protein	NA
PFLU2628	-2.401	-3.368	3-hydroxybutyrate dehydrogenase	3-hydroxybutyrate dehydrogenase
PFLU2642	3.529	2.779	3 membrane-bound lytic murein transglycosylase D	3 membrane-bound lytic murein transglycosylase D
PFLU2644	-3.360	-3.727	hypothetical protein	hypothetical protein
PFLU2651	2.193	2.437	hypothetical protein	NA
PFLU2659	-2.416	-3.820	hypothetical protein	NA
PFLU2664	-3.557	-2.922	hypothetical protein	hypothetical protein
PFLU2686	4.245	4.368	hypothetical protein	NA
PFLU2689	-2.766	-2.524	hypothetical protein	hypothetical protein
PFLU2694	2.897	2.963	hypothetical protein	NA
PFLU2695	-2.102	-3.543	sigma-54 interacting regulatory protein	sigma-54 interacting regulatory protein
PFLU2699	2.130	8.345	hypothetical protein	NA
PFLU2700	4.672	8.318	hypothetical protein	NA
PFLU2706	-2.261	-2.749	hypothetical protein	NA

PFLU2711	-3.299	-3.486	putative methyl-accepting chemotaxis protein	putative methyl-accepting chemotaxis protein
PFLU2721	2.381	3.262	putative efflux system inner membrane protein	putative efflux system inner membrane protein
PFLU2739	-3.762	-3.167	fructokinase	fructokinase
PFLU2748	2.233	2.727	putative thiol peroxidase	putative thiol peroxidase
PFLU2752	-2.264	-2.321	putative outer membrane efflux protein	putative outer membrane efflux protein
PFLU2754	-2.540	-2.411	putative short chain dehydrogenase	putative short chain dehydrogenase
PFLU2761	-2.243	-2.055	putative alpha-amylase	putative alpha-amylase
PFLU2762	-2.267	-2.374	putative trehalose synthase protein	putative trehalose synthase protein
PFLU2768	-2.631	-2.781	LysR family transcriptional regulator	LysR family transcriptional regulator
PFLU2780	-2.414	-2.715	putative transmembrane phosphatidylcholine synthase	putative transmembrane phosphatidylcholine synthase
PFLU2787	-3.218	-2.130	heme uptake regulator	heme uptake regulator
PFLU2792	4.013	2.072	putative molybdenum-pterin binding protein II	NA
PFLU2798	-2.281	-2.375	putative alpha/beta hydrolase	NA
PFLU2802	-2.019	-2.304	isoquinoline 1-oxidoreductase subunit alpha	isoquinoline 1-oxidoreductase subunit alpha
PFLU2824A	2.707	2.303	hypothetical protein	NA
PFLU2830	2.252	2.602	hypothetical protein	NA
PFLU2832	3.905	2.752	phage protein	NA
PFLU2842	4.238	5.077	hypothetical protein	NA
PFLU2844A	2.315	2.118	hypothetical protein	NA
PFLU2857A	3.741	4.877	hypothetical protein	NA

PFLU2858	**2.757**	**3.838**	**hypothetical protein**	**NA**
PFLU2865	**6.212**	**6.041**	**hypothetical protein**	**NA**
PFLU2871	**7.233**	**6.271**	**hypothetical protein**	**NA**
PFLU2876	**-2.904**	**-3.279**	**hypothetical protein**	**NA**
PFLU2887	**3.991**	**3.239**	**hypothetical protein**	**NA**
PFLU2888A	**3.845**	**2.671**	**putative phage-like protein**	**NA**
PFLU2890	**-2.638**	**-2.031**	**hypothetical protein**	**NA**
PFLU2891	**2.016**	**2.884**	**putative phage tail assembly protein**	**NA**
PFLU2906	**-3.154**	**-2.850**	**putative ABC transporter membrane protein**	**putative ABC transporter membrane protein**
PFLU2912	**-2.309**	**-2.121**	**hypothetical protein**	**hypothetical protein**
PFLU2916	**-4.227**	**-3.743**	**TetR family transcriptional regulator**	**TetR family transcriptional regulator**
PFLU2918	**3.114**	**3.675**	**putative lipoprotein**	**NA**
PFLU2924	**3.321**	**2.624**	**hypothetical protein**	**hypothetical protein**
PFLU2927	**2.361**	**2.074**	**hypothetical protein**	**NA**
PFLU2928	**3.540**	**3.093**	**hypothetical protein**	**NA**
PFLU2935	**-3.368**	**-2.682**	**putative glycine betaine/L-proline ABC transporter substrate-binding periplasmic protein**	**putative glycine betaine/L-proline ABC transporter substrate-binding periplasmic protein**
PFLU2949A	**2.084**	**2.228**	**hypothetical protein**	**NA**
PFLU2958	**-2.781**	**-2.656**	**chemotactic transduction protein**	**chemotactic transduction protein**
PFLU2959	**-2.148**	**-2.423**	**AraC family transcriptional regulator**	**AraC family transcriptional regulator**
PFLU2974	**-3.145**	**-2.198**	**hypothetical protein**	**NA**
PFLU2989	**2.082**	**2.292**	**alkyl hydroperoxide reductase protein**	**alkyl hydroperoxide reductase protein**

PFLU2991	2.405	3.139	lactoylglutathione lyase	lactoylglutathione lyase
PFLU3000	-3.117	-2.961	LysR family transcriptional regulator	LysR family transcriptional regulator
PFLU3001	-2.699	-2.260	putative ACP reductase	NA
PFLU3004	-2.198	-2.440	glycerate kinase	glycerate kinase
PFLU3007	-2.355	-2.696	hypothetical protein	NA
PFLU3026	-2.495	-2.037	hypothetical protein	NA
PFLU3042	2.311	2.546	putative glycosyl transferase	putative glycosyl transferase
PFLU3045	-2.269	-2.151	putative oxidoreductase	putative oxidoreductase
PFLU3048	-2.416	-2.565	hypothetical protein	NA
PFLU3052	3.223	2.557	hypothetical protein	NA
PFLU3062	-2.320	-2.296	putative aerobic C4-dicarboxylate transport protein	putative aerobic C4-dicarboxylate transport protein
PFLU3080	-3.994	-3.328	putative 2-keto-4-pentenoate hydratase	putative 2-keto-4-pentenoate hydratase
PFLU3086	-3.102	-2.538	putative phenylacetaldehyde dehydrogenase	putative phenylacetaldehyde dehydrogenase
PFLU3091	-2.749	-2.929	putative amino acid permease	putative amino acid permease
PFLU3107	-3.454	-3.841	putative transcriptional regulator	NA
PFLU3138	-2.437	-2.078	hypothetical protein	hypothetical protein
PFLU3147	-3.397	-3.358	putative family S58 peptidase	NA
PFLU3158	-2.703	-2.921	putative aminotransferase	putative aminotransferase

PFLU3160	-3.055	-3.260	putative quinone oxidoreductase	putative quinone oxidoreductase
PFLU3163	-2.766	-2.483	hypothetical protein	NA
PFLU3179A	-2.323	-2.538	LysR family transcriptional regulator	LysR family transcriptional regulator
PFLU3198	2.172	2.315	putative acyl CoA oxidase	putative acyl CoA oxidase
PFLU3202	-2.422	-3.226	hypothetical protein	hypothetical protein
PFLU3229	3.520	3.647	putative secreted pectate lyase	NA
PFLU3236	3.074	2.634	general secretion pathway protein G/T	general secretion pathway protein G/T
PFLU3241	2.496	2.154	hypothetical protein	NA
PFLU3242	3.820	3.968	hypothetical protein	NA
PFLU3242A	3.214	3.123	hypothetical protein	NA
PFLU3243	3.643	3.315	hypothetical protein	NA
PFLU3264	-2.468	-2.031	hypothetical protein	NA
PFLU3265	-3.296	-3.407	AraC family transcriptional regulator	AraC family transcriptional regulator
PFLU3273	-3.155	-3.225	6 5-carboxymethyl-2-hydroxymuconate delta-isomerase	6 5-carboxymethyl-2-hydroxymuconate delta-isomerase
PFLU3285	-2.161	-2.226	DNA-binding transcriptional activator FeaR	DNA-binding transcriptional activator FeaR
PFLU3288	-2.947	-2.725	hypothetical protein	NA
PFLU3291	-2.205	-2.319	putative aldehyde dehydrogenase	putative aldehyde dehydrogenase
PFLU3295	-2.503	-2.186	GntR family transcriptional regulator	GntR family transcriptional regulator
PFLU3297	-2.317	-2.225	putative acetyl-CoA acetyltransferase	putative acetyl-CoA acetyltransferase

PFLU3334	-3.004	-3.093	TetR family transcriptional regulator	TetR family transcriptional regulator
PFLU3343	2.426	2.099	hypothetical protein	NA
PFLU3344	5.641	4.929	hypothetical protein	NA
PFLU3355	2.419	2.430	hypothetical protein	NA
PFLU3374	2.481	2.145	hypothetical protein	NA
PFLU3375	-4.408	-3.748	putative D-serine/D-alanine/glycine transporter	putative D-serine/D-alanine/glycine transporter
PFLU3403	2.017	2.309	putative lipoprotein	NA
PFLU3413	3.867	3.095	hypothetical protein	NA
PFLU3460	-2.043	-2.527	GntR family transcriptional regulator	GntR family transcriptional regulator
PFLU3474	-3.374	-4.023	hypothetical protein	hypothetical protein
PFLU3497	-3.400	-2.805	putative monooxygenase	NA
PFLU3499	-2.159	-2.435	putative DNA-3-methyladenine glycosylase I	putative DNA-3-methyladenine glycosylase I
PFLU3502	-3.016	-4.354	GntR family transcriptional regulator	GntR family transcriptional regulator
PFLU3533	4.349	3.568	hypothetical protein	NA
PFLU3534	2.384	2.022	hypothetical protein	NA
PFLU3550	-2.630	-2.433	hypothetical protein	NA
PFLU3551	-2.468	-2.372	putative aldo/keto reductase	putative aldo/keto reductase
PFLU3571	-2.206	-2.150	putative GGDEF domain signaling protein	putative GGDEF domain signaling protein
PFLU3574	-2.228	-2.984	putative ABC transporter ATP-binding protein	putative ABC transporter ATP-binding protein
PFLU3580	2.711	2.629	hypothetical protein	hypothetical protein
PFLU3586	2.090	2.315	hypothetical protein	NA

PFLU3596	-3.253	-3.949	hypothetical protein	hypothetical protein
PFLU3604	-2.707	-2.498	hypothetical protein	hypothetical protein
PFLU3615	-2.521	-2.378	putative protease	NA
PFLU3628	-3.132	-2.382	putative acetyltransferase	putative acetyltransferase
PFLU3629	2.269	2.878	hypothetical protein	NA
PFLU3630	2.438	3.648	putative acetyltransferase	putative acetyltransferase
PFLU3644	-3.549	-3.417	putative bicyclomycin resistance protein	putative bicyclomycin resistance protein
PFLU3723	-2.256	-2.811	glycerol kinase	glycerol kinase
PFLU3724	-3.628	-3.637	C-terminal region of transketolase	C-terminal region of transketolase
PFLU3726	-2.518	-2.239	putative ribose transporter permease	putative ribose transporter permease
PFLU3728	-2.212	-2.211	putative ribose ABC transporter ATP-binding protein	putative ribose ABC transporter ATP-binding protein
PFLU3735	-3.648	-5.101	hypothetical protein	NA
PFLU3736	-3.499	-2.995	hypothetical protein	NA
PFLU3757	-2.726	-4.186	hypothetical protein	NA
PFLU3761	2.608	2.613	hypothetical protein	NA
PFLU3763	3.764	3.009	hypothetical protein	NA
PFLU3775	-2.387	-2.180	hypothetical protein	hypothetical protein
PFLU3787	-3.895	-4.418	hypothetical protein	NA

PFLU3805	-2.716	-2.382	ATP-dependent Clp protease ATP-binding subunit ClpA	ATP-dependent Clp protease ATP-binding subunit ClpA
PFLU3840	-2.405	-2.653	hypothetical protein	hypothetical protein
PFLU3841	-8.454	-3.228	hypothetical protein	NA
PFLU3851	-3.386	-3.641	hypothetical protein	NA
PFLU3873	2.568	3.093	peptidyl-prolyl cis-trans isomerase B	peptidyl-prolyl cis-trans isomerase B
PFLU3884	-4.059	-3.937	putative acyl-CoA dehydrogenase family protein	putative acyl-CoA dehydrogenase family protein
PFLU3894	2.610	2.425	hypothetical protein	NA
PFLU3913	-3.537	-3.756	cytochrome B561	cytochrome B561
PFLU3926	3.149	2.661	DNA-binding protein HU-beta	DNA-binding protein HU-beta
PFLU3942	-2.420	-2.206	phenylhydantoinase	phenylhydantoinase
PFLU3946	2.324	2.060	putative copper resistance protein	putative copper resistance protein
PFLU3947	-3.096	-2.892	putative copper resistance protein D	putative copper resistance protein D
PFLU3950	-2.260	-2.088	hypothetical protein	NA
PFLU3975	3.157	4.356	putative L-ornithine 5-monooxygenase	NA
PFLU3977	3.072	4.144	putative periplasmic protein	putative periplasmic protein
PFLU3992	-2.466	-2.885	putative gluconokinase	putative gluconokinase
PFLU3993	-2.618	-2.159	putative zinc-binding dehydrogenase	putative zinc-binding dehydrogenase
PFLU3999	3.087	4.158	hypothetical protein	NA
PFLU4004	2.946	3.020	4-amino-4-deoxy-L-arabinose transferase	4-amino-4-deoxy-L-arabinose transferase
PFLU4011	-3.059	-3.148	putative ABC transporter membrane protein	NA

PFLU4035	-3.385	-3.804	hypothetical protein	NA
PFLU4037	-2.459	-2.843	putative 2-hydroxyacid dehydrogenase	putative 2-hydroxyacid dehydrogenase
PFLU4038	-2.237	-2.086	putative tartrate dehydrogenase	putative tartrate dehydrogenase
PFLU4040	-2.270	-2.978	acetylornithine deacetylase	acetylornithine deacetylase
PFLU4048	-3.706	-3.316	putative oxidoreductase	putative oxidoreductase
PFLU4056	-3.463	-3.082	putative betaine aldehyde dehydrogenase	putative betaine aldehyde dehydrogenase
PFLU4063	2.485	2.562	hypothetical protein	hypothetical protein
PFLU4083	-2.021	-2.287	TetR family transcriptional regulator	TetR family transcriptional regulator
PFLU4116	-2.680	-2.552	putative sensory box GGDEF transmembrane protein	NA
PFLU4128A	3.608	3.048	hypothetical protein	NA
PFLU4144	2.231	2.508	phenylalanyl-tRNA synthetase subunit alpha	phenylalanyl-tRNA synthetase subunit alpha
PFLU4161	2.139	2.276	putative L-asparaginase II	putative L-asparaginase II
PFLU4162	2.789	3.321	hypothetical protein	NA
PFLU4165	2.014	2.546	carbon storage regulator	carbon storage regulator
PFLU4170	2.178	2.317	hypothetical protein	NA
PFLU4177	2.930	2.923	putative lipoprotein	NA
PFLU4193	-3.468	-3.272	3-isopropylmalate dehydrogenase	3-isopropylmalate dehydrogenase
PFLU4195	-2.687	-2.419	isopropylmalate isomerase small subunit	isopropylmalate isomerase small subunit
PFLU4205	-2.825	-2.754	TetR family transcriptional regulator	TetR family transcriptional regulator
PFLU4211	-3.738	-3.710	LysR family transcriptional regulator	LysR family transcriptional regulator

PFLU4219	2.079	2.210	putative ABC transporter cobalamin-binding protein	NA
PFLU4228	-2.890	-3.085	hypothetical protein	NA
PFLU4235	2.410	2.037	putative phosphoglycolate phosphatase	putative phosphoglycolate phosphatase
PFLU4242	4.781	4.008	hypothetical protein	NA
PFLU4256	-2.070	-2.808	hypothetical protein	hypothetical protein
PFLU4265	-2.928	-2.689	acetylornithine deacetylase	acetylornithine deacetylase
PFLU4269	-3.175	-2.069	putative phosphorous compounds metabolism-related dioxygenase	NA
PFLU4277	2.076	2.413	methionine sulfoxide reductase A	methionine sulfoxide reductase A
PFLU4295	2.871	3.952	putative heat shock protein A	NA
PFLU4306	-2.404	-2.675	putative GGDEF/GAF domain sensory box protein	NA
PFLU4321	-2.497	-2.403	putative cyanophycin synthetase	putative cyanophycin synthetase
PFLU4329	-2.716	-3.722	hypothetical protein	NA
PFLU4355	-2.844	-3.209	Xanthine/uracil permeases family protein	Xanthine/uracil permeases family protein
PFLU4366	2.592	3.062	hypothetical protein	hypothetical protein
PFLU4377	3.974	4.451	hypothetical protein	NA
PFLU4378	3.991	4.945	diaminobutyrate--2-oxoglutarate aminotransferase	diaminobutyrate--2-oxoglutarate aminotransferase
PFLU4388	2.518	3.727	putative thioesterase	putative thioesterase
PFLU4445	-2.261	-2.388	flagellar protein FliS	flagellar protein FliS
PFLU4457	-2.462	-2.352	transcriptional regulation of aroF, aroG, tyrA and aromatic amino acid transport	transcriptional regulation of aroF, aroG, tyrA and aromatic amino acid transport

PFLU4464	-4.245	-5.677	hypothetical protein	NA
PFLU4465	-2.430	-3.307	hypothetical protein	NA
PFLU4473	3.495	3.526	hypothetical protein	hypothetical protein
PFLU4478	-3.079	-2.800	putative glutathione peroxidase	putative glutathione peroxidase
PFLU4479	-3.378	-2.920	putative transporter	putative transporter
PFLU4502	4.510	4.377	hypothetical protein	NA
PFLU4508	-2.118	-2.659	hypothetical protein	NA
PFLU4517	-2.847	-3.315	hypothetical protein	NA
PFLU4533	3.335	3.713	peptidyl-prolyl cis-trans isomerase A	peptidyl-prolyl cis-trans isomerase A
PFLU4549	-2.674	-3.865	hypothetical protein	hypothetical protein
PFLU4552	-3.027	-2.258	hypothetical protein	hypothetical protein
PFLU4554	3.475	2.870	cbb3-type cytochrome c oxidase subunit II	cbb3-type cytochrome c oxidase subunit II
PFLU4555	3.310	3.086	putative cytochrome C oxidase subunit	NA
PFLU4574	-2.938	-2.722	putative acyl-CoA dehydrogenase	putative acyl-CoA dehydrogenase
PFLU4598	5.392	3.713	hypothetical protein	NA
PFLU4615	2.207	2.097	hypothetical protein	NA
PFLU4622	-2.162	-2.375	GntR family transcriptional regulator	GntR family transcriptional regulator
PFLU4634	2.561	2.510	hypothetical protein	NA
PFLU4638	2.773	3.050	hypothetical protein	hypothetical protein
PFLU4649	2.850	2.747	hypothetical protein	NA
PFLU4650	3.903	3.896	hypothetical protein	NA

PFLU4657	-2.927	-2.759	enoyl-CoA hydratase	enoyl-CoA hydratase
PFLU4658	2.047	2.270	putative acyltransferase	putative acyltransferase
PFLU4672	-2.456	-2.609	GntR family transcriptional regulator	GntR family transcriptional regulator
PFLU4679	-2.376	-2.369	AraC family transcriptional regulator	AraC family transcriptional regulator
PFLU4682	-4.340	-4.361	L-arabinose transporter permease	L-arabinose transporter permease
PFLU4683	-3.285	-3.468	L-arabinose transporter ATP-binding protein	L-arabinose transporter ATP-binding protein
PFLU4685	-2.876	-3.167	short chain dehydrogenase	short chain dehydrogenase
PFLU4686	-2.223	-2.836	putative GNAT family acetyltransferase	putative GNAT family acetyltransferase
PFLU4704	5.089	3.708	acyl carrier protein	acyl carrier protein
PFLU4708	5.977	4.813	50S ribosomal protein L32	50S ribosomal protein L32
PFLU4709	2.587	2.511	hypothetical protein	NA
PFLU4721	3.709	4.309	hypothetical protein	NA
PFLU4741	-4.106	-4.248	hypothetical protein	NA
PFLU4765	2.403	2.770	putative histidine-binding periplasmic protein	putative histidine-binding periplasmic protein
PFLU4769	3.251	2.379	hypothetical protein	NA
PFLU4769A	2.726	2.056	putative insertion element	NA
PFLU4772	-3.296	-3.665	hypothetical protein	NA
PFLU4790	3.744	5.795	hypothetical protein	NA
PFLU4797	-3.436	-4.009	hypothetical protein	hypothetical protein
PFLU4798	-3.289	-3.933	LysR family transcriptional regulator	LysR family transcriptional regulator

PFLU4811	3.560	3.343	putative gluconokinase	putative gluconokinase
PFLU4814	3.385	3.245	hypothetical protein	NA
PFLU4842	2.180	2.739	putative porin	putative porin
PFLU4848	2.516	2.065	hypothetical protein	NA
PFLU4859	2.524	2.892	hypothetical protein	NA
PFLU4865	2.278	2.047	hypothetical protein	NA
PFLU4880	-2.554	-2.646	hypothetical protein	hypothetical protein
PFLU4885	4.272	6.780	hypothetical protein	NA
PFLU4888	-3.010	-2.582	putative DNA-3-methyladenine glycosylase II	putative DNA-3-methyladenine glycosylase II
PFLU4891	2.690	3.363	arginine deiminase	arginine deiminase
PFLU4892	2.409	3.102	ornithine carbamoyltransferase	ornithine carbamoyltransferase
PFLU4896	4.805	4.687	glycine cleavage system protein H	glycine cleavage system protein H
PFLU4897	3.207	3.328	glycine dehydrogenase	glycine dehydrogenase
PFLU4919	-2.074	-2.439	hypothetical protein	NA
PFLU4939	2.218	2.535	putative transcriptional regulator	NA
PFLU4955	2.710	3.621	alpha-ketoglutarate permease	alpha-ketoglutarate permease
PFLU4956	-2.389	-2.445	hypothetical protein	NA
PFLU4965	2.586	2.930	glyceraldehyde 3-phosphate dehydrogenase 1	glyceraldehyde 3-phosphate dehydrogenase 1
PFLU4968	2.791	3.457	putative exported heme receptor protein	putative exported heme receptor protein
PFLU4980	-3.869	-5.116	hypothetical protein	NA
PFLU4987	4.159	5.001	chaperonin GroEL	chaperonin GroEL
PFLU4988	3.992	4.400	co-chaperonin GroES	co-chaperonin GroES
PFLU4992	-3.193	-3.286	putative 6-O-methylguanine DNA methyltransferase family protein	putative 6-O-methylguanine DNA methyltransferase family protein
PFLU5012	4.139	3.375	30S ribosomal protein S16	30S ribosomal protein S16

PFLU5029	5.576	4.831	hypothetical protein	NA
PFLU5038	3.657	3.724	maltoporin	maltoporin
PFLU5039	2.059	2.210	trehalose-6-phosphate hydrolase	trehalose-6-phosphate hydrolase
PFLU5040	3.428	3.079	PTS system sucrose-specific transporter subunit IIBC	PTS system sucrose-specific transporter subunit IIBC
PFLU5061	3.028	3.323	nucleoside diphosphate kinase	nucleoside diphosphate kinase
PFLU5066	-2.595	-2.737	HesB family protein	HesB family protein
PFLU5076	2.449	2.367	preprotein translocase subunit YajC	NA
PFLU5077	2.309	2.327	queuine tRNA-ribosyltransferase	queuine tRNA-ribosyltransferase
PFLU5083	2.770	2.284	putative ATP-binding protein	NA
PFLU5083A	2.690	2.316	hypothetical protein	NA
PFLU5099	2.026	2.040	hypothetical protein	NA
PFLU5102	2.686	2.094	hypothetical protein	NA
PFLU5112	-3.779	-2.201	hypothetical protein	NA
PFLU5134	2.643	3.719	hypothetical protein	NA
PFLU5135	3.575	4.452	putative aminotransferase	putative aminotransferase
PFLU5137	2.829	3.097	cytochrome C oxidase (ubiquinol oxidase) subunit IV	cytochrome C oxidase (ubiquinol oxidase) subunit IV
PFLU5139	3.356	3.438	cytochrome C oxidase (ubiquinol oxidase) subunit I	cytochrome C oxidase (ubiquinol oxidase) subunit I
PFLU5140	3.546	3.315	cytochrome C oxidase (ubiquinol oxidase) subunit II	cytochrome C oxidase (ubiquinol oxidase) subunit II
PFLU5144	-2.804	-3.055	hypothetical protein	hypothetical protein
PFLU5170	3.342	2.580	50S ribosomal protein L27	50S ribosomal protein L27
PFLU5171	2.604	3.138	50S ribosomal protein L21	50S ribosomal protein L21
PFLU5180	-2.113	-2.269	putative gluconate permease	putative gluconate permease

PFLU5192A	-2.719	-2.201	cat operon regulatory protein	cat operon regulatory protein
PFLU5196	-3.288	-2.714	anthranilate dioxygenase reductase	anthranilate dioxygenase reductase
PFLU5202	-2.426	-3.015	3-hydroxyisobutyrate dehydrogenase	3-hydroxyisobutyrate dehydrogenase
PFLU5208	2.424	2.134	hypothetical protein	hypothetical protein
PFLU5249	2.358	2.566	polynucleotide phosphorylase/polyadenylase	polynucleotide phosphorylase/polyadenylase
PFLU5256	5.415	4.204	preprotein translocase subunit SecG	preprotein translocase subunit SecG
PFLU5268	2.143	2.817	chaperone protein DnaJ	chaperone protein DnaJ
PFLU5269	3.595	4.525	molecular chaperone DnaK	molecular chaperone DnaK
PFLU5270	2.885	3.451	heat shock protein GrpE	heat shock protein GrpE
PFLU5298	2.302	2.391	hypothetical protein	NA
PFLU5325	-2.977	-2.316	putative transcription elongation factor	putative transcription elongation factor
PFLU5345	-2.211	-2.475	putative cytochrome oxidase subunit II	putative cytochrome oxidase subunit II
PFLU5348	-2.577	-2.669	putative dehydrogenase	putative dehydrogenase
PFLU5359	5.747	6.024	putative heme-binding protein	NA
PFLU5373	-2.269	-2.263	putative hydrolase	putative hydrolase
PFLU5380	-2.298	-2.008	putative AsnC family regulatory protein	putative AsnC family regulatory protein
PFLU5386	2.166	2.088	hypothetical protein	NA
PFLU5397	-2.563	-3.069	putative dehydrogenase	putative dehydrogenase
PFLU5432	-2.409	-2.355	hypothetical protein	NA
PFLU5436	-5.382	-4.651	hypothetical protein	hypothetical protein

PFLU5440	-2.210	-2.140	putative regulatory protein	putative regulatory protein
PFLU5479	2.935	3.083	hypothetical protein	NA
PFLU5483	5.141	4.223	putative ABC transporter outer membrane exported protein	putative ABC transporter outer membrane exported protein
PFLU5487	-2.251	-2.187	putative endonuclease	NA
PFLU5493	-2.016	-2.286	putative hydrolase	putative hydrolase
PFLU5501	3.697	3.221	50S ribosomal protein L17	50S ribosomal protein L17
PFLU5503	2.439	3.370	30S ribosomal protein S4	30S ribosomal protein S4
PFLU5504	2.863	3.803	30S ribosomal protein S11	30S ribosomal protein S11
PFLU5505	2.777	3.015	30S ribosomal protein S13	30S ribosomal protein S13
PFLU5506	3.593	3.335	50S ribosomal protein L36	50S ribosomal protein L36
PFLU5510	2.366	3.019	30S ribosomal protein S5	30S ribosomal protein S5
PFLU5511	2.052	2.628	50S ribosomal protein L18	50S ribosomal protein L18
PFLU5514	2.050	2.624	30S ribosomal protein S14	30S ribosomal protein S14
PFLU5515	2.147	3.082	50S ribosomal protein L5	50S ribosomal protein L5
PFLU5517	2.740	3.238	50S ribosomal protein L14	50S ribosomal protein L14
PFLU5518	2.793	3.982	30S ribosomal protein S17	30S ribosomal protein S17
PFLU5519	2.616	3.678	50S ribosomal protein L29	50S ribosomal protein L29
PFLU5521	2.418	3.120	30S ribosomal protein S3	30S ribosomal protein S3
PFLU5522	2.146	3.101	50S ribosomal protein L22	50S ribosomal protein L22
PFLU5523	2.821	3.485	30S ribosomal protein S19	30S ribosomal protein S19
PFLU5524	2.106	3.099	50S ribosomal protein L2	50S ribosomal protein L2
PFLU5528	2.457	2.779	30S ribosomal protein S10	30S ribosomal protein S10
PFLU5529	2.411	3.267	elongation factor Tu	elongation factor Tu
PFLU5531	2.176	3.122	30S ribosomal protein S7	30S ribosomal protein S7
PFLU5532	2.746	2.270	30S ribosomal protein S12	30S ribosomal protein S12
PFLU5535	3.115	3.529	50S ribosomal protein L7/L12	50S ribosomal protein L7/L12

PFLU5536	2.431	3.399	50S ribosomal protein L10	50S ribosomal protein L10
PFLU5547	-2.312	-2.478	iron-sulfur cluster insertion protein ErpA	iron-sulfur cluster insertion protein ErpA
PFLU5551	2.239	2.667	hypothetical protein	hypothetical protein
PFLU5558	-3.182	-2.918	indole-3-glycerol-phosphate synthase	indole-3-glycerol-phosphate synthase
PFLU5565	-3.215	-2.916	putative ABC transporter membrane protein	putative ABC transporter membrane protein
PFLU5566	-2.394	-2.467	putative ABC transporter membrane protein	putative ABC transporter membrane protein
PFLU5572	-2.748	-2.895	putative heat shock protein	NA
PFLU5590	4.903	3.318	hypothetical protein	NA
PFLU5609	3.400	3.921	putative dehydrogenase	putative dehydrogenase
PFLU5610	-4.769	-5.920	hypothetical protein	NA
PFLU5611	-3.962	-4.433	dithiobiotin synthetase	dithiobiotin synthetase
PFLU5617	-2.680	-2.088	putative regulatory protein	putative regulatory protein
PFLU5624	-4.706	-5.278	putative response regulator	putative response regulator
PFLU5632	-2.311	-2.252	putative ornithine cyclodeaminase	NA
PFLU5636	-4.186	-2.841	putative ABC transporter ATP-binding protein	putative ABC transporter ATP-binding protein
PFLU5678	-2.182	-2.067	AraC family transcriptional regulator	AraC family transcriptional regulator
PFLU5694	-2.672	-3.007	hypothetical protein	NA
PFLU5700	3.063	2.708	hypothetical protein	NA

PFLU5704	-2.202	-2.221	hypothetical protein	NA
PFLU5729	-3.046	-2.997	putative ABC transporter substrate-binding exported protein	NA
PFLU5730	-2.510	-2.797	putative endoribonuclease L-PSP family protein	NA
PFLU5731	-5.398	-5.365	putative D-amino acid dehydrogenase small subunit	putative D-amino acid dehydrogenase small subunit
PFLU5760	-2.760	-2.866	hypothetical protein	NA
PFLU5763	2.221	2.555	putative recemase	putative recemase
PFLU5788	-2.217	-2.170	putative dehydrogenase	putative dehydrogenase
PFLU5789	-3.254	-2.753	hypothetical protein	NA
PFLU5793	-2.344	-2.085	formamidopyrimidine-DNA glycosylase	formamidopyrimidine-DNA glycosylase
PFLU5822	-2.019	-2.363	hypothetical protein	NA
PFLU5841	-2.288	-2.610	putrescine ABC transporter permease	putrescine ABC transporter permease
PFLU5901	2.843	2.575	thioredoxin	thioredoxin
PFLU5918	-3.696	-4.014	hypothetical protein	hypothetical protein
PFLU5923	-2.076	-2.435	putative ABC transporter membrane protein	putative ABC transporter membrane protein
PFLU5926	-3.627	-3.406	hypothetical protein	NA
PFLU5939	2.249	2.304	hypothetical protein	NA
PFLU5953	-2.429	-2.551	nitrogen regulatory protein P-II 2	nitrogen regulatory protein P-II 2
PFLU5956	-3.679	-3.841	putative magnesium chelatase protein	putative magnesium chelatase protein

PFLU5959	-2.504	-3.384	multidrug efflux protein NorA	multidrug efflux protein NorA
PFLU5979	5.178	4.749	50S ribosomal protein L33	50S ribosomal protein L33
PFLU5980	4.683	3.845	50S ribosomal protein L28	50S ribosomal protein L28
PFLU5998	-2.733	-3.106	hypothetical protein	hypothetical protein
PFLU6004	-2.957	-2.665	hypothetical protein	hypothetical protein
PFLU6006	2.324	2.519	hypothetical protein	NA
PFLU6019	2.195	2.225	hypothetical protein	NA
PFLU6020	2.299	2.145	hypothetical protein	NA
PFLU6021	3.734	3.566	hypothetical protein	NA
PFLU6022	3.477	2.870	hypothetical protein	NA
PFLU6032	2.467	2.489	DNA-binding protein HU1	DNA-binding protein HU1
PFLU6041	2.380	2.072	putative transporter-like membrane protein	putative transporter-like membrane protein
PFLU6076	2.876	3.062	hypothetical protein	NA
PFLU6080	2.664	2.469	putative lipoprotein	NA
PFLU6101	-2.250	-2.518	putative cation transporter ATPase	putative cation transporter ATPase
PFLU6115	2.810	2.591	glucitol operon repressor	glucitol operon repressor
PFLU6118	2.270	2.793	F0F1 ATP synthase subunit beta	F0F1 ATP synthase subunit beta
PFLU6134	2.091	2.211	putative inner membrane protein translocase component YidC	putative inner membrane protein translocase component YidC
PFLU6136	3.454	2.229	50S ribosomal protein L34	50S ribosomal protein L34
PFLU6137	3.001	3.975	peptide synthase	peptide synthase

Supplementary Table 3. Genes with differential expression (>2 $\log_2$ FC) in *Acanthamoeba* when interacting with selected evolved strains, compared to interaction with WT SBW25.

Gene ID	Fold Change (log)		Annotation
	Ac + WS1	Ac + WFE	
ACA1_000330	2.745	3.268	Myotubularin, putative
ACA1_002500	-1.600	-2.188	hypothetical protein
ACA1_007750	-1.023	-2.244	protein kinase domain containing protein
ACA1_007760	-0.890	-2.061	PH domain containing protein
ACA1_011810	-1.968	-2.169	AT hook motif domain containing protein
ACA1_013670	2.699	2.493	copper chaperone Atox1, putative
ACA1_018120	-1.767	-2.289	hypothetical protein
ACA1_020670	1.460	3.106	hypothetical protein
ACA1_022330	-1.840	-2.014	carbamoyl phosphate synthase L chain, ATP-binding, putative
ACA1_022710	-2.025	-2.617	H(+)-transporting atpase family protein
ACA1_023180	3.221	3.265	hypothetical protein
ACA1_024960	2.693	2.695	amine oxidase, flavin containing superfamily protein
ACA1_027500	-1.428	-2.029	hypothetical protein
ACA1_031150	-2.244	-3.166	hypothetical protein
ACA1_034100	2.678	2.852	hypothetical protein
ACA1_035540	-4.674	-4.048	hypothetical protein
ACA1_035640	-2.510	-2.649	betalactamase
ACA1_036990	-1.469	-2.118	peptidase M20, putative
ACA1_038270	3.069	3.024	hypothetical protein
ACA1_038380	3.050	3.291	dlcB : dynein light chain 1, cytoplasmic, putative
ACA1_039660	-2.131	-2.403	NAD+ dependent glutamate dehydrogenase

ACA1_042000	2.843	3.035	snRNP core protein SMX5d, putative
ACA1_043170	3.010	2.976	hypothetical protein
ACA1_050630	2.754	2.374	hypothetical protein
ACA1_051820	2.946	2.999	ubiquitin family protein
ACA1_052500	-0.999	-2.028	WD domain, G-beta repeat-containing protein
ACA1_054200	-2.357	-3.020	Sadenosyl-L-homocysteine hydrolase, putative
ACA1_054290	2.837	3.078	hypothetical protein
ACA1_054340	-1.535	-2.261	ifdA : Eukaryotic initiation factor 4A, putative
ACA1_057180	-1.233	-2.170	Nucleosome assembly protein (NAP), putative
ACA1_058810	-1.615	-2.102	Inositol3-phosphate synthase
ACA1_058850	-2.255	-2.631	chaperone protein DnaK, putative
ACA1_061430	3.418	3.199	hypothetical protein
ACA1_062250	3.359	3.034	C2 and SH3 domain containing protein
ACA1_062280	3.260	2.944	hypothetical protein
ACA1_062310	3.360	3.037	HIT zinc finger protein
ACA1_062590	-1.931	-2.236	HEAT repeat domain containing protein
ACA1_063550	2.662	2.953	cytidine and deoxycytidylate deaminase zincbinding region domain containing protein
ACA1_063570	-2.914	-3.740	hypothetical protein
ACA1_064500	2.728	2.654	elongation factor SIII p15 subunit, putative
ACA1_066010	2.722	2.984	nuclear transport factor 2, putative
ACA1_066310	0.723	5.022	hypothetical protein
ACA1_069310	-1.639	-2.055	CTP synthase
ACA1_069460	-1.428	-2.136	hypothetical protein
ACA1_071090	-1.627	-2.261	ABC transporter, putative
ACA1_071570	-1.831	-2.301	hypothetical protein

ACA1_071930	3.531	3.820	hypothetical protein
ACA1_072540	3.197	3.394	Smlike protein LSm6, putative
ACA1_073360	-2.341	-3.619	RNA recognition motif domain containing protein
ACA1_074620	3.648	3.560	hypothetical protein
ACA1_074910	3.370	3.192	hypothetical protein
ACA1_076550	2.050	3.114	hypothetical protein
ACA1_076620	1.268	3.067	thymidylate synthase
ACA1_077080	2.861	3.585	guanylyl cyclase
ACA1_077150	2.703	3.276	hypothetical protein
ACA1_077170	1.979	2.949	hypothetical protein
ACA1_079570	2.991	3.026	hypothetical protein
ACA1_080570	-1.660	-2.278	nuclear transport factor 2 (ntf2) domain containing protein
ACA1_080660	-1.117	-2.168	nucleosome assembly protein family
ACA1_082860	-2.014	-2.374	peptidase S9, prolyl oligopeptidase active site region, putative
ACA1_083780	2.076	3.017	ankyrin repeat-containing protein
ACA1_086860	-1.588	-2.009	Magnesium-ATPase
ACA1_088330	2.680	1.129	hypothetical protein
ACA1_088680	2.778	1.917	oxidoreductase, 2OGFe(II) oxygenase family protein
ACA1_088880	2.743	1.898	opioid growth factor receptor (ogfr) region protein, putative
ACA1_089300	-1.133	-2.205	hypothetical protein
ACA1_091530	-1.394	-2.095	pemtA : Phospholipid methyltransferase
ACA1_091670	-1.346	-2.152	metK : ATP:L-methionine S-Adenosyltransferase
ACA1_091710	-1.146	-2.289	PAS domain Sbox domain containing protein
ACA1_091820	-2.543	-2.930	peptidase family M13, putative
ACA1_091940	-1.744	-2.125	metallopeptidase
ACA1_092600	-2.121	-2.591	NlpC/P60 domain containing protein

ACA1_093690	-1.908	-2.069	hypothetical protein
ACA1_094400	-2.013	-1.996	tetratricopeptide repeat domain containing protein
ACA1_095900	-1.607	-2.023	hypothetical protein
ACA1_099600	2.971	3.192	hypothetical protein
ACA1_100780	3.998	3.965	hypothetical protein
ACA1_101390	3.357	2.764	complex 1 protein (lyr family) protein
ACA1_101410	4.416	4.354	hypothetical protein
ACA1_101470	3.125	3.228	dynE : dynactin 4 isoform 2, putative
ACA1_101480	4.033	3.850	Prokumamolisin, activation domain containing protein
ACA1_101500	3.282	3.143	PH domain containing protein
ACA1_101520	2.696	2.522	ankyrin repeat-containing protein
ACA1_101540	2.643	2.166	ubiquitin carboxyl-terminal hydrolase
ACA1_101550	2.822	2.506	WD domain, G-beta repeat-containing protein
ACA1_101690	2.718	2.566	hypothetical protein
ACA1_103640	-1.337	-2.111	peroxidase
ACA1_104780	1.897	3.163	hypothetical protein
ACA1_108830	-1.484	-2.096	cycloartenol synthase
ACA1_112860	2.633	2.480	EF hand domain containing protein
ACA1_114580	-1.578	-2.259	hyaluronan / mrna binding family protein
ACA1_114650	2.988	3.214	hypothetical protein
ACA1_116220	-1.256	-2.027	steroid isomerase
ACA1_119150	-1.936	-2.174	Interferoninducible protein Gig2, putative
ACA1_119250	3.500	3.499	hypothetical protein
ACA1_119440	-1.550	-2.148	Serine carboxypeptidase S28
ACA1_123850	3.457	3.205	LIM domain containing protein
ACA1_127200	-1.786	-2.196	aconitate hydratase

ACA1_128510	-2.389	-2.821	chaperonin GroL, putative
ACA1_128580	-1.385	-2.016	RasGEF domain containing protein
ACA1_134130	2.239	3.095	hypothetical protein
ACA1_137930	-2.427	-1.604	hypothetical protein
ACA1_138040	-1.639	-2.006	elongation factor 1alpha, somatic form, putative
ACA1_140060	-2.327	-2.545	ATPase family associated with various cellular activities (AAA) domain containing protein
ACA1_142620	-2.214	-2.594	ATPdependent RNA helicase dbp2, putative
ACA1_143810	-1.712	-2.114	hypothetical protein
ACA1_143920	-1.581	-2.157	nicalin, putative
ACA1_144570	-1.342	-2.141	X7, putative
ACA1_144920	-1.586	-2.117	IgA Peptidase M64 protein
ACA1_152960	-1.528	-2.303	mdhB : malate dehydrogenase
ACA1_155100	2.772	2.822	Tim10/DDP family zinc finger superfamily protein
ACA1_155690	-2.798	-3.053	NADP oxidoreductase coenzyme F420-dependent protein
ACA1_159790	-2.112	-2.016	hypothetical protein
ACA1_163860	-1.748	-2.180	fthS : formate-tetrahydrofolate ligase
ACA1_164050	-1.764	-2.298	Antiquitin, putative
ACA1_164110	2.894	2.776	hypothetical protein
ACA1_164970	3.029	3.026	hypothetical protein
ACA1_167330	2.370	2.972	hypothetical protein
ACA1_169070	-1.470	-2.062	stt3 : integral membrane protein 1 isoform 5, putative
ACA1_170260	3.928	4.055	hypothetical protein
ACA1_171100	-2.021	-2.798	VATPase subunit A, putative
ACA1_174000	2.828	2.854	hypothetical protein
ACA1_175060	-1.688	-2.078	vatM : vacuolar proton ATPase, putative

ACA1_175690	4.225	3.422	hypothetical protein
ACA1_181700	1.393	3.034	hypothetical protein
ACA1_181920	2.723	2.317	hypothetical protein
ACA1_183270	-1.048	-2.099	tyrosine protein kinase, putative
ACA1_183620	-1.567	-2.241	citrate synthase, mitochondrial, putative
ACA1_183930	2.750	2.596	signal recognition particle 9 kDa protein
ACA1_184650	-1.916	-2.139	hypothetical protein
ACA1_185300	-2.979	-3.319	hypothetical protein
ACA1_185330	4.150	4.636	hypothetical protein
ACA1_189820	2.587	2.910	protein bcp1, putative
ACA1_195290	-1.380	-2.083	hypothetical protein
ACA1_199970	-2.001	-2.467	glycoside hydrolase family protein
ACA1_199990	-1.459	-2.326	guanine nucleotide-binding protein beta subunit, putative
ACA1_200430	-1.635	-2.133	elongation factor 1-alpha, putative
ACA1_201100	2.219	3.155	hypothetical protein
ACA1_201140	2.817	3.739	hypothetical protein
ACA1_201190	2.023	2.967	endonuclease/exonuclease/phosphatase family protein
ACA1_201370	-1.864	-2.190	allantoicase repeat domain containing protein
ACA1_206510	-1.519	-2.188	hypothetical protein
ACA1_207970	-1.872	-2.248	Myb-like DNA-binding domain containing protein
ACA1_208090	-1.716	-2.160	DnaJ domain containing protein
ACA1_214330	-1.662	-2.120	hypothetical protein
ACA1_218640	-1.507	-2.221	nucleoside diphosphate kinase 1, putative
ACA1_220140	-2.280	-3.033	eukaryotic translation elongation factor 2, putative
ACA1_220200	-1.557	-2.120	hypothetical protein

ACA1_225890	-2.219	-2.254	nramp1 : solute carrier family 11 member 1 [Source: Projected from Dictyostelium discoideum (DDB_G0276973)]
ACA1_227830	-1.714	-2.278	PhoPQactivated pathogenicity-related protein-like protein, putative
ACA1_230570	2.257	2.979	hypothetical protein
ACA1_231400	3.177	3.675	hypothetical protein
ACA1_231410	2.445	3.543	pol polyprotein
ACA1_234620	-1.547	-2.099	polyadenylate-binding protein family protein
ACA1_237560	2.787	2.924	R3H domain containing protein
ACA1_239920	2.671	2.797	hypothetical protein
ACA1_240370	1.932	2.992	hypothetical protein
ACA1_244340	2.025	2.964	hypothetical protein
ACA1_245470	3.231	3.094	4F5 protein family
ACA1_245660	-1.362	-2.264	hypothetical protein
ACA1_247220	-1.315	-2.056	isoprenylcysteine carboxyl methyltransferase (icmt) family protein
ACA1_247490	-1.756	-2.075	hypothetical protein
ACA1_248210	-1.676	-2.172	xylosidase
ACA1_248540	2.829	2.935	dynein light chain tctextype, putative
ACA1_249280	2.750	3.067	hypothetical protein
ACA1_251170	0.355	-2.043	serine/threonineprotein phosphatase
ACA1_252500	2.663	2.993	commd6 : COMM domain containing protein 6, putative
ACA1_253340	3.309	4.090	hypothetical protein
ACA1_253460	3.978	3.647	protein kinase
ACA1_257300	2.970	3.021	Nicotinamide-nucleotide adenylyltransferase
ACA1_257430	2.795	2.729	pyridoxamine 5'phosphate oxidase family superfamily protein
ACA1_264110	-1.231	-2.004	ribosomal protein L3, putative
ACA1_266040	0.825	2.980	hypothetical protein

ACA1_266970	3.320	3.272	DnaK family superfamily protein
ACA1_267070	3.303	2.946	hypothetical protein
ACA1_267220	3.109	3.208	hypothetical protein
ACA1_270690	-1.635	-2.183	lysine-tRNA ligase
ACA1_271380	-1.366	-2.058	ribosomal protein L10, putative
ACA1_271560	-1.763	-2.181	hypothetical protein
ACA1_277790	-1.360	-2.016	protease, serine, 16 (thymus), putative
ACA1_277830	-1.579	-2.069	LIM domain containing protein
ACA1_278780	-1.814	-2.188	hypothetical protein
ACA1_280720	2.667	2.571	calmodulin, putative
ACA1_282890	-1.501	-2.115	prmt1 : arginine nmethyltransferase, putative
ACA1_283480	4.162	4.110	LIM domain containing protein
ACA1_286170	-1.700	-2.067	alanyl dipeptidyl peptidase
ACA1_287820	-1.581	-2.219	transketolase
ACA1_289060	-1.357	-2.018	hypothetical protein
ACA1_295770	2.592	2.984	Protein yippeelike 1, putative
ACA1_295880	-1.799	-2.224	NAD-dependent malic enzyme, putative
ACA1_296040	2.459	3.128	hypothetical protein
ACA1_296070	-0.625	-2.129	hypothetical protein
ACA1_300720	-1.911	-2.032	WD repeat domain 43 isoform 5, putative
ACA1_312480	-1.594	-2.001	hypothetical protein
ACA1_313730	-1.581	-2.202	glycosyltransferase, group 2 domain containing protein
ACA1_315750	3.333	3.506	hypothetical protein
ACA1_318090	-1.812	-2.285	glycosyl hydrolase family 20, catalytic domain containing protein
ACA1_319220	-1.847	-2.262	cellular apoptosis susceptibility protein
ACA1_320100	2.632	2.017	hypothetical protein

ACA1_320310	1.874	2.967	hypothetical protein
ACA1_320830	-1.607	-2.136	hypothetical protein
ACA1_321730	-1.537	-2.047	gabT : 4aminobutyrate aminotransferase
ACA1_322580	2.629	2.967	calmodulin, putative
ACA1_323450	-1.464	-2.130	hypothetical protein
ACA1_324680	2.378	3.616	hypothetical protein
ACA1_324790	1.801	3.443	DNA repair family protein
ACA1_324810	3.583	4.397	hypothetical protein
ACA1_324840	2.227	3.049	hypothetical protein
ACA1_324900	2.985	3.411	hypothetical protein
ACA1_325260	-1.640	-2.024	peptidylprolyl cis-trans isomerase, FKBP-type domain containing protein
ACA1_327940	2.725	2.933	hypothetical protein
ACA1_330530	3.275	3.782	CsbD family protein
ACA1_330770	3.250	3.759	CsbD family protein
ACA1_333710	-2.355	-2.770	hypothetical protein
ACA1_336910	2.940	3.679	actin subfamily protein
ACA1_338010	2.486	2.991	raslike protein
ACA1_353190	2.652	1.891	cytochrome p450 superfamily protein
ACA1_353220	3.064	2.320	hypothetical protein
ACA1_356170	-1.295	-2.245	hypothetical protein
ACA1_356420	-1.519	-2.048	hypothetical protein
ACA1_356920	2.913	3.300	hydrolase, NUDIX domain containing protein
ACA1_357160	3.367	3.722	actin subfamily protein
ACA1_357480	3.338	3.742	F-box domain containing protein
ACA1_357610	2.822	3.192	RasGEF domain containing protein

ACA1_358070	2.790	2.973	hypothetical protein
ACA1_359750	-1.676	-2.167	succinyl coenzyme A synthetase alpha subunit
ACA1_360490	3.935	6.838	hypothetical protein
ACA1_360910	-2.322	-3.223	hypothetical protein
ACA1_360920	-2.071	-2.479	La domain containing protein
ACA1_367310	-1.782	-2.205	zinc knuckle domain containing protein
ACA1_367940	-2.042	-2.543	atp5b : ATP synthase, putative
ACA1_369110	2.641	2.499	small nuclear ribonucleoprotein G, putative
ACA1_369520	-1.318	-2.077	ribosomal protein L6e, putative
ACA1_370160	2.987	2.960	hypothetical protein
ACA1_371310	-1.298	-2.233	3,4dihydroxy-2-butanone-4-phosphate synthase
ACA1_373620	3.531	3.460	amino acidbinding ACT domain containing protein
ACA1_373630	3.573	3.048	RNA recognition motif domain containing protein
ACA1_373680	3.081	2.759	hypothetical protein
ACA1_373690	2.843	2.877	ADPribosylglycohydrolase superfamily protein
ACA1_373720	3.181	3.305	exonuclease
ACA1_373760	3.284	3.424	bifunctional GlmU protein
ACA1_373780	3.505	3.641	hypothetical protein
ACA1_376780	2.767	3.208	hypothetical protein
ACA1_379630	0.707	3.048	Fbox domain containing protein
ACA1_380340	0.470	3.328	leucine rich repeat-containing protein
ACA1_381510	-2.021	-2.003	NADH dehydrogenase, putative
ACA1_382630	-1.863	-2.144	LBP / BPI / CETP family, Cterminal domain containing protein
ACA1_384020	2.856	2.968	hypothetical protein
ACA1_384080	2.688	2.085	PLAC8 family protein
ACA1_385240	2.865	3.158	hypothetical protein

ACA1_385410	-1.729	-2.078	transketolase, putative
ACA1_390170	-1.859	-2.275	laminin egflike (domains iii and v) domain containing protein
ACA1_393040	2.607	3.052	hypothetical protein
ACA1_396930	-1.426	-2.165	hypothetical protein
ACA1_400260	2.730	3.772	ranlike small GTPase

Chapter 3 Supplementary

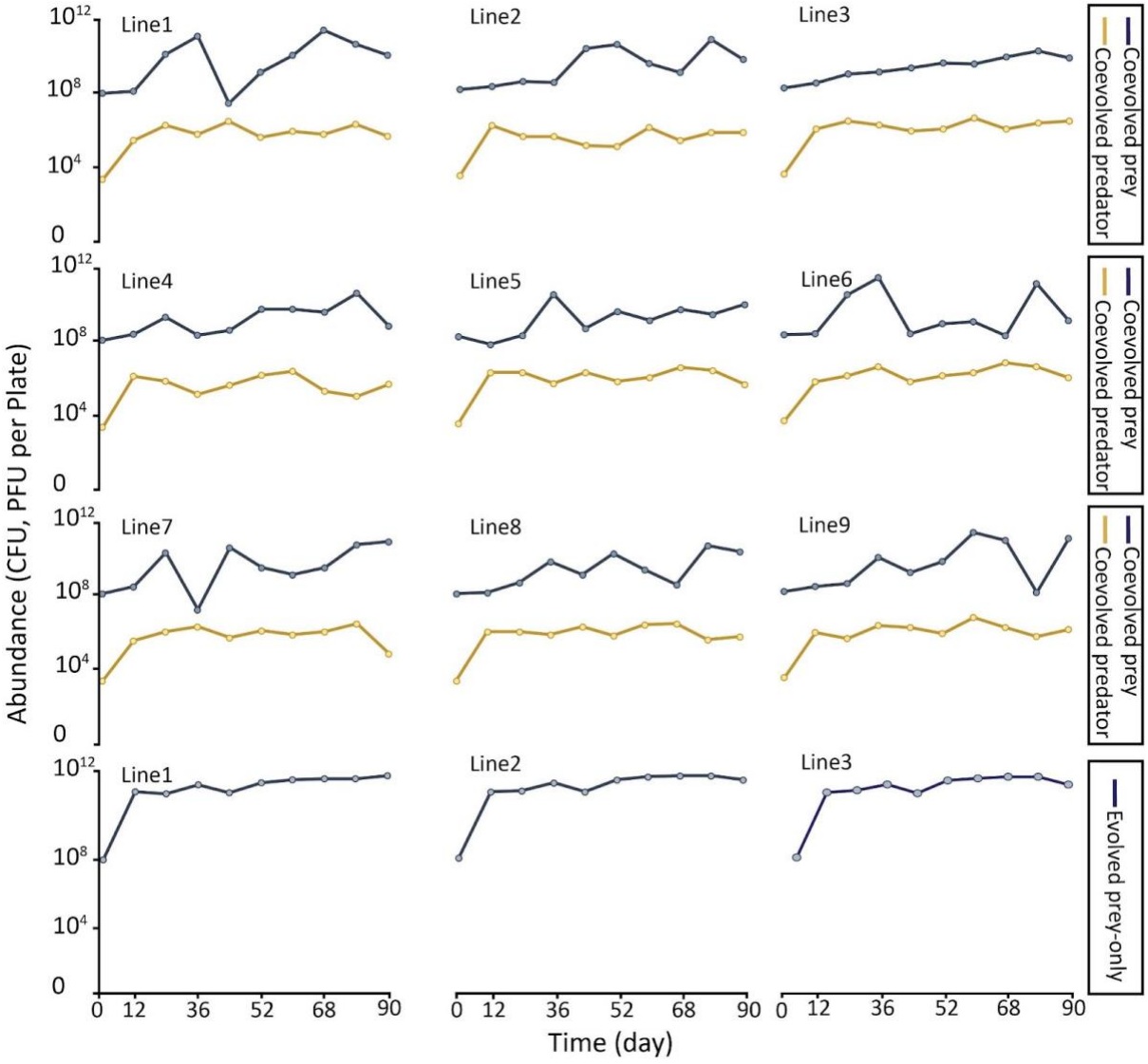

Supplementary Figure 1. Estimates of the abundance of population size at every second transfer for each organism in nine coevolution and three evolved prey-only lines over 90-days of evolution. (CFU, PFU per experimental plate).

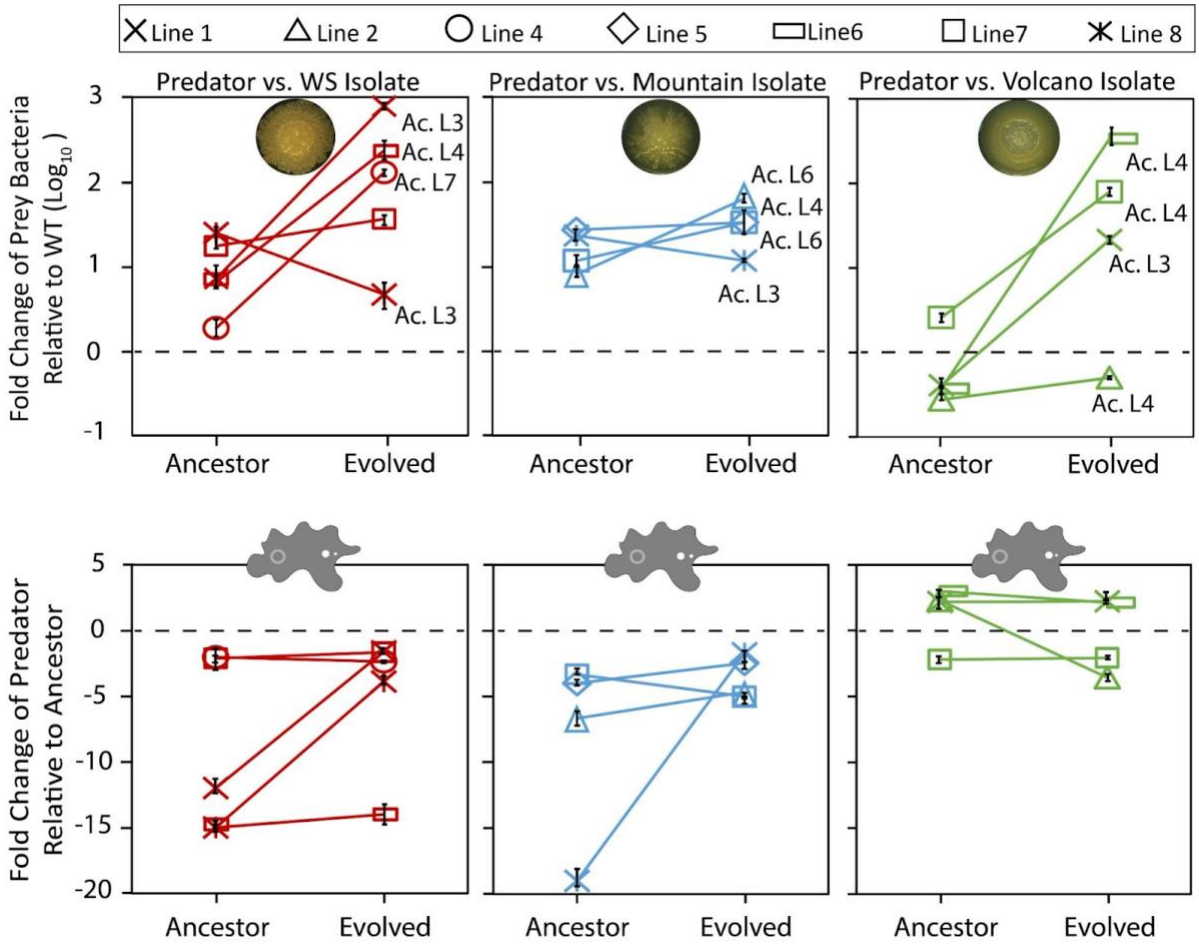

Supplementary Figure 2. Performance test assay results; A) showing the fold change in the number of the bacterial population (CFU) after four days of predation by ancestral and evolved *Acanthamoebae* sp. relative to WT prey while growing with ancestral predators (dashed lines). B) Fold change in the number of ancestral and evolved *Acanthamoeba* cells (PFU) while predating upon evolved isolates relative to the ancestral predator with WT prey (dashed lines). Error bars represent standard division (n=6).

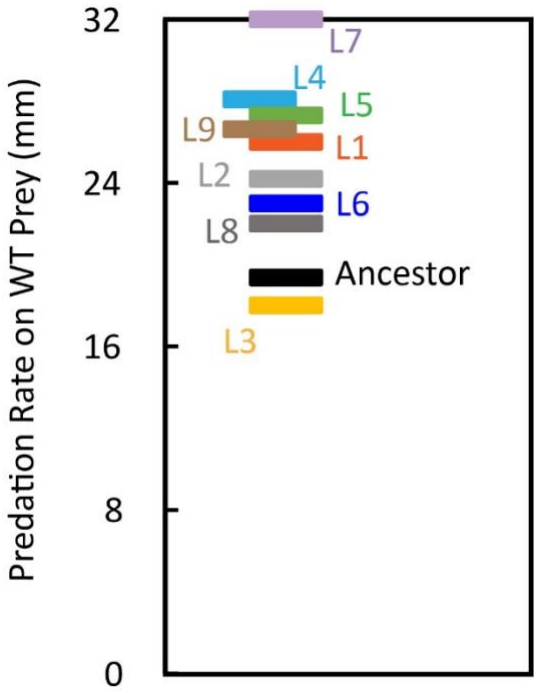

Supplementary Figure 3. Line test assay; The predation rate of each of the predator types while consuming WT prey from line test assay in four days. With the exception of CE L3-predator, all the predator types have shown higher predation rate on WT prey (n=6).

Supplementary Table 1. All colony morphologies tested in this study against their coevolved, ancestor or evolved predators from other lines. There is data lacking for some of the colonies and this is because they were not involved in both line and performance test assays. NA means that the experiment does Not Apply.

	Line Test Assay (Relative Prey Fitness)		Performance Test (Fold Change Relative to WT Bacteria)		
Strains	Bacteria vs. CoEv. Ac.	Bacteria vs. Ev. Ac.	Bacteria vs. Anc. Ac.	Bacteria vs. CoEv .Ac.	Bacteria vs. Ev. Ac.
WT	NA	0.5 (L2)	NA	NA	NA
		0.57 (L6)			
		0.43 (L7)			
		0.54 (L9)			
LWT-L9	0.42	0.2 (L2)	1.8	-9	127 (L6)
		0.24 (L6)			
		0.21 (L7)			
VOL-L1	ND	ND	-2.5	170	22 (L3)

VOL-L2	0.21	0.21 (L6)	-3.7	3	-2 (L4)
		0.12 (L7)			
		0.28 (L9)			
VOL-L6	0.07	0.15 (L2)	-3	45	337 (L4)
		0.0 (L7)			
		0.2(L9)			
VOL-L7	0.04	0.12 (L2)	2.6	34	80 (L4)
		0.17 (L6)			
		0.02(L9)			
Mnt-L2	0.58	0.65 (L6)	8	3.5	63 (L6)
		0.52 (L7)			
		0.7 (L9)			
Mnt-L5	ND	ND	27	1.5	20
Mnt-L6	0.77	0.69 (L2)			
		0.63 (L7)			
		0.7 (L9)			
Mnt-L7	0.59	0.55 (L2)	12	27	33 (L4)
		0.8 (L6)			
		0.75 (L7)			
Mnt-L8	ND	ND	23	8.4	12 (L3)
Mnt-L9	0.78	0.68 (L2)			
		0.79 (L6)			
		0.72 (L7)			
WS-L1	ND	ND	7	35	782 (L4)
WS-L2	0.87	0.91(L6)	8	5	5.5 (L4)
		0.88 (L7)			
		0.98 (L9)			

WS-L4	ND	ND	1.9	26	129 (L7)
WS-L6	0.98	0.98 (L2)	6.5	3.9	233 (L4)
		0.97 (L7)			
		0.97 (L9)			
WS-L7	0.9	0.9 (L2)	17	10	36 (L4)
		0.94 (L6)			
		0.92 (L9)			
WS-L8	ND	ND	25	3	4.6 (L4)

Chapter 4 Supplementary

DRC 16

MASSEY UNIVERSITY
GRADUATE RESEARCH SCHOOL

STATEMENT OF CONTRIBUTION
DOCTORATE WITH PUBLICATIONS/MANUSCRIPTS

We, the candidate and the candidate's Primary Supervisor, certify that all co-authors have consented to their work being included in the thesis and they have accepted the candidate's contribution as indicated below in the *Statement of Originality*.

Name of candidate:	Farhad Golzar
Name/title of Primary Supervisor:	Dr Heather Hendrickson
Name of Research Output and full reference:	
In which Chapter is the Manuscript /Published work:	Chapters 2 & 4
Please indicate:	
• The percentage of the manuscript/Published Work that was contributed by the candidate:	90%
and	
• Describe the contribution that the candidate has made to the Manuscript/Published Work:	
Chapter 2: All work with the exception of the biofilm strength assay. Capther 4: All work with the exception of RNA sequencing.	
For manuscripts intended for publication please indicate target journal:	
Munuscript 1: Plos bio - Manuscript 2: ISME - Manuscript 3: MBE	
Candidate's Signature:	Golzar, Farhad Digitally signed by Golzar, Farhad Date: 2022.03.03 16:29:28 +13'00'
Date:	03/03/2022
Primary Supervisor's Signature:	Heather Hendrickson Digitally signed by Heather Hendrickson Date: 2022.03.04 08:44:48 +13'00'
Date:	04/03/2022

(This form should appear at the end of each thesis chapter/section/appendix submitted as a manuscript/ publication or collected as an appendix at the end of the thesis)

GRS Version 4– January 2019

Supplementary Table 1. Population sequencing results of coevolved (CE) and evolved prey-only (PO) at four different time points from 90-day experiment.

Line/PFLU	ORF nucleotide Change/position	Day0	Day16	Day40	Day64	Day90
L1-3677	1,199 C>G	0	0.2	0	0	0
L1-3750	1,226 G>T	0	0.22	0	0	0
L1-4037	871 C>G	0	0.2	0.13	0.08	0.2
L1-4287	495, 499, 491 A>C	0	0.3	0	0.28	0.31
L1-0883	525 T>C	0	0.12	0.2	0	0.07
L1-2181	T>C	0	0	0.27	0	0
L1-0882	1,092 T>G	0	0	0	0.76	0.51
L1-4974	∆A643-A1065	0	0	0	0.97	0.65
L1-4975	∆A1-A1098	0	0	0	0.97	0.65
L1-0300	(-)103 A>G	0	0	0	0	0.12
L1-1537	581 C>T	0	0	0	0.11	0.42
L1-1224	822 G>T	0	0	0	0	0.25
L1-3978	1,778 G>C	0	0	0	0	0.21
L1-4829	∆D1-G330	0	0	0	0	0.41
L1-4830	∆G350-T1689	0	0	0	0	0.23
L2-0924	789 C>T	0	0	0	0	0.09
L2-1795	260 C>*	0	0	0	0	0.1
L2-4443	619 G>C	0	0	0	0	0.15
L2-1373	89 T>G	0	0.2	0.1	0.07	0.06
L2-3091	841 A>C	0	0.22	0.13	0.13	0.08

L2-4287	495, 499, 491 A>C	0	0.32	0.32	0.32	0.3
L2-0458	T>G	0	0.13	0.2	0.13	0.05
L2-1224	151 -CTGATGGACCTGATC	0	0	0.78	0.12	0.35
L2-2143	304 T>A	0	0.15	0.21	0.07	0.1
L2-3978	1,777 G>C	0	0.08	0.12	0.22	0.23
L2-4201	1,216 A -> T	0	0	0	0.2	0
L2-4744	154 T>C	0	0	0	0	0.23
L2-4974	∆A643-A1065	0	0	0	0	0.23
L2-4975	∆A1-A1098	0	0	0	0	0.23
L2-4829	275 G>C	0	0	0	0	0.07
L3-0458	1,304 A>C	0	0.2	0.17	0.11	0.08
L3-3850	80 T>C	0	0.23	0.13	0.14	0.15
L3-4287	503, 495, 499, 491 A>C	0	0.25	0.3	0.28	0.32
L3-1224	151 -CTGATGGACCTGATC	0	0	0.46	0.3	0.27
L3-2711	602 G>A	0	0	0.2	0.09	0
L3-3091	841 A>C	0	0.15	0.21	0.13	0.1
L3-3517	752A -> G - 749 C -> G	0	0	0.21	0	0
L3-3521	244T -> C	0	0	0.2	0	0
L3-3615	151 T -> G	0	0	0.2	0	0
L3-3978	1,777 GCGGCCTGTGCGGCATTG> CCGTATCATTAAAAAATG	0	0.11	0.23	0.1	0.2
L3-1231	111 T>G	0	0	0	0.46	0
L3-1849	993 T>G	0	0	0	0.58	0

L3-3750	1,256 CGCGGCCAGGC>CT	0	0.1	0	0.21	0.1
L3-3879	2,254 T -> C	0	0	0	0.21	0
L3-4974	∆A643-A1065	0	0	0	0.24	0.39
L3-4975	∆A1-A1098	0	0	0	0.24	0.39
L3-1130	514 C>T	0	0	0	0	0.28
L3-1588	595 A -> G	0	0	0	0	0.2
L3-4038	1,058T -> C	0	0	0	0	0.25
L3-0924	790 C -> T	0	0	0	0	0.26
L3-0923	139 TGGGGGCGA>TGGGGGGCGA	0	0	0	0	0.17
L3-1164	241 +CTTGACCAG	0	0	0	0	0.19
L3-1585	625 C>T	0	0	0	0	0.14
L3-3422	379 G>A	0	0	0	0	0.14
L3-4395	945 G>A	0	0	0	0	0.08
L3-4712	280 ACCCCCTCG>ACCCCCCTCG	0	0	0	0	0.13
L4-2744	716 G>T	0	0.22	0	0	0.05
L4-4287	502 A>C	0	0.21	0.28	0.32	0.06
L4-1224	151 -CTGATGGACCTGATC	0	0	0.5	0.4	0.6
L4-1849	122 T>G	0	0	0.06	0	0
L4-0924	789 C>T	0	0	0	0	0.16
L4-4477	194 CCAGCAAATC>CC	0	0	0	0	0.1
L4-3978	1,787 G -> T - 1,787GC -> TA	0	0	0.15	0.22	0

L4-2181	2,181 C>T	0	0	0	0.72	0
L4-4974	∆A643-A1065	0	0	0	0	0.24
L4-4975	∆A1-A1098	0	0	0	0	0.23
L5-4287	490 AG -> CC	0	0.35	0.29	0	0
L5-1224	151 -CTGATGGACCTGATC	0	0	0.4	0.17	0.11
L5-4745	1,000 AT -> CC / CGAACAGCCCGAT -> TACGGGAAGTTCC	0	0	0.27	0.07	0
L5-4974	∆A643-A1065	0	0	0.2	0.42	0.50
L5-4975	∆A1-A1098	0	0	0.2	0.42	0.50
L5-5507	121 G>A	0	0	0.62	0.2	0.17
L5-5685	560 A -> C	0	0	0.2	0.09	0
L5-1849	122 TGGGGGGGGCGG>TGGGGGGGCGG	0	0	0	0.54	0.74
L5-4037	871C -> G	0	0.13	0.15	0.23	0.11
L5-4287	495, 499, 491 A>C	0	0	0	0.31	0.25
L5-3978	1,778 G -> C	0	0	0	0	0.2
L5-4201	1,258 A -> T	0	0	0	0	0.21
L6-3517	749 C>G	0	0.2	0	0	0
L6-3677	1,186 C>T	0	0.21	0	0	0
L6-3978	1,778 G>C-T>C- G>T	0	0.22	0	0	0.23
L6-4287	495, 499, 491 A>C	0	0.29	0.31	0.37	0.32
L6-4974	∆A643-A1065	0	0.92	0.91	0.96	0.87
L6-4975	∆A1-A1098	0	0.92	0.91	0.96	0.87
L6-4420	1,826 +GGTGA	0	0	0.32	0	0

L6-4201	1,239T -> C	0	0	0	0.21	0
L6-4829	∆D1-G330	0	0	0	0.38	0.2
L6-4830	∆G350-T1689	0	0	0	0.26	0.2
L6-5897	306 CC>GA	0	0.08	0	0.21	0
L6-1224	822 G>T	0	0	0	0	0.13
L7-3091	779 A>C	0	0.24	0	0	0
L7-3521	252 A>T	0	0.22	0	0	0
L7-4287	502 ACCCACCCG>CCCCCCCCC	0	0.27	0.27	0.27	0.34
L7-3850	81 T -> C	0	0	0.24	0	0
L7-4829	∆D1-G330	0	0	0.25	0.75	0.26
L7-4830	∆G350-T1689	0	0	0	0.26	0.26
L7-4974	∆A643-A1065	0	0	0.98	0.92	0.95
L7-4975	∆A1-A1098	0	0	0.98	0.96	0.95
L7-1849	68 A>T	0	0	0	0	0.21
L7-3901	1,022 C -> T	0	0	0	0	0.2
L7-4201	1,216 A -> T	0	0	0	0	0.22
L7-4436	523 G>A	0	0	0.06	0.08	0.55
L7-4712	280 A>C	0	0	0	0.17	0.7
L7-4712	76 TCGACGATCC>TC	0	0	0	0.1	0.1
L7-5685	ACCCTGAAACTGGC>AC	0	0.1	0.1	0.06	0.21
L7-5034	2,812 G>A	0	0	0	0	0.07
L7-5210	G188A	0	0	0	0	0.03
L8-2711	602 T>C	0	0.2	0	0	0

L8-2744	699 A>C	0	0.21	0.06	0.06	0.07
L8-3750	1,211 G>T	0	0.21	0	0	0
L8-4287	495, 499, 491 A>C	0	0.3	0.27	0.27	0.32
L8-4936	1,776 A>T	0	0.21	0.17	0.09	0.08
L8-3978	1,777 G>C	0	0	0.2	0.21	0.15
L8-4974	∆A643-A1065	0	0	1.0	0.94	1.0
L8-4975	∆A1-A1098	0	0	1.0	0.94	1.0
L8-4976	903 GCCCCCCCCGAT>GCCCCCCCCCGAT	0	0	0	0	0.21
L8-3850	122T -> G	0	0	0	0.24	0
L8-5190	661 T>C	0	0	0.08	0.68	0
L8-1849	68 A>T	0	0	0	0	0.3
L8-4436	523 G>A	0	0	0	0	0.5
L8-4712	280 A>C	0	0	0	0	0.54
L8-4712	76 TCGACGATCC>TC	0	0	0	0	0.21
L8-4829	275 G>C	0	0	0	0	0.26
L8-5034	2,812 G>A	0	0	0	0	0.29
L8-5210	G188-A	0	0	0	0	0.04
L9-3521	226 C>T	0	0.22	0	0	0
L9-3615	155 T>C	0	0.22	0	0	0
L9-3677	1,196 GA>GC	0	0.22	0	0	0
L9-3978	1,777 G>C	0	0.22	0.21	0.13	0.2
L9-4287	495, 499, 491 A>C	0	0.3	0.27	0.21	0.32
L9-1849	67 A>T	0	0	0.54	1.0	0.97

L9-4712	280 A>C	0	0	0.34	1.0	0.99
L9-4974	∆A643-A1065	0	0	0.95	0.98	1.0
L9-4975	∆A1-A1098	0	0	0.95	0.98	1.0
L9-4443	928 A>G	0	0	0	0.64	0.39
L9-0882	640T -> G	0	0	0	0	0.54
L9-4037	880 C -> G	0	0	0	0	0.21
L9-5897	317T -> C	0	0	0	0	0.25
L9-5927	899 A -> G	0	0	0	0	0.21
Cont1-0458	1,304 A -> C	0	0.21	0	0	0
Cont1-4287	499 A -> C	0	0.3	0	0	0.27
Cont1-3978	1,784 T -> C	0	0	0.22	0	0
Cont1-2711	602 T -> C	0	0	0	0	0.2
Cont1-4936	1,766 T -> C	0	0	0	0	0.21
Cont2-3615	161 A -> C	0	0.23	0	0	0
Cont2-3879	2,254 T -> C	0	0.2	0	0	0
Cont2-4037	890 A -> G	0	0.2	0	0	0
Cont2-4287	479 A -> C	0	0.26	0.29	0	0
Cont2-4287	499 T -> G	0	0	0	0	0.27
Cont2-3091	779 T -> G	0	0	0	0	0.16
Cont3-3677	1,193 T -> G	0	0.22	0	0	0
Cont3-3850	81T -> C	0	0.21	0	0.21	0

Cont3-3879	2,254 T -> C	0	0.2	0	0	0
Cont3-4287	499 A -> C	0	0.42	0.28	0.30	0
Cont3-4201	1,258 T -> A	0	0	0	0	0.22
Cont3-5249	1,171 T -> G	0	0	0	0	0.2
Cont3-5927	899 A -> G	0	0	0	0.21	0

Supplementary Table 2. The locations and details of mutations observed in this study by whole-genome sequencing of 29 colony morphotypes from the end of the experiment.

Strains	Gene name	PFLU	ORF AA Change	ORF Nucleotide Change
L1-LWT	rpoN	0882	T365P	T1093G
	fadD1	4829	ΔM1-T110	ΔD1-G330
	fadD2	4830	ΔA117-563	ΔG350-T1689
	hypothetical protein	4974	ΔQ215-355	ΔA643-A1065
	hypothetical protein	4975	ΔA1-M366	ΔA1-A1098
L1-Vol	(LuxR) malT	0925	V892G	T2675G
	fadD1	4829	ΔM1-T110	D1-G330
	fadD2	4830	ΔA117-563	ΔG350-T1689
L1-WS	wspF	1224	G275C	G823T
L2-Mnt	putative exported protein	0924	R264C	C790T
	hypothetical protein	4974	ΔQ215-355	ΔA643-A1065
	hypothetical protein	4975	ΔA1-M366	ΔA1-A1098

L2-Vol	flrA, fleQ, flaK	4443	P207R	C620G
	fadD1	4829	ΔM1-T110	ΔD1-G330
	fadD2	4830	ΔA117-563	ΔG350-T1689
	hypothetical protein	4974	ΔQ215-355	ΔA643-A1065
	hypothetical protein	4975	ΔA1-M366	ΔA1-A1098
L2-WS	wspF	1224	ΔLMDLI 51-55	Δ151-165
	amrZ	4744	R20C	C58T
L3-LWT	hypothetical protein	4974	ΔQ215-355	ΔA643-A1065
	hypothetical protein	4975	ΔA1-M366	ΔA1-A1098
L3-Mnt	mutS	1164	+LVK81-83	+241-249
	hypothetical protein	4974	Δ Q215-355	ΔA643-A1065
	hypothetical protein	4975	ΔA1-M366	ΔA1-A1098
	awsR	5210	S240P	A718G
	pilE	0776	T48I	T143C
	phoD	0807	P26S	T76C
	motY	1155	R25C	C73T
	nagZ	1562	A173V	C518T
	talB	1585	G209D	C626T
	phage major capsid pr.	1588	F199L	A595G
	Putative amidase	1992	V152A	A476G
	gsmt	2095	Y234C	A701G

	Iron receptor protein	2593	A74T	C220T
	livM	3422	R127H	G380A
	exuT	3436	P459S	G1375A
	fadE	3529	G231S	C691T
	etk-wzc	3677	Y735C	T2204C
	atuD	4395	A316T	G946A
	flgA	4734	D130N	G388A
	leuA	5050	G347S	G1039A
	ispB	5172	A206T	G616A
	trxA	5901	K98E	T292C
L3-WS	wspF	1224	ΔLMDLI 51-55	Δ151-165
L3-WS1	wspE	1225	YH132-LV133	ATCA395-TGGT398
	metZ	4182	A103T	C307T
	hypothetical protein	1231	F38V	T112G
L4-LWT	OmpR family	1849	T331P	T991G
	hypothetical protein	4974	ΔQ215-355	ΔA643-A1065
	hypothetical protein	4975	ΔA1-M366	ΔA1-A1098
L4-Mnt	putative exported protein	0924	R264C	C790T
	fadL	4477	Frameshift deletion ΔQ66	Δ198-205 (-GCAAATCA)
	hypothetical protein	4974	ΔQ215-355	ΔA643-A1065
	hypothetical protein	4975	ΔA1-M366	ΔA1-A1098

L4-WS1	wspF	1224	ΔLMDLI 51-55	Δ151-165
	wspC	1221	M250R	T749G
L4-WS	wspF	1224	ΔLMDLI 51-55	Δ151-165
	malT	0925	V892G	T2,675G
L5-Mnt[1]	OmpR family	1849	Frameshift deletion P38	G112
	hypothetical protein	4974	ΔQ215-355	ΔA643-A1065
	hypothetical protein	4975	ΔA1-M366	ΔA1-A1098
L5-Mnt[2]	hypothetical protein	4974	Q215-355	A643-A1065
	hypothetical protein	4975	ΔA1-M366	ΔA1-A1098
L5-WS1	wspF	1224	ΔLMDLI 51-55	Δ151-165
	leucine rich-repeat protein	4319	T490I	G1469A
	secY	5507	P41L	G122A
	amrZ	4744	ΔM1-109	Δ1-327
	mgtE	4745	ΔL343-481	Δ1029-1443
L6-Mnt	hypothetical protein	4974	ΔQ215-355	A643-A1065
	hypothetical protein	4975	ΔA1-M366	ΔA1-A1098
L6-Vol	fadD1	4829	ΔM1-105N	ΔD1-317T
	fadD2	4830	ΔN111-563	ΔT316-1689T
	hypothetical protein	4974	ΔQ215-355	A643-A1065
	Hypothetical Protein	4975	ΔA1-M366	A1-A1098
L6-WS	wspC	1221	Frameshift deletion F8L	T24

	wspF	1224	G275C	G823T
L7-Mnt	OmpR family	1849	L22Q	A65T
	Gph	4712	V94G	A281C
	hypothetical protein	4974	ΔQ215-355	ΔA643-A1065
	hypothetical protein	4975	ΔA1-M366	ΔA1-A1098
	PFAS, purL	5034	A938V	G2813A
L7-Vol	fadD1	4829	Q197 Stop codon	GTT589ATT
	Gph	4712	V94G	A281C
	hypothetical protein	4974	ΔQ215-355	ΔA643-A1065
	hypothetical protein	4975	ΔA1-M366	ΔA1-A1098
	fliI	4436	A175V	G524A
L7-WS	awsR	5210	A63V	G188A
	Gph	4712	Frameshift deletion GRI 22-25	65-74 (-GATCCGAC)
	hypothetical protein	4974	ΔQ215-355	A643-A1065
	hypothetical protein	4975	ΔA1-M366	A1-A1098
	fliI	4436	A175V	G524A
L8-SWS	awsR	5210	A63V	G188A
	Gph	4712	Frameshift deletion GRI 22-25	65-74 (-GATCCGAC)
	hypothetical protein	4974	ΔQ215-355	A643-A1065
	hypothetical protein	4975	ΔA1-M366	ΔA1-A1098
	fliI	4436	A175V	G524A

	dppD	0820	G60S	C178T
L8-LWS	EIF1, SUI1	0625	I99V	A295G
	fliI	4436	A175V	G524A
	Gph	4712	Frameshift deletion GRI 22-25	65-74 (-GATCCGAC)
	hypothetical protein	4974	ΔQ215-355	ΔA643-A1065
	hypothetical protein	4975	ΔA1-M366	ΔA1-A1098
L8-Mnt	OmpR family, sensor kinase	1849	L22Q	A65T
	Gph	4712	V94G	A281C
	hypothetical protein	4974	ΔQ215-355	ΔA643-A1065
	hypothetical protein	4975	ΔA1-M366	ΔA1-A1098
	acrA, mexA, adeI, smeD	4976	D305R	913 (+C)
	PFAS, purL	5034	A938V	G2813A
L8-Vol	fadD1	4829	Q197 Stop codon	GTT589ATT
	Gph	4712	V94G	A281C
	fliI	4436	A175V	G524A
	hypothetical protein	4974	ΔQ215-355	ΔA643-A1065
	hypothetical protein	4975	ΔA1-M366	ΔA1-A1098
L9-Mnt	OmpR family	1849	L22Q	A65T
	Gph	4712	V94G	A281C
	hypothetical protein	4974	ΔQ215-355	A643-A1065
	hypothetical protein	4975	ΔA1-M366	A1-A1098

	acrA, mexA, adeI, smeD	4976	Frameshift deletion ΔP304	ΔC912
L9-LWT	OmpR family	1849	L22Q	A65T
	flrA, fleQ, flaK	4443	F310S	A929G
	Gph	4712	V94G	A281C
	hypothetical protein	4974	ΔQ215-355	ΔA643-A1065
	hypothetical protein	4975	ΔA1-M366	ΔA1-A1098

Supplementary Table 3. Primers used in this study.

Name	Description	Sequence
fadD1-A (XbaI)	Complementation	5'- ggacttctagaCCTCCCACATGGGTATAGCG-3'
fadD1-B (KpnI)		5'-ggactggtaccGATGAATTCGCGTCGCTGAC-3'
fadD2-A (XbaI)	Complementation	5'-ggacttctagaCAGCGCATTTCAGATCAGGC-3’
fadD2-B (KpnI)		5’-ggactggtaccCACTCAGGTAAGAGGACAAG-3’
fadD1/2-A (XbaI)	Complementation	5'- ggacttctagaCCTCCCACATGGGTATAGCG-3'
fadD1/2-B (KpnI)		5’-ggactggtaccCACTCAGGTAAGAGGACAAG-3’
	Complementation	
Volcano-A (Bgl II)	Deletion	5'-ggacagatctCCATCCCATGGGAGAGCATC-3'
Volcano-B (Bgl II)		5’-ggacagatctGATCAGCATCATCGCCATGC -3'
fadD1-A (Bgl II)	Deletion	5’-ggacagatctGCGGCCAACCCACGAGAATG-3’
fadD1-B		5’-cgtcgctgacCGCTATACCCATGTGGGAGG-3’

fadD1-C		5’-gggtatagcgGTCAGCGACGCGAATTCATC-3’
fadD1-D (Bgl II)		5’-ggacagatctGGCGTACCGGATGATCGCAC-3’
fadD2-A (Bgl II)	Deletion	5’-ggacagatctGGTTGCTGAAAGCCGGTTTG-3’
fadD2-B		5’-ctcaggtaagCGTGAGTCGTTGCCGATGAC-3’
fadD2-C		5’-acgactcacgCTTACCTGAGTGTGTCCGGC-3’
fadD2-D (Bgl II)		5‘-ggacagatctGGCCTGGGCGATGTAACTGC-3’
fadD1fadD2-A (Bgl II)	Deletion	5’-ggacagatctGCGGCCAACCCACGAGAATG-3’
fadD1/2-B		5’-ctcaggtaagCGCTATACCCATGTGGGAGG-3’
fadD1/2-C		5’-gggtatagcgCTTACCTGAGTGTGTCCGGC-3’
fadD1fadD2-D (Bgl II)		5’-ggacagatctGGCCTGGGCGATGTAACTGC-3’
Mountain-A (BglII)	Deletion	5’-ggacttaattaaGATTCTGCCCACCTACAGCC-3’
Mountain-B (SalI)		5’-ggacttaattaaCGATCACCGTACCGCTTTGC-3’
4974-A (BglII)	Deletion	5’-ggacagatctCTGCAAACAAGCCCCTAACG-3’
4974-B		5’-acggccaaagGCTCCCTTCTGTAATTGGGG-3’
4974-C		5’-agaagggagcCTTTGGCCGTTGGCAGCGTG-3’
4974-D (SalI)		5’-ggacagatctCATCCACGACACCTGGTGCG-3’
4975-A (BglII)	Deletion	5’-ggacagatctCCCGTTACTGCCCACTGCTG-3’
4975-B		5’-ggacgcgcagGTTGGATGCCCAGCGCCTTG-3’
4975-C		5’-ggcatccaacCTGCGCGTCCTTCATGCAAC-3’

4975-D (SalI)		5’-ggacagatctGTCACCCAGATCCACTTGGC-3’
49744975-A (BglII)	Deletion	5’-ggacagatctCTGCAAACAAGCCCCTAACG-3’
4974/75-B		5’-ggacgcgcagGCTCCCTTCTGTAATTGGGG-3’
4974/75-C		5’-agaagggagcCTGCGCGTCCTTCATGCAAC-3’
49744975-D (SalI)		5’-ggacagatctGTCACCCAGATCCACTTGGC-3’

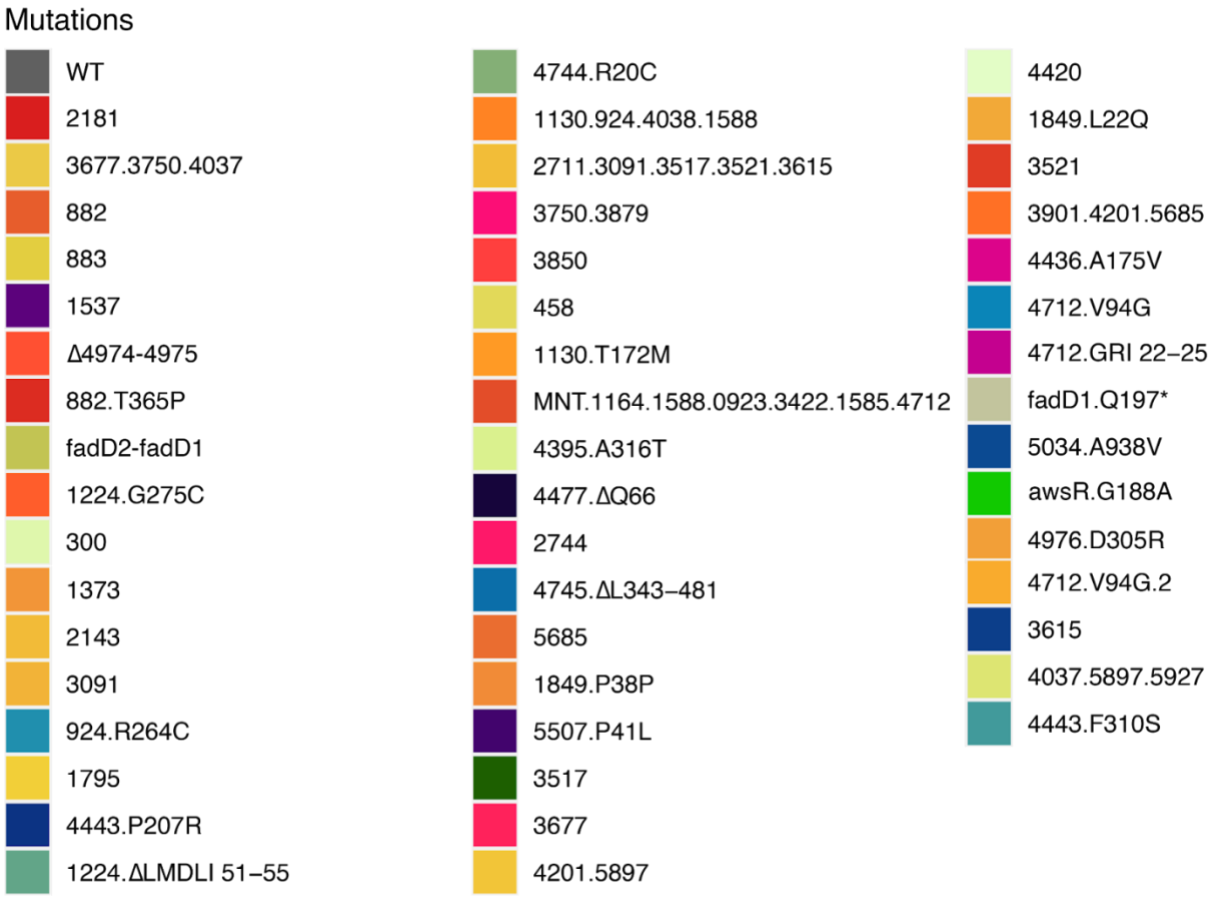

Supplementary Figure 1. Muller plot Legend. Labelled colour is representative of a unique mutation associated with gene PFLU number in *P. fluorescens* SBW25.

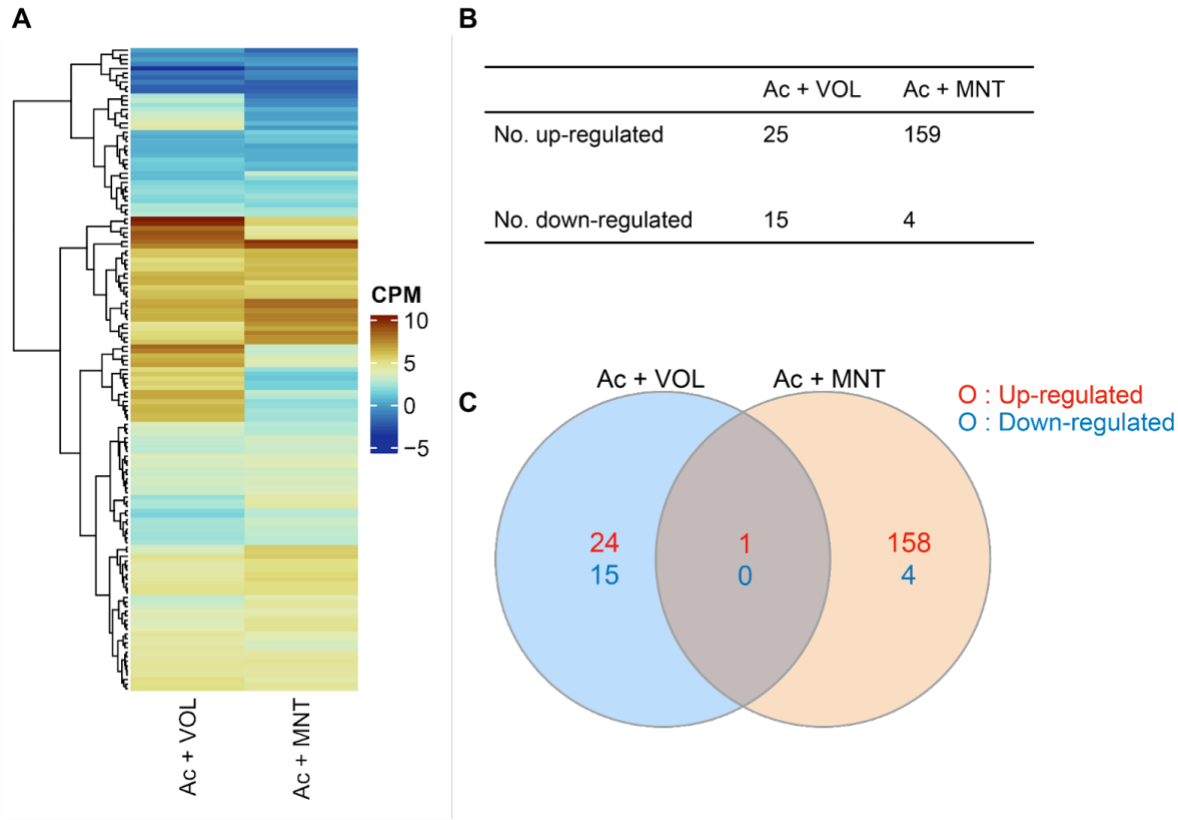

Supplementary Figure 2. Overview of significant changes in gene expression of *Acanthamoeba sp.* when predating upon evolved Vol and Mnt strains. A) Gene expression in log_2 counts per million (CPM) when interacting with each evolved strain as a heatmap clustered by count. B) The number of genes upregulated or downregulated (>2-fold change, p-value < 0.05). C) Venn diagram showing the number of overlapping genes differentially expressed between the two conditions. Ac; *Acanthamoeba sp.*, Vol; Volcano, Mnt; Mountain.

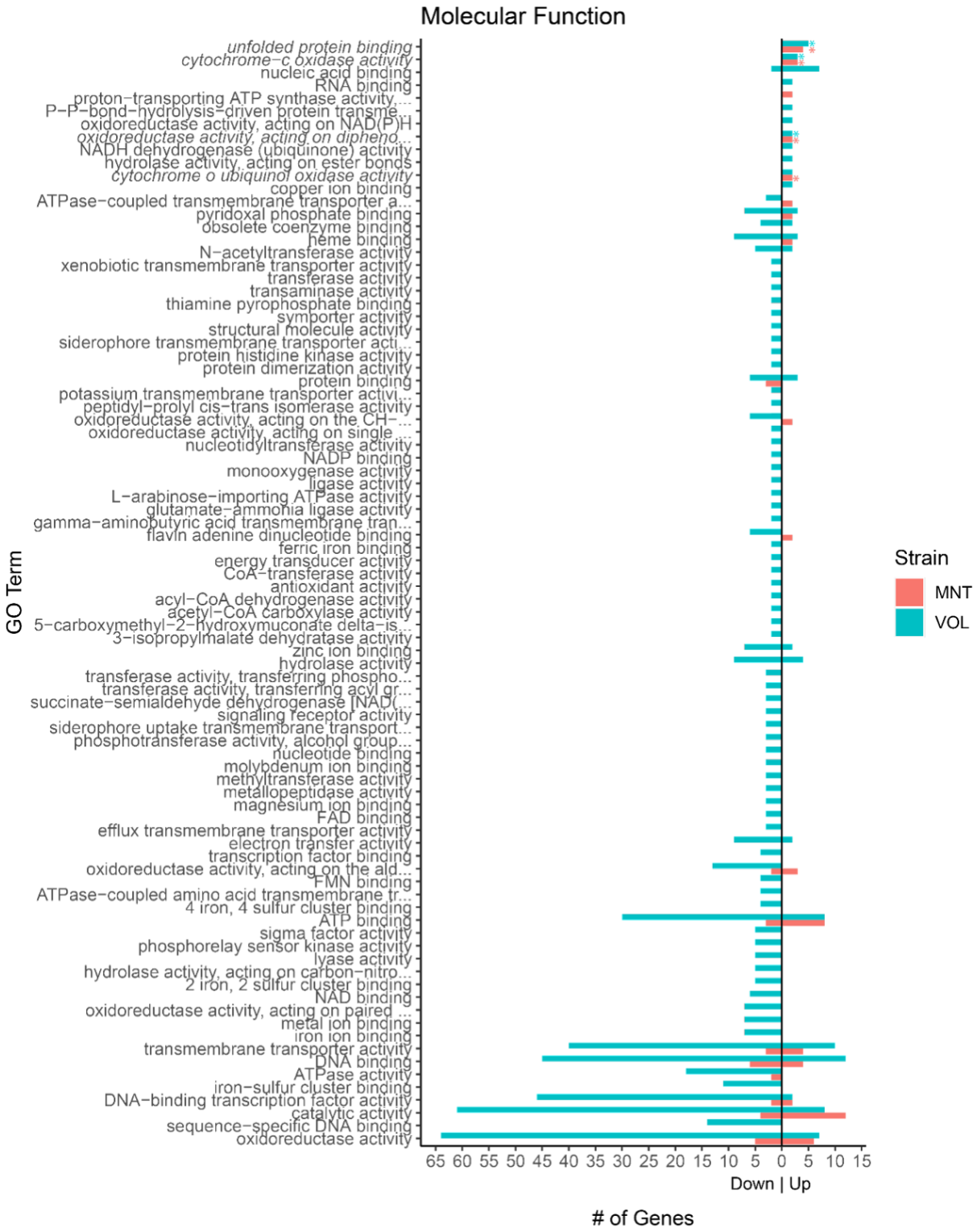

Supplementary Figure 3. Distribution of gene ontology (GO), molecular function classifications. GO analysis of upregulated (right) and downregulated (left) genes in Vol-L1 and Mnt-L2 when exposed to ancestral *Acanthamoeba sp.* as indicated. Stars denote enriched GO terms (One-tailed Fisher's exact test, P value <0.05).

Supplementary Table 4. Genes with differential expression (>2 log_2 FC) in Vo-L1l or Mnt-L2 when interacting with *Acanthamoeba*, compared to interaction with WT SBW25.

Gene.Name	Vol_Ac	Mnt_Ac	WT_Ac	Product.Description
PFLU0030	-2.617	-1.903	-2.057	putative 2-dehydro-3-deoxygalactonokinase
PFLU0031	-3.282	-1.410	-1.769	2-dehydro-3-deoxy-6-phosphogalactonate aldolase
PFLU0038	2.404	0.512	-0.327	hypothetical protein
PFLU0054	-2.010	-0.449	-0.922	hypothetical protein
gltP	2.654	1.346	2.131	glutamate/aspartate:proton symporter
PFLU0127	2.171	0.632	1.523	hypothetical protein
PFLU0131	-3.162	-0.951	-1.010	putative ABC transporter lipoprotein
gabD	-2.642	-0.440	-0.498	succinate-semialdehyde dehydrogenase I
PFLU0196	-2.658	-1.514	-1.184	AraC family transcriptional regulator
PFLU0199	-6.289	-0.147	-0.508	putative ABC sulfur transporter ATP-binding protein
PFLU0200	-7.843	-1.126	-1.224	putative ABC sulfur transporter membrane protein
PFLU0209	-2.185	-0.060	-0.874	putative TonB-dependent membrane protein
PFLU0211	-4.000	-1.742	-0.959	putative transporter-like membrane protein
PFLU0213	-3.152	-0.185	0.774	hypothetical protein
PFLU0219	-4.092	-2.492	-0.962	hypothetical protein
PFLU0228	2.196	3.482	1.299	putative amino acid ABC transporter membrane protein
PFLU0240	-7.210	1.024	2.060	putative monooxygenase
PFLU0250	-8.041	-1.070	-0.682	hypothetical protein
tauB	-4.418	0.756	0.853	taurine transporter ATP-binding subunit
PFLU0278	-2.376	-0.853	-0.348	putative molybdopterin oxidoreductase
PFLU0279	-2.115	-1.197	-0.406	hypothetical protein
PFLU0295	-2.119	-0.668	0.271	putative iron-transport related exported protein
gabP	-2.754	-1.014	-0.754	GABA permease

secB	**2.057**	**1.068**	**1.786**	**preprotein translocase subunit SecB**
PFLU0364	**-2.419**	**-1.231**	**-0.726**	**putative histidine ABC transporter membrane protein**
PFLU0365	**-2.500**	**-1.372**	**-1.283**	**putative histidine ABC transporter ATP-binding protein**
PFLU0376	**2.421**	**1.439**	**1.621**	**putative ABC transporter exported protein**
hslU	**3.241**	**3.336**	**4.124**	**ATP-dependent protease ATP-binding subunit HslU**
hslV	**2.260**	**2.585**	**3.103**	**ATP-dependent protease peptidase subunit**
rpmE	**4.293**	**1.995**	**2.193**	**50S ribosomal protein L31**
PFLU0437	**-2.643**	**-0.448**	**-0.285**	**putative acyltransferase**
trxC	**2.184**	**2.017**	**2.886**	**thioredoxin**
PFLU0442	**-2.277**	**-0.902**	**-0.342**	**hypothetical protein**
PFLU0443	**-2.399**	**-0.586**	**-0.326**	**hypothetical protein**
putA	**1.968**	**2.341**	**2.717**	**trifunctional transcriptional regulator/proline dehydrogenase/pyrroline-5-carboxylate dehydrogenase**
thiC	**-2.144**	**-1.265**	**-0.110**	**thiamine biosynthesis protein ThiC**
rplI	**0.917**	**2.469**	**2.442**	**50S ribosomal protein L9**
azu	**4.238**	**0.390**	**1.159**	**azurin**
ureE	**-2.690**	**-2.232**	**0.172**	**urease accessory protein UreE**
PFLU0570	**-2.487**	**0.297**	**-1.115**	**hypothetical protein**
cbpA	**3.236**	**2.502**	**4.249**	**curved DNA-binding protein**
PFLU0581	**-2.748**	**-0.776**	**-1.209**	**putative acetyltransferase**
PFLU0588	**-2.637**	**-1.382**	**-0.532**	**putative amino acid ABC transporter substrate-binding protein**
fis	**3.061**	**0.833**	**1.798**	**DNA-binding protein Fis**
PFLU0660	**-2.836**	**-0.264**	**-0.749**	**putative substrate-binding periplasmic protein**
PFLU0663	**-3.032**	**-2.006**	**-0.744**	**putative dehydrogenase**
PFLU0669	**-2.209**	**-0.518**	**-0.738**	**hydroxydechloroatrazine ethylaminohydrolase**
PFLU0673	**-3.259**	**-1.310**	**-1.640**	**putative purine transporter-like permease**

mmsA	**-0.204**	**2.193**	**1.658**	**methylmalonate-semialdehyde dehydrogenase**
PFLU0700	**-2.998**	**-0.961**	**-0.710**	**putative two-component system sensor kinase**
PFLU0731	**2.320**	**1.581**	**2.514**	**50S ribosomal protein L25/general stress protein Ctc**
ipk	**3.922**	**3.511**	**2.672**	**4-diphosphocytidyl-2-C-methyl-D-erythritol kinase**
PFLU0751	**-0.974**	**-2.037**	**-0.933**	**putative MerR family regulatory protein**
PFLU0754	**-2.164**	**-1.389**	**-1.038**	**hypothetical protein**
PFLU0755	**-3.163**	**-2.041**	**-1.398**	**hypothetical protein**
PFLU0762	**2.220**	**1.082**	**1.476**	**putative acyltransferase**
rpsT	**5.465**	**1.623**	**2.324**	**30S ribosomal protein S20**
PFLU0779	**2.140**	**0.953**	**1.302**	**putative lipoprotein**
PFLU0788	**2.742**	**3.624**	**4.201**	**zinc-binding protein**
rpsI	**3.252**	**1.210**	**1.559**	**30S ribosomal protein S9**
PFLU0849	**-2.745**	**-1.287**	**-1.343**	**5-dehydro-4-deoxyglucarate dehydratase**
garD	**-2.200**	**-0.472**	**-1.191**	**D-galactarate dehydratase**
PFLU0855	**2.354**	**0.511**	**1.912**	**hypothetical protein**
PFLU0856	**-2.168**	**-0.742**	**-0.642**	**Membrane transport protein**
mreD	**2.346**	**1.025**	**1.445**	**rod shape-determining protein**
fumC	**-1.222**	**-2.149**	**0.724**	**fumarate hydratase**
sodA	**-2.049**	**-2.062**	**0.679**	**superoxide dismutase**
rpoN	**-2.265**	**-0.911**	**-0.609**	**RNA polymerase factor sigma-54**
opdC	**-3.164**	**-1.230**	**-1.821**	**histidine porin opdC ***
PFLU0958	**-2.009**	**-0.606**	**-0.750**	**putative two-component system sensor kinase**
cusR	**-3.926**	**-2.168**	**-1.452**	**tw-component system, response regulator**
PFLU0960	**-2.221**	**-0.806**	**-0.495**	**hypothetical protein**
PFLU0971	**-2.400**	**-1.365**	**-1.103**	**putative fusaric acid resistance protein fusion**

PFLU1004	-2.671	-0.874	-0.500	hypothetical protein
PFLU1005	-5.316	-0.910	-0.249	hypothetical protein
PFLU1026	1.780	2.315	2.991	putative fumarylacetoacetase
PFLU1038	-3.068	-0.100	0.100	putative transporter-like membrane protein
PFLU1050	2.596	0.883	0.063	putative DNA-binding protein
PFLU1073	-6.474	-0.942	-0.024	putative deacetylase
PFLU1087A	2.521	-0.390	0.569	hypothetical protein
PFLU1089	-1.135	-2.098	-0.282	putative iron utilisation protein
PFLU1103	2.656	1.691	1.886	putative amino acid transporter-like membrane protein
PFLU1148	-2.622	-1.250	-1.487	putative formate dehydrogenase
PFLU1187	-2.057	-1.641	-1.165	hypothetical protein
PFLU1197	2.185	1.934	3.375	LysR family transcriptional regulator
wspF	-2.867	-1.608	-0.991	chemotaxis-specific methylesterase
PFLU1229	-2.842	-1.260	-0.189	TetR family transcriptional regulator
cspA1	2.449	1.054	1.407	major cold shock protein
PFLU1279	2.932	1.612	1.935	hypothetical protein
PFLU1296	-2.147	-0.696	-0.417	putative esterase
capB	6.268	1.604	1.948	cold shock protein
PFLU1363	-2.355	0.429	-0.188	putative amino acid degradation-related transferase
gctB	-3.544	0.419	-0.147	glutaconate CoA-transferase subunit B
pcaH	-2.035	-0.610	-0.196	protocatechuate 3,4-dioxygenase subunit beta
PFLU1388	-2.346	-0.605	-0.555	putative transporter-like membrane protein
PFLU1408	-2.835	-0.544	-0.490	putative dihydrodipicolinate synthase
PFLU1412	3.432	3.819	5.067	alcohol dehydrogenase
PFLU1413	2.487	2.082	3.147	putative transporter-like membrane protein

PFLU1418	**-2.643**	**-1.161**	**-0.165**	**putative transporter-like membrane protein**
rsuA	**-2.695**	**-1.536**	**-1.814**	**ribosomal small subunit pseudouridine synthase A**
algU	**-2.641**	**-1.427**	**-1.037**	**RNA polymerase sigma factor AlgU**
mucA	**-3.614**	**-1.649**	**-1.269**	**sigma factor negative regulatory protein**
PFLU1491	**-2.672**	**-0.552**	**-1.022**	**short chain dehydrogenase**
PFLU1504	**-3.078**	**-1.346**	**-0.969**	**LysR family transcriptional regulator**
PFLU1533	**-2.174**	**-1.073**	**-0.896**	**LysR family transcriptional regulator**
PFLU1534	**-2.591**	**-1.391**	**-1.441**	**LamB/YcsF family protein**
PFLU1597	**4.188**	**0.653**	**0.662**	**(p)ppGpp synthetase**
PFLU1605	**-2.833**	**-0.985**	**-1.702**	**putative two-component system sensor kinase**
PFLU1608	**-6.946**	**0.039**	**-0.496**	**putative fimbrial-like protein**
PFLU1611	**-6.688**	**-1.591**	**-2.181**	**putative fimbrial-like chaperone protein**
PFLU1615	**-2.075**	**-0.410**	**-0.020**	**LysR family transcriptional regulator**
argD	**-2.758**	**-2.195**	**-1.138**	**acetylornithine aminotransferase**
PFLU1628	**-3.245**	**-0.596**	**-0.888**	**putative transporter-like membrane protein**
PFLU1632	**2.085**	**-0.661**	**-0.337**	**putative peptide ABC transporter permease**
PFLU1652	**2.595**	**0.333**	**0.665**	**hypothetical protein**
PFLU1653	**6.572**	**1.682**	**2.614**	**putative transporter-like membrane protein**
PFLU1655	**7.318**	**1.933**	**2.060**	**Nucleotide-diphospho-sugar transferase**
fnl2	**2.170**	**0.703**	**0.768**	**NAD dependent epimerase/dehydratase**
fnl3	**2.805**	**0.793**	**1.015**	**UDP-N-acetylglucosamine2-epimerase**
PFLU1662	**3.653**	**1.162**	**1.592**	**hypothetical protein**
PFLU1674	**-7.715**	**-0.577**	**-0.565**	**putative amino acid transporter-like, membrane protein**
kdpA	**-6.824**	**0.181**	**-0.064**	**potassium-transporting ATPase subunit A**
kdpB	**-7.213**	**0.161**	**0.027**	**potassium-transporting ATPase subunit B**

PFLU1687	2.973	1.971	2.951	putative methyl-accepting chemotaxis protein
greB	2.309	1.190	0.992	transcription elongation factor
PFLU1714	2.934	1.406	2.017	elongation factor P
PFLU1718	-6.574	0.401	-0.522	LysR family transcriptional regulator
PFLU1720	-3.402	-1.446	-1.169	LysR family transcriptional regulator
PFLU1725	-3.545	-2.020	-2.341	enoyl-CoA hydratase
deaD	2.719	1.989	2.461	cold-shock dead-box protein A
PFLU1727	-2.019	-0.260	-0.684	putative aromatic ring dioxygenase
dsbE	2.089	1.316	1.949	cytochrome C biogenesis, thiol:disulfide interchange protein
PFLU1766	2.481	1.447	2.161	putative cytochrome C biogenesis protein
PFLU1773	2.417	1.003	0.664	hypothetical protein
PFLU1774	2.391	0.472	0.643	putative methyltransferase
PFLU1775	2.740	0.540	0.412	putative oxidoreductase
phnN	-3.152	-1.557	-1.385	phosphorous compounds metabolism-related ATP-binding protein
PFLU1790	-2.344	0.245	-0.042	LysR family transcriptional regulator
PFLU1791	-6.790	-1.877	-0.753	hypothetical protein
PFLU1793	-2.667	-1.636	-0.881	putative metalloprotease
gcl	-3.086	-1.641	-1.796	glyoxylate carboligase
htpG	2.164	3.133	4.029	heat shock protein 90
PFLU1843	-2.916	-0.800	-0.912	putative AMP-binding protein
PFLU1870	-2.123	0.113	-0.424	TetR family transcriptional regulator
PFLU1873	-2.189	0.185	-0.694	putative ABC transporter membrane protein
PFLU1876	-2.644	-1.462	-1.520	putative transporter-like membrane protein
PFLU1891	-2.407	-1.290	-0.812	putative cytochrome C oxidase (monoheme and diheme subunits)

PFLU1892	**-2.314**	**-1.511**	**-0.869**	**putative cytochrome C subunit protein**
PFLU1893	**-2.155**	**-1.247**	**-0.873**	**hypothetical protein**
PFLU1894	**-2.315**	**-1.351**	**-0.649**	**hypothetical protein**
PFLU1895	**-2.849**	**-1.815**	**-1.107**	**putative cytochrome C dehydrogenase-like protein**
PFLU1896	**-3.295**	**-2.447**	**-1.371**	**hypothetical protein**
PFLU1898	**-5.515**	**-3.808**	**-2.450**	**putative transporter-like membrane protein**
PFLU1924	**2.633**	**0.527**	**0.764**	**putative HTH-type regulatory protein**
gabD2	**-2.222**	**-0.746**	**-0.921**	**succinate-semialdehyde dehydrogenase**
PFLU1949	**-2.073**	**-0.288**	**-1.017**	**histidinol dehydrogenase**
PFLU1950	**-2.763**	**-0.183**	**-2.442**	**putative dehydrogenase**
PFLU1951	**-2.617**	**-0.934**	**-1.870**	**putative fumarylacetoacetate hydrolase family protein**
PFLU1955	**-2.076**	**-0.229**	**-0.368**	**hypothetical protein**
PFLU1988	**-2.460**	**-0.845**	**-0.561**	**3-oxoacyl-ACP reductase**
PFLU1989	**-2.777**	**-1.018**	**-0.689**	**3-oxoacyl-ACP reductase**
PFLU1990	**-2.340**	**-1.136**	**-1.334**	**putative transporter-like membrane protein**
PFLU1991	**-2.542**	**-1.899**	**-1.861**	**putative polysaccharide deacetylase**
PFLU1995	**-4.361**	**2.114**	**-1.619**	**hypothetical protein**
PFLU1996	**-5.013**	**2.097**	**-1.640**	**hypothetical protein**
accC	**-2.742**	**1.690**	**-1.214**	**acetyl-CoA carboxylase biotin carboxylase subunit**
PFLU2010	**-3.356**	**-1.063**	**-1.358**	**putative AsnC family regulatory protein**
cycA	**2.298**	**1.294**	**1.496**	**D-serine/D-alanine/glycine transporter**
PFLU2021	**2.197**	**0.205**	**0.360**	**putative transporter-like membrane protein**
PFLU2035	**-6.483**	**0.713**	**-0.211**	**putative ABC transporter ATP-binding protein**
PFLU2042	**2.538**	**2.125**	**2.721**	**putative ABC transporter membrane protein**
soxR	**-2.605**	**-0.999**	**-0.683**	**redox-sensitive transcriptional activator**

PFLU2055	**-4.946**	**-2.449**	**-1.605**	**putative sigma54-dependent regulatory protein**
PFLU2061	**-2.151**	**-0.255**	**-0.749**	**putative peptidase**
PFLU2088	**-2.055**	**-0.022**	**-1.416**	**putative hydrolase**
PFLU2126	**2.457**	**2.404**	**3.125**	**hypothetical protein**
PFLU2128	**-9.861**	**-2.405**	**-1.095**	**hypothetical protein**
PFLU2134	**-2.433**	**-0.895**	**-0.660**	**shikimate 5-dehydrogenase**
PFLU2164	**-3.119**	**-1.161**	**0.064**	**putative regulatory protein**
PFLU2173	**-6.901**	**-1.083**	**0.467**	**putative hydrolase**
PFLU2176	**-2.906**	**-1.929**	**-0.402**	**putative isomerase**
PFLU2177	**-2.232**	**-1.293**	**-0.642**	**putative acetyltransferase**
PFLU2180	**-3.283**	**-1.628**	**-1.571**	**putative LuxR family regulatory protein**
PFLU2185	**-2.084**	**-0.355**	**-1.186**	**putative hydrolase**
PFLU2199	**-8.110**	**-0.589**	**-1.827**	**putative carboxypeptidase**
PFLU2210	**-2.585**	**-0.283**	**0.080**	**putative monooxygenase**
PFLU2211	**-2.950**	**-1.095**	**-0.510**	**putative monooxygenase**
PFLU2212	**-2.074**	**-0.698**	**-0.543**	**putative monooxygenase**
PFLU2215	**-2.265**	**0.151**	**-0.901**	**putative monoxygenase**
PFLU2220	**-3.114**	**-0.615**	**-0.214**	**putative ABC transporter exported protein**
PFLU2224	**-6.721**	**0.560**	**0.939**	**putative hydrolase**
PFLU2226	**-1.862**	**2.728**	**2.560**	**putative ABC transporter substrate-binding protein**
PFLU2227	**-2.922**	**1.876**	**2.355**	**putative homocysteine S-methyltransferase**
PFLU2232	**-3.737**	**-0.553**	**-0.077**	**putative oxidoreductase**
gabP	**-2.307**	**0.289**	**-0.343**	**GABA permease**
PFLU2273	**-2.348**	**-0.735**	**-0.812**	**GntR family transcriptional regulator**
PFLU2281	**-2.289**	**-0.362**	**-1.570**	**putative ABC transporter membrane protein**

PFLU2283	-2.435	-0.204	-0.418	putative ABC transporter ATP-binding protein
pnl	-1.401	-2.039	-1.836	pectin lyase
xylH	-3.083	-0.960	-1.139	xylose ABC transporter permease
PFLU2305	-5.428	-0.750	-0.931	putative IclR family regulatory protein
PFLU2310	-2.969	-1.362	-2.087	putative monooxygenase
PFLU2313	-2.845	-1.574	-0.971	putative reductase
PFLU2317	-3.084	-0.893	-0.243	putative sarcosine oxidase subunit alpha
soxB	-2.611	-2.441	-1.432	sarcosine oxidase subunit beta
PFLU2322	-4.962	-0.564	0.173	putative DNA-binding protein
PFLU2325	-7.254	-0.451	-0.969	putative glutamate synthase
PFLU2326	-2.733	-0.724	-0.306	putative glutamate synthase large subunit
PFLU2327	-2.787	-0.720	-0.375	ammonia transporter
PFLU2337	-2.112	-0.593	-2.158	putative two-component system sensor kinase
PFLU2339	-5.858	-2.063	-0.058	hypothetical protein
PFLU2340	-2.956	-2.124	-1.805	putative polyamine ABC transporter ATP-binding protein
PFLU2342	-5.076	-2.860	-1.330	putative polyamine ABC transporter membrane protein
PFLU2349	-3.425	-0.761	-1.558	putative aldehyde dehydrogenase
PFLU2350	-3.426	-1.177	-1.795	putative lactonase
PFLU2352	-4.070	-1.396	-0.580	putative oxidoreductase
PFLU2367	-2.754	-1.530	-1.228	dihydroxy-acid dehydratase
PFLU2368	-3.124	-1.563	-1.802	putative transporter-like membrane protein
PFLU2369	-4.177	-0.588	-1.452	hypothetical protein
PFLU2370	-3.694	-1.509	-1.950	putative aldehyde dehydrogenase
araF	-2.931	-0.403	-2.070	L-arabinose ABC transporter substrate-binding periplasmic protein
araG	-3.478	-1.607	-1.441	L-arabinose transporter ATP-binding protein

araH	**-2.897**	**0.006**	**-1.229**	**L-arabinose transporter permease**
PFLU2375	**-2.542**	**-0.328**	**-1.411**	**putative aldose 1-epimerase**
PFLU2376	**-2.373**	**-0.504**	**-1.261**	**putative short-chain dehydrogenase/reductase**
PFLU2381	**-2.145**	**-0.752**	**-1.096**	**hypothetical protein**
PFLU2390	**-2.731**	**-0.099**	**-0.949**	**putative desaturase**
PFLU2403	**-2.025**	**-0.402**	**-1.576**	**putative dehydrogenase**
PFLU2412	**-2.572**	**-1.413**	**-1.646**	**putative TonB-ferrisiderophore receptor protein**
PFLU2419	**-1.440**	**-2.831**	**-1.127**	**putative type II secretion pathway protein G**
PFLU2423	**-3.016**	**-1.375**	**-1.662**	**putative type II secretion pathway protein D**
PFLU2440	**-6.557**	**-0.831**	**-0.329**	**putative peptidylprolyl isomerase**
PFLU2442	**-2.986**	**-1.738**	**-0.697**	**LysR family transcriptional regulator**
PFLU2450	**-3.303**	**-0.897**	**-0.789**	**hypothetical protein**
PFLU2469	**-2.607**	**-0.185**	**-0.641**	**putative dehydrogenase**
polS	**-7.452**	**-0.114**	**0.024**	**sorbitol dehydrogenase**
PFLU2493A	**1.534**	**2.363**	**1.443**	**AraC family transcriptional regulator**
PFLU2498	**2.435**	**1.795**	**1.377**	**putative methyl-accepting chemotaxis protein**
PFLU2529	**-4.755**	**-2.659**	**-1.793**	**putative IcrL family regulatory protein**
PFLU2530	**-6.865**	**-2.252**	**-1.938**	**putative LuxR family regulatory protein**
PFLU2532	**-3.421**	**-1.667**	**-1.479**	**GntR family transcriptional regulator**
fmdA	**-8.768**	**-1.243**	**-1.064**	**formamidase**
amiE	**-7.733**	**-1.134**	**-0.281**	**acylamide amidohydrolase**
PFLU2540	**-2.050**	**-0.951**	**-0.457**	**putative transporter-like membrane protein**
PFLU2547	**2.218**	**0.142**	**3.507**	**putative pyoverdine synthetase F**
pvdO	**2.699**	**-1.351**	**3.529**	**pyoverdine biosynthetic process ***
viscC	**2.229**	**-0.480**	**0.378**	**putative non-ribosomal peptide synthetase**

PFLU2557	**2.426**	**0.468**	**0.996**	**putative LuxR family regulatory protein**
PFLU2559	**-2.580**	**-1.599**	**-1.626**	**AsnC family regulatory protein**
PFLU2561	**-6.339**	**-0.602**	**0.305**	**hypothetical protein**
PFLU2584	**-2.802**	**-1.011**	**-1.416**	**putative ABC transporter ATP-binding protein**
PFLU2586	**2.732**	**1.732**	**2.989**	**putative DnaK suppressor protein**
PFLU2593	**-3.143**	**-1.588**	**-1.225**	**putative TonB-dependent receptor**
PFLU2598	**-2.001**	**-1.348**	**-0.394**	**TonB-dependent siderophore receptor**
PFLU2601	**-7.466**	**0.015**	**-0.083**	**putative transmembrane protein**
PFLU2603	**-2.032**	**0.042**	**-0.174**	**AraC family transcriptional regulator**
PFLU2618	**-7.163**	**-1.799**	**-0.387**	**glutamine high-affinity transport system; membrane component**
PFLU2620	**-3.425**	**-1.548**	**-0.916**	**ABC transporter ATP-binding protein**
PFLU2622	**-2.318**	**-0.812**	**-0.851**	**putative transcriptional regulator**
PFLU2624	**-2.345**	**-0.639**	**-0.482**	**2-dehydro-3-deoxygluconokinase**
PFLU2627	**-2.783**	**-0.009**	**-0.058**	**acetoacetyl-CoA synthetase**
PFLU2642	**3.263**	**1.617**	**2.087**	**3 membrane-bound lytic murein transglycosylase D**
PFLU2644	**-2.419**	**-0.773**	**-1.279**	**hypothetical protein**
PFLU2655	**-2.346**	**-0.921**	**0.005**	**putative transcriptional regulator**
PFLU2664	**-3.374**	**-1.673**	**-1.318**	**hypothetical protein**
PFLU2695	**-2.005**	**-1.183**	**-1.556**	**sigma-54 interacting regulatory protein**
fapD	**-6.929**	**-0.800**	**-0.049**	**amyloid fibril formation ***
PFLU2704	**-2.025**	**-0.619**	**-1.540**	**putative dehydrogenase**
PFLU2709	**-2.300**	**-0.420**	**-0.805**	**hypothetical protein**
PFLU2711	**-3.570**	**-1.704**	**-1.509**	**putative methyl-accepting chemotaxis protein**
PFLU2730	**-7.156**	**-0.326**	**-0.101**	**luciferase-like monooxygenase**
PFLU2733	**-2.331**	**-0.521**	**-0.863**	**methionine aminopeptidase**

PFLU2739	**-3.091**	**-1.674**	**-1.958**	**fructokinase**
PFLU2741	**-2.548**	**-0.762**	**-0.860**	**putative mannitol 2-dehydrogenase**
PFLU2743	**-3.216**	**-1.235**	**-0.661**	**putative ABC transporter permease**
PFLU2754	**-2.089**	**-0.460**	**-0.920**	**putative short chain dehydrogenase**
PFLU2768	**-3.217**	**-1.197**	**-1.477**	**LysR family transcriptional regulator**
PFLU2780	**-2.002**	**-1.060**	**-1.460**	**putative transmembrane phosphatidylcholine synthase**
PFLU2787	**-3.246**	**-1.427**	**-0.222**	**heme uptake regulator**
PFLU2790	**-6.711**	**-0.411**	**-0.063**	**putative integral membrane transport protein**
PFLU2793	**0.804**	**2.078**	**3.216**	**putative aminotransferase**
PFLU2799	**-7.439**	**0.240**	**0.486**	**putative monooxygenase**
PFLU2803	**-2.116**	**-0.072**	**-0.507**	**putative cytochrome C aldehyde dehydrogenase**
PFLU2817	**-2.484**	**-0.870**	**-0.683**	**putative phage integrase**
PFLU2837	**-0.704**	**-2.420**	**-0.725**	**hypothetical protein**
PFLU2897	**-2.507**	**-0.193**	**-0.879**	**putative phage-like protein**
PFLU2906	**-2.969**	**-1.082**	**-1.588**	**putative ABC transporter membrane protein**
PFLU2916	**-3.844**	**-1.857**	**-1.243**	**TetR family transcriptional regulator**
PFLU2924	**2.667**	**0.660**	**1.163**	**hypothetical protein**
PFLU2935	**-3.001**	**-1.984**	**-1.403**	**putative glycine betaine/L-proline ABC transporter substrate-binding periplasmic protein**
PFLU2939	**-3.193**	**0.672**	**0.190**	**putative two-component system sensor kinase**
PFLU2940	**-2.380**	**-1.941**	**0.507**	**hypothetical protein**
PFLU2957	**-2.467**	**-1.336**	**-1.694**	**Mg(2+) transport ATPase protein B**
chpE	**-2.525**	**-0.757**	**-0.740**	**chemotactic transduction protein**
PFLU2995	**-6.356**	**-0.019**	**1.012**	**putative transcriptional regulator**
PFLU3006	**-5.743**	**2.315**	**-1.248**	**hypothetical protein**
PFLU3037	**2.296**	**0.654**	**0.157**	**hypothetical protein**

PFLU3062	-2.197	-0.881	-1.057	putative aerobic C4-dicarboxylate transport protein
PFLU3073	-2.414	-0.112	0.054	AraC family transcriptional regulator
PFLU3079	-2.273	-0.675	-0.873	AraC family transcriptional regulator
PFLU3080	-4.217	-0.938	-1.670	putative 2-keto-4-pentenoate hydratase
mhpA	-3.135	-1.252	-1.048	3-(3-hydroxyphenyl)propionate hydroxylase
PFLU3084	-5.459	-1.046	-1.038	hypothetical protein
PFLU3086	-3.353	-1.712	-1.688	putative phenylacetaldehyde dehydrogenase
PFLU3087	-3.609	-0.857	-0.778	hypothetical protein
PFLU3090	-2.324	-0.365	-1.440	putative aldehyde dehydrogenase
PFLU3091	-2.420	-0.576	-1.504	putative amino acid permease
PFLU3094	-2.392	-0.199	-0.702	putative transmembrane permease
PFLU3097	-8.484	0.301	-1.108	putative phenylacetaldehyde dehydrogenase
PFLU3108	-3.824	-1.346	-1.170	3-oxoacyl-(acyl carrier protein) synthase II
PFLU3124	-6.471	0.125	-1.018	short chain dehydrogenase
PFLU3137	-2.932	-0.800	-1.037	putative epoxide hydrolase
PFLU3138	-2.374	-1.428	-1.359	hypothetical protein
PFLU3142	2.028	-0.715	-0.093	putative outer membrane secretion protein
PFLU3143	2.316	-0.753	-0.625	putative HlyD family secretion protein
PFLU3158	-3.205	-0.861	-0.926	putative aminotransferase
PFLU3160	-3.012	-1.638	-1.060	putative quinone oxidoreductase
PFLU3176	-2.933	-0.231	-0.345	aspartate aminotransferase
PFLU3179A	-2.345	-0.713	-0.846	LysR family transcriptional regulator
PFLU3202	-2.142	-0.348	-1.761	hypothetical protein
PFLU3209	-5.471	2.017	-0.008	putative high-molecular weight cobalt-containing nitrile hydratase subunit alpha
PFLU3235	-3.261	-2.035	-1.593	general secretion pathway protein K/X

PFLU3236	2.800	0.586	1.155	general secretion pathway protein G/T
PFLU3263	-7.163	-0.240	-1.684	putative efflux protein
PFLU3264	-2.015	-0.713	-0.985	Putative MetA-pathway of phenol degradation
PFLU3265	-3.115	-1.871	-1.301	AraC family transcriptional regulator
PFLU3269	-6.829	-1.061	-0.027	fumarylacetoacetate (FAA) hydrolase family protein
PFLU3273	-2.596	-2.092	-1.351	6 5-carboxymethyl-2-hydroxymuconate delta-isomerase
PFLU3287	-3.808	-0.942	-1.461	putative amino acid permease
PFLU3293	-3.422	-0.934	-0.379	oxidoreductase subunit alpha
PFLU3296	-2.059	-0.536	-0.616	putative acyl-CoA dehydrogenase oxidoreductase protein
PFLU3297	-2.273	0.084	-1.136	putative acetyl-CoA acetyltransferase
PFLU3298	-2.706	-0.341	-1.581	feruloyl-CoA synthase
PFLU3299	-3.767	-0.421	-0.965	aldehyde dehydrogenase family protein
PFLU3300	-2.431	-0.687	-0.169	p-hydroxycinnamoyl CoA hydratase/lyase
PFLU3301	-2.084	-0.032	-0.040	putative MarR family regulatory protein
PFLU3303	-2.016	-0.360	-1.418	putative 3-hydroxyphenylpropionic transporter MhpT
PFLU3306	-2.790	-0.989	-1.266	putative aldehyde dehydrogenase
PFLU3307	-2.266	-0.479	-1.070	putative nif-specific regulatory protein
PFLU3323	2.948	3.223	3.332	putative amino acid permease membrane protein
PFLU3325	2.073	3.362	2.993	putative rhizopine biosynthesis/dihydropicolinate synthase
PFLU3326	1.825	3.287	3.190	putative fatty aldehyde dehydrogenase
PFLU3327	0.829	2.394	2.492	putative D-amino acid dehydrogenase
PFLU3334	-3.849	-1.717	-1.456	TetR family transcriptional regulator
PFLU3375	-3.654	-2.532	-1.950	putative D-serine/D-alanine/glycine transporter
PFLU3383	-2.861	0.047	0.318	putative proline/betaine transporter
PFLU3419	-7.676	0.457	0.163	hypothetical protein

PFLU3433	-2.053	-0.755	-0.444	putative positive regulator of gcv operon
PFLU3435	-4.534	-0.730	-0.369	putative MarR family transcriptional regulator
PFLU3442	-2.800	-0.473	-1.099	putative transporter
ampC	-2.366	-0.342	-0.541	beta-lactamase
PFLU3474	-2.474	-1.797	-1.459	hypothetical protein
PFLU3486	2.054	1.399	1.301	tRNA hydroxylase
PFLU3492	-3.146	-0.114	-0.655	putative 2-hydroxyacid dehydrogenase
PFLU3496	-4.447	-0.087	-0.797	GntR family transcriptional regulator
PFLU3499	-2.540	-0.624	-1.190	putative DNA-3-methyladenine glycosylase I
PFLU3501	-2.759	0.106	0.111	GntR family transcriptional regulator
PFLU3502	-2.691	-1.766	-1.438	GntR family transcriptional regulator
PFLU3529	-0.467	2.446	2.008	acyl-CoA dehydrogenase
PFLU3568	-2.237	-0.852	-0.568	putative RNA polymerase sigma factor
PFLU3574	-2.165	-0.258	-0.519	putative ABC transporter ATP-binding protein
PFLU3580	2.365	1.967	1.696	hypothetical protein
PFLU3596	-2.517	-0.461	-0.647	hypothetical protein
PFLU3644	-3.026	-0.624	-1.121	putative bicyclomycin resistance protein
PFLU3651	0.514	2.040	0.408	putative amino acid exporter
PFLU3655	5.551	4.369	1.300	hypothetical protein
PFLU3657	4.875	2.668	0.838	hypothetical protein
PFLU3662	3.813	4.034	0.392	putative polysaccharide export protein
PFLU3664	3.693	3.431	0.545	mannose-1-phosphate guanylyltransferase
PFLU3665	3.102	2.789	-0.945	GDP-mannose mannosyl hydrolase
PFLU3667	2.918	3.001	0.332	GDP-fucose synthetase
PFLU3668	4.615	3.853	1.026	putative GDP-mannose 4,6-dehydratase

PFLU3674	**5.085**	**4.424**	**0.911**	**putative lipopolysaccharide biosinthesis-related acetyltransferase**
udg	**5.075**	**4.257**	**1.460**	**putative nucleotide sugar dehydrogenase**
PFLU3677	**5.366**	**4.467**	**1.398**	**tyrosine-protein kinase**
PFLU3678	**6.113**	**4.926**	**1.209**	**putative protein-tyrosine phosphatase**
PFLU3689	**-2.844**	**0.598**	**-0.312**	**putative alkanesulfonate ABC transporter periplasmic binding protein**
PFLU3691	**-6.252**	**-0.267**	**0.816**	**hypothetical protein**
PFLU3692	**-2.679**	**0.509**	**-0.636**	**hypothetical protein**
PFLU3694	**-2.502**	**1.080**	**-0.455**	**putative TonB protein**
PFLU3702	**2.197**	**2.453**	**0.196**	**putative isochorismatase**
PFLU3703	**1.549**	**2.669**	**-1.090**	**hypothetical protein**
PFLU3709	**2.117**	**2.441**	**-0.894**	**putative transcriptional regulator**
PFLU3724	**-3.570**	**-1.406**	**-1.385**	**C-terminal region of transketolase**
PFLU3726	**-2.890**	**-2.503**	**-1.556**	**putative ribose transporter permease**
PFLU3728	**-2.336**	**-1.859**	**-1.164**	**putative ribose ABC transporter ATP-binding protein**
PFLU3733	**2.487**	**1.561**	**2.067**	**putative aquaporin Z**
PFLU3738	**-2.511**	**-0.915**	**-0.564**	**hypothetical protein**
PFLU3773	**2.636**	**0.775**	**1.549**	**biopolymer transport protein**
PFLU3782	**2.780**	**1.036**	**2.165**	**putative arsenate reductase**
infA	**3.462**	**0.182**	**0.882**	**translation initiation factor IF-1**
PFLU3807	**2.655**	**0.400**	**0.754**	**putative cold-shock protein**
PFLU3818	**3.579**	**0.416**	**0.484**	**NADH dehydrogenase subunit A**
PFLU3826	**2.122**	**1.045**	**0.720**	**NADH dehydrogenase subunit J**
PFLU3827	**2.222**	**0.713**	**-0.133**	**NADH dehydrogenase subunit K**
PFLU3843	**2.172**	**0.982**	**0.510**	**hypothetical protein**

PFLU3854	-7.456	-0.842	-1.984	putative branched-chain amino acid ABC transporter permease
PFLU3862	-3.498	-0.238	0.972	putative integral membrane protein
PFLU3873	2.534	1.225	1.311	peptidyl-prolyl cis-trans isomerase B
PFLU3874	2.084	0.737	0.753	UDP-2,3-diacylglucosamine hydrolase
PFLU3884	-3.168	-2.024	-1.748	putative acyl-CoA dehydrogenase family protein
PFLU3891	1.434	2.815	1.854	gamma-carboxygeranoyl-CoA hydratase
PFLU3897	-2.446	-0.659	-1.497	putative catalase
PFLU3911	-6.870	-0.505	0.376	2-aminoethylphosphonate--pyruvate transaminase
PFLU3912	-6.458	-0.581	-1.377	phosphonoacetaldehyde hydrolase
PFLU3913	-2.494	-1.413	-1.645	cytochrome B561
PFLU3915	-2.328	-0.565	-0.698	putative 2,4-dienoyl-CoA reductase
PFLU3920	-2.585	-0.494	-0.491	2-oxoacid dehydrogenase subunit E1
PFLU3926	2.996	0.809	0.993	DNA-binding protein HU-beta
PFLU3936	-2.259	-0.817	-0.744	putative transporter-like membrane protein
PFLU3938	-2.848	-0.568	-0.972	putative lipoprotein
PFLU3942	-3.017	-1.339	-1.462	phenylhydantoinase
PFLU3943	-2.384	-0.789	-0.917	putative oxidoreductase
PFLU3947	-3.473	-1.224	-1.913	putative copper resistance protein D
PFLU3958	2.059	0.268	2.405	putative sodium:sulfate symporter
PFLU3960	-2.868	-1.852	-1.728	putative oxidoreductase
PFLU3969	-2.143	-0.174	-0.814	putative acetyltransferase
PFLU3976	-2.372	-0.320	-0.574	RNA polymerase sigma factor
PFLU3991	-7.422	-0.073	-0.404	short chain dehydrogenase
PFLU3992	-3.078	-0.753	-1.382	putative gluconokinase
PFLU3993	-4.256	-0.561	-1.751	putative zinc-binding dehydrogenase

PFLU3994	-2.109	-0.210	-1.074	putative sugar transporter permease
PFLU3995	-2.636	-0.719	-1.084	putative sugar transporter ATP-binding protein
arnT	2.310	0.572	0.757	4-amino-4-deoxy-L-arabinose transferase
viscA	2.439	-0.580	-0.390	putative non-ribosomal peptide synthetase
PFLU4008	2.735	-0.049	-0.079	putative LuxR family regulatory protein
PFLU4012	-2.769	-0.108	-1.026	putative ABC transporter ATP-binding protein
PFLU4018	-6.549	0.621	-0.283	amino acid ABC transporter permease
PFLU4025	-6.308	-0.342	-0.043	putative biotin carboxyl carrier protein of acetyl-CoA carboxylase
PFLU4028	-2.168	-1.343	-0.345	putative ABC transporter membrane protein
PFLU4039	-7.199	0.175	-1.421	putative succinate-semialdehyde dehydrogenase
PFLU4040	-3.240	0.889	-1.426	acetylornithine deacetylase
PFLU4045	-3.257	-0.168	-0.843	putative ABC transporter integral membrane protein
PFLU4046	-2.230	-0.587	-1.686	putative oligopeptide ABC transporter integral membrane protein
PFLU4048	-2.542	-0.200	-1.151	putative oxidoreductase
PFLU4055	-8.475	-1.806	-1.193	hypothetical protein
PFLU4065	-6.761	-1.211	0.323	putative oxidase
PFLU4067	-6.464	-1.865	-0.163	ABC transporter ATP-binding protein
PFLU4080	-7.297	-0.409	0.158	general secretion pathway protein
PFLU4082	-2.625	0.075	-0.494	putative beta-glucosidase
PFLU4087	-2.516	-0.621	-0.102	alkanesulfonate transporter substrate-binding subunit
PFLU4094	-7.515	-0.210	-0.749	putative transcriptional regulator
PFLU4103	-2.219	-1.003	-1.128	putative two-component system regulator
PFLU4119	-2.075	-1.138	-0.421	multidrug efflux protein
PFLU4120	-4.073	-1.466	-0.984	putative acriflavine resistance protein A

PFLU4132	2.257	-0.375	0.666	putative lipopolysaccharide modification acyltransferase
cspA2	2.334	0.425	0.096	major cold shock protein
PFLU4193	-3.611	-1.923	-1.068	3-isopropylmalate dehydrogenase
PFLU4194	-2.344	-0.191	-0.254	putative methyltransferase
leuD	-2.102	-0.775	-0.936	isopropylmalate isomerase small subunit
PFLU4196	-2.107	-0.887	-0.344	isopropylmalate isomerase large subunit
PFLU4204	-3.024	-0.831	-0.655	Alpha/beta hydrolase family
PFLU4205	-3.541	-0.737	-0.867	TetR family transcriptional regulator
PFLU4211	-3.477	-1.463	-0.907	LysR family transcriptional regulator
PFLU4213	-3.366	-0.291	0.234	LysR family transcriptional regulator
PFLU4231	-2.172	0.374	-0.302	putative quinone oxidoreductase
PFLU4247	-3.944	-2.051	-0.484	LysR family transcriptional regulator
PFLU4256	-2.439	-0.828	-1.210	hypothetical protein
PFLU4273	-6.471	-0.520	-1.966	putative zinc-binding dehydrogenase
PFLU4277	2.189	3.625	4.572	methionine sulfoxide reductase A
PFLU4283	-3.234	-0.036	-0.351	hypothetical protein
PFLU4287	-2.057	0.203	-0.086	transporter-like membrane protein
PFLU4293	-7.770	-0.135	-1.324	aspartate aminotransferase
PFLU4294	-2.818	-1.612	-0.703	putative proton glutamate symport protein
PFLU4309	-2.096	-2.060	-1.242	putative ABC transporter ATP-binding protein
PFLU4310	-2.153	-0.084	-0.886	hypothetical protein
PFLU4316	-2.312	-1.342	-0.850	putative thiolase
PFLU4355	-3.313	-1.350	-1.919	Xanthine/uracil permeases family protein
PFLU4363	-2.202	-0.613	-1.524	hypothetical protein
PFLU4366	2.344	1.636	1.807	hypothetical protein

PFLU4377	3.712	0.947	3.998	MbtH-like protein
PFLU4378	2.150	-0.399	3.275	diaminobutyrate--2-oxoglutarate aminotransferase
PFLU4383	-2.807	-1.084	-0.854	putative thiol:disulfide interchange protein
pvdG	2.291	0.213	3.996	putative thioesterase
PFLU4394	-2.465	-0.794	-0.982	acetyl-CoA carboxylase carboxyltransferase
PFLU4396	-2.708	-1.108	-0.392	putative enoyl-CoA hydratase/isomerase
PFLU4397	-2.069	-0.697	-1.051	putative acetyl-/propionyl-coenzyme A carboxylase alpha chain protein
fliS	-2.056	-2.180	-1.024	flagellar protein FliS
PFLU4457	-2.259	-0.823	-0.476	transcriptional regulation of aroF, aroG, tyrA and aromatic amino acid transport
PFLU4478	-2.116	-0.739	-1.033	putative glutathione peroxidase
PFLU4479	-3.118	-1.941	-1.632	putative transporter
PFLU4510	-2.175	-1.008	-0.988	agmatinase
PFLU4512	-2.554	-0.831	-0.117	putative transmembrane transport protein
PFLU4513	-2.550	-0.376	-0.519	putative sodium/solute symporter
PFLU4518	-2.039	-0.736	-0.669	putative transporter-like membrane protein
PFLU4549	-3.135	-1.605	-1.293	hypothetical protein
PFLU4552	-2.484	-1.282	-0.918	hypothetical protein
PFLU4554	4.000	5.058	5.215	cbb3-type cytochrome c oxidase subunit II
PFLU4568	3.020	2.173	2.791	coproporphyrinogen III oxidase
PFLU4574	-3.895	-1.716	-1.545	putative acyl-CoA dehydrogenase
PFLU4581	-2.157	-1.737	-1.702	hypothetical protein
PFLU4593	-2.144	-1.103	-1.599	putative xanthine dehydrogenase large subunit
PFLU4638	2.014	0.679	1.687	hypothetical protein
PFLU4657	-2.490	-1.093	-1.615	enoyl-CoA hydratase

PFLU4679	-2.290	-0.457	-0.834	AraC family transcriptional regulator
araH	-4.039	-1.006	-2.121	L-arabinose transporter permease
araG	-3.117	-1.840	-2.062	L-arabinose transporter ATP-binding protein
PFLU4684	-3.000	-1.460	-2.038	L-arabinose-binding periplasmic protein
PFLU4685	-2.638	-1.820	-1.646	short chain dehydrogenase
PFLU4693	-2.075	-1.385	-1.033	GntR family transcriptional regulator
PFLU4696	-2.163	-1.259	-0.988	putative molybdenum cofactor biosynthesis protein A
acpP	4.431	1.130	1.250	acyl carrier protein
rpmF	4.725	1.765	2.377	50S ribosomal protein L32
PFLU4771	2.262	0.682	0.970	putative 5-methylcytosine-specific restriction enzyme
PFLU4790	1.237	2.166	0.821	Peptidase propeptide and YPEB domain
PFLU4792	-3.089	-0.446	-1.055	putative methyl-accepting chemotaxis protein I
PFLU4797	-3.758	2.057	-1.486	hypothetical protein
PFLU4798	-3.367	-1.448	-1.262	LysR family transcriptional regulator
PFLU4806	2.435	0.390	-0.020	putative acetyltransferase
PFLU4811	2.456	0.259	2.098	putative gluconokinase
PFLU4830	-2.284	-0.222	-1.094	long-chain-fatty-acid--CoA ligase
PFLU4884	-2.815	-0.210	-1.338	putative two-component system response regulatory protein
PFLU4888	-3.016	-0.781	-0.795	putative DNA-3-methyladenine glycosylase II
PFLU4890	2.936	1.629	3.098	arginine/ornithine antiporter
PFLU4891	2.582	1.869	3.583	arginine deiminase
PFLU4892	2.394	1.700	3.314	ornithine carbamoyltransferase
PFLU4896	4.444	4.746	4.089	glycine cleavage system protein H
PFLU4897	2.217	2.561	2.411	glycine dehydrogenase
PFLU4912	2.116	1.515	1.786	putative thioesterase

PFLU4975	**-0.302**	**-9.749**	**0.374**	**hypothetical protein**
PFLU4976	**-0.861**	**2.813**	**0.688**	**putative HlyD family secretion protein**
groEL	**2.518**	**2.297**	**3.207**	**chaperonin GroEL**
groES	**3.432**	**2.445**	**2.931**	**co-chaperonin GroES**
PFLU4993	**2.417**	**0.623**	**1.023**	**beta-lactamase induction signal transducer AmpG**
rplS	**2.173**	**2.101**	**1.983**	**50S ribosomal protein L19**
rpsP	**3.717**	**1.428**	**2.011**	**30S ribosomal protein S16**
PFLU5025	**-2.918**	**-0.337**	**-0.426**	**putative N-acetylglucosamine-6-phosphate deacetylase**
serA	**5.298**	**0.745**	**2.682**	**D-3-phosphoglycerate dehydrogenase**
PFLU5038	**2.953**	**2.260**	**1.340**	**maltoporin**
PFLU5040	**2.953**	**1.660**	**1.984**	**PTS system sucrose-specific transporter subunit IIBC**
PFLU5066	**-2.368**	**-0.772**	**-1.289**	**HesB family protein**
PFLU5067	**-2.223**	**-0.828**	**-1.060**	**scaffold protein**
PFLU5091	**2.389**	**0.766**	**-0.073**	**putative chemotaxis protein CheW**
PFLU5095	**2.290**	**-0.164**	**-0.549**	**putative chemotaxis two-component system response regulator**
PFLU5138	**2.038**	**2.073**	**3.328**	**cytochrome C oxidase (ubiquinol oxidase) subunit III**
PFLU5139	**2.580**	**2.192**	**3.315**	**cytochrome C oxidase (ubiquinol oxidase) subunit I**
PFLU5140	**3.082**	**2.940**	**3.937**	**cytochrome C oxidase (ubiquinol oxidase) subunit II**
PFLU5142	**-2.176**	**-1.295**	**-0.987**	**nitric oxide dioxygenase**
PFLU5150	**1.022**	**2.628**	**2.439**	**putative hydrolase**
PFLU5152	**-3.182**	**-1.263**	**-1.469**	**flavodoxin**
PFLU5165	**-2.609**	**-1.464**	**-0.396**	**oxidoreductase**
rpmA	**2.558**	**1.963**	**1.863**	**50S ribosomal protein L27**
rplU	**1.639**	**2.218**	**2.329**	**50S ribosomal protein L21**
PFLU5187	**-2.263**	**-0.841**	**-0.743**	**putative amino acid transporter membrane protein**

PFLU5190	**-2.333**	**0.075**	**0.386**	**catechol 1,2-dioxygenase**
PFLU5191	**-7.629**	**-0.455**	**0.876**	**muconolactone delta-isomerase**
PFLU5192	**-9.338**	**-0.186**	**0.012**	**muconate cycloisomerase 1**
PFLU5194	**-2.573**	**-0.663**	**-0.120**	**benzoate 1,2-dioxygenase subunit alpha**
PFLU5195	**-2.401**	**-1.172**	**-0.860**	**benzoate 1,2-dioxygenase subunit beta**
antC	**-2.103**	**-1.252**	**-0.380**	**anthranilate dioxygenase reductase**
PFLU5202	**-2.647**	**-0.834**	**-1.228**	**3-hydroxyisobutyrate dehydrogenase**
PFLU5208	**2.248**	**-0.673**	**-0.087**	**hypothetical protein**
secG	**5.161**	**2.200**	**2.074**	**preprotein translocase subunit SecG**
PFLU5262	**3.104**	**0.508**	**0.505**	**hypothetical protein**
dapB	**1.639**	**2.415**	**3.046**	**dihydrodipicolinate reductase**
dnaJ	**1.619**	**2.283**	**3.056**	**chaperone protein DnaJ**
dnaK	**2.879**	**3.659**	**4.724**	**molecular chaperone DnaK**
grpE	**2.107**	**2.516**	**3.715**	**heat shock protein GrpE**
pdhR	**-2.619**	**-0.502**	**-0.084**	**pyruvate dehydrogenase complex repressor**
PFLU5292	**2.767**	**0.794**	**1.336**	**hypothetical protein**
PFLU5306	**2.232**	**1.069**	**1.820**	**putative transposase**
PFLU5311	**2.985**	**1.408**	**0.931**	**hypothetical protein**
PFLU5325	**-2.244**	**-1.199**	**-1.948**	**putative transcription elongation factor**
PFLU5350	**-2.108**	**-0.328**	**-2.562**	**putative dehydrogenase**
PFLU5357	**2.491**	**-0.266**	**3.646**	**hypothetical protein**
hasAp	**2.405**	**0.034**	**4.009**	**Heme-binding protein A ***
aroQ	**-7.968**	**-0.639**	**-0.613**	**3-dehydroquinate dehydratase**
PFLU5366	**-2.120**	**0.250**	**0.049**	**TetR family transcriptional regulator**
tesB	**-2.096**	**-0.576**	**-0.783**	**acyl-CoA thioesterase II**

PFLU5380	-2.021	-1.690	-1.235	putative AsnC family regulatory protein
PFLU5397	-2.557	-0.755	-1.101	putative dehydrogenase
PFLU5436	-4.575	-2.564	-1.917	hypothetical protein
PFLU5441	-2.192	0.533	-1.235	putative aldehyde dehydrigenase
PFLU5444	-3.006	0.004	-1.225	ethanolamine ammonia-lyase small subunit
PFLU5483	5.698	4.019	5.578	putative ABC transporter outer membrane exported protein
rplQ	3.035	0.869	1.485	50S ribosomal protein L17
rpmJ	2.280	1.018	1.853	50S ribosomal protein L36
rpsN	0.628	2.029	1.515	30S ribosomal protein S14
rplE	1.505	2.107	1.820	50S ribosomal protein L5
rpmC	1.512	2.052	2.247	50S ribosomal protein L29
rpsC	1.467	2.158	1.961	30S ribosomal protein S3
rpsS	2.324	2.056	2.250	30S ribosomal protein S19
rpsL	2.146	0.833	1.330	30S ribosomal protein S12
rplL	2.088	1.870	2.224	50S ribosomal protein L7/L12
nusG	2.351	1.582	1.319	transcription antitermination protein NusG
secE	2.329	1.265	1.069	preprotein translocase subunit SecE
PFLU5547	-2.205	-0.273	-0.733	iron-sulfur cluster insertion protein ErpA
crp	-2.069	-1.548	-1.200	cAMP-regulatory protein
trpC	-3.052	-1.801	-1.624	indole-3-glycerol-phosphate synthase
PFLU5573	-3.007	-0.621	-0.391	hypothetical protein
pqqA	2.208	0.518	1.524	coenzyme PQQ synthesis protein PqqA
PFLU5607	-2.878	-1.027	-0.747	putative dehydrogenase
PFLU5609	0.797	2.919	2.243	putative dehydrogenase
bioD	-3.314	-1.898	-1.934	dithiobiotin synthetase

PFLU5612	**-3.050**	**-1.113**	**-1.574**	**putative biotin biosynthesis-like protein**
bioB	**-3.310**	**0.350**	**-1.389**	**biotin synthase**
PFLU5624	**-4.127**	**-2.310**	**-1.903**	**putative response regulator**
PFLU5626	**-2.191**	**-0.254**	**-0.801**	**putative DNA poymerase**
PFLU5634	**-6.665**	**-0.919**	**-0.167**	**putative amino acid ABC transporter membrane protein**
PFLU5636	**-5.199**	**-1.373**	**-1.760**	**putative ABC transporter ATP-binding protein**
soxA	**-2.153**	**0.214**	**0.259**	**sarcosine oxidase subunit alpha**
PFLU5675	**-2.621**	**-0.635**	**-1.112**	**3-hydroxybutyryl-CoA dehydrogenase**
PFLU5678	**-2.652**	**-1.343**	**-1.395**	**AraC family transcriptional regulator**
PFLU5688	**-2.058**	**-0.775**	**-0.871**	**hypothetical protein**
PFLU5731	**-2.132**	**-0.788**	**-2.432**	**putative D-amino acid dehydrogenase small subunit**
PFLU5733	**-2.420**	**-0.121**	**-0.244**	**putative hemolysin**
PFLU5736	**-3.471**	**-0.432**	**-0.614**	**putative malonate transporter-like membrane protein**
PFLU5737	**-2.144**	**0.506**	**-1.249**	**putative malonyl-CoA-acyl carrier protein transacylase**
PFLU5738	**-2.339**	**0.293**	**-1.123**	**phosphoribosyl-dephospho-CoA transferase**
PFLU5739	**-2.023**	**-0.054**	**-0.668**	**putative malonate decarboxylase subunit gamma**
PFLU5743	**-2.103**	**0.813**	**0.073**	**putative decarboxylase**
PFLU5763	**2.110**	**2.026**	**2.071**	**putative recemase**
PFLU5788	**-2.273**	**-2.122**	**-1.991**	**putative dehydrogenase**
PFLU5808	**-2.399**	**-0.582**	**-1.673**	**putative oxidoreductase**
PFLU5846	**-2.188**	**-0.311**	**-0.431**	**putative aminotransferase**
PFLU5847	**-2.313**	**-0.638**	**-0.509**	**putative glutamine synthetase**
PFLU5849	**-2.654**	**-0.584**	**-0.386**	**putative glutamine synthetase**
ssuA	**-0.064**	**2.341**	**3.856**	**putative aliphatic sulfonatesABC transporter substrate-binding protein**
trxA	**2.069**	**1.732**	**1.601**	**thioredoxin**

PFLU5906	**-2.768**	**-0.056**	**-0.883**	**putative ABC transporter ATP-binding protein**
elbB	**-2.242**	**-0.323**	**-0.393**	**isoprenoid biosynthesis protein with amidotransferase-like domain**
PFLU5918	**-3.278**	**-1.172**	**-1.092**	**hypothetical protein**
comM	**-2.948**	**-1.491**	**-1.412**	**putative magnesium chelatase protein**
PFLU5959	**-2.291**	**-0.960**	**-1.120**	**multidrug efflux protein NorA**
PFLU5973	**-2.149**	**-0.364**	**-0.338**	**GntR family transcriptional regulator**
rpmG	**4.223**	**1.937**	**2.716**	**50S ribosomal protein L33**
rpmB	**3.933**	**1.596**	**2.191**	**50S ribosomal protein L28**
PFLU5998	**-2.148**	**-1.020**	**-1.263**	**hypothetical protein**
PFLU6004	**-2.159**	**-1.076**	**-1.138**	**hypothetical protein**
clpB2	**2.126**	**-0.263**	**0.228**	**chaperone**
PFLU6056	**-2.405**	**-0.485**	**-0.493**	**LysR family transcriptional regulator**
PFLU6060	**-2.512**	**0.005**	**-0.334**	**putative regulatory protein**
PFLU6091	**-3.393**	**-1.126**	**-0.885**	**putative ABC transporter periplasmic protein**
hisI	**-6.921**	**-0.417**	**-0.641**	**phosphoribosyl-AMP cyclohydrolase**
PFLU6102	**-2.386**	**0.576**	**-0.360**	**hypothetical protein**
PFLU6103	**-6.978**	**1.156**	**-2.467**	**hypothetical protein**
srlR	**2.613**	**1.904**	**1.792**	**glucitol operon repressor**
atpD	**1.826**	**2.005**	**2.119**	**F0F1 ATP synthase subunit beta**
atpG	**1.264**	**2.065**	**1.814**	**F0F1 ATP synthase subunit gamma**
atpB	**2.409**	**1.671**	**2.008**	**F0F1 ATP synthase subunit A**
rpmH	**2.443**	**1.583**	**1.830**	**50S ribosomal protein L34**